Integration of exteroceptive and interoceptive cues in spatial localization

Denise van Barneveld

Integration of exteroceptive and interoceptive cues in spatial localization

Een wetenschappelijke proeve op het gebied van de

Natuurwetenschappen, Wiskunde en Informatica

Proefschrift

ter verkrijging van de graad van doctor

aan de Radboud Universiteit Nijmegen

op gezag van de rector magnificus, prof. mr. S.C.J.J. Kortmann,

volgens besluit van het college van decanen

in het openbaar te verdedigen op donderdag 2 februari 2012

om 10.30 uur precies door

Denise Cornelia Petrus Barbara Maria van Barneveld
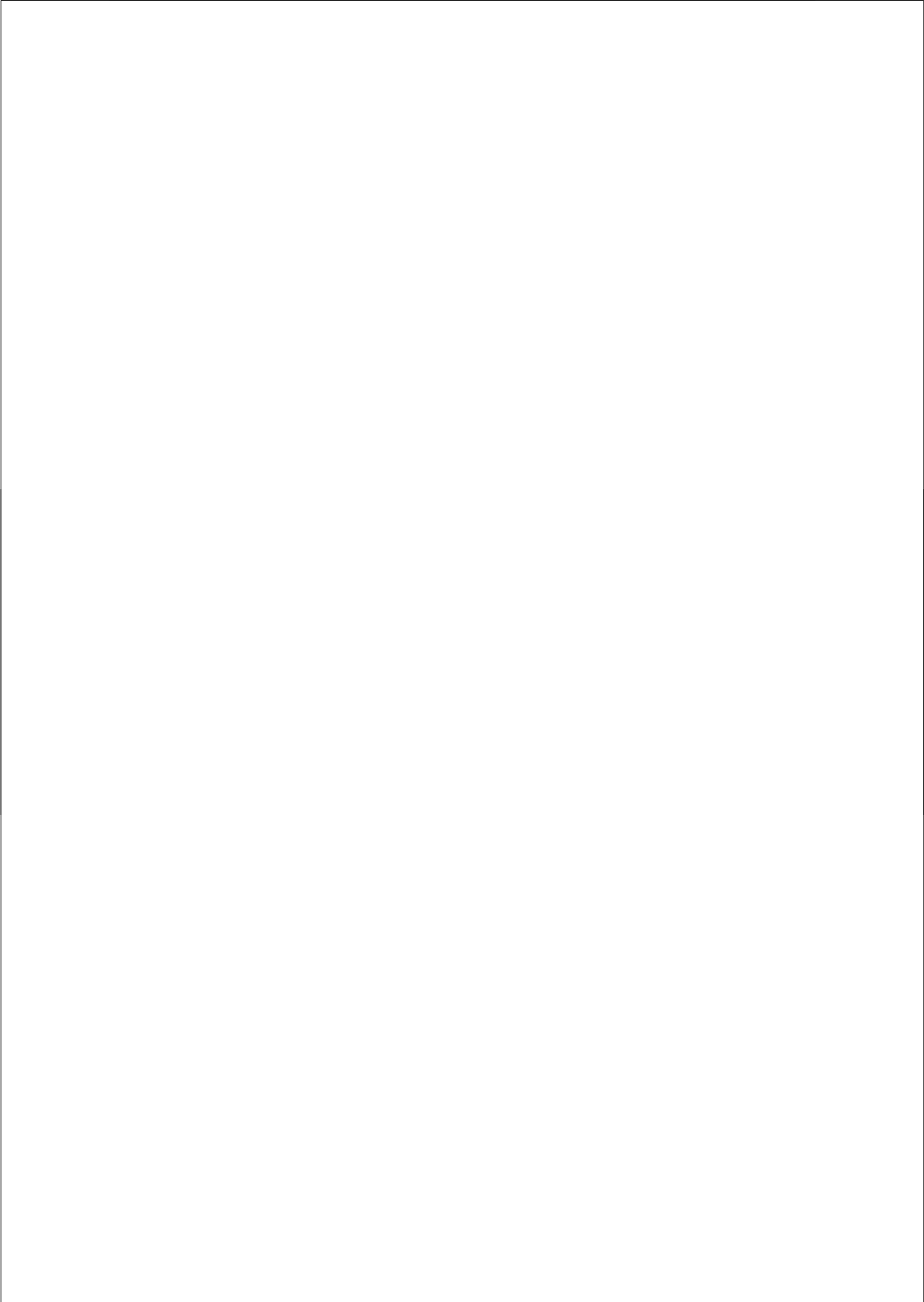
geboren op 1 juli 1983

te Geleen

Promotor: Prof. Dr. A.J. van Opstal

Copromotor: Dr. M.M. van Wanrooij

Manuscriptcommissie: Prof. Dr. R.G.J. Meulenbroek
Prof. Dr. A.V. van den Berg
Dr. H. Versnel (University Medical Center Utrecht)

TABLE OF CONTENTS

1

General introduction

Despite seemingly effortless goal-directed behavior like turning around if you hear someone shout your name, our brain is presented with complex computational challenges that have to be solved to enable such localization. Our localization abilities rely on neural computations that translate object information from our sensory systems into a coherent perception of their locations in space. This often requires that information from different senses is combined: a process called multisensory integration. Moreover, information about object location must be updated with every movement we make to correctly perceive that we are moving through a usually stationary environment. This subtype of multisensory integration is called spatial updating. The first chapter of this thesis provides a brief overview of the relevant topics that that determine multisensory integration and spatial updating: the structure and functioning of hearing, vision and the vestibular system, the mechanism of sound localization, and the problems the brain encounters when information of multiple senses need to be combined.

VISUAL SYSTEM

To safely navigate through space, it is important to avoid obstacles. Vision is the most important sense we use to determine the location of these obstacles. Visual information enters the system through our eyes and the lens topographically projects objects onto the two retinas, so that each neighboring point in visual space corresponds to a neighboring point on the retina. This retinotopic organization is preserved throughout the visual pathway up to the visual cortex (Sereno et al., 1995). As will be made clear below, the retinal information alone is not sufficient for adequate spatial localization in daily life, as the system also needs to incorporate the position of the eyes in the orbit and head on the body and in space to calculate the absolute positions of objects in space.

Although the visual field is large, the visual system's capacity to analyze fine spatial detail is limited to the fovea, a small (about 0.5° viewing angle) specialized area at the center of the retina where color-sensitive photoreceptors (cones) are densely packed. Visual acuity and color-vision deteriorate fast from the fovea to the peripheral retina, where receptor density (rods) is relatively low providing blurred and color-weak vision, but with a high sensitivity in near darkness and to visual motion. As a result, when we want to examine fine details of an object in the visual periphery, the fovea should be directed towards it. To meet this need, primates (and other foveate frontal-eyed animals, like cats) have evolved the ability to make very fast eye movements, saccades, which can shift the gaze line to a new point of interest.

These fast eye movements, however, give rise to a serious problem for the visual system that needs to be overcome: as every eye movement sweeps the visual scene across the retina and moves objects to different retinal locations, vision needs to update its internal representation of the world after each eye movement, to perceive that the eyes are scanning a stable environment, rather than that the environment itself moves around the observer. Below I will discuss the spatial updating process and the associated coordinate transformations in more detail.

SOUND LOCALIZATION

Although vision is an important sense to localize objects in the world around us, the role of audition, however, should not be underestimated; we can hear sounds originating from behind, at locations far beyond the visual field, and precisely determine their locations in complete darkness. The first stages of the auditory processing system (Fig. 1.1) are, unlike the

Figure 1.1   Schematic representation of the outer and inner ear.

visual system, not arranged in a spatial format. In contrast, it is organized tonotopically: each point on the basilar membrane peaks to a tone of a certain frequency, regardless its location with respect to the head. The cochlea thus acts as a frequency analyzer unraveling the identity of the sound and does not provide direct information about its location. Therefore, the auditory system needs to deduce position information about sounds in a different way than the visual system. It calculates the position of a sound source from implicit acoustic cues that arise from the interaction of the sound waves with the two ears, the head and the torso.
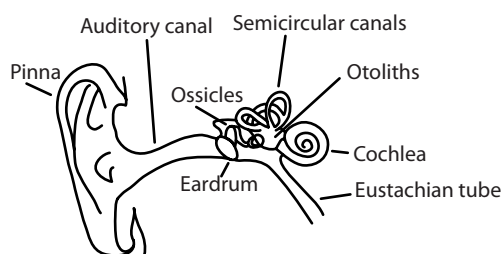
Sound localization cues in azimuth

Sound localization in the horizontal plane (in this thesis described by azimuth angle α) is based on interaural difference cues in arrival time and loudness (Blauert, 1997). Because of the finite sound velocity (343 m/s), a sound wave enters the ear ipsilateral to the sound source earlier than the far ear, creating an interaural time difference (ITD). ITDs vary in a systematic way with the sound's azimuth (Fig. 1.2A) and correspond to unique ongoing interaural phase differences (IPD). These IPDs are processed in the medial superior olive (MSO) of the auditory brainstem. At higher frequencies phase differences become ambiguous and may exceed 2π (one period) radians. For these frequencies the head becomes a significant obstacle for sound pressure waves, which causes a head shadow leading to interaural level differences (ILD; Fig. 1.2B). These ILDs are processed by cells in the lateral superior olive (Yin, 2002).
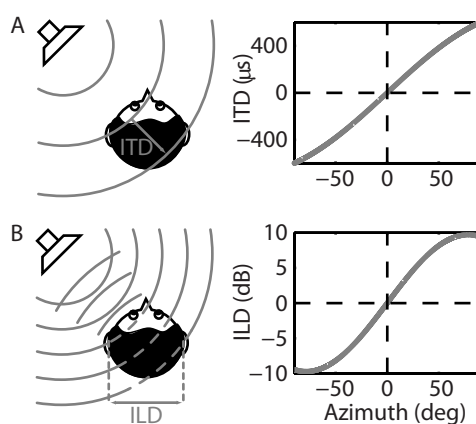
Figure 1.2   Sound localization cues in azimuth: interaural time and level differences. A) The relation between azimuth (α) and ITD is approximated for a spherical head by $ITD=r/c\,(\alpha+sin\,\alpha)$, where r denotes head radius (about 8 cm) and c is sound velocity of 343 m/s. B) The ILD relation for broad-band sounds is described by $ILD=9.7\cdot sin(0.02\cdot\alpha)$ (Van Wanrooij and Van Opstal, 2004). Note that ILDs are highly frequency dependent.
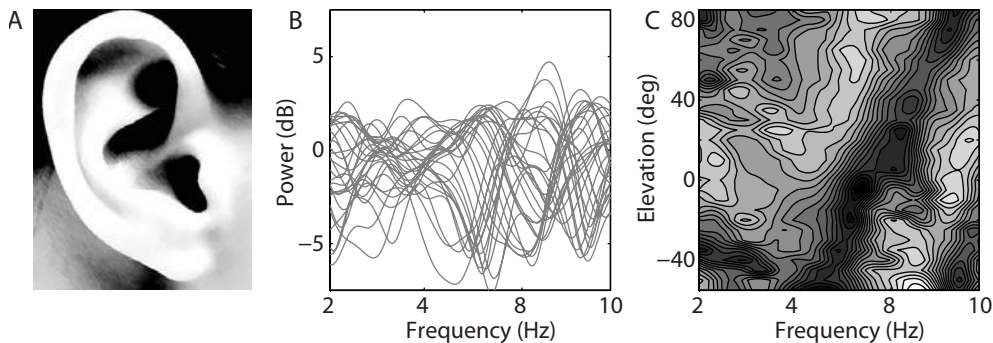
Figure 1.3 Directional transfer functions (DTF). The ear (A) filters sounds in a direction-dependent way. B) The power of the DTFs as a function of frequency. C) Contour plot of the same DFTs with the gray-scale presenting power (black: low, white: high). Note the clear direction- and frequency-dependent notch.

Sound localization cues in elevation

The binaural difference cues vary systematically with azimuth, but remain ambiguous with respect to vertical location of the source (elevation, ε) because the ears are usually at the same height. Also mirrored front-back locations have the same ITD and ILD. More precisely, there is a cone of locations with identical ITD and ILD: the cone of confusion. To resolve these confusions, the convoluted pinna cavities reflect and diffract sounds from different elevations differently, causing direction-dependent patterns of attenuation and amplifications in the spectra of the sounds arriving at the eardrum; the so-called directional transfer functions (DTFs) or spectral cues (Fig. 1.3; Wightman and Kistler, 1989; Middlebrooks, 1992). By comparing the sound energy across different frequency bands, the auditory system can determine the sound source's location in the vertical and front-back direction (Hofman and Van Opstal, 2002). Physiological evidence suggests that the dorsal cochlear nucleus might play a role in analyzing the directional features of sounds (Young and Davis, 2002).

VESTIBULAR SYSTEM

In daily life we are constantly moving and to achieve a stable percept of the world around us, the brain needs to monitor these movements, for which it could use a variety of signals. Since we usually plan our movements ourselves, the brain has access to the efference copies and corollary discharges of the planned movement signals that drive the muscles (Crapse and Sommer, 2008). Furthermore, muscle spindles sense movements of the head on the trunk, the trunk on the hips etc (Armstrong et al., 2008). In addition, our head movements in space are detected by the organs of balance, the vestibular system. The vestibular system continuously converts head movement and orientation relative to gravity into neural signals that are sent to the brainstem (Angelaki and Cullen, 2008). All these different types of interoceptive signals can be combined to determine our body orientation and its changes in space.

In this thesis, I focus on the role of the vestibular system in spatial localization. The vestibular system is located in the inner ears at both sides of the head (Fig. 1.1). It consists of
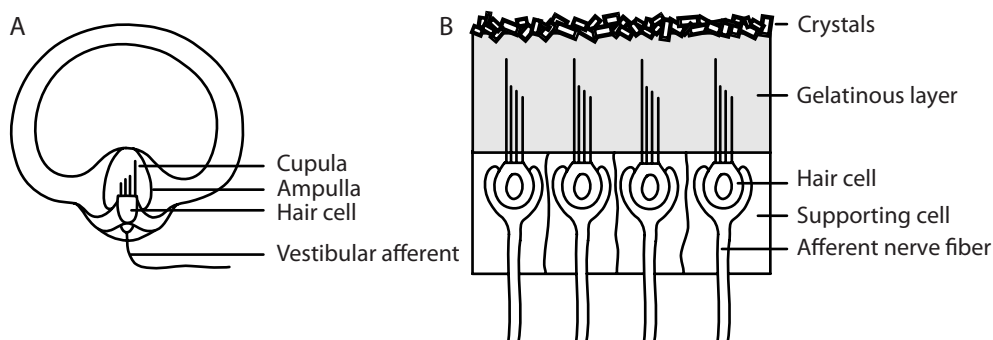
Figure 1.4   Schematic representation of the anatomy of (A) semicircular canals and (B) otoliths.

three semicircular canals (Fig. 1.4A) and two otoliths: the utricle and saccule (Fig. 1.4B).

The three canal pairs are angular head-velocity sensors. They are oriented orthogonally to each other and consist of an endolymph-filled duct, being closed off by a gelatinous mass called the cupula. When the head rotates, the inertia of the fluid causes the cupula to displace, which is sensed by embedded hair cells and causes an increase or decrease of the firing rate of afferent neurons. Since the canals on both sides of the head form pairs with hair cells that are oppositely polarized, a turn of the head simultaneously causes an increase of firing at the side of the head toward which the rotation is directed, and a decrease at the other side. Because the canals respond to angular acceleration, a double integration is needed to estimate head orientation under passive rotations. A first peripheral integration is carried out within the vestibular apparatus itself, because of their narrow ducts and the high viscosity of the fluid (Young, 1984), and the second is carried out in the central nervous system (Robinson, 1989).

The net difference in firing rates leads to slow movements of the eyes to counter head rotation. This vestibulo-ocular reflex (VOR) thus keeps the image of the outside world stationary on the retina. Due to the limited oculomotor range the eye cannot turn indefinitely in the orbit. Therefore, the slow compensatory movements of the eyes in the opposite direction are periodically interrupted by vestibular quick phases, rapid eye movements in the direction of rotation. The resulting characteristic saw tooth pattern of eye movements is called nystagmus.

When the head keeps rotating at a constant speed, however, the fluid will slowly catch up with the canal and the cupula will return to its neutral position. As a result, the vestibular slow-phase response decays to zero after about 30-40 s, and the subject does no longer experience a sense of rotation. As such, the slow-phase VOR acts as a high-pass linear filter to head velocity.

The second part of the vestibular organ, the otoliths, senses linear accelerations of the head, such as those induced by tilting with respect to the direction of gravity, or to translational movements. These organs contain a sensory epithelium, the macula, which consists of hair cells and associated supporting cells. On top of these cells and their hair bundles lies a gelatinous layer covered with a fibrous structure, the otolithic membrane. Crystals of calcium carbonate called otoconia are embedded in this membrane. These crystals give the otoliths their names

(otolith is Greek for "ear stones"). When the head is linearly accelerated or tilted, the crystals are displaced due to their inertia, causing the hair cells to deflect. This deflection either increases or decreases the firing rate, a signal to the brain about linear head acceleration.

MULTISENSORY INTEGRATION

Most of the time our sensory organs receive information about the world around us and the status of our own body. Integrating these different signals, a process called multisensory integration, might be beneficial for a number of reasons. First, one sensor could complement missing information of other senses; for example we cannot see audiovisual targets that are presented behind us, but we do hear them. Furthermore, combining information from multiple sensors could resolve potentially ambiguous information provided by individual sensors. E.g. efference copies of eye movements can distinguish visual motion on the retina originating from a moving stimulus relative to a stationary eye from the situation of a moving eye relative to a stationary object. Combing signals can also lead to more precise localization responses and reduced saccadic reaction times as has been shown for audiovisual integration (Frens et al., 1995; Colonius and Arndt, 2001; Corneil et al., 2002).

When the brain can rely on multiple sources of sensory information, this raises the question how these signals are weighted centrally. As an example, I here show how audiovisual integration is thought to originate from the optimal combination of auditory and visual percepts according to maximum-likelihood estimation (MLE; Alais and Burr, 2004; Körding et al., 2007). The unimodal sensory signals are assumed to be statistically independent, each with their own reliability (Fig. 1.5). A signal is reliable if the probability distribution of stimulus location given the sensory signal has a relatively small variance, otherwise a sources is regarded as unreliable. More-reliable sources are assigned a larger weight, and less-reliable sources are assigned smaller weights. Combining noisy sources affords the opportunity to improve signal-to-noise ratio, but may introduce errors.

Mathematically, the MLE model of sensory integration is characterized in the following way (Alais and Burr, 2004). The optimal combination of the independent auditory and visual estimates $\widehat{T}_A$ and $\widehat{T}_V$ of the target in space is given by:

$$\widehat{T}_{AV} = w_A\widehat{T}_A + w_V\widehat{T}_V \tag{1.1}$$

where w_A and w_V are the relative weights for each modality, inversely proportional to their reliabilities σ^2:

$$w_A = \frac{\sigma_V^2}{\sigma_A^2 + \sigma_V^2} \quad \text{and} \quad w_V = \frac{\sigma_A^2}{\sigma_A^2 + \sigma_V^2} \tag{1.2}$$

From this reasoning it follows that the audiovisual variance is always smaller than the unisensory variances:

$$\sigma_{AV}^2 = \frac{\sigma_A^2 \cdot \sigma_V^2}{\sigma_A^2 + \sigma_V^2} \tag{1.3}$$
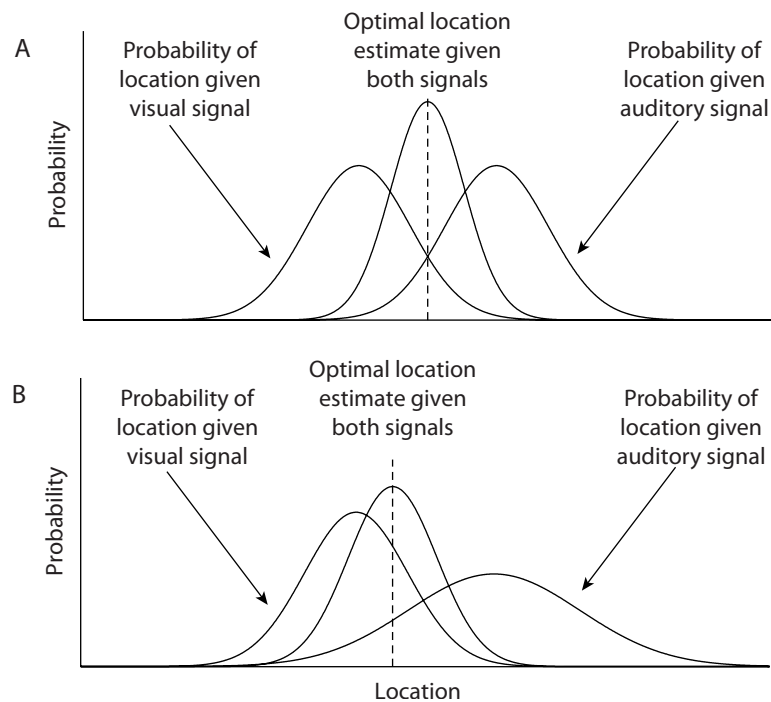
Figure 1.5 Optimal integration model for sensory integration based on MLE theory. A) Visual and auditory signals are equally reliable. B) Visual signals are more reliable than auditory signal. Adapted from Battaglia et al., 2003.

Moreover, according to Eqn 1.1 the audiovisual estimate lies between the unisensory estimates (Fig. 1.5), with the reliabilities as weighting factors. Thus, although the multimodal percept is more precise than the unimodal percepts, multisensory integration could create a localization bias. Below I will discuss the ventriloquist effect and the Aubert effect as examples of such a bias.

REFERENCE FRAME TRANSFORMATION

Multisensory integration is complicated by the fact that sensors and effectors encode information in different reference frames. As explained above, auditory information is encoded in a head-centered reference frame (T_H), whereas visual information is encoded in an eye-centered or retinotopic reference frame (T_R), and eye movements need eye-centered motor commands (Fig. 1.6A). To utilize these signals some of them need to be converted between reference frames. For example, in order to correctly plan an eye movement (ΔG) to the location of a sound, head-centered auditory information (T_H) needs to be transformed into a frame of reference suitable of accessing the oculomotor pathway. Conventionally, this is assumed to be a gaze-centered frame of reference, based on oculomotor representations in the superior colliculus (Jay and Sparks, 1984; 1987a,b). This transformation requires incorporation of eye-in-head orientation (E_H) if the eyes are eccentric in the head:

$$\Delta G = T_H - E_H \tag{1.4}$$

Experiments in our lab have shown that such transformations take place correctly in unaligned fixation conditions ($E_H \neq 0$) (Frens and Opstal, 1994), even with eccentric eye position due to drift or multiple saccades in total darkness (Van Grootel and Van Opstal, 2009; 2010). These latter two studies suggest that these transformations are based on an actual eye position signal rather than on the commonly accepted feedback of eye displacement (Jurgens et al., 1981; Goldberg and Bruce, 1990).

Visual targets, on the other hand, can be maintained in an eye-centered reference frame:

$$\Delta G = T_R \tag{1.5}$$

This simplification does not account for the fact that gaze displacement is a result of non-commutative eye rotations in multiple dimensions that arise from muscle contractions (for review: Crawford et al., 2011) that need rate-coded motor commands. Also, other motor behaviors, like goal-directed arm or head movements, require transformations into different reference frames (e.g. head-, body- or space-centered), and self motion needs to be accounted for as well (see spatial updating).

SPATIAL UPDATING

Usually, we are not motionless when planning goal-directed eye and head movements. Initial target directions become immediately obsolete when the eyes look into another direction. Moreover, making whole-body movements changes the position of the head in space and needs also be taken into account. Therefore, relying only on the initial target position for goal-directed movements would cause significant localization errors (Fig. 1.6B). Using visual feedback to determine the new location of the object would be too slow. To avoid delays, the brain should compute the new location; a process called spatial updating.

Spatial updating can be considered a reference frame transformation. For example, to react to a world-fixed visual target (T_R, Fig 1.6B), its initial eye-centered coordinates need to be converted into eye motor commands (ΔG), incorporating head-in-space (ΔH_S) and eye-in-head movements (ΔE_H) made during the reaction time:

$$\Delta G = T_R - \Delta H_S - \Delta E_H \tag{1.6}$$

For a target moving along with the head, on the other hand, head rotation should not be compensated. Thus, for appropriate spatial updating the brain should determine whether targets are moving or stationary in space. In order to do so, it should dissociate eye, head and body movements from object motion as exactly the same retinal motion pattern can result from a moving object relative to a stationary eye and a stationary object relative to a moving eye.
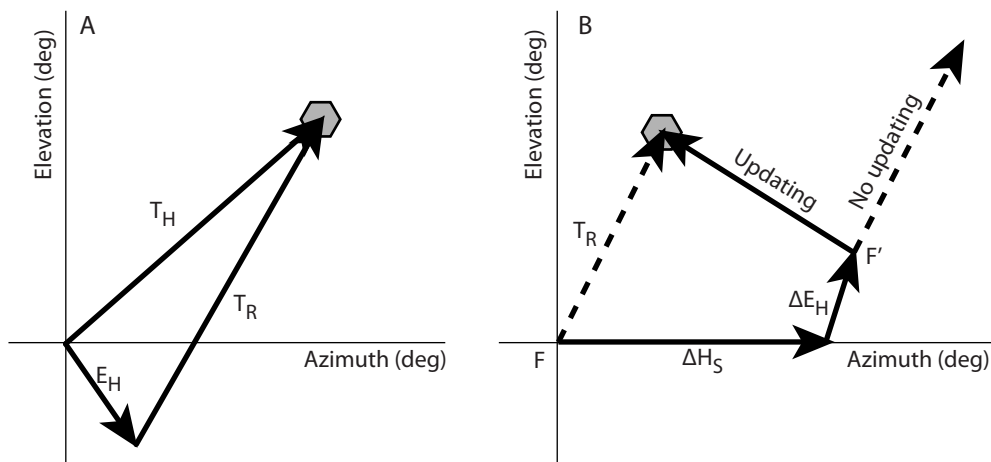
Figure 1.6 Reference frame transformations and spatial updating. In a mathematical sense, a reference frame is a set of rigid axes that are usually perpendicular to each other and intersect at one point, the origin. These axes allow the spatial location of an object to be defined by a set of coordinates. A) With the eyes eccentric in the head (E_H) and thus deviated from the straight ahead direction [a,ε] = [0,0], target location relative to the head (T_H) differs from target location on the retina (T_R). B) Illustration of one of the experimental paradigms described in chapter 3 of this thesis. At time zero a brief target (T_R) is presented while the head and eye is at [a,ε] = [0,0]. During the reaction time the head (and body) is passively rotated (ΔH_S) to the right. The eyes are not stationary either due to the ongoing vestibular ocular reflex and nystagmus and the absence of visual landmarks and land on fixation point F'. Correct spatial updating would fully incorporate intervening head and eye displacement signals and would be directed towards the world-centered location of the target (solid arrow). If the system does not update, it results in significant localization errors (dashed arrow).

Chapters 2 and 3 deal with spatial updating of visual and auditory targets, respectively. We analyzed head-restrained localization saccades to short and long-duration targets during passive whole-body rotation, where head and eye are displaced during the reaction time. Passive head rotations withhold the brain corollary discharge and proprioceptive information. Therefore, it could only rely on vestibular canal and auditory or visual stimulus motion information to determine the amount of head rotation and the possible movement of the stimulus through space. In chapter 2 we showed that long visual flashes provide sufficient retinal motion information for spatial updating, as head-fixed and world-fixed visual targets were appropriately localized. Short flashes, on the other hand, were kept in an eye-centered reference frame, which implies no spatial updating for both head and eye displacements, despite the fact that these latter signals were readily available to the system. In chapter 3 we extended these results to head-fixed short and long-duration sound bursts. Our results showed that these were all kept in head-centered coordinates. Our measurements also indicated that subjects were unable to reliably detect the auditory motion direction for the short noise bursts. Taken together, these findings suggest that if the brain is unsure about stimulus motion, it keeps targets in their initial reference frame.

MULTISENSORY INTEGRATION CAN INTRODUCE ERRORS

Although multisensory integration can be beneficial in many ways, it also can introduce errors under certain conditions (see above). In this thesis, I present data on three such errors: the ventriloquist effect (chapter 4), the Auditory Aubert-effect (chapter 5) and the audiogyral illusion (chapters 6 and 7).

Ventriloquist effect

Traditionally, visual information is regarded superior and dominant in spatial perception over other sensory systems (Welch and Warren, 1980). For example, in the ventriloquist effect the ventriloquist talks, but we perceive the sound to originate from the moving mouth of the puppet, even though we know that it is the ventriloquist that makes the sound and not the puppet (Fig. 1.7). Although it might seem that multisensory integration is failing here, according to the wide-spread MLE view (see above) it is actually a result of optimal integration of multimodal stimuli. This scheme of integration has the side-effect of introducing inaccuracies (the perceived sound location is biased towards the visual stimulus; Eqn 1.1), yet will reduce uncertainty in that audiovisual percept (Eqn 1.3).

This reduction in uncertainty can be clearly observed, as responses to audiovisual targets are more precise (Van Wanrooij et al., 2009; 2010). Another benefit of audiovisual integration is a reduced saccadic reaction time (Frens et al., 1995; Hughes et al., 1998; Colonius and Diederich, 2004) for audiovisual targets compared to their unimodal counterparts.

Intuitively one might argue that only signals stemming from the same event, either spatially or temporally, should be integrated. This intuition is corroborated by experimental evidence as the effects of integration decreases with increasing disparity between sound and light (Bertelson and Radeau, 1981; Frens et al., 1995; Van Wanrooij et al., 2009). In order to do so, the brain should deduce the single modality locations in space, decide whether the auditory and visual signals originated from the same source (Körding et al., 2007; Van Wanrooij et al., 2010), integrate the information according to that decision (Alais and Burr, 2004) and prepare and initiate a response towards the target (Corneil et al., 2002). As auditory targets enter the brain in a head-centered reference frame and visual targets are encoded in an eye-centered reference frame, the auditory and visual signals should be converted to a common presentation (either head-, eye-, body- or space-centered), before deciding whether these signals originated from the same spatial source.

This is not a trivial hypothesis as neurophysiological data suggests that

Figure 1.7   A cartoon of a ventriloquist

neurons in areas that are involved in multimodal localization behavior, such as superior colliculus (Jay and Sparks, 1984), lateral intraparietal area (Mullette-Gillman et al., 2005) and ventral intraparietal area (Schlack et al., 2005), have auditory and visual receptive fields that are not coded in a common frame. Moreover, behavioral data suggest spatially-incorrect integration for perceptual decisions on audiovisual fusion areas (Hartnagel et al., 2007) and for the recalibration of sounds in the ventriloquist aftereffect (Kopčo et al., 2009).

Chapter 4 investigated whether the ventriloquist effect indeed acted in a common reference frame. To that end, we let subjects localize sounds in the presence of a co-occurring visual distractor while the initial eye and head orientations were varied over a large range to disentangle uncommon (or hybrid) from common reference frame. Our results suggest that the ventriloquist effect acts in a common reference frame. Furthermore, our results demonstrate that humans accurately incorporate the different head and eye orientations required for the appropriate sensory-coordinate transformations.

Aubert-effect

Under normal conditions the direction and strength of the gravity vector is constant. Therefore, one could assume that knowledge about the direction of gravity would be sufficient to estimate actual body tilt with respect to the earth, and object verticality in space. Paradoxically, even though tilted subjects can accurately estimate their body orientation in the absence of visual cues (dashed line Fig. 1.8, e.g. Mittelstaedt, 1983; Mast and Jarchow, 1996; Van Beuzekom et al., 2001), they are not able to align a luminous line to the earth-vertical (thick solid line Fig. 1.8). Their responses depend systematically on body roll (Aubert, 1861; Mittelstaedt, 1983; Kaptein and Van Gisbergen, 2004), or on head-on-neck orientation (Van Beuzekom et al., 2001). Typically, errors are negligible for near-upright orientations. For tilt angles below about 30°, the line settings might show a small overcompensation (E-effect; Müller, 1916)
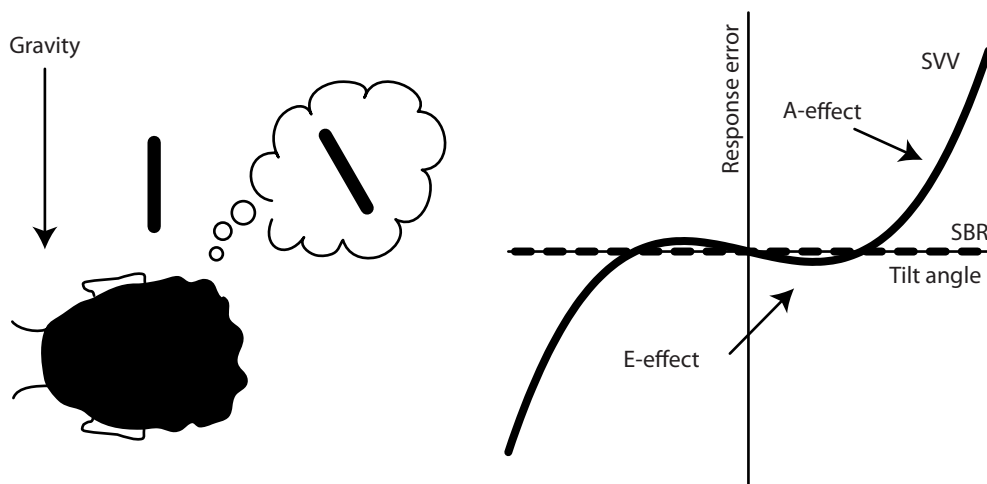
Figure 1.8   Aubert-effect. A line that is in reality aligned to gravity can be perceived tilted as much as 30° for a subject that is tilted 90°. Subject makes large errors when aligning a luminous line to the earth vertical when subjected to sideward body tilt (roll). The subjective visual vertical (SVV; thick solid line) shows overcompensation (E-effect) at small tilt angles and undercompensation at large tilt angles (A-effect). Subjective body roll (SBR; dashed horizontal line), on the other hand, is veridical.

and at tilt angles exceeding about 60° errors show an undercompensation that systematically varies with body-tilt angle (Aubert (A)-effect; Aubert, 1861). For example, when tilted 90° to the right, a single line that is in reality earth-vertical can appear to be tilted to the left by as much as 30°.

To account for the errors in the line setting task and their absence in body-tilt percepts, Mittelstaedt (1983) proposed that an internal bias signal, the so-called idiotropic vector, plays a crucial role in visual verticality perception, but not in the estimation of body tilt. According to this hypothesis, the otolith estimate is not aligned with gravity because of an imperfect fusion of utricle and saccule information originating from the difference in number of afferents (Rosenhall, 1972). Adding an idiotropic vector prevents errors at small tilt angles at the expense of errors at large tilt angles.

An alternative explanation of the bias in the responses is a Bayesian approach (De Vrijer et al., 2008), which states that it is useful to utilize existing (prior) knowledge in the interpretation of new sensory data. In contrast to Mittelstaedt's proposal, the head tilt signal stemming from the otoliths is assumed to be veridical, but corrupted with noise. Combining this noisy signal with a prior assumption that the head is usually upright results in a statistically optimal estimation of head orientation in space that is biased toward the prior distribution but is less variable than the original otolith signal. The perception of the line in space results then from the vector summation of the biased head-tilt signal with the precise and accurate retinal information of the luminous line.

In chapter 5 we extended these results to the auditory domain. We investigated the role of the otoliths and proprioception of neck muscles in determining the auditory zenith, as an analogue to the visual vertical. When upright, subjects could accurately indicate the auditory zenith. When they tilted their heads sideways, the head-centered zenith shifted accordingly. The world-centered zenith, however, shifted systematically in the direction of head tilt and the response variability increased. Although this shift was larger it resembled the visual Aubert-effect.

Audiogyral illusion

Active intervening head movements before and during eye-head gaze shifts towards a brief broadband auditory target do not affect the accuracy of sound localization behavior (Goossens and Van Opstal, 1999; Vliegen et al., 2004). Passive whole-body rotation in darkness, however, introduces systematic errors in sound localization of head-fixed sounds in the direction opposite to rotation (Fig. 1.9). This phenomenon is known as the audiogyral illusion (AGI; Münsterberg and Pierce, 1894; Clark and Graybiel, 1949). As a consequence of this apparent sound displacement, the subjective auditory median plane (AMP, the plane where the binaural difference cues are perceived to be zero) shifts in the opposite direction, which is in the direction of body rotation. As a result, sounds need to be presented physically in the direction of rotation to be perceived in the middle of the head.

Various hypotheses have been proposed to explain the underlying mechanism of the AGI. It was first thought to arise from an erroneous sense of rotation (Clark and Graybiel, 1949). Alternatively, kineasthetic factors like a misperceived head-on-trunk orientation might underlie the AGI (Lester and Morant, 1969; 1970; Lackner, 1974). Also, spatial attention might
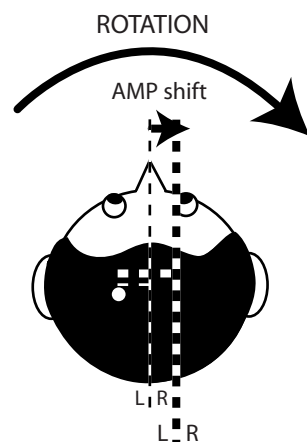
ROTATION

AMP shift

L R

L R

Figure 1.9   The audiogyral illusion. Sounds presented in the AMP are perceived in the centre of the head. For normal hearing and stationary listeners, this corresponds to sounds with ILD = 0 dB and ITD = 0 µs (thin vertical dashed line). If during whole-body rotation in darkness, the AMP shifts in the direction of rotation (thick vertical dashed line), a head fixed sound (white dot) shifts in the opposite direction, which is presented by the longer thick horizontal dashed line.

influence sound localization (Bohlander, 1984). Furthermore, the eyes are not stationary during whole-body rotation in darkness due to the VOR. The quick phases of the ocular nystagmus pattern shift the average eye position in the direction of head rotation ('Look where you go', Chun and Robinson, 1978; Vidal et al., 1983; Carpenter, 1988). Importantly, both ocular nystagmus (Arnoult, 1950; Thurlow and Kerr, 1970) and eccentric eye position (Lewald and Ehrenstein, 1996; Razavi et al., 2007) have been shown to effect sound localization and lateralization, as well as perceived body-orientation (Quarck et al., 2009).

In chapters 6 and 7 of this thesis we propose that the deviation in eye position is the major factor underlying the AGI. In chapter 6 we tested this hypothesis by determining the AMP during sinusoidal whole-body rotation and during smooth pursuit tracking of a sinusoidally moving visual target without vestibular stimulation. The AMP shifted in the direction of rotation in darkness and this shift disappeared in the presence of a fixation light at straight ahead. Furthermore, the pursuit experiments showed that the AMP shifted with eye position and not with eye velocity, indicating that indeed the shift in average eye position, and not the vestibular stimulation per se, underlies the audiogyral illusion. Chapter 7 confirmed these results, as neither patients with acute unilateral vestibular neuronitis, nor healthy subjects that underwent bilateral bipolar galvanic stimulation of the vestibular afferents, showed a shift in AMP when the eyes were kept at straight ahead.

Adapted from: Van Barneveld, D.C.P.B.M., Kiemeneij, A.C.M. and Van Opstal, A.J. (2011) Absence of spatial updating when the visuomotor system is unsure about stimulus motion. J Neurosci, 31(29): 10558-10568

2

Absence of spatial updating when the visuomotor system is unsure about stimulus motion

Denise C.P.B.M. Van Barneveld
Anne C.M. Kiemeneij
A. John Van Opstal

INTRODUCTION

To maintain a stable visual representation despite self-motion, the visuomotor system should account for intervening movements of eyes and head. As the original retinocentric coordinates of a target are not appropriate after self-motion, they need to be updated (spatial updating). The system could adjust its internal representations through extraretinal sources, such as vestibular signals, muscle proprioception, efference copies, or corollary discharges (Crapse and Sommer, 2008).

Humans (Hallett and Lightstone, 1976; Becker and Jurgens, 1979; Goossens and Van Opstal, 1997a; Vliegen et al., 2005) and monkeys (Van Grootel, 2010) accurately orient to brief visual flashes in the double-step paradigm despite an intervening saccadic eye, or eye-head gaze shift. Interestingly, spatial updating does not require visual-evoked programming of the intervening saccadic gaze-shift. For example, when eliciting a saccade by microstimulation of the superior colliculus, the subsequent saccade to an extinguished flash is still goal-directed (Mays and Sparks, 1980; Sparks and Mays, 1983). Long-latency saccades towards brief flashes presented before (Herter and Guitton, 1998) or during (Blohm et al., 2003; Daye et al., 2010) smooth-pursuit eye movements remain accurate, and also saccades to brief head-fixed flashes appear to incorporate eye movements caused by passive vestibular nystagmus (Van Beuzekom and Van Gisbergen, 2002).

Localizing a stimulus requires the visuomotor system to dissociate self-motion from target motion. Whereas extraretinal signals may provide accurate estimates of head-in-space and eye-in-head movements, retinal signals could provide information about target movement with respect to the eyes. But how much retinal motion is needed to decide whether a target is stationary in space, or moves relative to the eyes, head or body? What is the prior assumption about the stimulus reference frame when retinal-motion information is insufficient?

To answer these questions, we investigated the role of retinal input and the vestibular canals in spatial updating. We rotated head- and body-fixed subjects sinusoidally around an earth-fixed vertical axis, while they localized visual flashes that were either stationary in space, or moved with the head. The experiments excluded the use of neck-proprioception and efference copies of head movements, so that only brief retinal motion signals, intervening eye-movements, and vestibular head-movement information during the saccade reaction time remained for updating target coordinates. We analyzed flash-evoked gaze shifts (ΔG) according to models (Fig. 2.1A) that differ in the compensation of intervening eye and head movements:

$$\Delta G = T_R - b \cdot \Delta H_S - c \cdot \Delta E_H \qquad (2.1)$$

with T_R the initial retinal location of the target flash, ΔH_S the vestibular-induced passive head-in-space movement during the reaction time, and ΔE_H the eye-in-head displacement. For example, accurate localization of stationary stimuli in world coordinates requires full compensation of eye and head displacements ($b = c = 1$). Localization in retinal coordinates (no compensation) corresponds to $b = c = 0$, while spatial updating into head-centered coordinates, appropriate when stimuli move with the head, only incorporates eye-in-head displacement ($b = 0$, $c = 1$). Our results demonstrate that spatial updating depends on the reliability of target-
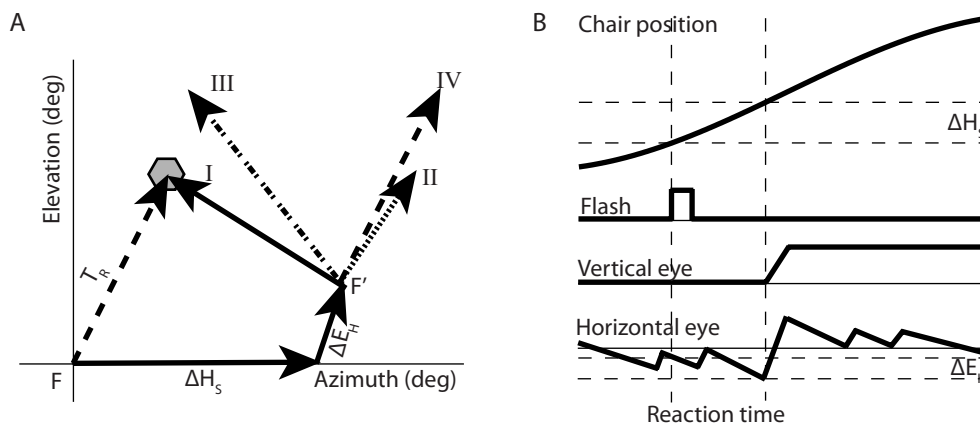
Figure 2.1   A) Four models for visuomotor spatial updating during passive whole-body rotation. At time = 0 a visual target (T_R) is presented while the subject fixates at *F*. During the response reaction time the head (and body) is passively rotated (ΔH_S). Due to vestibular nystagmus and absence of visual landmarks, the eyes undergo an eye displacement (ΔE_H) and end at location *F'* in the world. Model I predicts a response in world-centered coordinates, and fully incorporates intervening head and eye displacements. Model II predicts a head-centered response, as it incorporates only the change in eye position. Model III only accounts for the head displacement, while model IV keeps the target in the initial retinocentric reference frame. B) Temporal order of chair position, visual target and eye movements.

motion information across the retina, as subjects adequately remapped the target location into head-centered (head-fixed targets), or world-centered (world-fixed targets) coordinates for long-duration stimuli only. In contrast, responses to very short flashes (0.5 ms) were best described in retinocentric coordinates (no spatial updating), regardless whether targets were head or world fixed.

METHODS

Subjects
Six subjects (three of either sex) participated in the experiments. Three participants (the authors, one male, two female) were familiar with the purpose of the experiments. All subjects had normal or corrected to normal vision, except for JO, who is amblyopic in his right, recorded eye. Experiments were conducted after obtaining full understanding and written consent from the subject. The experimental procedures were approved by the Local Ethics Committee of the Radboud University Nijmegen and adhered to The Code of Ethics of the World Medical Association (Declaration of Helsinki), as printed in the British Medical Journal of July 18, 1964.

Apparatus

Vestibular setup
Experiments were conducted in a completely dark room. The subject was seated in a computer-controlled vestibular stimulator (Van Barneveld and Van Opstal, 2010), with the head firmly

stabilized in an upright position with a padded adjustable helmet. We measured chair position with a digital position encoder at an angular resolution of 0.04°. The present study employed sinusoidal yaw rotation with an amplitude of 70° at a frequency of 1/6 Hz, which corresponded to a peak chair-velocity of 73°/s. This rotation profile was applied using a custom-made Matlab program on a PC (Precision T3400, Dell, Limerick, Ireland) that controlled a second PC that steered the position of the chair.

Visual stimuli

The same Matlab program also controlled the visual stimuli via a PCIE-2214 card (Pericom, San Jose, CA, USA). Visual stimuli emanated from an array of red light-emitting diodes (LED type HLMP-3301), with a response speed of 90 ns. LEDs were positioned on the intersections of seven concentric circles at viewing angles of 5, 10, …, 35° (at a distance to the cyclopean eye of 39 cm), and 12 directional meridians placed at every 30°. The visual stimulus array was either attached to the vestibular chair (head-fixed condition), or stationary in space (world-fixed condition). Due to comfortable positioning of the head, the center LED was positioned on the naso-occipital axis at a distance to the cyclopean eye that varied slightly between subjects (head-fixed condition: 32 - 41 cm; world-fixed condition: 129 – 134 cm). LEDs were flashed for 0.5, 4 or 100 ms. Timing precision of LED onset and offset (0.1 ms, or better) was verified by recording the LED's input signal at 50 kHz.

Eye-movement measurements

We measured two-dimensional eye movements of the right eye with the double-magnetic induction technique (Bour et al., 1984; Bremen et al., 2007) using oscillating magnetic fields at 30, 48 and 60 kHz generated by three pairs of orthogonal coils (0.77 x 0.77 m) inside the vestibular stimulator. The horizontal, vertical and frontal eye-position signals were amplified, demodulated by tuned lock-in amplifiers (Princeton Applied Research, NJ, USA, model PAR 128A), low-pass filtered (150 Hz, custom-built 4th order Bessel) and subsequently sampled at 500 Hz per channel (1401 Plus, using Spike 2 software, Cambridge Electronic Design, Cambridge, England) for storage on the computer's hard disk (Precision 360, Dell, Limerick, Ireland) together with the chair position.

Conventions

Coordinate system

We express the coordinates of visual target locations and eye-in-head positions in a double polar coordinate system, in which the origin coincides with the center of the head (Knudsen and Konishi, 1979). In this system the left/right azimuth coordinate, α, is defined as the angle within a horizontal plane with the vertical midsagittal plane. The up/down elevation angle, ε, is defined as the angle within a vertical plane with the horizontal plane through the subject's eyes. The straight-ahead position is defined by $[\alpha, \varepsilon] = [0,0]°$.

Experimental paradigms

Subjects participated in six different experiments (two paradigms with three target durations) that were performed on different days. The order was varied over subjects. In three world-centered experiments, the visual targets were stationary in space, whereas in the other three head-centered experiments the targets rotated along with the subject. As a precaution we avoided the potential use of binocular vision and depth estimation by blindfolding the right (measured) eye, for all experiments except for the 4 ms head-fixed targets, for which only subject MK was blindfolded. JO was never blindfolded, since his amblyopia precluded the use of any visual depth-related cues.

Calibration

A calibration run preceded each experimental run, in which the subject fixated 37 (head-fixed condition) or 49 (world-fixed condition) LEDs that covered the oculomotor range. At fixation the subject pressed a joystick, which triggered 50 ms sampling of horizontal, vertical and frontal eye-position signals. These data were used for offline calibration of the eye-position signals. As described above, the distance between the head and LED array, and thus the LEDs' eccentricity varied slightly across subjects, resulting in different calibration ranges from 29 - 40°.

Static condition

We assessed the subject's baseline visual-localization behavior to the target flashes in a static run presented at the beginning of the experimental sessions with the head-fixed targets. An LED was flashed for 0.5, 4 or 100 ms (as used in the different vestibular sessions) at an eccentricity of (about) 20° in one of eight randomly chosen oblique directions (±30, ±60, ±120, ±150°), where 0° denotes rightward, and 90° upward. The targets were presented in a pseudo-random order with an inter-stimulus interval of 3.5 seconds, such that in total 96 targets (12 repetitions of 8 stimuli) were presented. The subject had to redirect gaze as fast and as accurately as possible to the perceived location of the visual target, keep gaze there for a moment, and then return to straight ahead. During localization trials we did not present an initial fixation light at straight ahead.

Dynamic condition

In the dynamic condition, the subject was rotated sinusoidally around the Earth-vertical axis at a frequency of 1/6 Hz, with a peak amplitude of 70°. To avoid discontinuities in velocity and acceleration at motion onset, angular velocity increased linearly over the first two sinusoidal periods during which no visual targets were presented. After these two periods, 96 targets were presented during 48 sinusoidal periods, at an inter-stimulus interval of on average 3 seconds. Subjects participated in 3-4 dynamic runs per condition.

We tested two conditions:
1. Head-fixed condition. The LED array was attached to the chair. The same LEDs as in the static condition were used (12 repetitions of 8 stimuli). Stimuli were presented at pseudo-random times during the vestibular cycle.

2. World-fixed condition. The LED array was stationary in space and placed in front of the chair. Two LEDs (elevation: 11°, azimuth: 0° with respect to stationary straight-ahead) were presented randomly within the period of ± 200 ms around peak chair velocity, during which the chair moved approximately 28°. Since the chair's position (and hence the head-in-space) varied with respect to the LEDs, the two LED locations resulted in various target re. head locations, with initial azimuth components between ± 14° (left-right).

The subject's task was to make an eye movement towards the perceived location of the target as fast and as accurately as possible, to briefly fixate this position, and then return to the perceived head-centered straight ahead location. We gave no additional instructions regarding the reference frame (head-centered, world-centered, or otherwise) of the responses. Note that we neither presented a fixation light at straight ahead, nor did we present any practice trials preceding the experiments.

Data Analysis

Calibration of eye-position data
We determined the relation between raw eye-position signals and the corresponding LED positions by training two neural networks for the azimuth and elevation eye-position components, respectively (for details, see Goossens and Van Opstal, 1997b). Each run's raw data were calibrated with networks of the calibration run, that were presented immediately before this run.

Saccade detection
A custom-made Matlab (The Mathworks, Natick, MA, USA) program detected saccades and vestibular quick phases from the calibrated eye-movement signals offline by setting separate thresholds for eye velocity at saccade onset (70°/s) and offset (60°/s). We visually checked the saccade detection markings and made manual changes when deemed necessary. To differentiate between quick phases of vestibular nystagmus and goal-directed saccades, we required the goal-directed saccades to have a vertical component, since the visual targets were presented at different elevations, and the reflexive vestibular quick phases had a negligible vertical component. Responses with extremely short latencies were regarded as anticipatory, and very long reaction times as inattentiveness of the subject. We therefore discarded saccades with latencies shorter than 80 ms and longer than 800 ms. Eye positions exceeding the head-centered calibration range of 29 - 40° (see Experimental paradigms - Calibration) were also excluded. Correction saccades in darkness were very rare (0.73 ± 0.60%), and therefore we report only on the first goal-directed saccade in each trial.

Statistics
For the static localization experiment we quantified the final eye-in-head positions in the azimuth (α_R^{stat}) and elevation (ϵ_R^{stat}) direction by determining the optimal linear fit through the data:

$$\alpha_R^{stat} = a_{stat} \cdot \alpha_T + b_{stat} \qquad (2.2a)$$

and
$$\epsilon_R^{stat} = c_{stat} \cdot \epsilon_T + d_{stat} \qquad\qquad (2.2b)$$

where α_T and ε_T are actual target azimuth and elevation relative to the head, b_{stat} and d_{stat} are the biases (offset, in °) whereas a_{stat} and c_{stat} are the gains (slope, dimensionless) of azimuth and elevation responses, respectively. Parameters were found by minimizing the mean-squared error (Press et al., 1992). From the linear fit we also determined the correlation coefficient (r) between data and model prediction, the coefficient of determination (r²), and the standard deviation of the residual error (σ).

Ideal static localization performance yields gains of 1.0 and biases of 0.0°. However, parameters a_{stat}, b_{stat}, c_{stat} and d_{stat} could deviate from the ideal values in an idiosyncratic way. To enable data pooling across subjects and conditions, we normalized the target locations with respect to the data obtained in the static localization condition for the 4 ms targets:

$$T_H^{Az} = a_{stat} \cdot \alpha_T + b_{stat} \text{ and hence } \alpha_R^{stat} = T_H^{Az} \qquad (2.3a)$$
$$T_H^{El} = c_{stat} \cdot \epsilon_T + d_{stat} \text{ and hence } \epsilon_R^{stat} = T_H^{El} \qquad (2.3b)$$

These normalized target locations T_H^{Az}, and T_H^{El}, were then used to perform regression on the *dynamic* localization responses of the vestibular stimulation experiments.

$$\alpha_R^{dyn} = a_{dyn} \cdot T_H^{Az} + b_{dyn} \qquad\qquad (2.4a)$$
and
$$\epsilon_R^{dyn} = c_{dyn} \cdot T_H^{El} + d_{dyn} \qquad\qquad (2.4b)$$

Because the vestibular stimulation only affected the horizontal eye-movement components and induced only horizontal head displacements, we do not present the regression results on the elevation data in detail.

Modeling

To determine to what extent the visuomotor system incorporated the intervening vestibular-induced eye and head movements during the reaction-time period, we performed a multiple linear regression analysis on the horizontal saccade components, as these were the components perturbed by the vestibular stimulation. The horizontal saccadic eye displacement (ΔG) was described as a linear combination of the horizontal initial target location on the retina (T_R), the horizontal vestibular-induced eye displacement (ΔE_H) in the head, and the horizontal passive displacement of the head in space (ΔH_S), both between target onset and response onset (cf. Eqn 2.1):

$$T_R = T_H^{Az} - E_H^{ini} \qquad\qquad (2.5)$$
$$\Delta G = a \cdot T_R + b \cdot \Delta H_S + c \cdot \Delta E_H + d \qquad\qquad (2.6)$$

in which a, b, and c are dimensionless response gains and d is the response bias (in °). In this chapter we consider four potential spatial updating models to explain visual-evoked saccade responses (Fig. 2.1, Table 2.1). In model I, full compensation of eye- and head-displacement signals corresponds to a world-centered target representation. In model II, only the vestibular-induced change in eye position is accounted for and the target remains in an updated head-

Table 2.1   Theoretical regression coefficients of Eqn 2.6 for the four models.

Model	Details	a	b	c	d
I (world-centered)	Full eye-head compenstaion	1	-1	-1	0
II (head-centered)	EYe-only compensation	1	0	-1	0
III	Head-only compensation	1	-1	0	0
IV (retinocentric)	No compensation	1	0	0	0

centered reference frame. Model III only incorporates the passive change in head orientation, while the visuomotor system is unaware of the intervening vestibular nystagmus. Finally, in model IV none of the intervening movement signals are accounted for and the target remains in its initial eye-centered reference frame. Table 2.1 summarizes the theoretical coefficients that correspond to each of the models.

Regression parameters were determined by applying the least-squares error criterion. We applied the bootstrap method to obtain confidence limits for the optimal fit parameters in the regression analysis. To that end, 1,000 data sets were generated by random selection of data points from the original data, which yielded 1,000 different fit parameters. The standard deviation (SD) of these fit parameters was taken as an estimate for the confidence levels of the parameter values obtained in the original data set (Press et al., 1992).

To determine whether the variability of azimuth or elevation endpoint data for the different stimulus durations were significantly different, we applied the Kolmogorov-Smirnov test on the response error.

The effect of stimulus duration on the regression parameters ΔH_s and ΔE_H was determined with a one-way ANOVA with duration as factor.

Determining VOR gain

We fitted the chair-velocity and the horizontal eye-velocity signals over 40 cycles of each run by a sinusoid with a frequency of 1/6 Hz, with amplitude and phase as free parameters. The vestibulo-ocular reflex (VOR) gain was then determined as the amplitude of the eye velocity divided by the amplitude of the chair velocity. The VOR gains presented in Table 2.2 are averaged over all runs (about 23 runs per subject).

Table 2.2   Average VOR gain and standard deviation of individual subjects.

Subject	VOR gain
AK	0.65 ± 0.10
DA	0.56 ± 0.13
DB	0.65 ± 0.05
JO	0.53 ± 0.11
TG	0.71 ± 0.07
MK	0.76 ± 0.07

RESULTS

Head and eye movements during the saccade reaction-time

The design of the dynamic experiments was to ensure a considerable and variable amount of head and eye displacements during the reaction time of the subjects, who were instructed to make rapid eye movements towards brief visual flashes across the visual field. The upper panels of Figure 2.2 show the latency distributions pooled over all subjects and all stimulus durations for the three localization conditions (static: 223 ± 52.2 ms, head-fixed condition: 229 ± 65.5 ms, world-fixed condition: 242 ± 80.5 ms). There was a considerable amount of
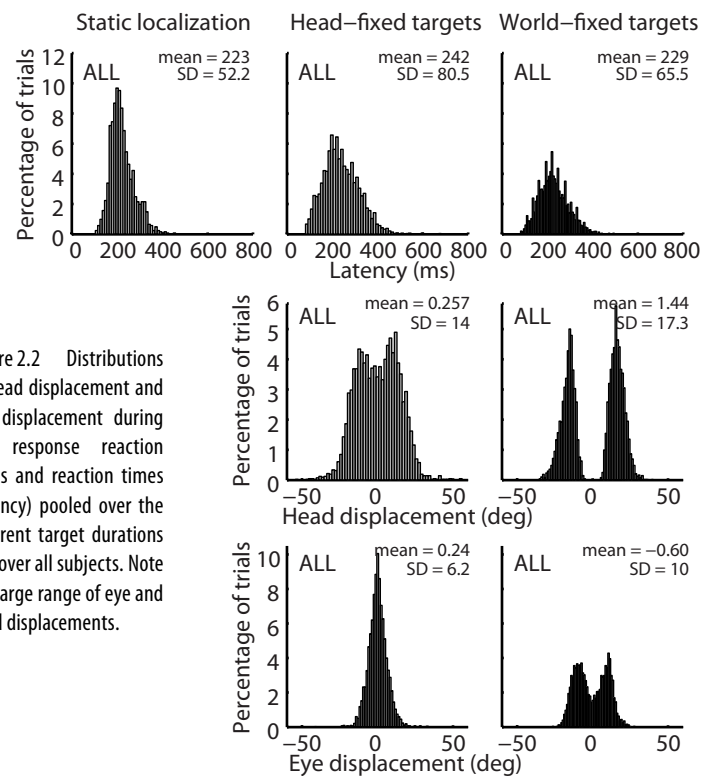
Figure 2.2 Distributions of head displacement and eye displacement during the response reaction times and reaction times (latency) pooled over the different target durations and over all subjects. Note the large range of eye and head displacements.

passive head displacement during the reaction time (Fig. 2.2, center panels): the mean is around zero, but with a large standard deviation (SD). In the experiments with world-fixed targets, the head displacement distributions were bimodal, since the world-fixed targets were always presented around maximal chair velocity and thus large head displacements dominated the distribution (see Methods). We verified that the near absence of small head displacements in the world-fixed experiments did not introduce a bias in the results, by also analyzing only large head displacement trials for the head-fixed target experiments (not shown). The eye-displacement distributions in the lower panels (Fig. 2.2) show that the eyes were not stationary during the reaction time either. Although subjects were instructed to redirect their gaze towards the perceived straight ahead after the goal-directed response and to keep their eyes there, they were unable to do so because of the ever-present vestibular nystagmus, and of a potential bias in their own percept of straight-ahead. For the analysis of the responses, however, this variability in initial eye positions was immaterial, as we always calculated actual stimulus locations on the retina on the basis of real eye-in-head positions, rather than on the intended positions.

Static localization

To assess baseline visual localization performance for the brief flashes, subjects made saccadic eye movements without vestibular stimulation. The upper two rows of Figure 2.3 shows the results for subject MK to 0.5 ms, 4 ms and 100 ms visual flashes. The subject was able to
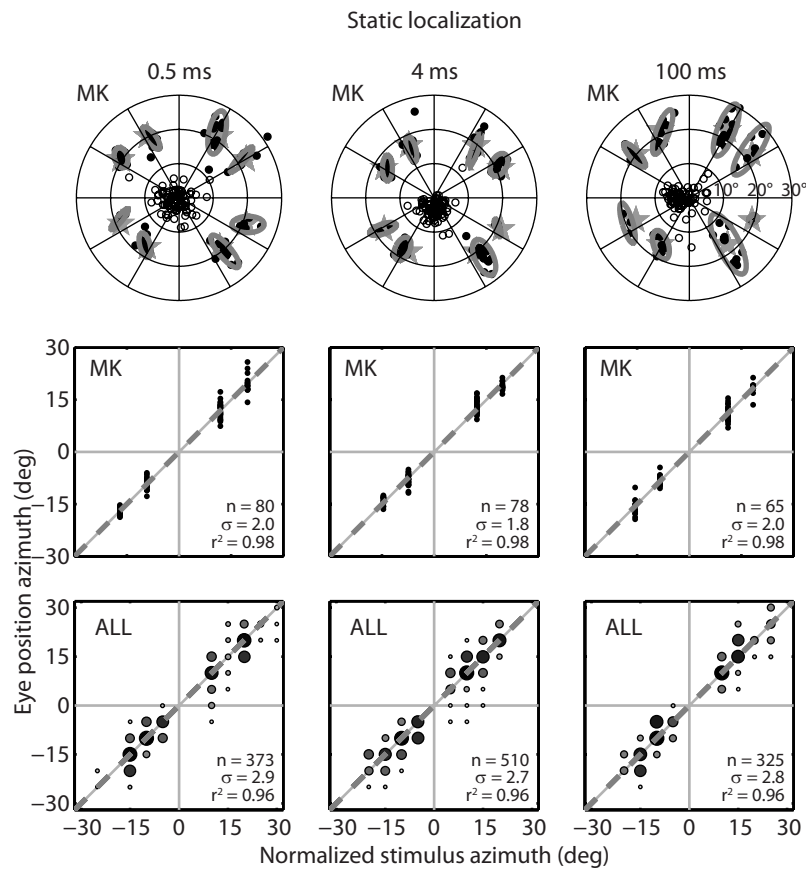
Figure 2.3   Standard localization behavior of subject MK to 0.5 ms (left), 4 ms (middle) and 100 ms (right) visual targets. The upper row is a 2D response representation. The eye position at the beginning of the first goal-directed saccade (, open circles) and the end points of the first goal-directed saccades (closed circles) are presented in head-coordinates. Gray ellipses denote the 2 x SD of the end points. Normalized targets locations (see Methods) are presented by gray stars. The center row shows the normalized linear regression results (Eqns 2.3a,b) on azimuth response components of the same data as in the upper row. The bottom row shows normalized linear regression results on azimuth responses pooled over all subjects. Data points were binned for graphical purposes (5°-wide bins); symbol size and grayscale correspond to the likelihood of the responses.

localize the visual flashes quite accurately ($r^2 = 0.98$, $\sigma \approx 2°$), and response variability did not depend on stimulus duration (Kolmogorov-Smirnov (KS) test: $P > 0.05$). The bottom row of Figure 2.3 shows that all subjects accurately localized the visual targets ($r^2 = 0.96$, $\sigma < 2.9°$) in the static condition. Note that in these figures target locations were normalized per subject (Eqns 2.3a and 2.3b). These results indicate that all visual flashes, including 0.5 ms, were well visible and localizable.

Visual information on the retina
For correct spatial updating, the visuomotor system should know whether the stimulus was stationary in space, or moving with the head. This motion can in principle be deduced from the visual motion streak on the retina when appropriately compared to the eye, head, and

A Head–fixed targets   World–fixed targets

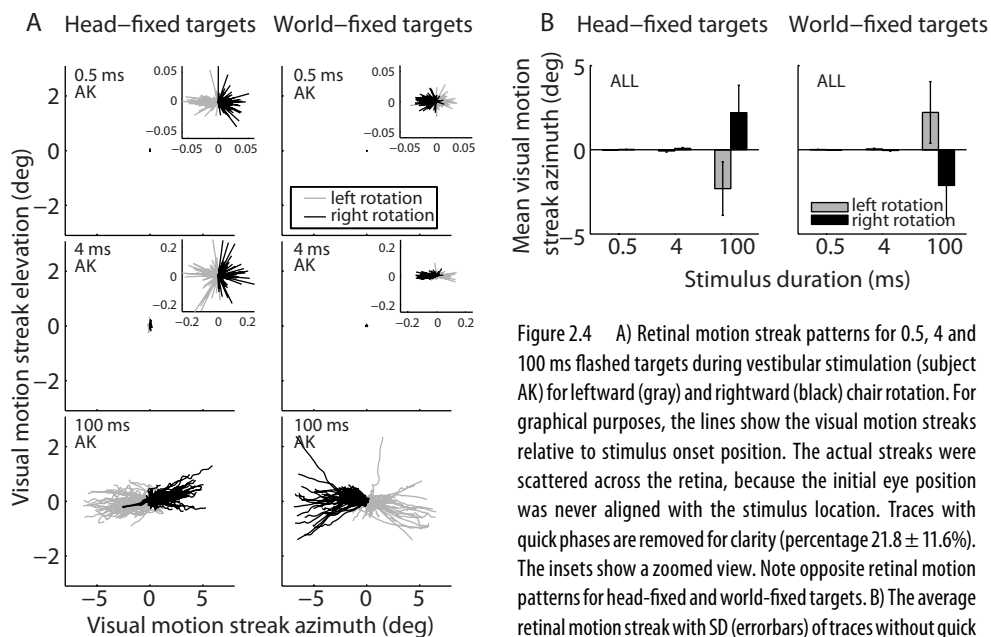B Head–fixed targets   World–fixed targets

Figure 2.4   A) Retinal motion streak patterns for 0.5, 4 and 100 ms flashed targets during vestibular stimulation (subject AK) for leftward (gray) and rightward (black) chair rotation. For graphical purposes, the lines show the visual motion streaks relative to stimulus onset position. The actual streaks were scattered across the retina, because the initial eye position was never aligned with the stimulus location. Traces with quick phases are removed for clarity (percentage $21.8 \pm 11.6\%$). The insets show a zoomed view. Note opposite retinal motion patterns for head-fixed and world-fixed targets. B) The average retinal motion streak with SD (errorbars) of traces without quick phases of all subjects pooled.

body movements during stimulus presentation. Presumably, the patterns of visual motion streaks on the retina would differ for world-fixed and for head-fixed targets. This can indeed be readily verified for the 100 ms target flashes in Figure 2.4A (lower panels), which shows the reconstructed visual movement excursions on the retina during the vestibular slow phases of subject AK, which, for graphical purposes, were all aligned with the center of the plot (the actual streaks were scattered across the retina, as the initial eye position was never aligned with the stimulus location). Note that if the vestibular-ocular reflex (VOR) would be perfect (gain = 1.0), there would be no motion on the retina when the target is stationary in space, as the eye-in-space would be stationary too. A head-fixed target would then yield maximum motion on the retina in the direction of head motion. However, because the gain of the VOR did not reach the optimal value (see Table 2.2), motion of the world-fixed targets resulted to be opposite to the direction of head motion, while retinal motion was in the same direction, but at lower speed, as the head for head-fixed targets. In Figure 2.4A this is visible for the rightward (black) and leftward (gray) directions of the passive head-in-space movements. For the short-duration stimuli, however, the visual motion streak resulted to be very small (for 0.5 ms: $0.00 \pm 0.01°$, maximum $0.19°$; for 4 ms: $0.01 \pm 0.08°$: maximum $0.77°$). Figure 2.4A (center and top rows) shows the visual streaks on the same scale as the 100 ms flashes, as well as on expanded scales (which show essentially the same patterns as for the 100 ms stimuli). Given the extremely small retinal excursions for the briefest stimuli, it is highly unlikely that these cues could have been used to discriminate target motion relative to the head from target movement relative to space. Figure 2.4B shows the average retinal motion streaks pooled over all subjects. The data show a consistent trend for all subjects: only the 100 ms stimuli could have provided a reliable dissociation of head-fixed and world-fixed targets
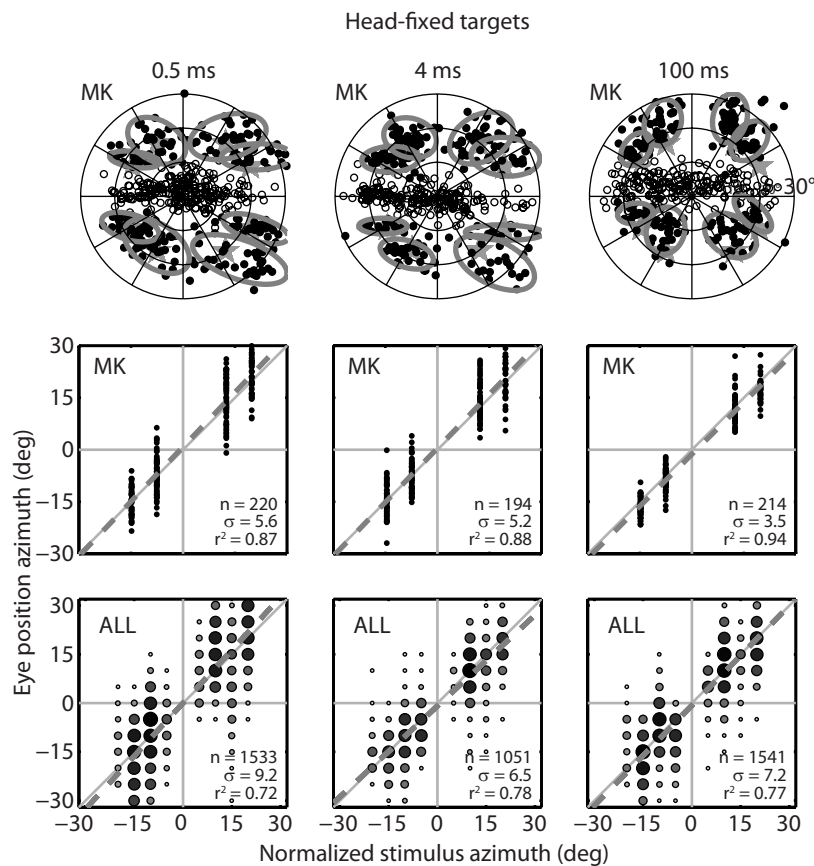
Head-fixed targets

Figure 2.5   Dynamic localization behavior of subject MK (upper rows) and all subjects pooled (lower row) to 0.5 ms (left), 4 ms (center) and 100 ms (right) head-fixed visual targets, presented in head-fixed coordinates. Same conventions as in Fig. 2.3.

during vestibular stimulation.

Dynamic localization of head-fixed targets

The upper two rows of Figure 2.5 show subject MK's localization performance for head-fixed targets during vestibular stimulation, with responses represented in a head-fixed reference frame. Accurate localization would mean that the visuomotor system would note that targets were indeed rotating along with the head; responses should scatter near the normalized target locations (gray stars; upper panels), and lie around the identity line of the stimulus-response plots (center panels). On average, localization responses (closed circles) were close to the target (slope close to one, and bias close to zero). The horizontal scatter (σ), however, was larger than in the static condition (Fig. 2.3) (KS test: $P < 0.05$ in 5 subjects), and it decreased systematically with stimulus duration, as scatter was smallest for the 100 ms stimuli (KS test: scatter 0.5 ms > scatter 4 ms, $P < 0.05$ in 5/6 subjects; scatter 4 ms > scatter 100 ms, $P < 0.05$ in 5/6 subjects). The bottom row of Figure 2.5 shows a similar trend when localization responses are pooled over all subjects. Also the scatter in response elevation was larger than for the
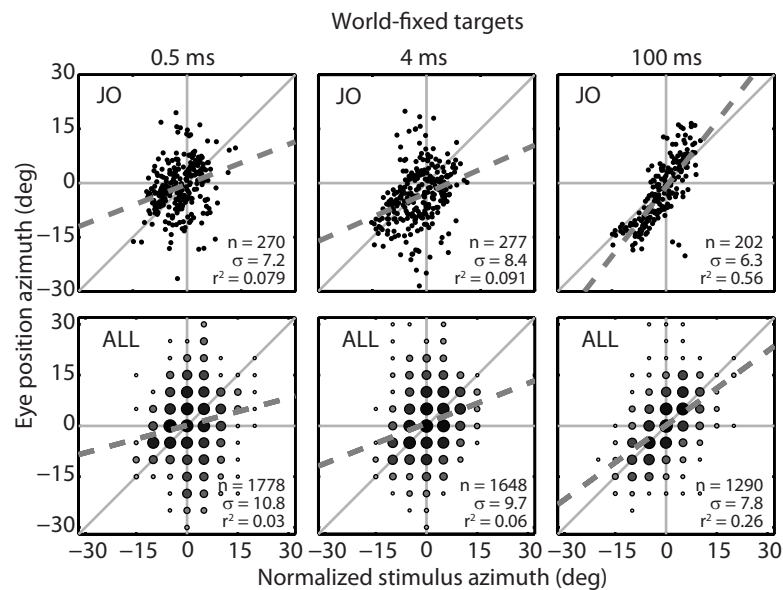
Figure 2.6   Dynamic localization of subject JO (upper row) and all subjects pooled (lower row) to 0.5 (left), 4 (center) and 100 ms (right) world-fixed visual targets, presented in world-fixed coordinates. Same conventions as Fig. 2.3.

static condition (KS test: $P < 0.05$ in 5/6 subjects; not shown). Note also the large variability in initial eye positions (open circles) due to the vestibular nystagmus.

Dynamic localization of world-fixed targets

The upper row of Figure 2.6 shows the dynamic localization behavior of subject JO to world-fixed targets; responses are represented in world coordinates. If the visuomotor system would detect that targets were indeed stationary in space, responses should scatter around the unity line in the stimulus-response plot. For the shortest stimuli of 0.5 and 4 ms this was clearly not the case. Responses showed a large variability (exceeding variability of the stationary condition: KS test $P < 0.01$ in all subjects), and a low correlation between normalized stimulus azimuth and response. For the 100 ms stimuli, response variability was much lower (KS test: scatter 4 ms > scatter 100 ms, $P < 0.05$ in 5/6 subjects), and the stimulus-response correlation was higher than for the short stimuli. Thus, for the long-duration stimuli, spatial updating may have occurred (see below, for a more detailed analysis). The same pattern is observed in the localization data pooled across subjects (Fig. 2.6, bottom row). The response variability in elevation was slightly larger than for static localization for the 4 and 100 ms targets (KS test: $P < 0.01$ in 5/6 subjects), but not for the 0.5 ms flashes (KS test: $P > 0.05$ in 4/6 subjects; data not shown).

Testing spatial updating models

To determine which of the different updating models (Introduction, Fig. 2.1A, and Methods) would best describe the dynamic responses, we first applied the ideal regression coefficients of Table 2.1 to the pooled intervening head- and eye-movement data shown in the distributions of
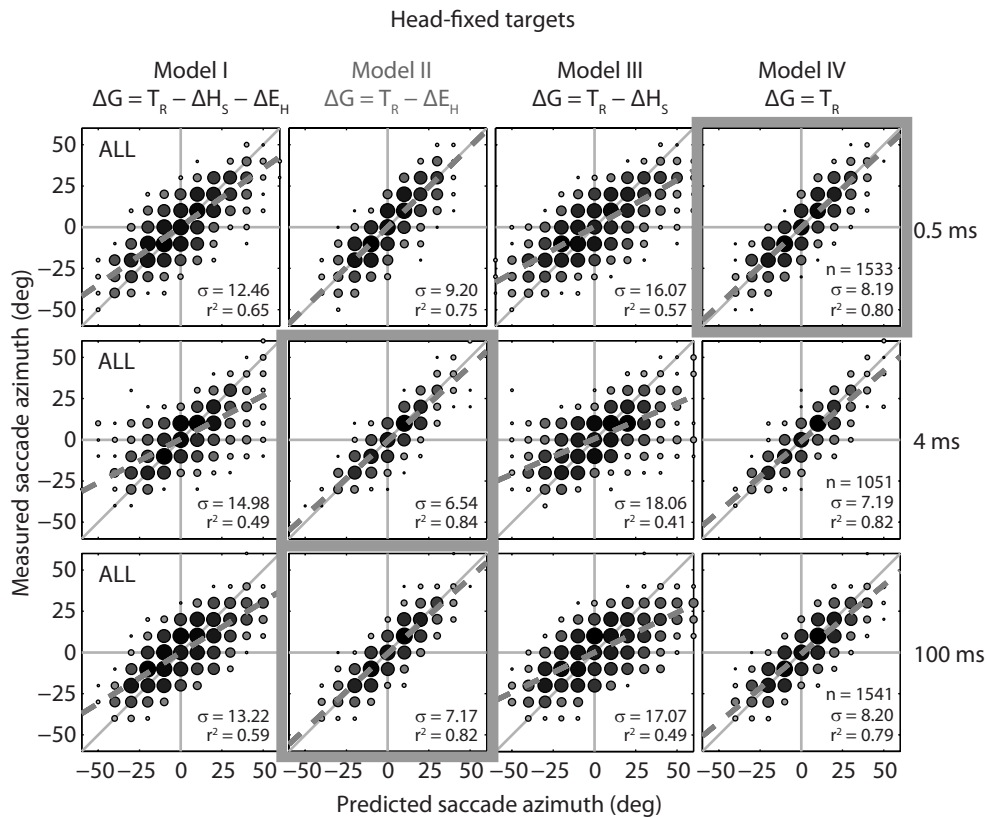
Figure 2.7   Measured saccade amplitude in azimuth for the four models described in Methods (columns) plotted against predicted saccade azimuth of head-fixed targets; data pooled for all subjects. Rows correspond to different stimulus durations. Data points were binned for graphical purposes (10°-wide bins); symbol size and grayscale correspond to log-likelihood of the responses. Dashed gray line shows linear regression results on the individual responses. Coefficients of determination (r^2) and standard deviation of the errors to the corresponding model (σ) are given in the lower-right corners of each subplot. If the model would predict the subject's responses perfectly, responses would fall on the unity line, and $r^2 = 1$. The gray-boxed panels have the highest coefficient of determination between predicted and response saccade azimuth. Model II, presented in gray font, is the appropriate model.

Figure 2.2 to predict the associated saccadic eye displacements. Figure 2.7 plots the measured vs. the predicted horizontal saccade components for the four spatial updating models in the head-fixed stimulus condition. The model that best describes the data should yield the highest coefficient of determination (r^2) and the smallest residual variance (σ^2). For the 4 and 100 ms stimuli, the results indicate best performance for the head-centered model (II), which suggests that the goal-directed saccade incorporated the intervening eye displacement, and at the same time ignored the intervening head displacement. This was the appropriate response, since the targets were indeed head-fixed. However, the retinocentric model (IV) best predicted the responses to the 0.5 ms stimuli, which indicates that the saccades incorporated neither the intervening passive head movements, nor the vestibular-induced eye displacements for these very short flashes.

World-fixed targets

Model I	Model II	Model III	Model IV
$\Delta G = T_R - \Delta H_S - \Delta E_H$	$\Delta G = T_R - \Delta E_H$	$\Delta G = T_R - \Delta H_S$	$\Delta G = T_R$

Measured saccade azimuth (deg)

0.5 ms
- Model I: ALL, $\sigma = 10.80$, $r^2 = 0.73$
- Model II: $\sigma = 11.14$, $r^2 = 0.37$
- Model III: $\sigma = 18.38$, $r^2 = 0.63$
- Model IV: $n = 1778$, $\sigma = 5.81$, $r^2 = 0.82$

4 ms
- Model I: ALL, $\sigma = 9.66$, $r^2 = 0.76$
- Model II: $\sigma = 11.61$, $r^2 = 0.30$
- Model III: $\sigma = 17.24$, $r^2 = 0.67$
- Model IV: $n = 1648$, $\sigma = 6.51$, $r^2 = 0.76$

100 ms
- Model I: ALL, $\sigma = 7.77$, $r^2 = 0.81$
- Model II: $\sigma = 14.34$, $r^2 = 0.27$
- Model III: $\sigma = 15.21$, $r^2 = 0.69$
- Model IV: $n = 1290$, $\sigma = 8.37$, $r^2 = 0.73$
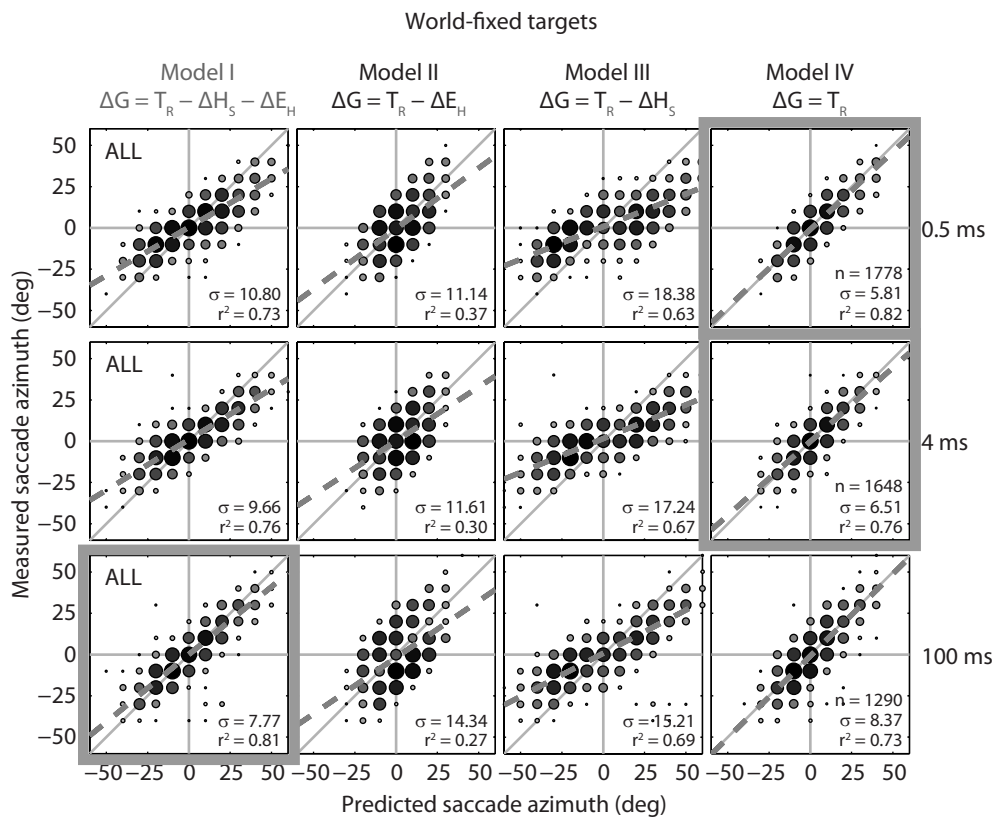
Predicted saccade azimuth (deg)

Figure 2.8   Measured saccade amplitude in azimuth for the four models described in Methods plotted against the predicted saccade azimuth of world-fixed targets; data pooled for all subjects. Same conventions as Fig. 2.7. Model I, presented in gray font, is the appropriate model.

To test for the significance of the seemingly small differences, we performed KS tests on the cumulative error distributions between measured vs. predicted saccades. Models II (appropriate updating into head-centered coordinates) and IV (no spatial updating) by far outperformed the other two models (highest correlations and smallest variances; KS-test: P $\ll 10^{-4}$). Also the differences between models II and IV were significant for the three stimulus durations: for the 0.5 ms flashes model IV outperformed model II (KS-test: P < 0.001), whereas for the 4 and 100 ms flashes, model II was significantly better than model IV (KS-test: for 4 ms: P < 0.001, and for 100 ms: P $\ll 10^{-4}$).

Figure 2.8 shows the results for the world-fixed stimulus condition in the same format as Figure 2.7. In this case the world-centered model (I) now best describes the data for the 100 ms stimuli, which is the appropriate localization response. In contrast, the retinocentric scheme (model IV) best predicts the results for the 0.5 and 4 ms flashes, indicating no (or very little) updating for the intervening eye and head movements, despite the considerable variation in these variables (see Fig. 2.2).

We compared the predictions of model I (updating in world-centered coordinates) vs. model IV (no spatial updating; retinocentric), as these two models both outperformed by far
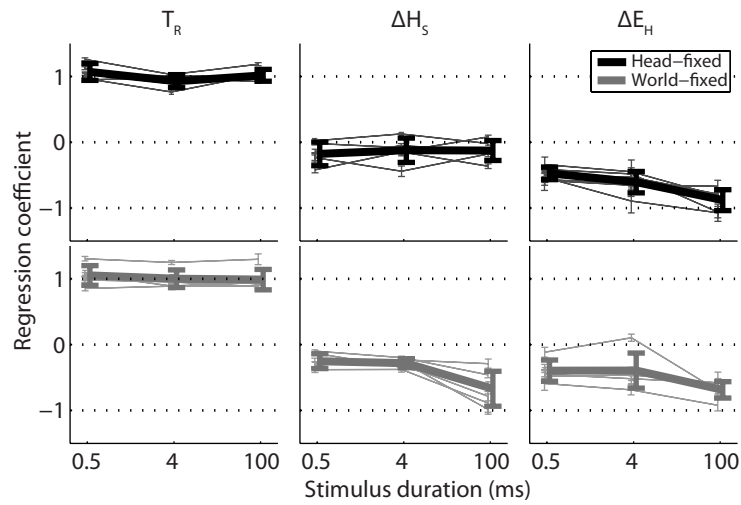
Figure 2.9   Multiple linear regression results (Eqn 2.6) on the subject's responses to 0.5, 4 and 100 ms visual targets during passive whole-body rotation averaged across subjects for head-fixed (black) and world-fixed targets (gray). Data points represent the regression coefficients of Eqn 2.6 for individual subjects (thin lines) and their average (bold lines). Left column: retinal target coefficient (T_R); center column: head-displacement coefficient (ΔH_S); right column: eye-in-head position coefficient (ΔE_H). Error bars represent one standard deviation. The horizontal dotted lines at +1, 0 and -1 correspond to ideal regression values. For head-centered targets: [a,b,c]=[1,0,-1]; for world-centered targets: [1,-1,-1] (Table 2.1). These ideal values are only approached for the 100 ms targets.

the other two models. For the 0.5 and 4 ms flashes, model IV was significantly better than model I (KS-test: for 0.5 ms: $P \ll 10^{-4}$, and for 4 ms: $P \ll 10^{-4}$), whereas for the 100 ms targets, model I significantly outperformed model IV (KS-test: 100 ms: $P < 0.001$).

Taken together, the results indicate that only the long-duration visual stimuli, which may have provided a consistent dissociation of the retinal streak patterns for head-fixed vs. world-fixed targets (Fig. 2.4), incurred appropriate spatial updating of targets into the head-centered or world-centered reference frame. In contrast, spatial updating was severely hampered, or even absent, when retinal motion was highly likely to be too small to be detected by the visual system. As Figures 2.7 and 2.8 provide a preliminary analysis of the results, based on idealized versions of the different updating models, we next provide a quantitative regression analysis of the responses.

Multiple linear regression
To quantify the actual amount of compensation of intervening eye-in-head and passive head-in-space displacements within the saccade reaction time, we performed a multiple linear regression analysis on the subject's responses (Eqn 2.6) for the six dynamic stimulation conditions. Figure 2.9 shows the resulting gains of the individual subjects (thin lines) together with the averaged results pooled across subjects (bold) for the three stimulus durations and the two spatial target conditions (black: head-fixed targets; gray: world-fixed targets). The results show that for all target flashes, and for all subjects, the gain of the retinocentric target location (a) was close to the ideal value of $a = +1.0$ (left column, T_R), indicating that all stimuli were well visible, also in the dynamic paradigm. For the 100 ms target durations (right-most

values in each subplot) the gains for ΔH_S (center column) and ΔE_H (right-hand column) approximated their ideal values, which would be $(b, c) = (0, -1)$, for the head-fixed targets (black), and $(b, c) = (-1, -1)$ for the world-fixed stimuli (gray). Note, however, that the ΔH_S gain did not reach the ideal value of -1.0, indicating an underestimation of the actual amount of head rotation. For the shortest stimuli of 0.5 ms (left-most data points in each subplot) the ΔH_S gain was even close to zero for both the head-fixed and world-fixed stimulus conditions. The data show that the ΔH_S gain for world-fixed stimuli depended significantly on stimulus duration (ANOVA: $F_{(2,15)} = 11.19$ P = 0.001). For the head-fixed stimuli this was not the case (ANOVA: $F_{(2,15)} = 0.16$ P = 0.86), and values did not differ significantly from 0 (t-test: P > 0.05). For 0.5 ms targets the head-displacement gain did not differ between head-fixed and world-fixed targets (Wilcoxon rank sum test: P = 0.39). For 4 and 100 ms targets the world-fixed condition induced a stronger updating response, than the head-fixed condition, as the head-displacement gain was significantly larger for world-fixed flashes (Wilcoxon rank sum test: 4 ms P = 0.04, 100 ms P = 0.004). Also the eye-movement (ΔE_H) gain for the shortest stimuli was strongly reduced to about -0.4, or less, for head- and world-fixed stimuli. The result for the 4 ms stimuli was typically close to that of 0.5 ms flashes, although inter-subject variability was more pronounced for the intermediate stimulus duration. For both conditions, the ΔE_H gain depended significantly on stimulus duration (ANOVA: $F_{(2,15)} = 11.96$ P = 0.001 (head-fixed targets); $F_{(2,15)} = 4.55$ P = 0.03 (world-fixed targets). The eye-displacement gain did not differ significantly between head-fixed and world-fixed targets (Wilcoxon rank sum test: P = 0.09 for each stimulus duration).

When using the regression coefficients (Eqn 2.6, Fig. 2.9) to predict the saccade amplitude in azimuth, we compared the MLR model to each of the four ideal models described in Methods and Table 2.1 (Figs. 2.7 and 2.8). The regression model describes the data with the highest correlation for all conditions (mean $r^2 \pm$ SD: 0.86 ± 0.07).

To summarize, appropriate spatial updating occurred for the long-duration stimuli (100 ms) only, as responses were directed toward the head-centered or world-centered location of the target, as required for accurate localization. Responses to the shortest targets, however, remained close to the initial retinocentric target coordinates, regardless the target's reference frame, or the intervening movements.

DISCUSSION

Summary
We investigated visual-vestibular integration in spatial updating of saccades. Our results show that updating relied on the integrity of visual information about the direction of target motion across the retina, as the only factor influencing spatial updating was visual flash duration. Long-duration flashes provided sufficient visual motion information (Fig. 2.4), for which the visuomotor system correctly incorporated passive intervening eye-head movements for world-fixed targets, and ignored head-movements for head-fixed targets. For very short flashes, however, the visual system could not reliably infer retinal stimulus motion, and thus could not dissociate whether stimuli moved with the head, or were stationary in space. In

those cases the system tended to ignore intervening eye-head displacements altogether, and kept targets in eye-centered coordinates. We believe that this is a remarkable result, as in real life it is highly unlikely that visual stimuli are fixed to the retina.

Related studies

Vliegen et al. (2005) used dynamic visual double-steps by presenting a visual target flash (50 ms) during actively programmed eye-head gaze shifts, and showed that gaze shifts went towards the world-centered goal. These data are in line with our current findings for long-duration (100 ms) visual stimuli. Our current paradigm denied the gaze-control system access to corollary discharges of head movements and neck-muscle proprioception, by imposing head and eye movements through passive whole-body rotation. In line with earlier microstimulation studies in monkey midbrain superior colliculus (Mays and Sparks, 1980; Sparks and Mays, 1983), active programming of an intervening saccade is not required for accurate spatial updating. Presumably, the visuomotor system interprets the colliculus-induced signal as an internally programmed corollary discharge signal. This is supported by recent evidence that indicates a colliculus to frontal-eye-field pathway carrying an eye-displacement signal that could be used for spatial updating (Sommer and Wurtz, 2002). In contrast, microstimulation in the parapontine reticular formation evokes an intervening eye movement that is not compensated (Sparks et al., 1987), suggesting that the corollary discharge signal arises upstream from the pons.

Our data further indicate that the visuomotor system needs adequate information about retinal stimulus motion. Retinal motion information during the high-velocity (>400°/s) gaze shifts in the Vliegen et al. (2005) study was probably sufficient for the visuomotor system to conclude that targets were stationary in space, as retinal streaks extended up to 30°. However, we cannot exclude the possibility that extremely brief flashes, like in our experiments, cannot be accurately localized after active gaze shifts either.

Visual localization performance during vestibular rotation was first studied by Van Beuzekom and Van Gisbergen (2002), who specifically instructed subjects to look at the head-centered location of 4 ms head-fixed flashes. Their results suggested compensation for the induced ocular nystagmus, but with increased horizontal endpoint scatter. However, since the data were not analyzed in terms of different updating models, it remained unclear to what extent subjects executed the task requirement, or whether a different instruction ("localize in world coordinates") would have mattered. Our results show that instruction was probably immaterial, as subjects did not perceive a difference between head-centered vs. world-centered targets for these brief stimuli, and they responded in the appropriate reference frame for longer stimuli without specific instructions.

The whole-body movements in our paradigm had comparable dynamics as the intervening gaze shifts in smooth pursuit studies. Those experiments demonstrated that extraretinal information about the pursuit gaze-motor command is available to the saccadic system (Schlag et al., 1990; Herter and Guitton, 1998), as long-latency saccades (> 200 ms) were directed to the world-centered location (Blohm et al., 2003; 2005; Daye et al., 2010). However, short-latency saccades (< 175 ms) landed near the eye-centered location, and thus lacked spatial updating (McKenzie and Lisberger, 1986; Blohm et al., 2003; 2005; Daye et al.,

2010), like for our briefest flash durations. In our experiments, however, we did not observe a latency-dependent effect (data not shown), as spatial updating varied exclusively with flash duration. Saccade reaction time was not a factor for spatial updating in the double-step saccade paradigm either (Goossens and Van Opstal, 1999; Vliegen et al., 2005). Note that the brief visual flashes in our experiment did not induce smooth-pursuit eye movements, as the brief target flashes appeared at unpredictable locations and never fell on the fovea. Besides, we did not use a visual fixation light to cancel the VOR.

Underestimation of head rotation

While visual target localization during active saccadic eye-head gaze shifts is typically accurate (Vliegen et al., 2005), passive head displacements appear to be slightly underestimated (this study: Fig. 2.9; Blouin et al., 1995a;b; 1997; 1998; Israel et al., 1999; Li et al., 2005; Klier et al., 2006). During active head movements, the brain has access to various sources of information about self-movement: vestibular, neck-muscle proprioception, corollary discharges, efference copies, and retinal motion signals. During passive whole-body rotation, however, only vestibular and, in our paradigm, retinal motion signals are present. Possibly, the underestimation of head displacement could be related to an incomplete VOR gain (see Table 2.2), in combination with the absence of supporting evidence from proprioceptive and efferent signals.

Proprioception is indeed used in target updating (Blouin et al., 1998). For example, neck-muscle vibration causes illusory motion of foveated targets (Biguer et al., 1988), and vibration of monkey dorsal neck-muscles shifts memory-guided saccade endpoints upwards (Corneil and Andersen, 2004).

The vestibular labyrinths are also involved in spatial updating: their surgical ablation severely compromises accurate updating of monkeys during yaw rotations (Wei et al., 2006). However, these deficits recover over time, suggesting that other signals (e.g. tactile, or body-proprioceptive cues) may take over the function of the vestibular apparatus.

We believe that perceptual learning (e.g. Israel et al., 1999) could not have played a role in our experiments, as subjects made automatic, short-latency saccade responses under open-loop conditions, and they were not instructed to respond in a particular reference frame. Moreover, their awareness of actual eye-in-head orientation was relatively poor, considering the substantial scatter in initial eye positions, despite the explicit instruction to look at straight ahead after the response.

No updating of extremely brief stimuli

The only way to dissociate the head-centered and spatial reference frames in our experiment was to deduce stimulus motion from the retinal target movement, appropriately combined with intervening eye- and head-movements. It is quite remarkable that the system could distinguish head-fixed vs. world-fixed targets. As the VOR attempts to stabilize the retinal image, stimuli should on average be stationary on the retina when stable in space (the typical visual world condition), and move at head velocity when head-fixed (a rather unlikely situation in the real world). For long-duration flashes, retinal motion patterns were indeed different for the two conditions, but did not conform to the typical real-world situation with an optimal VOR: head-fixed targets moved along with the head at a lower speed, whereas world-fixed targets

moved in the opposite direction (Fig. 2.4). Rather than assuming that the stimulus was also moving through space, the system generated the appropriate oculomotor responses, despite the unlikely stimulus in the head-fixed condition, and the non-ideal VOR (Table 2.2).

That short-duration stimuli were not updated cannot be explained by poor stimulus visibility, because localization accuracy and precision in the stationary condition did not depend on stimulus duration (Fig. 2.3). Furthermore, the retinal target coefficient during vestibular stimulation was close to ideal for all flash durations (Fig. 2.9). Perceptually, these extreme brief flashes seemed indistinguishable from the 4 ms flashes. This may be explained by the fact that neural activity in the central visual system to brief visual probes is prolonged to several tens of ms (Duysens et al., 1985). Since the retinal motion streak at the visual periphery for these short flashes (Fig. 2.4) was far below the retinal spatial resolution, the system could not deduce stimulus motion with respect to the eye to update targets in the appropriate reference frame. In line with this, Festinger and Holtzman (1978) showed that poorly-defined visual smear hampers perceptual estimates of stimulus motion. Our data show that under those conditions the visuomotor system tends to keep targets in eye-centered coordinates, which have been suggested to be the coordinates also used by visual memory (Baker et al., 2003). This default strategy is surprising for several reasons. First, the integrity of the extraretinal signals was the same for all stimulus conditions, so that the visuomotor system did have adequate information about intervening self-movements of eyes and head. Second, it is highly unlikely in daily life that visual stimuli move along with the eyes or head. Thus, one would rather expect a default strategy to localize targets in world-centered coordinates, since all signals required for this transformation (Eqn 2.6) were available. The only difference between the six conditions, not captured by the different spatial-updating models, is the amount and direction of retinal motion during stimulus presentation. This strongly suggests that during passive vestibular stimulation the integrity of this signal is required to induce spatial updating. Whether this conclusion also holds for actively generated gaze shifts remains to be studied.

ACKNOWLEDGEMENTS

Adapted from: Van Barneveld, D.C.P.B.M., Binkhorst, F. and Van Opstal, A.J. (2011) Absence of compensation for vestibular-evoked passive head rotations in human sound localization. Eur J Neurosci, 34, 1149–1160

3

Absence of compensation for vestibular-evoked passive head rotations in human sound localization

Denise C.P.B.M. Van Barneveld
Floor Binkhorst
A. John Van Opstal

INTRODUCTION

Acoustic cues, generated by the interaction of sound waves with the head and pinnae, specify sound locations with respect to the head. Interaural timing (ITD) and level differences (ILD) refer to horizontal plane locations (azimuth), whereas spectral pinna cues define vertical directions (elevation) (Wightman and Kistler, 1989; Middlebrooks, 1992; Blauert, 1997). Thus, programming a goal-directed eye movement toward a sound should incorporate the initial eye-in-head orientation ('spatial updating') (Poppel, 1973; Jay and Sparks, 1984; 1987; Van Grootel and Van Opstal, 2010). Indeed, changes in eye and/or head posture influence spatial hearing (Lewald, 1997; Goossens and Van Opstal, 1999; Kopinska and Harris, 2003; Königs et al., 2007; Van Barneveld and Van Opstal, 2010), and open-loop gaze-orienting studies have shown that the auditory system accurately incorporates intervening eye-head movements made after, or during, sound presentation (Goossens and Van Opstal, 1999; Vliegen et al., 2004; Van Grootel and Van Opstal, 2010).

How does the auditory system dissociate target motion from self-motion? Under natural conditions, neck-muscle proprioception, corollary discharges of planned movements, and vestibular signals could all contribute to these transformations (e.g. Angelaki and Cullen, 2008; Armstrong et al., 2008; Crapse and Sommer, 2008, for reviews). Such signals could in principle determine to what extent changes in acoustic cues correlate with (estimated) motion of the head. Because target and head movements would typically be uncorrelated, the default assumption could be that sounds originate from a world-centered reference frame. Indeed, free-field eye-localization of tones (Goossens and Van Opstal, 1999), and eye-head orienting studies to brief noise bursts have supported this idea (Goossens and Van Opstal, 1999; Vliegen et al., 2004).

The present study concerns saccade responses towards brief noise bursts (3, 10 and 100 ms) under passive whole-body rotation to investigate the vestibular contribution to audio-spatial updating when corollary discharges and proprioceptive signals of head movements are absent. We analyzed saccades (ΔE) by applying models that differ in the amount of compensation for intervening passive head displacement (ΔH_S), and eye-in-head position (E_H) at saccade onset (Fig. 3.1A):

$$\Delta E = T_H + b \cdot \Delta H_S + c \cdot E_H \tag{3.1}$$

with T_H the head-centered location at sound onset. Localization in world coordinates requires full compensation for intervening movements ($b = c = -1$, Model I). When targets remain in head-centered coordinates only the eye-in-head position is accounted for ($b = 0$; $c = -1$, Model II), while Model IV lacks any spatial updating ($b = c = 0$).

Although sounds rotated along with the listener, we show that the amount of head displacement during the briefest sounds (< 1°) remained well below the minimal audible movement angle (MAMA; about 5°); the auditory system could thus not detect any changes in acoustic localization cues. These sounds are therefore perceived stationary in space and, like in Vliegen et al. (2004), expected to be localized in world-centered coordinates. Longer-duration (100 ms) stimuli could induce measurable changes in ITDs/ILDs that would anti-correlate
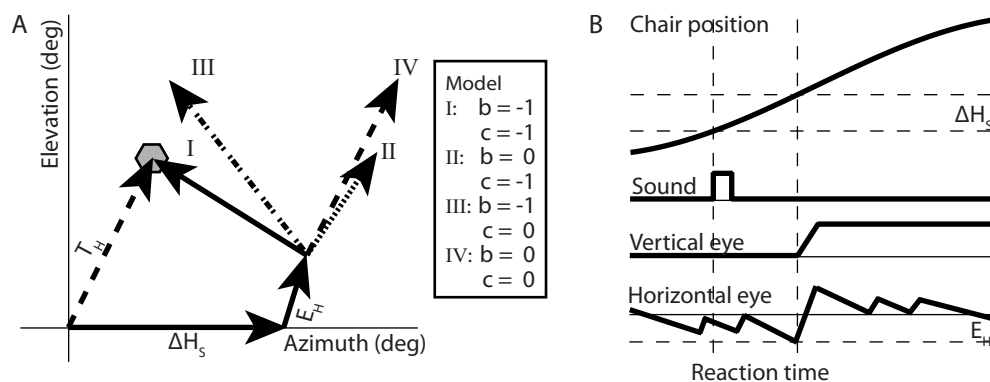
Figure 3.1 A) Four models for a saccadic eye movement toward an auditory target during passive whole-body rotation. At time = 0 a brief auditory target (T_H) is presented while the head is at $[\alpha,\varepsilon] = [0,0]$. During the reaction time the head (and body) is passively rotated (ΔH_S) to the right. At the response onset the eyes are not centered in the orbit (E_H) due to the ongoing vestibular ocular reflex and nystagmus and the absence of visual landmarks. Model I predicts a response in world-centered coordinates and fully incorporates intervening head- and eye displacement signals. Model II predicts a head-centered response, as it incorporates only the change in eye position. Model III only accounts for the head displacement, while model IV keeps the target in the initial head-centered reference frame. Note that model II is the ideal model, since the auditory targets were rotating together with the listeners. The ideal values of b and c of Eqn 3.1 are presented in the table. B) Temporal order of chair position, auditory target and response.

with self-generated head movements, and the auditory system might thus correctly infer that these sounds moved along with the head. Interestingly, our results demonstrate that listeners localized all sounds in head-centered coordinates (model II), suggesting that head movements are not incorporated in sound localization when only vestibular cues are present, and/or the system is unsure about stimulus motion.

METHODS

Listeners
Nine listeners, all with normal hearing, participated in the experiments. Three of the listeners (the authors) were familiar with the purpose of the experiment. All listeners had normal or corrected to normal vision, except for JO, who is amblyopic in his right, recorded eye. Experiments were conducted after obtaining full understanding and written consent from the listener. The experimental procedures were approved by the Local Ethics Committee of the Radboud University Nijmegen, and adhered to The Code of Ethics of the World Medical Association (Declaration of Helsinki), as printed in the British Medical Journal of July 18, 1964.

Apparatus

Vestibular setup
Experiments were conducted in a completely dark room (4.05 x 5.15 x 3.30 m³). The listener sat in a computer-controlled vestibular stimulator, with the head firmly stabilized in an upright

position with a padded adjustable helmet. Chair position was measured using a digital position encoder with an angular resolution of 0.04° (Van Beuzekom and Van Gisbergen, 2002).

Auditory stimuli emanated from two loudspeakers (Visaton, GmbH, SC5.9, Haan, Germany) mounted inside the vestibular chair at 10° above ear level, both left and right at an azimuth angle of 37°. The distance from the ears to the plane of the loudspeakers was 40 cm. Sounds were played at 70 dBA SPL (calibrated with a Brüel and Kjær BK2610 sound amplifier and BK4144 microphone at the position of the subject's head) and were well discernable from the low-frequency sinusoidal background noise produced by the motor (at the zenith) of the vestibular chair.

We measured two-dimensional eye movements with the scleral search-coil technique (Collewijn et al., 1975), using oscillating magnetic fields generated by two sets of orthogonal coils (0.77 x 0.77 m) inside the vestibular stimulator. The horizontal and vertical eye-position signals were amplified, demodulated by tuned lock-in amplifiers (Princeton Applied Research, NJ, USA, model PAR 128A), and subsequently sampled at 500 Hz per channel for storage on the computer's hard disk.

Sound stimuli

Coordinate system
We express the coordinates of auditory target locations as well as the eye-in-head position in a double-polar azimuth-elevation coordinate system, in which the origin coincides with the centre of the head (Knudsen and Konishi, 1979; Hofman and Van Opstal, 1998). In this system the azimuth angle, α, is defined as the angle within a horizontal plane with the vertical midsagittal plane. The elevation angle, ε, is defined as the direction within a vertical plane with the horizontal plane through the listener's ears. The straight-ahead position is defined by $[\alpha, \varepsilon] = [0, 0]°$.

Stationary free-field sounds
Six listeners localized stationary free-field sounds, which were digitally generated with Matlab software and consisted of broadband (0.3-12 kHz) Gaussian white noise of 3, 10 or 100 ms. The 3 and 10 ms sounds had onset and offset ramps of 0.5 ms; the 100 ms sounds had 1 ms ramps. Since all auditory stimuli were produced by two loudspeakers at $[\alpha, \varepsilon] = [\pm 37, 10]°$ with respect to the listener's head, we simulated free-field sound locations by filtering the stereo broadband noise bursts with the listener's own ITD and frequency-dependent ILD information (listeners DB, JO and FB), or with the ITD and ILDs of listener JO (listeners AJ, PB and JT). In this way, simulated sounds originated at $\alpha = [-20, -17.5, ..., 17.5, 20]°$, at elevation $\varepsilon = 10°$. Details on ITD and ILD measurements are provided in Supporting Information.

Moving free-field sounds
We measured the minimum audible movement angle (MAMA) for five of our listeners in the setup, by simulating moving sounds with the two fixed loudspeakers through variation of the amplitude and timing of each sample of the sound according to a linear velocity profile. Sounds thus moved symmetrically through the straight-ahead location ($\alpha = 0°$, where the

spatial resolution of the auditory system is best) at [±25, ±50, ±100, ±150, ±200, ±250, ±400]°/s, for a duration of 3, 10, 50 and 100 ms.

Experimental paradigms

Dynamic localization of free-field head-fixed sounds
Six listeners participated in two different dynamic localization experiments that were performed on different days. The first experiment contained only 100 ms sounds. The second experiment consisted of 3 and 10 ms sounds randomly intermingled. Each experiment consisted of a calibration run, two stationary runs and two dynamic runs.

Calibration
Each experimental session started with a calibration run in which 37 LEDs were presented (direction re. horizontal, Φ = 0 to 360° in 30° steps; eccentricity re. straight ahead, R = 0, 10, 20 and 30° for listeners JO and PB, R = 0, 13.2, 25 and 35° for listeners DB, FB, AJ and JT), which the listeners had to fixate. These data were used for offline calibration of the eye-coil signals to veridical eye-in-head orientations.

Stationary condition
We assessed the listener's baseline sound-localization behavior in two stationary runs, preformed at the beginning and at the end of an experimental session, by presenting simulated free-field sounds in a semi-random order with an inter-stimulus interval of 3.5 seconds (total: 68 stimuli per run, 4 repetitions for each location). The listener had to redirect gaze as fast and as accurately as possible to the perceived location of the sound source, keep gaze there for a moment, and then return to straight ahead. During localization trials we did not present an initial fixation light at straight ahead.

Dynamic condition
In the dynamic condition, listeners underwent sinusoidal rotation around the earth-vertical axis at a frequency of 1/9 Hz, with a peak amplitude of 160° (peak chair velocity 112°/s, except for JO in the 100 ms condition: peak amplitude 90°, peak chair velocity 63°/s). To avoid discontinuities in chair velocity and acceleration at motion onset, the angular chair velocity increased linearly over the first two sinusoidal periods, during which no sound stimuli were presented. After these two periods, 68 (4 repetitions of 17 sounds) stimuli were presented during 27 sinusoidal periods, at an inter-stimulus interval of 3.5 seconds. Because the chair had a cycle time of 9 seconds, stimuli were presented at 9 different chair positions, and at 18 different chair velocities and chair accelerations. The task of the listener was to make a saccadic eye movement to the perceived location of the sound as fast and as accurately as possible, briefly fixate this position, and then return to the estimated straight-ahead location. In general, listeners were not able to return to straight ahead due to the ongoing vestibulo-ocular reflex and corresponding ocular nystagmus, and to a potential bias in their estimate. Note, however, that this variation in eye-in-head position is important to disentangle the different potential models (Fig. 3.1). We gave no additional instructions regarding the reference

frame (head-centered, world-centered, or otherwise) of the responses. Note that we did not present a fixation light at straight ahead to counteract the VOR. In pilot experiments with the use of an initial fixation light we obtained the same results (data not shown).

Measuring the minimum audible movement angle (MAMA)

Five listeners (two of whom also participated in the dynamic localization experiments) participated in the MAMA experiment, which was designed to test whether listeners could reliably detect the movement direction of 3, 10, 50 and 100 ms sounds, and to estimate the MAMA from the 100 ms data for a stationary listener. To that end, listeners performed four runs of sound-movement discrimination in a two-alternative forced-choice task, in which they were asked to indicate whether the sound moved leftward or rightward. Stimuli were presented at an inter-stimulus interval of two seconds. Each run consisted of 168 stimuli of a single sound duration (12 repetitions of 14 moving sounds), resulting in four psychometric curves representing the probability of a rightward response as function of sound velocity, for each sound duration.

In an additional experiment, four listeners (two of whom also participated in the dynamic localization experiments) indicated the stimulus movement direction of 50 ms sounds during the same sinusoidal whole-body rotation as in the dynamic localization experiments. Stimuli were presented at peak chair velocity (i.e. at chair amplitude 0°), both in leftward and rightward chair rotation directions. For each of these two chair positions we presented 12 repetitions of 14 moving sound stimuli, resulting in two psychometric curves.

Psychometric curve fitting

The psychometric data of the MAMA experiment were modeled by a cumulative Gaussian by using the method of maximum likelihood (Wichmann and Hill, 2001a). The psychometric curve, $\psi(x)$ (x is stimulus velocity), is thus given by:

$$\Psi(x) = \lambda + (1 - 2\lambda) \cdot erf(x; \mu, \sigma) \tag{3.2},$$

in which $erf(x; \mu, \sigma)$ is the error function (mean μ, standard deviation σ). The lapse parameter, λ, represents stimulus-independent errors that may be due to mistakes, a bias, or to random guessing of the listener. This parameter was restricted to be maximally 10%. The 95% confidence intervals of thresholds were determined by bootstrapping (N = 1000). We defined the just-notable-difference (JND) as half the distance between the 0.25 and 0.75 fraction rightward judgements. We then estimated the MAMA from the 100 ms moving stimuli by multiplying the stimulus duration with the JND.

Head displacement during stimulus presentation

As explained in the Introduction, stimuli during which the amount of head rotation remains well below the auditory movement detection threshold (the MAMA, see above) are perceived as stationary in space. Since the peak chair velocity was 112°/s, the maximum chair displacements (and hence potential sound re. head displacements) during the 3, 10 and 100 ms were 0.33, 1.1 and 11°, respectively. Fig. 3.2 summarizes the actual passive head rotations during all
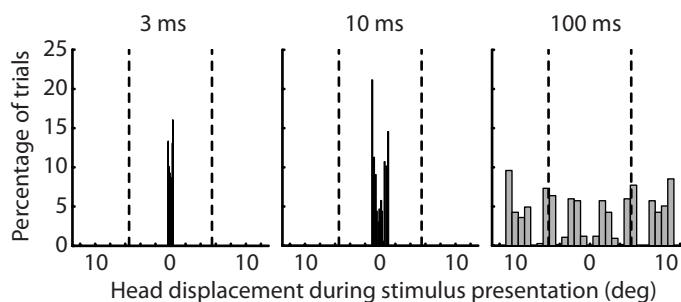
Figure 3.2 Histograms of head displacement during stimulus presentation together with the average minimum audible movement angle (dashed lines) of 5.5 ± 1.4° as measured in our setup (see Results).

applied stimulus presentations, together with the MAMA measured in our setup. Although the MAMA depends on target velocity (Perrott and Saberi, 1990; Chandler and Grantham, 1992), it is always higher than the minimum audible angle of stationary sounds (Mills, 1958).

Data Analysis

Calibration of eye data
The relation between raw eye-position signals and the corresponding LED positions were obtained by training two neural networks for the horizontal and vertical eye-position components, respectively. The trained networks were subsequently used to calibrate all eye-position signals (for details, see Goossens and Van Opstal, 1997b).

Saccade detection
A custom-made program detected saccades and vestibular quick phases from the calibrated eye-movement signals off-line by setting separate eye-velocity thresholds for saccade onset (70°/s) and offset (60°/s). To differentiate between quick phases of vestibular nystagmus and goal-directed saccades, we required the dynamic goal-directed saccades to have a vertical component (mean ± SD: 15.5 ± 10.9°), since the sounds emanated from loudspeakers at 10° elevation, and the vestibular quick phases had a negligible vertical component. We visually checked the saccade detection markings and made manual changes when deemed necessary. We discarded saccades with latencies shorter than 80 ms and longer than 800 ms. Responses with extremely short latencies were regarded as anticipatory, and very long reaction times as inattentiveness of the listener. Eye positions exceeding 30° (listeners JO and PB) or 35° (listeners DB, FB, JT, AJ) were excluded, because of the calibration range (see Experimental paradigms – Calibration). Typically, less than 10% of the data was excluded from this analysis. Listeners sometimes responded by making several correction saccades. We report on the first goal-directed saccade in each trial only.

Statistics
For the stationary localization condition, the eye-in-head endpoint of the saccadic response in the azimuth direction, E_{stat}, was quantified by determining the optimal linear fit through the data:

$$E_{stat} = g_{stat} \cdot \alpha_T + b_{stat} \qquad (3.3)$$

where α_T is the simulated target azimuth, b_{stat} is the bias (offset, in °) and g_{stat} the corresponding gain (slope, dimensionless). Parameters were found by minimizing the mean-squared error (Press et al., 1992). From the linear fit we also determined the correlation coefficient between data and model prediction.

Ideally, for stationary localization the gain is 1.0 and the bias is 0°. However, parameters g_{stat} and b_{stat} could deviate from the ideal values in an idiosyncratic way. To enable data pooling across listeners and conditions, we normalized the simulated target locations such that response gain and bias for all three stationary conditions were 1.0 and 0.0°, respectively:

$$T_H = g_{stat} \cdot \alpha_T + b_{stat} \qquad \text{and hence} \qquad E_{stat} = T_H \tag{3.4}$$

The normalized target locations, T_H, were then used to perform regression on the saccade endpoints of the dynamic localization responses during vestibular stimulation in world coordinates:

$$E_{dyn} = g_{dyn} \cdot T_H + b_{dyn} \tag{3.5}$$

Models

To determine to what extent the auditory system incorporated the intervening vestibular-induced eye and head movements during the reaction time period (see Fig. 3.1), we performed a multiple linear regression analysis on the horizontal saccadic eye-displacement responses (ΔE) by a linear combination of the normalized initial target location in head-centered coordinates (T_H, Eqn 3.4), the passive head displacement in space between sound onset and response onset (ΔH_S), and the onset position of the eyes in the head at the start of the response (E_H):

$$\Delta E = a \cdot T_H + b \cdot \Delta H_S + c \cdot E_H + d \tag{3.6}$$

in which a, b and c are dimensionless response gains, and d is the response bias (in °). In this paper we considered four potential spatial updating models to explain auditory-evoked saccade responses (Fig. 3.1). In model I, full compensation of eye and head-displacement signals corresponds to a world-centered target representation. In model II, only the vestibular-induced change in eye position is accounted for and the target remains in an updated head-centered reference frame. Model III only incorporates the passive change in head-orientation, while the audiomotor system is unaware of the intervening vestibular nystagmus. Finally, in model IV none of the intervening movement signals are accounted for, and the target remains in its initial head-centered reference frame.

Histograms

The bin-width (BW) of the histograms (see Fig. 3.5) was determined by $BW=range/\sqrt{N}$, where range is the difference between the largest and smallest values (excluding the two most extreme points), and N is the number of included points.
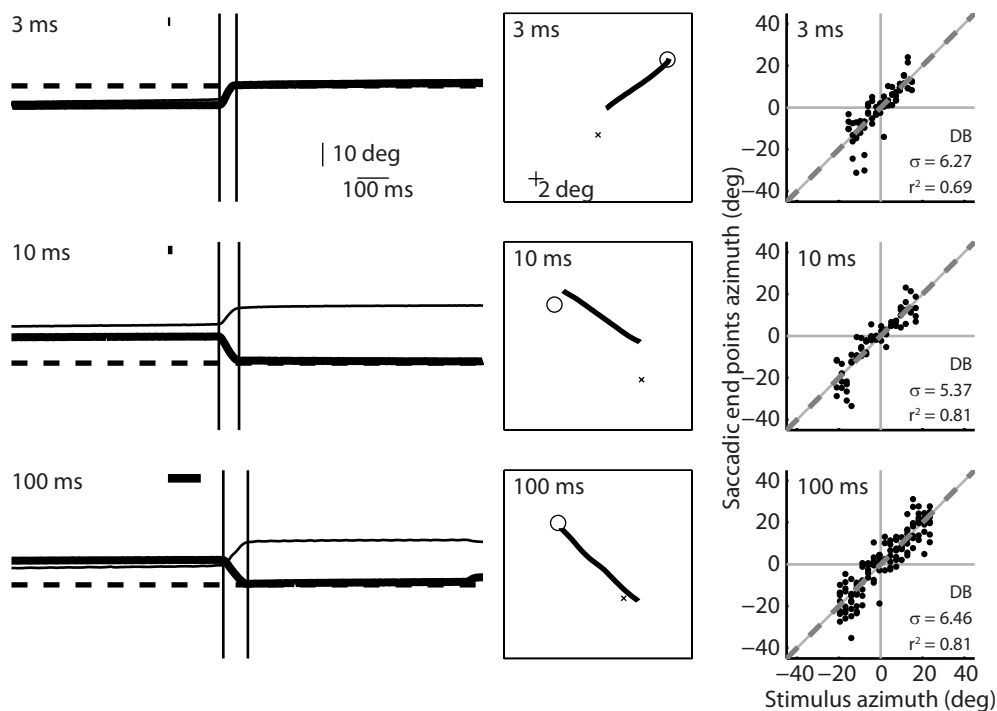
Figure 3.3   Stationary sound localization behavior of listener DB for the three sound durations (rows). First two columns: example eye movements in the stationary condition to 3, 10 and 100 ms noise burst presented in darkness. In the temporal plots (first column) azimuth (thick trace) and elevation (thin trace) components of eye position are plotted relative to target onset. The thin vertical lines show the localization saccade onsets and offsets. Thick horizontal bar shows target presentation time. The horizontal dashed line corresponds to the normalized stimulus azimuth (T_H; Eqn 3.4). The spatial plots (second column) present the saccades of the temporal data of the first column. The small x denotes straight ahead $[a,\varepsilon] = [0,0]$. Circles correspond to the target location. In the third column, the endpoints of all saccades of listener DB are plotted as a function of normalized stimulus azimuth in world coordinates. The dashed line shows a linear regression on these endpoints. Coefficients of determination (r^2) and response variability (σ) are given in the lower-right corners.

RESULTS

Stationary sound localization (baseline)

To assess baseline sound-localization performance of the listeners towards the simulated free-field noise bursts in the vestibular setup, they responded to brief sounds without vestibular stimulation during the first and last run of each experimental session. The first two columns of Fig. 3.3 show typical sound-localization trials of listener DB to 3 ms (top row), 10 ms (centre row) and 100 ms (bottom row) sounds. The left-most panels show the calibrated azimuth (bold) and elevation (thin) eye-movement traces relative to target onset, together with the sound's timing (black horizontal bar), and normalized (Eqn 3.4) azimuth target locations (dashed horizontal line). These examples show that the azimuth responses were reliably directed towards the normalized target locations, even for the briefest stimulus duration. The second column shows the spatial trajectories of the saccades (samples taken between the solid vertical

51

Table 3.1   Localization parameters for all subjects: Gain, bias and variance of uncorrected stationary localization (Eqn 3.3) and dynamic localization (Eqn 3.5).

		Stationary				Dynamic			
Duration (ms)	Listener	Uncorrected Gain (g_{stat})	Bias (b_{stat})	r^2	Variance	Gain (g_{dyn})	Bias (b_{dyn})	r^2	Variance
3	DB	0.76	-0.25	0.69	6.95	0.61	3.79	0.07	21.3
	FB	1.65	1.34	0.87	11.03	0.87	1.14	0.42	20.6
	J0	0.68	0.97	0.80	5.81	0.82	3.65	0.09	22.7
	PB	1.03	-8.07	0.72	7.71	0.73	5.28	0.19	18.0
	JT	1.02	6.15	0.70	8.41	0.80	-1.73	0.05	38.8
	AJ	1.03	9.88	0.72	7.90	0.46	5.91	0.02	36.8
10	DB	0.94	-2.12	0.81	5.77	0.41	1.05	0.05	21.6
	FB	1.69	-1.39	0.86	11.94	0.84	-0.19	0.37	21.4
	J0	0.66	0.25	0.67	7.15	0.75	-1.48	0.05	26.4
	PB	1.42	-9.96	0.76	9.78	0.51	-0.53	0.17	21.1
	JT	1.47	3.93	0.81	10.40	0.72	-10.24	0.11	37.0
	AJ	1.26	4.28	0.83	7.87	0.48	2.02	0.04	34.5
100	DB	1.08	2.02	0.81	6.53	0.67	3.78	0.28	15.3
	FB	1.37	-0.80	0.84	8.64	0.91	-1.11	0.42	18.1
	J0	1.38	-6.22	0.91	6.72	0.67	7.00	0.15	26.8
	PB	0.97	-12.69	0.87	4.67	0.92	-0.31	0.46	11.8
	JT	1.46	3.23	0.85	9.31	0.81	-0.56	0.20	28.3
	AJ	1.44	2.05	0.79	10.27	1.06	2.36	0.25	30.8

lines in the left-most column) together with the normalized sound locations (circles). Note that the azimuth components of the responses were accurate. In this paper we do not discuss the elevation response components, as listeners were rotated around the earth-vertical axis only, and stimulus elevation was always fixed at +10°.

As described in Methods (Eqn 3.4) we normalized the stimulus locations such that its linear regression line had a slope of 1.0 and no bias. Figure 3.3 (right-hand column) shows all end points of localization responses of listener DB plotted against normalized stimulus azimuth in the stationary condition. The response end points correlated well with the target location, indicating that the responses were indeed goal-directed, even for the very brief click-like sounds of 3 (top) and 10 ms (centre) ($r^2 > 0.7$). The left-hand side of Table 3.1 shows that all listeners had good baseline sound localization performance (uncorrected: 0.65 < gains < 1.7, biases < 13°, $r^2 > 0.65$ and variances < 12°), showing that their responses were indeed solely guided by simulated binaural acoustic information.
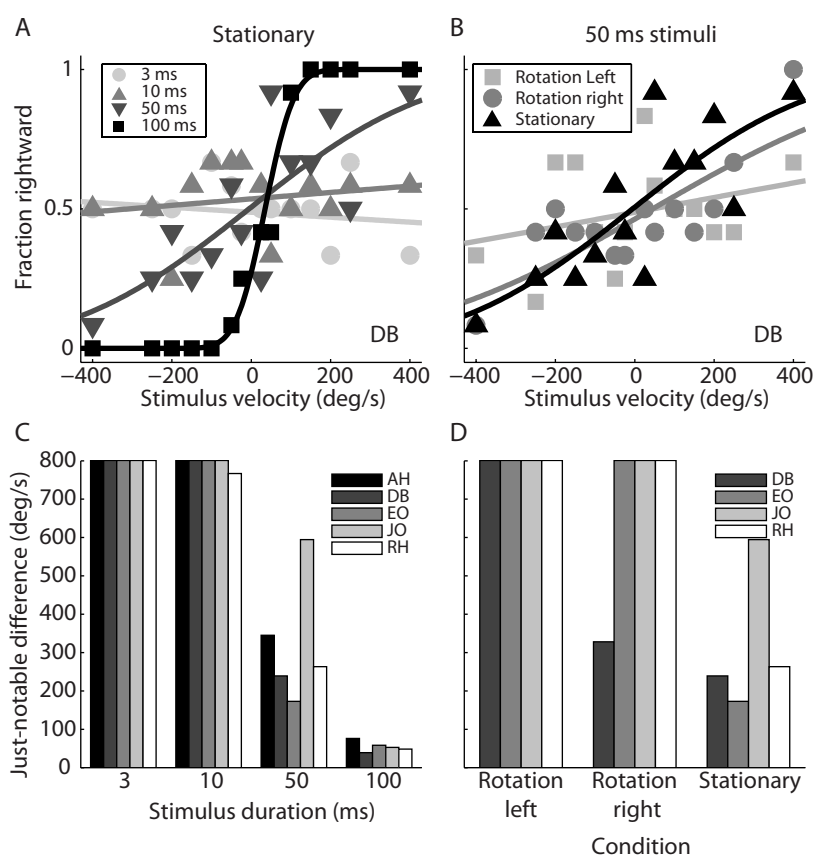
Figure 3.4   Detection of direction of sound motion. A) Fraction of rightward judgements as function of stimulus velocity (negative: leftward motion) for the four different sound durations for listener DB. C) individual just notable differences for the four stimulus durations. Note that the bars for 3 and 10 ms sounds extend well above the 800°/s. B) Fraction of rightward judgements as function of stimulus velocity for 50 ms sounds when listener DB was stationary (black triangles) or during rotation (gray squares and circles). D) individual just notable differences for 50 ms sounds when listeners were stationary or rotating. Note that the bars for rotation left and rotation right extend well above 800°/s (except for listener DB rotation right).

Sound-motion detection ability

As argued in the Introduction, adequate spatial updating requires the system to dissociate self-motion from target motion, for which it needs accurate information about movement of the sound source with respect to the moving head. We expected that the 100 ms stimuli could potentially provide sufficient acoustic information to determine that the sound-source moves along with the head, whereas the briefest sounds would be perceived as stationary in space. To test the auditory system's sensitivity for sound-source motion for a stationary and a rotating head, we performed two-alternative forced-choice psychophysics on sounds of 3, 10, 50 and 100 ms duration, moving at a range of leftward and rightward constant velocities (see Methods). As an example, Figure 3.4A shows the psychometric curves (Eqn 3.2) of listener DB for the four stimulus durations. The subject could reliably detect the direction of motion for 100 ms sounds, as the probability of rightward responses for rightward moving sounds is

one for speeds exceeding about 75-100°/s, and it's zero for sounds moving leftward at 75-100°/s and higher. The measured threshold is close to 0°/s. Figure 3.4C shows that the JND for the 100 ms sounds were well below 100°/s for all 5 listeners (mean ± SD: 55 ± 14°/s), indicating that the movement direction of these sounds could in principle be detected when moving through the straight-ahead direction. Because in the dynamic localization experiment the sounds were head-fixed, the auditory system might thus be confident about the detected absence of motion relative to the head, and should thus ignore the vestibular signals indicating head-through-space motion. These JNDs correspond to a MAMA of 5.5 ± 1.4° (Fig. 3.2).

In contrast, the psychometric curves for the 3 and 10 ms sounds were completely flat (Fig. 3.4A), as the listener could not hear any motion in these short click-like sounds. This can also be appreciated from the JND determined for all listeners (mean ± SD: 3ms: 5701 ± 5964°, 10 ms: 2454 ± 1825°; Fig. 3.4C), which were much larger (yielding unnaturally high values) than for the 100 ms sounds. The JND for the 50 ms sounds appeared to fall around 200-300°/s, indicating that a 50 ms stimulus moving at about 100°/s would not be reliably perceived as moving.

To check whether the JND would somehow strongly improve when the listener is subjected to whole-body rotation (at a maximum velocity of 112°/s), four listeners performed the same motion-discrimination task on the 50 ms sounds in the dynamic rotation condition. We specifically used the 50 ms sounds to detect any improvement in performance, as this stimulus duration lay closest to threshold performance (Fig. 3.4A,C). Although the example curves in Figure 3.4B suggest that during rotation the psychometric curves of listener DB may actually have had a lower slope (i.e. a higher JND, decreased sensitivity) than for the stationary condition, when pooled across listeners, the differences were not significant (t-test: P > 0.12). We conclude that during whole-body rotation the auditory system is not more sensitive to moving sounds than during the head-stationary condition.

Head and eye movements during the saccade reaction time

The dynamic experiments were designed to ensure considerable and variable passive head movements during the saccadic reaction time of the listeners, who were instructed to make a rapid saccadic eye movement toward the perceived sound location. Figure 3.5 quantifies the relevant variables from the experimental data, pooled for all listeners. The top row of Figure 3.5 shows the reaction-time distributions for the three stimulus durations (3 ms: mean ± SD: 222 ± 117 ms, 10 ms: 236 ± 123 ms, and 100 ms: 235 ± 100 ms). The centre row of Figure 3.6 shows distributions of head displacements during the measured reaction-time periods. Note that there was a considerable amount of head rotation: the mean was around zero degrees, but the distributions had a SD of about 20°, corresponding to a range from about -70 to +70°. The histograms in the bottom row show that the eyes were not stationary during the reaction time either. Although listeners were instructed to redirect their eyes toward the perceived straight ahead in preparation for the next localization response, the eyes deviated significantly from this location due to the ever-present vestibulo-ocular reflex and ocular nystagmus, and to a potential bias in their own estimate of straight ahead. The eye position variance at response-saccade onset was about 10°, so that initial eye-positions almost covered the entire oculomotor range of ±35°. Note that these variations in eye-in-head position and
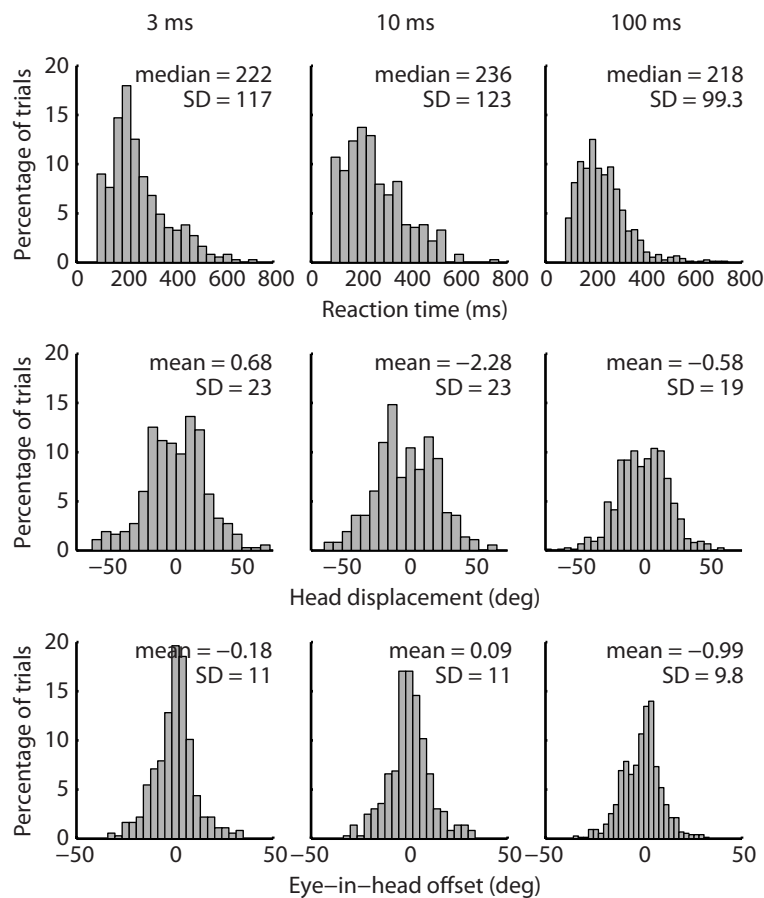
Figure 3.5   Distributions of reaction times (latency), head displacement during the reaction times and eye-in-head position at the time of the saccade response for the different sound durations, pooled over all listeners.

head displacements were required to disentangle the different models (outlined in Fig. 3.1) on dynamic sound-localization performance. Thus, the dynamic stimulation condition indeed challenged the auditory system to a substantial amount of spatial remapping to represent the target either in world coordinates, or to keep it in head-centered coordinates.

Dynamic sound localization

The left-hand side of Figure 3.6 shows three trials of subject DB during vestibular stimulation (same format as Fig. 3.3). Note the clear horizontal nystagmus pattern in the eye-movement traces (bold), which were not accompanied by vertical eye movements (thin). The sound-localization responses, in contrast, had a clear elevation component. Note that the responses in the three examples appear to be directed to the chair-fixed stimulus locations. In the following section we will further quantify these qualitative observations of the response patterns with respect to the different spatial updating models of Figure 3.1.

Figure 3.6 (right-hand column) shows the azimuth localization responses of listener DB in the dynamic conditions for the three stimulus durations (rows); we expressed final eye
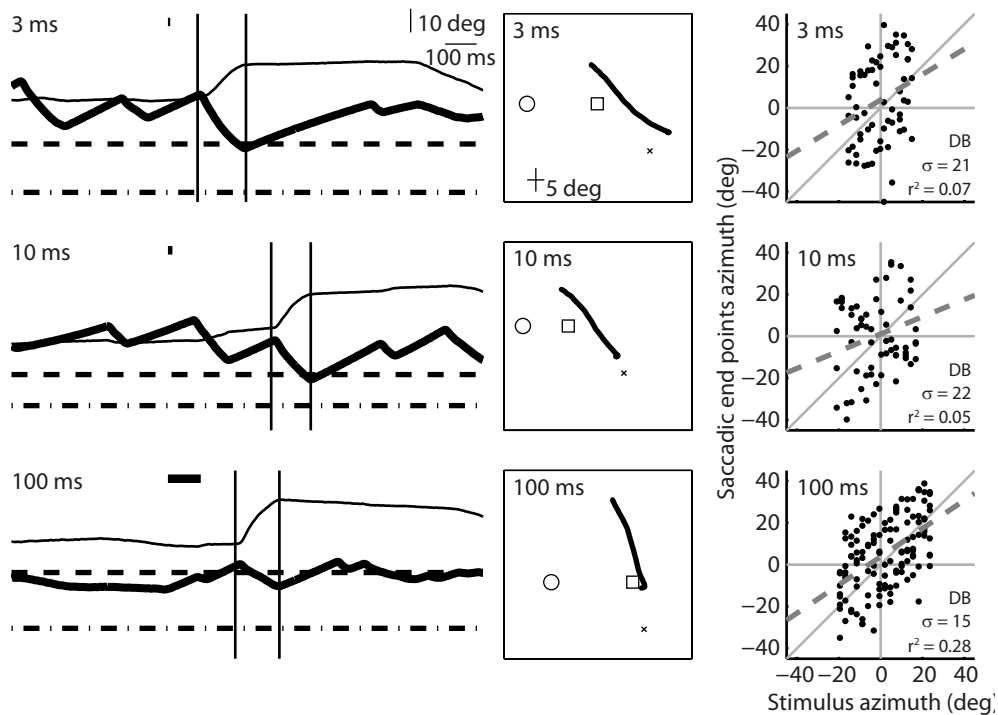
Figure 3.6   Dynamic sound localization behavior of listener DB for the three sound durations (rows). Same conventions as Fig. 3.3. Target locations are presented in head coordinates (T_H; Eqn 3.4; horizontal dashed lines in the first column and squares in the second column), and in world-coordinates ($T_W = T_H - \Delta H_S$; horizontal dot-dashed lines in the first column and circles in the second column).

position after the localization saccade in world coordinates (Eqn 3.5). Unlike the stationary condition (Fig. 3.3, right), the azimuth responses correlated poorly with the normalized world-centered target location for the dynamic vestibular condition. Linear regression yielded a large variability ($\sigma > 28°$) and a very low correlation ($r^2 < 0.2$). The right-hand side of Table 3.1 shows that this was the case for all listeners ($r^2 < 0.46$, variances $> 12°$). The horizontal scatter in the responses was significantly larger than in the static condition (KS test: $P < 10^{-7}$ for all listeners).

Testing the spatial updating models

The linear regression analysis on the response data in Figure 3.6 suggests that listener DB did not incorporate the passive head rotation in her localization responses. This holds for all listeners (Table 3.1). To test which of the four models described in Methods (Fig. 3.1, Eqn 3.6) best accounted for the behavior of all listeners, we applied the optimal regression coefficients of the models to the head and eye-movement data summarized in Figure 3.5 (centre and bottom rows) to predict the saccadic response. Figure 3.7 presents the predicted horizontal saccadic eye displacement of each model against the measured saccade component pooled for all listeners. The results make clear that for all sound durations the craniocentric model II ($\Delta E = T_H - E_H$, see Methods) yields by far the highest correlation (r^2) and lowest variability (σ) between predicted and measured saccadic responses (KS test on model I, III and IV errors
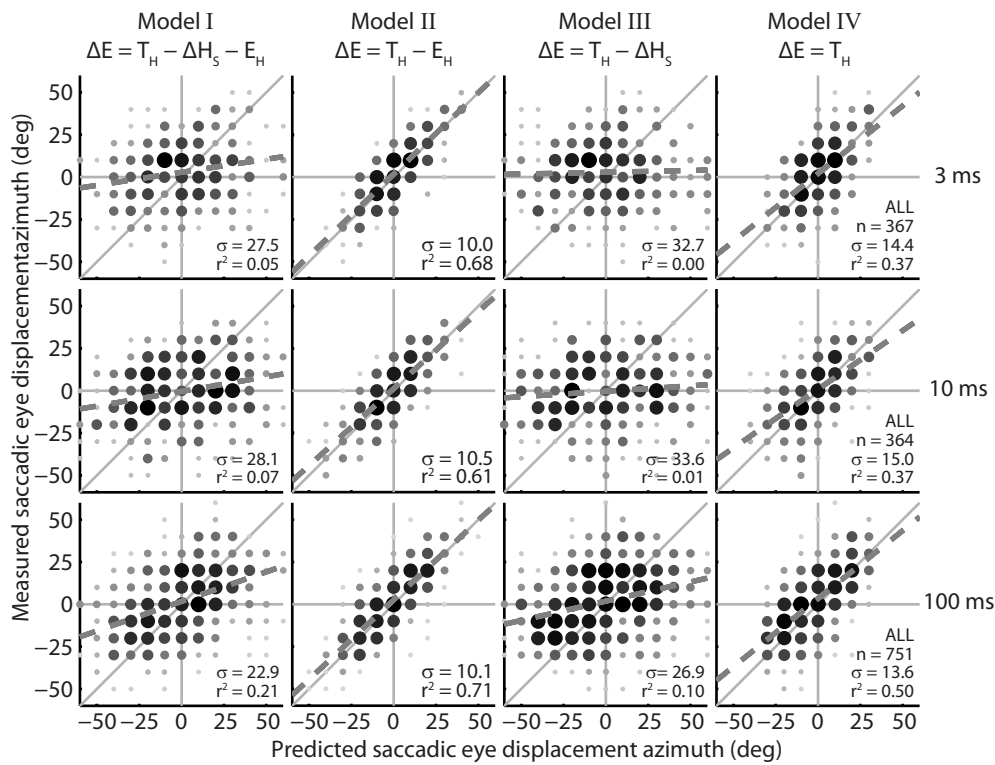
Figure 3.7 Predicted saccadic azimuth for the four models described in Methods plotted against the measured saccade azimuth pooled for all listeners. If the model would predict the listener's responses perfectly, responses would fall on the unity line and r^2 would be 1. Coefficients of determination (r^2) and response variability (σ) are given in the lower-right corners. Model II has the highest correlation and smallest variability between predicted and response saccade azimuth.

compared to model II errors: $P < 10^{-3}$ for all stimulus durations). This suggests that whereas the audiomotor system accounted for the vestibular induced changes in eye-in-head position (Fig. 3.5, bottom row), the substantial passive head rotations during the listener's reaction time (Fig. 3.5, centre row) were not incorporated in the responses.

Multiple linear regression analysis

To quantify the actual contributions of initial sound location, eye-in-head position and passive head displacement in sound-evoked saccades during vestibular stimulation, we performed a multiple linear regression analysis on the listener's saccadic eye displacements (Eqn 3.6). Table 3.2 provides the resulting coefficients for the individual listeners, and Figure 3.8 shows the averaged results across listeners for each of the three sound durations. The data show there is no effect of stimulus duration on the responses, as the gain of the craniocentric target location (T_H) (ANOVA: $F(2,15) = 0.12$ $P = 0.89$), gain of the passive head displacement during the reaction time (ΔH_s) (ANOVA: $F(2,15) = 0.83$ $P = 0.45$), and gain of the eye-in-head position at saccade onset (E_H) (ANOVA: $F(2,15) = 0.92$ $P = 0.42$) did not depend on stimulus duration. These results show that for all sounds, and for all listeners, the T_H gain did not differ from the
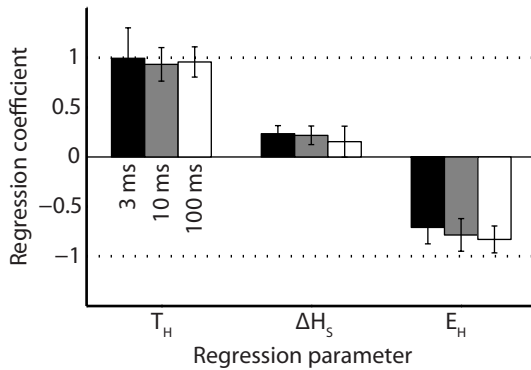
Figure 3.8 Multiple linear regression results (Eqn 3.6) on the listener's responses to 3, 10 and 100 ms noise bursts during passive whole-body rotation. Bars represent the regression coefficients of Eqn 3.6 averaged across listeners. Error bars represent standard deviation. The horizontal lines at +1 and -1 correspond to ideal regression values (see Fig. 3.1).

ideal value of +1 (t-test: P = 0.44), while the E_H gain was close to -1. The ΔH_S gain, however, remained close to 0 (even slightly positive, P < 0.05). In other words, the initial craniocentric target location (derived from simulated acoustic cues), as well as the change in eye-in-head position at the time of the response, were both incorporated in planning the saccadic response, although the eye-in-head orientation appeared to be slightly underestimated (mean ± SD: c = -0.77 ± 0.16). Importantly, the passive head displacements were not accounted for. These results therefore contrast markedly with the findings of the dynamic localization study by Vliegen et al. (2004), in which listeners made spatially accurate saccades to brief sound bursts under head-unrestrained conditions.
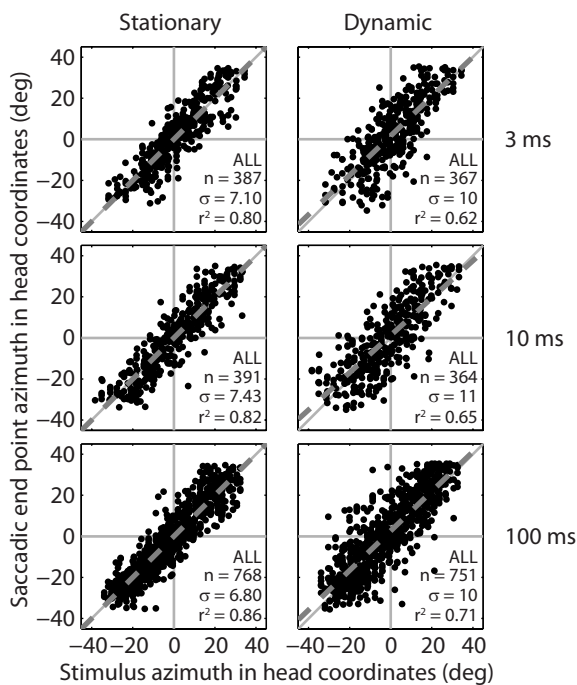

Figure 3.9 Comparison of stationary and dynamic localization conditions regarding response variability. Data are pooled across listeners and expressed in normalized head-centered coordinates. Despite the subjects' reported difficulty of the task, response variability in the dynamic condition (σ ≈ 10°) is only slightly larger than in the stationary condition (σ ≈ 7°).

Table 3.2   Multiple linear regression parameters of individual listeners. The horizontal component of the saccade was described as a function of the horizontal target position relative to the head (Target, T_H), head displacement in the reaction time (ΔH_S) and eye-in-head offset at the response (E_H, see Eqn 3.5). The table lists the regression coefficients (slopes a, b and c, bias d in °).

| Duration (ms) | Listener | Multiple Linear Regression Analysis | | | | |
		T_H a ± SD	ΔH_S b ± SD	E_H c ± SD	Bias d ± SD	r^2
3	AJ	0.90 ± 0.10	0.20 ± 0.06	-0.52 ± 0.17	3.94 ± 1.69	0.76
	DB	0.96 ± 0.07	0.16 ± 0.08	-0.65 ± 0.18	1.67 ± 0.97	0.75
	FB	0.98 ± 0.04	0.18 ± 0.06	-0.92 ± 0.15	-0.77 ± 1.06	0.87
	JO	0.89 ± 0.09	0.39 ± 0.10	-0.63 ± 0.17	8.06 ± 1.72	0.72
	JT	1.58 ± 0.12	0.24 ± 0.06	-0.63 ± 0.14	-6.60 ± 1.84	0.73
	PB	0.66 ± 0.08	0.24 ± 0.05	-0.91 ± 0.20	2.74 ± 0.67	0.75
10	AJ	0.96 ± 0.10	0.06 ± 0.05	-0.92 ± 0.21	1.61 ± 1.53	0.62
	DB	0.81 ± 0.06	0.32 ± 0.06	-0.56 ± 0.18	2.28 ± 0.90	0.75
	FB	1.11 ± 0.07	0.25 ± 0.08	-0.92 ± 0.20	2.85 ± 1.30	0.84
	JO	0.66 ± 0.09	0.30 ± 0.09	-0.75 ± 0.16	3.60 ± 2.43	0.63
	JT	1.03 ± 0.09	0.18 ± 0.06	-0.63 ± 0.11	-4.00 ± 1.68	0.74
	PB	1.03 ± 0.09	0.20 ± 0.04	-0.94 ± 0.20	0.77 ± 0.65	0.79
100	AJ	1.05 ± 0.06	0.04 ± 0.06	-0.73 ± 0.16	4.60 ± 1.45	0.65
	DB	0.87 ± 0.05	0.01 ± 0.04	-0.67 ± 0.12	2.23 ± 0.57	0.78
	FB	1.12 ± 0.04	0.13 ± 0.04	-0.95 ± 0.10	-0.44 ± 0.64	0.88
	JO	0.93 ± 0.04	0.42 ± 0.07	-0.74 ± 0.16	3.42 ± 0.79	0.83
	JT	1.06 ± 0.05	0.07 ± 0.05	-1.00 ± 0.10	0.53 ± 1.10	0.79
	PB	0.71 ± 0.05	0.26 ± 0.04	-0.89 ± 0.16	8.57 ± 0.79	0.70

Variability of stationary vs. dynamic conditions

Although listeners reported to find the localization task difficult, especially for the briefest noise bursts, their responses appeared to be quite consistent with only modest variability. To quantify this aspect of the data, Fig. 3.9 compares the saccadic end points of all listeners pooled for the stationary and dynamic conditions against the normalized target in head-centered coordinates. Note that the response variability for the dynamic condition (mean ± SD over subjects and stimulus durations: 9.59 ± 0.38°) is higher than for the stationary condition (7.02 ± 0.09°) (t-test: $P < 10^{-4}$).

DISCUSSION

We investigated spatial updating of auditory-evoked saccades towards short (3 and 10 ms) and long (100 ms) noise bursts during passive whole-body rotation. Although the auditory system could not detect the presence or absence of stimulus motion with respect to the head

for the shortest stimuli (Fig. 3.4), all sounds were localized in head-centered coordinates (Figs 3.7 and 3.8). In doing so, it ignored vestibular information about passive-induced head rotations, but accounted for changes in eccentric eye-in-head position imposed by vestibular nystagmus. These results contrast markedly with previous studies using brief (3-50 ms) sound bursts, presented either prior to, or during, actively generated intervening eye-head gaze shifts. Under such conditions sound-localization performance was spatially accurate (Goossens and Van Opstal, 1999; Vliegen et al., 2004). Below we will discuss possible explanations for this discrepancy.

Comparison with previous studies

Major differences between our study and previous studies are: (i) we denied the audiomotor system use of corollary discharge information of planned head movements; (ii) there was no proprioceptive information regarding changes of head-on-trunk orientation; (iii) the head was rotated passively; (iv) the sound source moved along with the head.

The visual-auditory double-step paradigm applied to head-unrestrained eye-head gaze shifts demonstrated that the audiomotor system updates its sound-localization responses in world (or body)-centered coordinates (Goossens and Van Opstal, 1999; Vliegen et al., 2004). Under such conditions, all sources of information about eye and head movements (neck proprioception, corollary discharges of planned movements, and vestibular signals) are available and consistent, and the listener is engaged in the active planning of a sequence of goal-directed gaze shifts. Vliegen et al. (2004) showed that accuracy (i.e. mean localization error) and precision (i.e. response variability) for static (sound presented before the voluntary head movement) and dynamic (sound presented during the head saccade) acoustic conditions were almost indistinguishable from sound-localization responses without intervening movements. In the current experiments response variability was slightly higher in dynamic localization trials than in static trials (Fig. 3.9). However, given that during the dynamic localization task the listener had to combine the acoustic localization cues with dynamic changes in eye position, while at the same time filter out acoustic background noise from the vestibular apparatus, as well as the vestibular head-movement signal, the difference in response variance (~37 % increase of the SD) was modest.

Interestingly, Vliegen et al. (2004) also showed that the auditory system continues to process acoustic-cue information under dynamic localization conditions, since gaze shifts were systematically better for longer-duration (50 ms) noise bursts, than for very brief (3 ms) sounds. The auditory system thus appeared to accumulate the processing of acoustic input as time progresses (Frens and Van Opstal, 1995; Hofman and Van Opstal, 1998; Vliegen et al., 2004). During head movements the acoustic localization cues change in a systematic and predictable way. Thus, for accurate localization, the head movement should be incorporated to compensate for these dynamic acoustic changes. This is not a trivial problem because of the different representations of the involved signals (e.g., tonotopic sensory codes vs. rate coding of neck muscle contractions).

Under head-fixed stationary conditions, self-generated dynamic changes in eye-position are almost fully incorporated in sound localization (with a gain of about -0.95) (Van

Grootel and Van Opstal, 2009; 2010). Because ocular responses also account for the involuntary drift of the eyes in darkness, spatial updating of sounds is based on an accurate representation of instantaneous eye position. The current experiments further extend these results to the eye-position changes of ocular nystagmus imposed by passive vestibular stimulation, with an eye-position gain of about -0.8 (Figs 3.5 and 3.7).

Two other studies have investigated spatial oculomotor behavior during whole-body vestibular stimulation around the yaw axis. Van Beuzekom and Van Gisbergen (2002) measured saccades to briefly-flashed (4 ms) visual targets that moved along with the head, and reported that subjects correctly localized stimuli in head-centered coordinates. We recently extended these experiments to visual flashes of different durations, presented at either head-fixed or world-fixed locations (Van Barneveld et al., 2011a). The results showed that spatial localization of brief visual flashes was only accurate if the visual system could reliably infer the direction of stimulus motion across the retina. Thus, long-duration (100 ms) flashes produced substantial visual streak patterns that could be updated in head-centered coordinates for head-fixed targets, and in world coordinates for world-stationary targets. In contrast, short flashes (0.5 and 4 ms) provided no detectable retinal motion cues and were kept in their initial sensory (i.e. retinal) coordinates. As a result, these brief stimuli were mislocalized.

Why no head-movement compensation?

We consider several possibilities to explain why in our experiments the audiomotor system did not compensate for the passive-induced head rotations, and instead kept sounds in an updated head-centered reference frame.

First, one might argue that listeners knew that the sounds were moving along with them, and could therefore have voluntarily adopted a craniocentric strategy. We believe this explanation is unlikely, because listeners were responding open loop and not instructed to localize the target in any particular reference frame. If they followed a voluntary strategy, part of the trials (or listeners) would have violated this strategy (either erroneously, or by adopting a different default). This was not observed. Moreover, if knowledge of the chair-fixed speaker locations would have played a role, part of the responses should have been directed toward the actual speaker locations (at ±37°), which never occurred. Instead, responses were reliably guided by the virtual, simulated sound locations at short reaction times, meanwhile incorporating the highly variable initial eye-position signal (Fig. 3.5). From this we infer the use of bottom-up acoustic and motor information sources, rather than top-down cognitive signals. Furthermore, although listeners made reliable and fast responses towards the sounds, they judged the task to be very difficult and were unable to reflect on their performance during the open-loop experiments. We therefore do not consider it feasible that listeners voluntarily disconnected the remapping of a (vestibularly-induced) dynamic head-movement signal, while at the same time remapping unpredictable eye positions.

Second, in the dynamic localization experiments, listeners were rotated at variable speeds during sound presentation, but received no dynamically changing acoustic cues, since the loudspeakers were attached to the chair. Could the auditory system have detected the absence of changing acoustic cues? For 100 ms sounds during high-velocity rotation, the answer might be yes, as our psychophysical results showed that fast-moving 100 ms sounds

were correctly perceived as moving (Figs 3.4A,C). For the 3 and 10 ms sounds, however, the amount of head rotation remained well below the MAMA (Fig. 3.2; Mills, 1958; Saberi and Perrott, 1990; Chandler and Grantham, 1992), and we also verified that whole-body rotation did not improve JNDs (Figs 3.4B,D). As a result, the auditory system appears to regard these short stimuli as stationary in space. Note also that since the head movements followed sinusoidal acceleration profiles, the head displacements didn't reach the MAMA in the majority of trials for 100 ms sounds either (Fig. 3.2). We therefore consider it improbable that the auditory system could have reliably discerned whether or not sounds were moving along with the chair on the basis of acoustic input. Yet, as evidenced by the near-perfect regression coefficients for the head-centered target location (a close to one (Eqn 3.6); Fig. 3.8), subjects accurately extracted the head-centered coordinates from the simulated acoustic cues during static and dynamic localization trials. Under natural hearing conditions the most likely situation for a world-stationary sound is a change in acoustic cues that anti-correlates with ongoing head movements, and it is highly unlikely that sounds are fixed to the head. We therefore reasoned that in the absence of evidence for dynamic changes in the acoustic cues, the auditory system's default assumption ('prior') would be that such sounds are regarded as stationary in space. This was indeed observed for head-unrestrained orienting responses (Vliegen et al., 2004), but our results indicate a different response mode for passive-induced head movements.

A third explanation might be that the auditory system uses signals for a coordinate transformation on the basis of their reliability. When motion cues are in conflict (here: vestibular information reports head motion in the absence of efference copies, neck-proprioceptive cues, and acoustic changes), the vestibular signal may contribute with only a small weight to the required coordinate transformations for world-centered stability. Although the eye movements were consistent with the interpretation of a vestibularly-induced head movement, the slow phase VOR showed that this compensation was far from perfect, as its gain was well above -1.0 (see also Van Barneveld et al., 2011a). Moreover, ocular nystagmus may also occur in the absence of vestibular stimulation, and would therefore be unreliable as a single source for spatial updating. Thus, if head-movement evidence is unreliable, it may be ignored altogether and the sound would be kept in its initial, head-centered, reference frame. Similar ideas, based on Bayesian statistical inference, have been proposed for perceptual tasks, multisensory integration, and sensorimotor performance (Battaglia et al., 2003; Niemeier et al., 2003; Alais and Burr, 2004; Körding et al., 2007; De Vrijer et al., 2009; Van Barneveld et al., 2011b).

Implications for spatial perception and behavior
Our recent visual-vestibular experiments demonstrated that the presence or absence of spatial updating of brief visual flashes relied on the integrity of the retinal motion signal (Van Barneveld et al., 2011a), rather than on the presumed reliability of the head-motion signal. Thus, the vestibular-only signal can be used for adequate spatial updating, despite the absence of efference copies or neck proprioception. We here conjecture that this is also the case for spatial updating of auditory stimuli. We hypothesize that the default strategy of the visual and auditory systems under vestibular-only stimulation would be to keep targets in their initial reference frame (audition: head-centered; vision: eye-centered) until sufficient sensory

evidence indicates stimulus motion relative to the head (or to the eye). Only if the sensory evidence is reliable, the system employs accurate spatial updating. These default strategies for auditory and visual remapping may seem surprising, or even suboptimal in the light of statistical inference models, as in daily life it is highly unlikely that sounds move along with the head, or that visual stimuli are fixed on the retina.

SUPPORTING INFORMATION

Simulation of free-field sound locations with two speakers
To simulate free-field sounds, we presented broadband noise bursts with personalized frequency-dependent ILD and ITD information. Here we describe how the sounds were created.

Setup
The listeners frequency-dependent ILDs and ITDs were measured in 3 x 3 x 3 m^3 dark room. The floor, ceiling and walls were covered by sound-attenuating black foam (50 mm thick with 30 mm pyramids, Uxem b.v., Lelystad, AX2250) to attenuate echoes for frequencies exceeding 500 Hz. The background noise level was about 30 dB SPL. The setup consisted of a vertical motorized hoop, 2.5 m in diameter, with 58 loudspeakers (Visaton, GmbH, SC5.9, Haan, Germany), that were mounted at 5° intervals.

ILD and ITD measurements
The ear's frequency response to sounds coming from locations in azimuth directions α = [-20, -17.5, ..., 17.5, 20]°, and at a fixed elevation angle ε = 0°, were measured simultaneously in both ears. We used a flat-spectrum Schroeder-phase signal (Schroeder, 1970; Hofman and Van Opstal, 1998) that contained 20 sweeps of 1024 samples, with a sample frequency of 48828 Hz. The first and the last sweeps were ramped (5 ms) and discarded from the analysis. The acoustic responses to the sweeps coming from the different locations were recorded with a probe microphone (Knowles EA1842) equipped with a short flexible tube (length 5.5 cm, 1.5 mm outer diameter). The end of the tube was placed at the entrance of the ear canal and fixated with tape without obstructing or deforming the pinnae. Listeners were seated in the center of the hoop and their head was kept in place by a headrest (Bremen et al., 2010).

The microphone signal was amplified (custom-built pre-amplifiers), band-pass filtered (0.2-20 kHz, Krohn-Hite 3343) and sampled at 48828 Hz (RP2.1 System 3, TDT). The subsequent offline analysis was performed in Matlab (MathWorks, Natick, MA). First, the average signal over sweeps 2 to 19 was calculated (1024 samples). Subsequently the magnitude spectra were computed with the fast Fourier transform. The obtained spectra were then smoothed using cepstral smoothing (smoothing factor 64). The ITD was measured from the relative onset times of the stimuli arriving at the two ears.

ITD and frequency dependent ILD filter

The smoothed spectra were used to create appropriate filters for the left and right loudspeaker. First, all spectra were divided by the spectrum for the straight-ahead location $[\alpha, \varepsilon] = [0, 0]°$ (reference spectrum). The result was transformed to a complex minimum-phase spectrum by Hilbert transformation. Subsequently, the minimum-phase impulse response in the time domain was determined by inverse Fourier transform, so it could be used as input for Finite Impulse Response (FIR) filters for each azimuth direction.

Broadband noise (see Methods) was convolved with the minimum-phase impulse response to provide the signals with position-dependent ILD information. Finally, the ITD information was provided by adding the appropriate delay (as additional zeros) between the left and right loudspeaker. This way stimuli could be perceived as a single sound source varying in their location between the two loudspeakers.

ACKNOWLEDGEMENTS

4

The reference frame of the
ventriloquist effect

Denise C.P.B.M. Van Barneveld
Marc M. Van Wanrooij

INTRODUCTION

The "ventriloquist effect" refers to the localization bias of sounds towards a co-occurring visual stimulus (Howard and Templeton, 1966; Jack and Thurlow, 1973). It is thought to originate from optimal integration of auditory and visual percepts (Alais and Burr, 2004; Körding et al., 2007), leading to faster and more precise orienting responses (Frens et al., 1995; Corneil et al., 2002). The shift in perceived sound location decreases with increasing spatiotemporal mismatch (Bertelson and Radeau, 1981; Frens et al., 1995), concomitant with a decrease in perceptual integration (Hillis et al., 2002; Hairston et al., 2003; Lewald and Guski, 2003; Wallace et al., 2004) and saccadic performance (Frens et al., 1995; Harrington and Peck, 1998; Hughes et al., 1998; Colonius and Arndt, 2001; Van Wanrooij et al., 2009; Van Wanrooij et al., 2010).
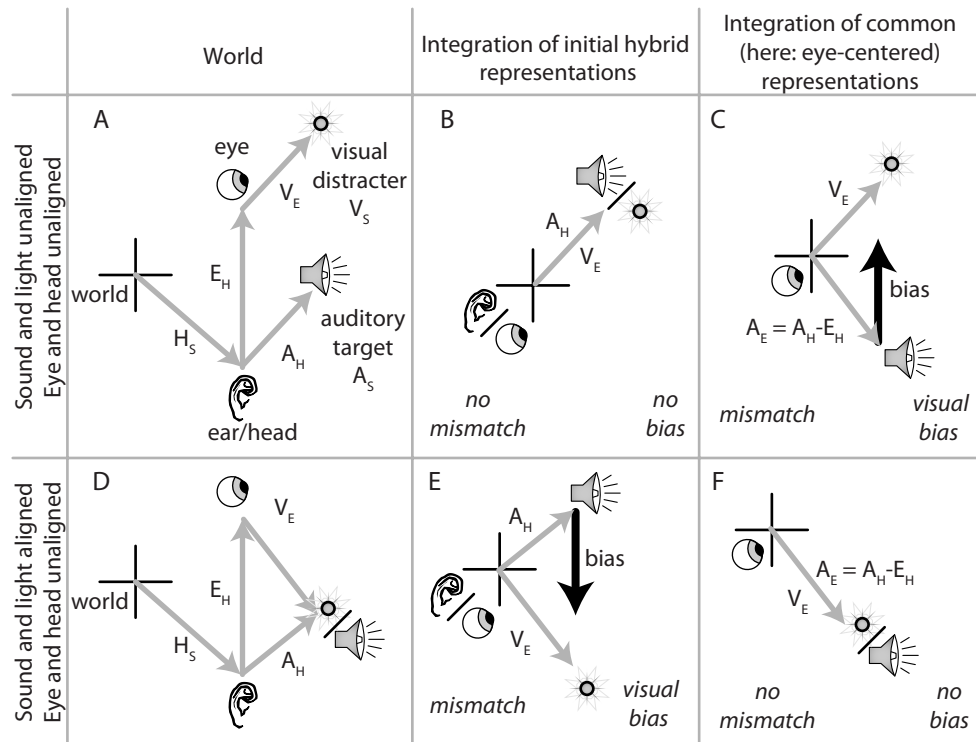

Figure 4.1   Rationale of the effect of reference frame transformations on cross-modal integration. A) Vector scheme for a situation in which there is not only a mismatch between the auditory target and the visual distracter, but also eye and head-in-space (H_S) position are unaligned due to rotation of the eye in the head (E_H). The initial representation of the target is head-centered for the sound (A_H) and eye-centered for the light (V_E). Black cross represents center of reference frame. Gray arrows denote various positions. B) Since there is no mismatch between the two representations for the situation shown in A, integration at this stage would not lead to a visual bias. C) A coordinate transformation to a common (here: eye-centered) reference frame would again introduce the mismatch between the auditory target and visual distracter as in the physical world. Integration at this stage would introduce a visual bias (indicated by black arrow). In contrast, for the situation in D), where the auditory target and visual distracter are spatially aligned, E) integration at a hybrid stage would now yield a visual bias, F) yet is absent at a common stage.

This integration effect poses a neuro-computational puzzle, since the different sensory signals are initially represented in different reference frames. Specifically, the brain computes sound locations from binaural and spectral cues relative to the ears (Blauert, 1997; Yin, 2002), whereas the retina contains a visual map of space with respect to the eyes. These signals have to be transformed into a common reference frame to maintain perceptual congruency and to generate common goal-directed behaviors (Stein and Stanford, 2008), as outlined in figure 1. Shortcomings in (or absence of) these transformations when integrating auditory and visual signals could lead to a cross-sensory spatial mismatch for a spatially-aligned audiovisual stimulus (Fig. 1D,E), or to cross-sensory alignment for a spatially-unaligned audiovisual stimulus (Fig. 1A,B), depending on the orientations of eye and head. Ideally, audiovisual integration should depend only on the actual spatial disparity between sound and light (Figs 1C,F).

We here ask whether the ventriloquist effect reveals any such shortcomings, or whether the visual bias on sound localization correctly operates in a common reference frame. This is a non-trivial question; audiovisual integration might already occur early in the brain (Kayser and Logothetis, 2007), while even at late stages modest single-neuron rate modulations by eye (Jay and Sparks, 1984) and head are different for auditory and visual signals (Jay and Sparks, 1987a), resulting in a dual or hybrid representation. Furthermore, behavioral data support the notion of a spatially-incorrect integration for perceptual decisions (Hartnagel et al., 2007), and for short-term recalibration of sound localization (Kopčo et al., 2009). However, these behavioral studies did not specifically address the ventriloquist effect, and were limited to only one change in eye position, without a change in head position, and the latter study only presented one audiovisual disparity.

To address this, subjects localized sounds in the presence of a visual distracter with rapid orienting movements, while we varied initial eye and head positions, auditory and visual stimulus locations, and audiovisual spatial mismatch over a substantial range in the midsagittal plane. We found that head and eye positions were accurately incorporated in the orienting movements, and that the ventriloquist effect acted at a unified common-integration stage.

METHODS

Subjects
Seven subjects participated in the experiments (age range, 22-53 years, median 31; 5 male, 2 female). All subjects except for both authors were naive about the purpose of the study. All had normal hearing (within 20 dB of audiometric zero, standard staircase audiogram test, ten frequencies, range 0.5-11.3 kHz, ½ octave separated), no uncorrected visual impairments, and showed normal baseline visual and auditory localization behavior (evidenced by the coefficient of determination of the stimulus-response relation ($r^2 > 0.7$), and a mean reaction time lower than 500 ms in unisensory localization experiments). Experiments were conducted after obtaining full understanding and written consent from the subject. The experimental procedures were approved by the Local Ethics Committee of the Radboud University Nijmegen,

and adhered to The Code of Ethics of the World Medical Association (Declaration of Helsinki), as printed in the British Medical Journal of July 18, 1964.

Experimental setup

During the experiments, subjects sat comfortably in a chair in the centre of a completely dark, sound-attenuated room ($3 \times 3 \times 3$ m^3). The floor, ceiling and walls were covered with sound-attenuating black foam (50 mm thick with 30 mm pyramids; AX2250, Uxem b.v., Lelystad, The Netherlands), effectively eliminating echoes for frequencies exceeding 500 Hz (Agterberg et al., 2011). The room had an ambient background noise level of 30 dB SPL (Bremen et al., 2010). The chair was positioned at the centre of a vertically oriented circular hoop (radius 1.2 m) on which an array of 29 small broadrange loudspeakers (SC5.9; Visaton GmbH, Haan, Germany) was mounted at 5° intervals from -55 to +85° in the midsagittal plane (elevation angles, with 0° at straight ahead; Van Barneveld et al., 2011b). Light-emitting diodes (LEDs) were mounted at the centre of each speaker.

Eye and head movements were recorded with the magnetic search-coil technique (Robinson, 1963). To this end, the listener wore a lightweight spectacle frame with a small coil attached to its nose bridge (Bremen et al., 2010). In the gaze-saccade experiments (see Audiovisual localization experiment section below), subjects wore a scleral search coil (Scalar Instruments, Delft, The Netherlands) in addition to the head coil. Three orthogonal pairs of square coils (6 mm^2 wires, 3 m x 3 m) were attached to the room's edges to generate oscillating horizontal (80 kHz), vertical (60 kHz) and frontal (48 kHz) magnetic fields, respectively. The eye- and head-coil signals were amplified and demodulated (EM7; Remmel Labs, Katy, TX, USA), low-pass-filtered at 150 Hz (custom built, fourth-order Butterworth), and digitized by a Medusa Head Stage and Base Station (TDT3 RA16PA and RA16; Tucker-Davis Technology) at a rate of 1017.25 Hz per channel. A button press was recorded along with the analog eye- and head-position signals, which enabled interaction between the subjects and a custom-written C++ program running on a PC (Precision 380; 2.8 GHz Intel Pentium D; Dell, Limerick, Ireland), which controlled data recording and stimulus generation.

Stimuli

Acoustic stimuli were digitally generated using Tucker-Davis System 3 hardware (Tucker-Davis Technologies, Alachua, FL, USA), with a real-time processor (RP2.1 System3, 48828 Hz sampling rate). All acoustic stimuli consisted of 50 dB (A-weighted), 150-ms duration Gaussian white noise (0.5-20 kHz bandwidth), with 5 ms sine-squared onset and cosine-squared offset ramps. Visual distracters consisted of green (wavelength 565 nm) light-emitting diodes (LEDs) mounted at the centre of each speaker (luminance 1.4 cd/m^2).

Experimental paradigms

Calibration experiment

Each experimental session started with a calibration experiment. To obtain the head-position data for the calibration procedure the subject accurately pointed a head-fixed laser pointer (attached to the spectacle frame required for head movement recording; see Experimental
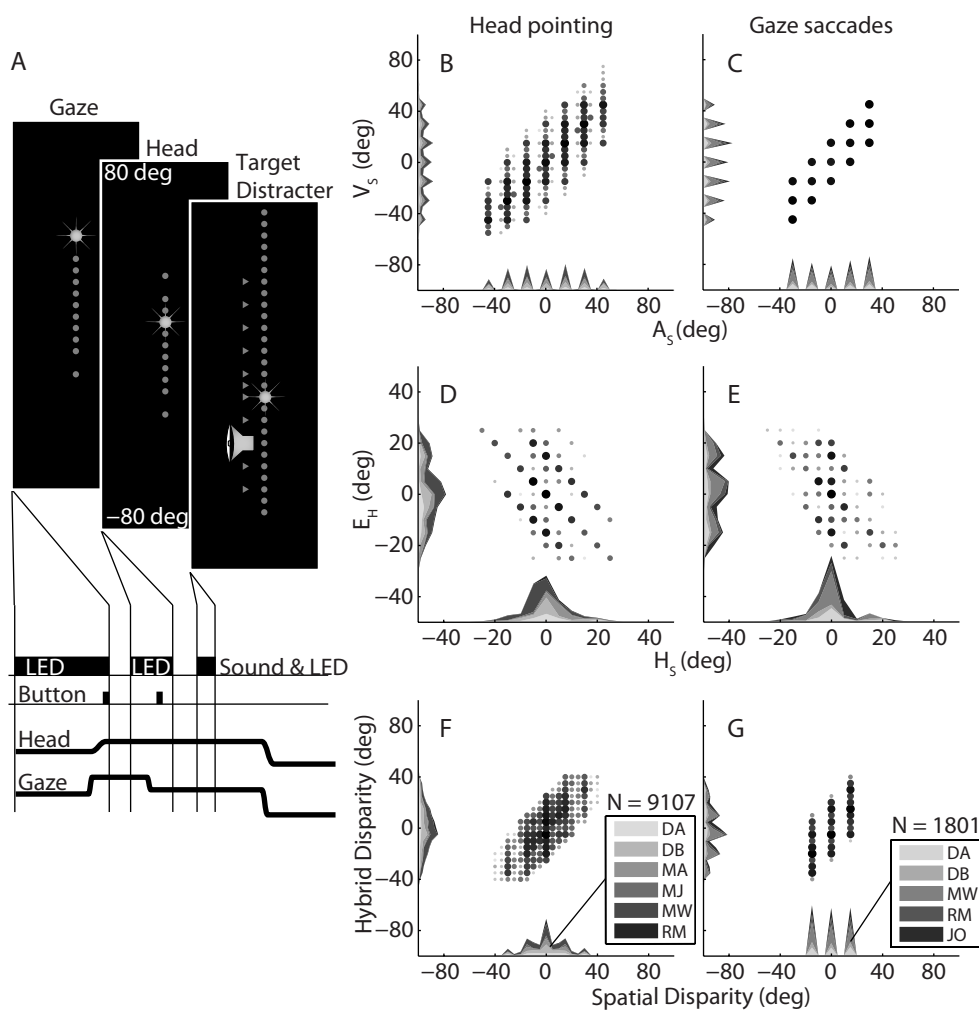
Figure 4.2   Spatial and temporal aspects of experimental paradigm. A) Spatial and temporal layout of example trial. Top: gray circles denote potential eye, head or visual distracter location, gray triangles denote potential auditory target. Example LED and speaker locations are indicated by star and speaker symbol(see Methods for details). B-G) Distributions and combinations of experimental parameters in (B,D,F) head-saccade and (C,E,G) gaze-saccade paradigms for all trails and subjects pooled. B,C) auditory-target-in-space A_s and visual-distracter-in-space V_s stimuli, D,E) eye-in-head E_H and head-in-space H_s orientation, F,G) disparity in a spatial reference frame stage and a hybrid reference frame stage. Data points were binned for graphical purposes (5 deg-wide bins); symbol size and gray-scale correspond to log-likelihood of particular stimulus configuration. Gray-scale in histograms indicate subject.

setup section) towards 56 LED locations in the two-dimensional frontal hemifield. The laser-pointer was turned on only during the calibration experiment. In the gaze-saccade experiments (described below), subjects also fixated the LEDs to obtain eye-position data for the calibration procedure.

Audiovisual localization experiment

Figure 4.2A illustrates the timing of each experimental trial. Each trial began with an LED to which subjects had to orient their heads. A button press extinguished this first head-fixation LED and a second LED was illuminated 200 ms later, which the subjects had to fixate with the eyes, while maintaining the initial head position as accurately as possible. A subsequent button press extinguished the second LED after a random delay (between 100 and 300 ms). An auditory target was then presented, simultaneously with a visual distracter, 200 ms after the extinction of the second fixation LED. To determine a potential effect of the pointer (head or eye movement) on the ventriloquist effect, subjects either had to generate a head movement (head-pointing experiments; five subjects) and/or a head-free gaze shift (gaze-saccade experiments; six subjects) as quickly and as accurately as possible to the sound, while ignoring the visual distracter.

The auditory target originated from one of 13 locations in the midsagittal plane: ± [0, 5, 15, 25, 30, 35, 45]° in elevation. A visual distracter was presented simultaneously at one of 27 locations: [-55, -50, -45, ..., 70, 75]° in elevation. The target and the distracter could thus originate from the same or from distinct spatial locations. Figures 4.2B and 4.2C show the distributions of the auditory target-in-space (A_S) and the visual-distracter-in-space (V_S) for all trials and subjects for head movements and gaze saccades, respectively.

The fixation LEDs for eye and head orientations were presented in the midsagittal plane at ± [0, 5, 10, 15, 20, 30]°. Since subjects did not have any visual reference to guide their head position, the actual alignment of the initial head-in-space (H_S) varied slightly from the actual fixation LED from trial to trial. In the gaze-saccade experiments, we calculated the initial eye-in-head position from the actual calibrated H_S and initial gaze position (E_S) by:

$$E_H = E_S - H_S \qquad (4.1)$$

We verified that the initial gaze position was always well aligned with the spatial location of the fixation LED in the gaze-saccade experiments (standard deviation between desired and actual gaze position was 1.4° across all subjects). Therefore, in the head-pointing experiments, where actual gaze position was not recorded, we took the fixation LED location as initial gaze position E_S, and estimated the eye-in-head orientation E_H from the actual calibrated H_S, and this E_S estimate, again according to Eqn 4.1. Figures 4.2D and 4.2E show the distributions of H_S and E_H of all trials, pooled over all subjects for head movements and gaze saccades respectively.

We presented a large number of randomly-selected combinations of sound and flash locations and initial E_H and H_S to the subjects in each experimental session. We did not present combinations of flash location and eye-in-space location that led to a visual-target-re-eye eccentricity $|V_E| > 60°$. Each subject performed multiple sessions on separate days, yielding a large number of responses per subject (ranging from 180 to 3439; see also Selection section), and ensuring that permutations of stimulus configurations (A_S x V_S x H_S x E_H) were evenly distributed for each subject.

By varying target and distracter locations, as well as eye and head orientations, the spatial disparity (D_{COMMON}) between the auditory target and visual distracter in space could

be dissociated from the hybrid disparity (D_{HYBRID}) between the head-centered auditory target location and the eye-centered visual distracter location. D_{COMMON} and D_{HYBRID} disparities are defined as follows:

$$D_{COMMON} = V_S - A_S \qquad \qquad (4.2a)$$
$$D_{HYBRID} = V_E - A_H \qquad \qquad (4.2b)$$

with $A_H = A_S - H_S$ the head-centered auditory target location and $V_E = V_S - E_H - H_S$ the eye-centered visual distracter location. Distributions of both disparities are shown in Fig. 4.2F and 4.2G for all trials and subjects for head movements and gaze saccades, respectively. We here choose to define D_{COMMON} in a world-centered reference frame, but note that the actual reference frame should remain unspecified. As long as the representations for auditory and visual signals are the same, a common world-centered, eye-centered or head-centered reference frame all yield the same common disparity (e.g. $D_{COMMON} = D_{SPACE} = D_{EYE} = D_{HEAD} = 0$ for the spatially aligned audiovisual stimulus in Fig. 4.1D).

Unisensory localization experiments

Subjects also participated in purely auditory and visual localization experiments with the same stimulus configurations (A_S or V_S x E_H x H_S) as in the audiovisual experiments, to ensure that they had normal localization performance, and could hear/see the auditory/visual stimuli (data not shown). Subject MW could not see visual stimuli with retinal eccentricities $V_E > 50°$. We excluded those trials in the audiovisual experiments from the analysis of this subject.

Data analysis

All data analysis was performed in Matlab R2010a (The Mathworks, Inc., Natick, MA).

Calibration

We determined the relation between raw head- and/or eye-position signals and the corresponding LED positions by training two neural networks for the horizontal and vertical head- and/or eye-position components, respectively (Neural Network Toolbox, Matlab; network structure: 3 input layers [horizontal, vertical and frontal field signals], 1 hidden layer with 5 units, 1 output layer [azimuth or elevation]; training: back-propagation algorithm according to Levenberg-Marquardt optimization, with Bayesian regularization). These networks corrected for small inhomogeneities in the magnetic fields, and coped with minor cross talk between the channels, which a non-linear goniometric regression (describing the theoretic relation between rotation of the coil within the magnetic field and current strength) cannot account for. Head- and/or eye-position data from the other experiments were calibrated off-line using these networks with an absolute precision < 3% over the entire range (120°). Note that head- and eye-position signals were calibrated by means of different networks.

Selection

Head and/or eye movements were automatically detected from calibrated data based on velocity criteria (head velocity: 10%; eye velocity: 20%). Onset and offset markings were

visually checked by the experimenter, and manually adjusted if necessary. Occasionally, subjects sometimes responded by making several orienting movements(< 3% of all trials). We report only on the first saccade in each trial. The results and conclusions, however, did not differ if the last saccade was analyzed (data not shown).

The total number of responses detected as such ranged per subject from 270 to 4154 (head: 540 to 4154, gaze: 270 to 808). We discarded responses with latencies shorter than 80 ms (deemed anticipatory) and longer than 800 ms (regarded as inattentive). Furthermore, we excluded extreme values of head and eye position and disparity (so that $|H_S|$ and $|E_H| \leq 25°$, $|D| \leq 40°$). These selection criteria yielded a total number of responses per subject ranging from 180 to 3439 (head: 490 to 3439, gaze: 180 to 681).

For a restricted disparity range ($|D| \leq 25°$, data not shown), the localization error was approximately a linear function of common or hybrid disparity. Therefore it was convenient to restrict $|D|$ further for the regression analyses (Eqns 4.3-4.7), as detailed below.

Sound localization

The localization endpoints of the saccadic responses, R, were quantified by determining the optimal linear fit through the data (e.g. Fig. 4.3A):

$$R = g \cdot A_S + o \tag{4.3}$$

where A_S is the target location, o is the offset (deg) and g the corresponding gain (slope, dimensionless), for absolute common and hybrid disparities $|D|$ up to 25°.

Ventriloquist effect

To quantify the visual bias on the sound localization responses, we fitted the response errors ($E = R - A_S$) as a function of either common (Fig. 4.3B), or hybrid (Fig. 4.3C), disparity:

$$E = b \cdot D + o \tag{4.4}$$

where o is a constant localization offset (deg; independent of auditory and visual stimulus) and b represents the visual bias (dimensionless; 1 entailing complete visual bias, and 0 no bias at all), for absolute disparities $|D|$ up to 25°.

Potential models for the reference frame of the ventriloquist effect

We consider two extreme hypotheses to explain audiovisual integration (Fig. 4.1). These models assume that the sound localization bias towards the visual distracter occurs in different reference frames; the common-integration model assumes that auditory and visual targets are integrated in a common reference frame, while the hybrid-integration model assumes integration at a stage where both auditory and visual targets are still represented in their initial head- and eye-centered reference frames, respectively.

We analyzed the localization responses as a function of the actual target location (A_S) and of both disparities with multiple linear regression (MLR-) analysis to test which model explained the data best (Fig. 4.3D):

$$R = g \cdot A_S + b \cdot D_{COMMON} + c \cdot D_{HYBRID} + o \qquad (4.5)$$

for absolute disparities $|D|$ up to 25°. Regression coefficients g, b and c reflect the contribution of a particular location variable (A_S, D_{COMMON}, D_{HYBRID} respectively) to the saccade end-point, irrespective of the other variables, and o is a constant offset (°).

Influence of eye and head orientation

MLR-analysis was also performed to determine the accuracy of coordinate transformations required to produce an orienting response. Ideally, the response should equal the motor error, ME, which is given by (the distance between current pointer position and the spatial target location):

$$ME = T_S - E_H - H_S \qquad \text{for gaze shifts, (4.6a)}$$
$$ME = T_S - H_S \qquad \text{for head movements, (4.6b)}$$

with T_s target-in-space. However, saccades towards peripheral targets typically undershoot the target location, so that actual responses might be a scaled version of the ideal motor error. The value for the gain may depend on many aspects, such as individual differences, the pointer used (eye, head, arm), task demands, species, or target modality (Knudsen et al., 1979; Perrott et al., 1987; Collewijn et al., 1988; Becker, 1989; Lemij and Collewijn, 1989; Frens and Van Opstal, 1995; Harris, 1995; Yao and Peck, 1997; Populin and Yin, 1998; Nodal et al., 2008). Therefore, we first determined the response gain (α) for each subject by:

$$\Delta R = \alpha \cdot ME \qquad (4.6c)$$

for a disparity $D_{COMMON} = 0$ (i.e. $T_s = A_s = V_s = AV_s$; Fig 4.4C).

Subsequently, we determined the accuracy of sensory coordinate transformations required to produce an orienting response, ΔR, towards an audiovisual target for absolute disparities $|D|$ up to 25° (Fig. 4.4):

$$\Delta R / \alpha = g \cdot A_S + b \cdot D_{COMMON} + c \cdot E_H + d \cdot H_S + o \qquad (4.7)$$

We restricted the MLR analysis to the common-reference frame model, as the analyses of Eqns 4.4 and 4.5 showed that integration was more likely to occur at a common stage (Fig. 4.3). Nevertheless, Eqn 4.7 can potentially further dissociate the common and hybrid reference frame models through the regression parameters c and d. If integration takes place in a common reference frame, there should be a complete incorporation of the initial eye and head orientations (see Fig. 4.1, $c = d = -1$) for gaze shifts. The hybrid model, in contrast, predicts no incorporation of eye and head orientation ($c = d = 0$). For head-only responses, eye position should not ($c = 0$, Fig. 4.1) and did not matter across subjects ($T_{df = 5} = -1.06$, P = 0.34). Since such a random variable added to an MLR analysis might affect the other regression coefficients in unpredictable ways, we omitted the E_H term from the head-saccade MLR as shown in Figure 4.4E.

Statistics

Parameters of all regressions were found by minimizing the mean-squared error. We determined the coefficient of determination (r^2) between data and model prediction, and the F-value and associated p-value for the full model.

We determined t-statistics and associated p-values for the regression coefficients mainly under the null-hypothesis: H_0: $\beta_K = 0$, where β_K denotes the parameter under consideration. For the gain-response analysis of Eqn 4.6 and the MLR analysis of Eqn 4.7, we also compared regression coefficients to ideal values of +1 (for α and g), or -1 (for c and d).

RESULTS

Ventriloquist effect

Subjects were by and large unable to ignore visual distracters when localizing sounds in the midsagittal plane. In Figures 4.3A-C this so-called ventriloquist effect is exemplified for the responses of subject MW (head and gaze responses pooled). Although localization responses are highly correlated with the sound locations ($r^2 = 0.85$, $F_{3245} = 1.9 \cdot 10^4$, $P < 0.001$, Fig. 4.3A), the localization errors still clearly depend on a common mismatch between the auditory target and the visual distracter (Fig. 4.3B). So, for example, when the light flash was presented 25° above the sound, responses were on average biased by approximately 14° towards the flash location. Up to a disparity of 25°, the localization error was approximately a linear function of common disparity (Fig. 4.3B, black line). The slope of this line (Eqn 4.4, b = 0.56, $T_{3245} = 40.3$, $P < 0.001$) is a measure of the strength of audiovisual integration, with 0 indicating no integration, and 1 total visual dominance. Responses of the other subjects to the spatially mismatched audiovisual stimuli were generally similar, although the amount of integration (Eqn 4.4, *b*) varied between 0.17 and 0.56 (mean ± SD: 0.38 ± 0.16, $T_{df>272} > 5.4$, $P < 0.001$).

Reference frame

To quantify whether the ventriloquist effect takes place in a common reference frame (Fig. 4.1C,F) or in a hybrid reference frame (Fig. 4.1B,E), we also analyzed the response endpoints as a function of hybrid mismatch (Eqn 4.4). For subject MW, localization errors are correlated with hybrid disparity (Fig. 4.3C; $r^2 = 0.09$, $F_{3245} = 328$, $P < 0.001$), although this relation was less profound than for common disparity (cf. Fig. 4.3B). Across subjects, the effect of hybrid disparity on localization error was typically small (Eqn 4.4: b; mean ± SD over all subjects: 0.20 ± 0.14), and although significantly larger than 0 (one-tailed t-test: $T_6 = 3.84$, $P = 0.004$), it was always smaller than the effect of common disparity (one-tailed paired t-test between hybrid and spatial slopes: $T_6 = 4.16$, $P = 0.003$).

Note that there exists a large covariation between the common and hybrid disparities (Fig. 4.2F-G) for both the gaze- and head-only responses. As such, the weak relationship between hybrid disparity and auditory localization error (Fig. 4.3C) could be a spurious one. To remove this confound we performed a multiple linear regression analysis (MLR; Eqn 4.5) on the pooled head and gaze responses of each subject, by including auditory-target location, common and hybrid disparity as independent variables, and the localization endpoint
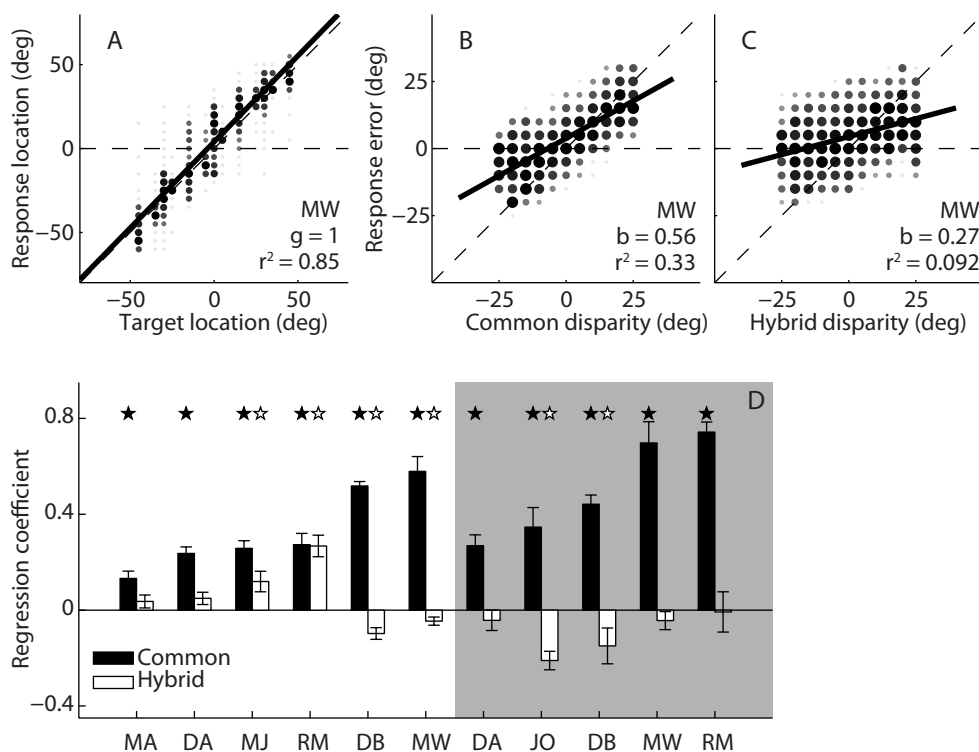
Figure 4.3   Audiovisual integration. A) Head- and gaze-saccade response locations of subject MW as a function of sound target location for absolute |D| up to 25 deg. Data points were binned for graphical purposes (5 deg-wide bins); symbol size and gray-scale correspond to log-likelihood of the target-response combination. The black line shows a linear fit through the individual data points. The slope (g; Eqn. 4.3) and the coefficient of determination (r^2) are given. B) The error between the target and response location as a function of common disparity of the same data as in A). If responses were not biased by the visual distracter, responses would lie around the dashed horizontal line. If the visual distracter would dominate the behavior, responses would lie around the unity line. The black line shows a linear fit (Eqn. 4.4) through the individual responses. The slope of this line (b) is a measure of audio-visual integration. The coefficient of determination (r^2) is given in the lower right corner. C) Localization error now as a function of hybrid disparity. D) The regression coefficients for common disparity (black) and hybrid disparity (white) of equation 5 (b and c, respectively) for the individual subjects for head orienting movements (white background) and gaze saccades (gray background). Stars indicate significant difference from zero (P<0.01).

as dependent variable. Figure 4.3D shows the contributions (regression coefficients) of the common and the hybrid disparity to the response endpoints. The contribution of common disparity (Fig. 4.3D, black bars) varied over subjects, from almost no contribution ($b = 0.1$ for head responses of subject MA, corresponding to only a 2° bias for 20° disparities) to a bias that clearly favors the visual distracter ($b > 0.5$; with an extreme 0.7 for gaze responses of subject MW). Nevertheless, despite this idiosyncratic variability, the common bias was significantly larger than 0 for each subject ($T_{df>131} > 4.1$, P < 0.001). Furthermore, the hybrid contribution was always smaller than the common contribution (one-tailed paired t-test all subjects: $T_{10} = 5.0$, P < 0.001), and its mean contribution across subjects was not significantly larger than 0 (one-tailed t-test: $T_{10} = -0.29$, P = 0.61). These results therefore strongly suggest that auditory

and visual coordinates are transformed into a common representation before integrating them based on their mismatch, as the common mismatch seems to be the dominant factor in explaining the visual bias. Furthermore, the response strategy did not depend on the pointer used, as the results were the same for gaze and head pointing.

Motor transformation

Irrespective of whether auditory and visual signals fuse within a common or a hybrid reference frame, for a goal-directed response the integrated signal (AV) needs to be transformed into a suitable motor command (e.g. Eqn 4.1). For example, making an eye movement to an audiovisual event requires at least a conversion from the head-centered representation of sound-source location (A_H) into an eye-centered oculomotor command (ΔG), which in theory can be simply achieved by subtracting the eye-in-head orientation (E_H; Van Grootel et al., in press):

$$\Delta G = A_H - E_H \tag{4.8}$$

while the eye-centered representation of an image can be maintained (Fig. 4.1). Obviously, this is an oversimplification (for reviews: Maier and Groh, 2010; Crawford et al., 2011) as for more complex tasks the brain needs to take into account, for example: non-commutative rotations of the eye-head-reach systems, self or induced motion (spatial updating), and the eventual effector (eye, head, and/or arm movement). Nevertheless, the integrated signal should be transformed into an eye-centered motor command for gaze saccades (Sparks and Mays, 1980; Robinson, 1975; Eqn 4.6a) and in a craniocentric motor command for head movements (Goossens and Van Opstal, 1997; Eqn 4.6b).

These motor commands yield movements that depend on the initial head position for both gaze shifts and head movements and on eye position for gaze shifts only. However, saccades tend to undershoot intended targets in an idiosyncratic way (for review: Becker 1989). Figures 4.4A and 4.4.B show two examples of this behavior by fitting Eqn 4.6a through the spatially aligned data. Subject JO had a larger undershoot of about 21% (α = 0.79; Fig. 4.4B), while subject DA only slightly undershot the AV target location (α = 0.91; Fig. 4.4A). Both subjects responded highly reliably to the stimuli, as evidenced from the high coefficient of variation, r^2. Figure 4.4C shows the individual response gains of all subjects for head pointing movements (mean ± SD over subjects: α = 0.79 ± 0.43; 5 out of 6 were significantly different from 1: $|T_{df>157}| > 7.4$, P < 0.001) and gaze saccades (mean ± SD over subjects: 0.88 ± 0.13, all 5 subjects were significantly different from 1: $|T_{df>93}| > 2.8$, P < 0.005).

Taking this general undershoot into account, the sensory coordinate transformations required for an accurate motor response yield an additional prediction of the common-integration model: the localization response should depend linearly on the auditory target location in space and on the audiovisual disparity that determines the amount of audiovisual integration. Moreover, the motor system should compensate for the initial head-in-space orientation and, for gaze saccades, also for the eye-in-head orientation. We tested these predictions by performing MLR analysis on the cross-modal data (Eqn 4.7), with the gain-compensated head displacements or gaze shift ($\Delta R/\alpha$) as the dependent variable, and the
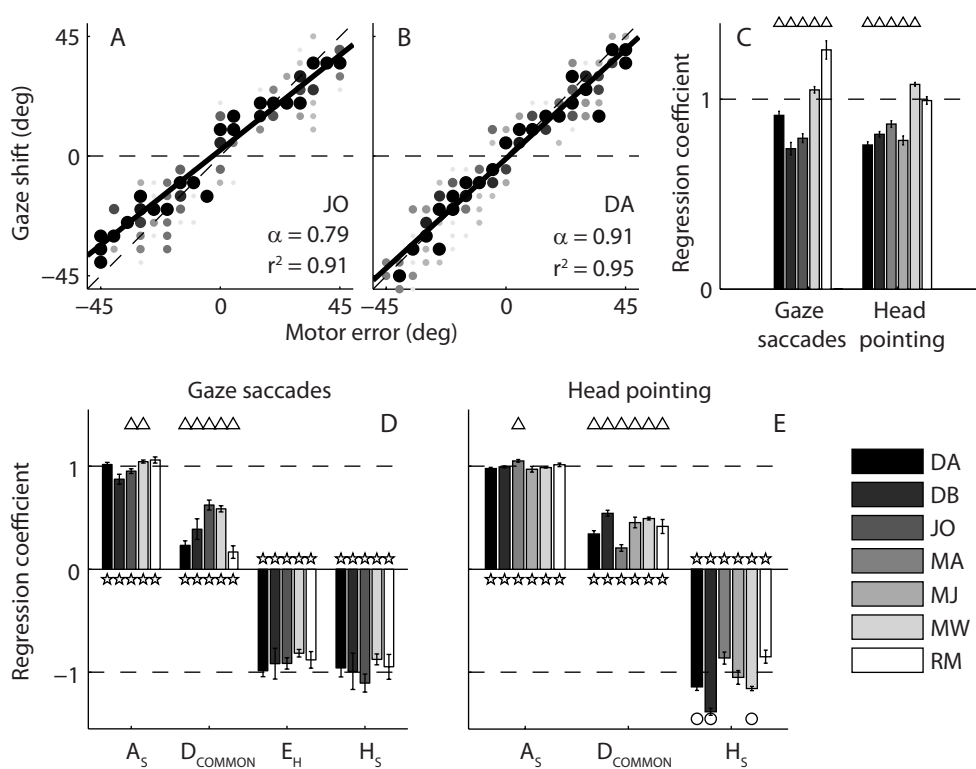
Figure 4.4   Coordinate transformations necessary for localization responses. A) and B) show all gaze saccades of two example subjects with a low (A) and a high (B) localization gain (Eqns 4.6). Data points were binned for graphical purposes (5 deg-wide bins); symbol size and gray-scale correspond to log-likelihood of particular configurations. The slope of the solid black line (a) is based on responses to audiovisual targets with common disparity of zero deg. C) Localization gains for all subjects for gaze saccades and head pointing separately. Triangles indicate significant differences from 1. The lower row shows MLR-results (Eqn 4.7) on localization responses for different initial eye (E_H) and head (H_S) orientations, for individual subjects for gaze saccades (D) and head movements (E). The common disparity (D_{COMMON}) coefficient shows the amount of audio-visual integration, with -1 entailing visual dominance. Error bars correspond to one standard deviation as obtained through bootstrapping. Dashed lines at plus one denote ideal auditory target representation in space (A_S), and at minus one full compensation of initial eye (E_H, for gaze saccades) and head orientation (H_S, for head pointing and gaze saccades). Stars indicate significant differences from 0, circles indicate significant differences from -1 and triangles indicate significant difference from +1 (P < 0.01).

spatial location of the sound (A_S), common audiovisual disparity (D_{COMMON}), head-in-space (H_S) and eye-in-head (E_H) as independent variables. Figures 4.4D and 4.4E present the regression coefficients for each of the subjects (grayscale bars) for gaze saccades and head movements, respectively.

When corrected for the response gain, all movements were goal directed, as the regression coefficients for A_S were indistinguishable from the ideal value of +1 (mean ± SD over subjects: head pointing: 1.00 ± 0.03, t-test over subjects: T_5 = -0.17, P = 0.87, gaze saccades: 0.99 ± 0.08 t-test over subjects: T_4 = -0.32, P = 0.76). In line with the results of Figure 4.3B, the responses were biased towards the visual distracter albeit with considerable idiosyncratic variability (D_{COMMON}: mean ± SD over subjects: head pointing: -0.41 ± 0.12, gaze saccades:

-0.40 ± 0.20). Importantly, the regression coefficients for E_H and H_S were close to -1, indicating that the system accounts for the initial eye and head position nearly completely (mean ± SD over subjects: H_S: head pointing : -1.07 ± 0.20, t-test over subjects: $T_4 = 0.90$, $P = 0.41$, gaze saccades: -0.98 ± 0.08, t-test over subjects: $T_5 = 0.63$, $P = 0.56$; E_H: gaze saccades: -0.90 ± 0.06, t-test over subjects: $T_4 = 3.5$, $P = 0.025$). Note that we omitted initial eye position from the analysis for head pointing as this did not have any systematical influence (see *Methods*). The full model has a high goodness-of-fit value (r^2, mean ± SD over subjects: 0.87 ± 0.07 for gaze saccades and 0.87 ± 0.04 for head pointing; $F_{df>131} > 97$, $P < 0.001$ for all subjects in both paradigms), indicating that the common spatial-integration model (Eqn 4.7) accounts well for the observed responses.

DISCUSSION

We used a novel paradigm to quantify the reference frame of the ventriloquist effect by instructing human subjects to generate either goal-directed head-free gaze shifts, or head movements to audiovisual stimuli that covered a large range of spatial disparities, from different initial eye and head positions. We found that subjects were unable to ignore visual distracters presented simultaneously with auditory targets (Fig. 4.3 and 4.4). Importantly, the evidence indicates that the ventriloquist effect takes place in a common reference frame, rather than at a stage where audition and vision are still represented in their initial respective head-centered and eye-centered reference frames (Fig. 4.3D). Furthermore, by accounting for the gaze-control system's tendency to undershoot targets, our findings suggest that the different eye and head orientations are fully incorporated in the planning of orienting responses to audiovisual stimuli (Fig. 4.4).

Disparity

The ventriloquist effect is a classic example of a multisensory illusion in which the spatial percept of a sound is 'captured' by the spatial location of a visual stimulus (Howard and Templeton, 1966; Jack and Thurlow, 1973; Radeau and Bertelson, 1977; 1978; Welch and Warren, 1980). These early studies indicated two important parameters that determine the strength of this illusion: the relative timing of and the spatial distance between the two stimuli. This has been termed the spatial and temporal "rules" of multisensory integration as it also holds for multisensory interactions in neurons (Stein and Meredith, 1993) and behavioral multisensory effects, such as: facilitation of stimulus detection (Hughes et al., 1994; Frens et al., 1995; Harrington and Peck, 1998; Colonius and Arndt, 2001; Frassinetti et al., 2002; Van Wanrooij et al., 2010; Colonius and Diederich 2011; see also: Slutsky and Recanzone, 2001) and higher audiovisual precision (Corneil et al., 2002). We only varied the spatial parameter substantially (presenting stimuli always synchronously), and found that in the midsagittal plane a spatially disparate visual distracter could have a strong impact on a subject's ability to localize a sound (e.g. Fig. 4.3B), even for disparities up to 25° (Thurlow and Jack, 1973). Similarly, other studies reported that auditory and visual stimuli must be presented within about 30° of each other within the horizontal plane to influence localization (Hairston et al.

2003; Wallace et al., 2004; see also: Van Wanrooij et al., 2009). As the first study reporting on the effect of eye and head position on audiovisual integration, our data adds to the "spatial rule", showing that spatial coincidence should be defined in a common reference frame.

This finding is surprising in the light of existing behavioral and neurophysiological data. These hint not only at imperfect reference frame transformations leading to heterogeneous unisensory representations running from eye- to head-centered, but more importantly also at different representations for the visual and auditory signals. Below we will discuss how these results can still be interpreted as integration in a common reference frame.

Behavioral representation

To our knowledge, only two behavioral studies focused on the reference frame of audiovisual integration (Hartnagel et al., 2007; Kopčo et al., 2009), but did not specifically test for the ventriloquist effect. By changing eye position from a central to an eccentric position, Hartnagel and coworkers (2007) found that audiovisual fusion areas were smallest between the current eye and head direction. This was interpreted as evidence for a misalignment of the visual and the auditory reference frames. However, the results can also be understood from a common representation by considering the spatial resolution of the visual and auditory systems. For vision resolution is highest near the fovea, while for audition it is highest near the centre of the head (Mills, 1958). Inferring whether or not a light and a sound were caused by the same source should therefore also be easier around and in-between the gaze and head directions. This alternative explanation still favors an alignment of the visual and auditory reference frames.

Kopčo and coworkers (2009) investigated the reference frame of the ventriloquist aftereffect (i.e. fast visual recalibration of spatial hearing: Held, 1955; Recanzone, 1998; Lewald, 2002; Woods and Recanzone, 2004; Wozny and Shams, 2011) by changing the eye position between training and test trials. They concluded that a hybrid reference frame guides this aftereffect, as neither a head-centered nor an eye-centered representation could account for their results. However, potentially confounding factors, such as saccade adaptation and/or an updating of prior expectation of sensor and target locations, could not be readily addressed as this would require a large variation in sensor (eye and ear) and target (sound and light) positions and disparities. Here we show that the immediate ventriloquist effect, which is presumably constantly subjected to such a variation in every-day life, operates on a common representation.

Neural representation

Multisensory influences on neuronal activity are already observed at low-level cortical areas that have been traditionally held as unisensory (e.g. Kayser et al., 2010; for reviews: Foxe and Schroeder, 2005; Schroeder and Foxe, 2005; Ghazanfar and Schroeder, 2006; Kayser et al., 2007; Koelewijn et al., 2010). Accordingly, if multisensory integration acts early, the common reference frame of sensory signals should emerge early too. In line with this view, eye position signals have been shown to modulate neural firing rates in auditory cortex (Werner-Reiss et al. 2003, Fu et al., 2004), and visual cortex (Weyand and Malpeli, 1993). Auditory and visual cortex are anatomically connected (Falchier et al., 2002; Rockland and Ojima, 2003; Bizley et

al., 2007), and neurons in visual cortex (area 18-19) respond to sounds in a spatially-specific manner (Morrell, 1972). Moreover, primary auditory and visual cortex both exhibit enhanced responses to aligned audiovisual stimuli (Martuzzi et al., 2007), which also enhance spatial processing in auditory cortex (Bizley and King., 2008). So far, however, studies on the spatial effects of audiovisual integration in low-level cortical areas are still lacking. Thus, although it cannot be excluded (Molholm et al., 2002; Stekelenburg et al., 2004; Bonath et al., 2007; Romei et al., 2007), there is as yet no clear evidence for a neuronal substrate at "early" cortical areas for the ventriloquist illusion.

Evidence for (mis)alignment of auditory and visual representations has been obtained at higher-level cortical, as well as at subcortical areas involved in spatial orienting behavior. Surprisingly, results do not unequivocally point to a common spatial representation. For example, there is a relatively poor correspondence between the representations of auditory and visual signals in the lateral intraparietal cortex (area LIP; Stricanne et al., 1996; Mullette-Gillman et al., 2005; 2009), and in the ventral intraparietal area (VIP; Schlack et al., 2005) of the posterior parietal cortex of the macaque monkey. Also in the monkey midbrain superior colliculus (SC), which is considered to fulfill a pivotal role in multisensory-guided orienting behavior (Meredith and Stein, 1983; 1986a;b; Stein and Meredith, 1993) are auditory and visual receptive fields misaligned (Jay and Sparks, 1987b), as the spatial tuning characteristics of many cells in the SC only partially shift with eye position (Jay and Sparks, 1984; Hartline et al., 1995). In contrast, McGuire and Sabes (2011) demonstrated a common representation for visual and proprioceptive targets.

How can multisensory integration at a common reference frame, as suggested by our behavioral findings be reconciled with these seemingly hybrid neurophysiological results? We consider several explanations for this apparent discrepancy. First, the neuronal representations might shift over time and become more aligned with the final common representation around the onset of a movement (Jay and Sparks, 1987a; Russo and Bruce, 1994; Linden et al., 1999; Cohen and Andersen, 2000). Second, while the majority of cells seem to exhibit heterogeneous reference frames for the visual and auditory signals separately, a substantial amount were shown to encode visual and auditory signals stemming from the same spatial location in a common reference frame (e.g. approximately 30% of recorded neurons in VIP). Integration of external multisensory stimuli might be predominantly governed by these neurons. Evidence for such a scheme has been observed in the dorsal medial superior temporal area (MSTd), where neurons with common heading preferences for visual and vestibular stimuli are more likely to contribute to crossmodal behavior (Gu et al., 2008). Third, these structures might not be crucial for the (perceptual) ventriloquist effect at all. For example, human studies (Phan et al., 2000; Bertelson et al., 2000; Meienbrock et al., 2007; Leo et al., 2008; Passamonti et al., 2009; Bertini et al., 2010) suggest that parietal cortex plays no essential role in the ventriloquist effect. However, as eye and head were always aligned in these studies, they cannot exclude that intact parietal cortex is important for aligning visual and auditory representations.

Overall, a straight-forward, hierarchical view of multisensory integration in the brain seems untenable, yet our data imply a simple outcome: a common representation of auditory and visual signals able to direct movements to targets in space. To establish a functional role for any brain structure in mediating the ventriloquist effect, however, experiments should

test neural and behavioral responses under a wide range of independent changes in sensor and target locations and disparities. Such experiments have not been conducted so far.

ACKNOWLEDGEMENTS

Adapted from: Van Barneveld, D.C.P.B.M., Van Grootel, T.J., Alberts, B. and Van Opstal, A.J.
(2011) The effect of head roll on perceived auditory zenith. Exp Brain Res, 21,
235-243

5

The effect of head roll on perceived auditory zenith

Denise C.P.B.M. Van Barneveld
Tom J. Van Grootel
Bart Alberts
A. John Van Opstal

INTRODUCTION

Spatial awareness relies on the integration of multisensory inputs, but as accuracy and variability of signals may differ and change under varying conditions, an interesting question is how different sources are integrated to construct a unified percept.

Spatial perception has been studied extensively with visual stimuli (Aubert, 1861; Mittelstaedt, 1983; Van Beuzekom et al., 2001; Kaptein and Van Gisbergen, 2004; 2005; De Vrijer et al., 2008). In visual-vestibular experiments subjects set the orientation of a luminous line, either parallel to their own body axis, or to the perceived earth-vertical (i.e. gravity). Subjects accurately estimate their body orientation, even in the absence of visual cues (e.g. Mittelstaedt, 1983; Mast and Jarchow, 1996; Van Beuzekom et al., 2001). However, when subjects have to set the luminous line earth-vertical, responses depend on body roll (Mittelstaedt, 1983; Kaptein and Van Gisbergen, 2004; Fig. 5.1), or on head-on-neck orientation (Van Beuzekom et al., 2001). For near-upright orientations, errors are typically negligible, but at intermediate tilt angles (around 30°) data may show a small overcompensation (E-effect; Müller, 1916). At larger rolls (> 60°), however, the luminous line setting is tilted in the direction of head roll (Aubert (A)-effect; Aubert, 1861), and response variability increases with roll angle.

Mittelstaedt (1983) explained the A-effect as a compromise between an imperfect gravicentric signal from the otoliths and a head-centered internal bias, called the idiotropic vector. According to this hypothesis, the otolith estimate is not aligned with gravity because of an imperfect fusion of utricle and saccule information. The head-roll estimate will then be biased towards the head axis after adding the imperfect otolith signal with the idiotropic vector. This computation minimizes the E-effect, but enhances the A-effect.

An alternative theory proposes a Bayesian principle (De Vrijer et al., 2008). This model is based on the summation of precise and accurate retinal information of the luminous line with a biased, but statistically optimal, estimate of head orientation in space. In contrast
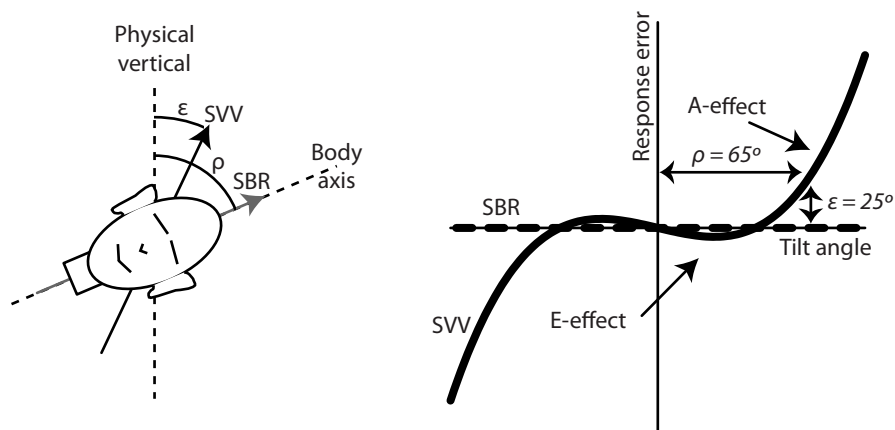

Figure 5.1   Visual-vestibular integration. Subject sets a luminous line either parallel to the perceived earth-vertical (black-white arrow), or estimate body orientation in space (gray arrow). With the body rolled over a large angle (ρ), the subjective visual vertical (SVV) deviates from physical vertical (error ε; A-effect). For small roll angles subjects may slightly overcompensate roll (E-effect). The error varies systematically with roll angle (solid black line, schematic data). The subjective body roll (SBR) aligns well with the actual body orientation for all roll angles (dached black line, schematic data).

to Mittelstaedt's proposal, the otoliths are assumed accurate, but contaminated with noise, which increases with roll angle. To cope with this neural variability, the Bayesian hypothesis assumes that in the visual task the brain uses prior assumptions about head orientations, e.g., upright is more likely than rolled. A Bayesian estimate (Dayan and Abbott, 2001) of head orientation is then biased toward the prior distribution (which explains the A-effect), but is less variable than the otoliths.

This study focuses on the integration of head-posture and acoustic spatial information. We wondered whether the auditory system is subjected to an A-effect when estimating a spatial auditory percept.

Sound localization

In contrast to the luminous line, the spatial representation of sound is far from perfect (Wightman and Kistler, 1989; Middlebrooks, 1992; Hofman and Van Opstal, 1998). Sound localization relies on implicit acoustic cues that are processed by independent neural pathways. Interaural time (ITD) and level (ILD) differences define locations in the horizontal plane (azimuth; Blauert, 1997); spectral-shape cues from the pinna encode vertical locations (elevation). Psychophysical experiments indicate that human sound- localization is accurate, but less precise when compared to visual localization (Frens and Van Opstal, 1995). Response variability is typically larger in elevation than in azimuth (Perrott and Saberi, 1990; Hofman and Van Opstal, 1998; Grantham et al., 2003), and varies with target eccentricity (Middlebrooks and Green, 1991; Frens and Van Opstal, 1995). Spatial resolution for azimuth decreases for far-lateral locations, and for elevation near the zenith (Hofman and Van Opstal, 1998).

Audio-vestibular integration

As there is no obvious equivalent of a vertical luminous line at straight ahead for audition, we presented auditory stimuli around the zenith, which for an upright head is straight above. We measured how subjects estimated the auditory zenith either straight above their head, or relative to the earth (i.e. opposite to gravity). In case of an auditory A-effect, one expects the world-centered zenith to shift in the direction of head roll.

To our knowledge, the only study on this topic is by Lechner-Steinleitner et al. (1981), who investigated how localization of a pure tone moving towards the zenith, is influenced by head orientation. Their data did not show an auditory A-effect.

By letting subjects actively roll their head either left-ear down, or right-ear down, we investigated the influence of head posture on perceived head-centered and earth-centered auditory zenith. We also determined the resolution of the auditory system around the zenith for sounds within different planes. We presented well-localizable broadband sounds at pseudo-random locations around the zenith, to prevent a potential effect of attention or prediction. Subjects indicated whether they perceived sounds left or right from the head- or world-centered zenith. In this way, listeners never indicated the zenith directly. Instead, we estimated perceived zenith (and its precision) by fitting psychometric curves through the responses for the different head-roll and plane conditions.

Our results show that subjects indicated the correct head-centered zenith regardless head roll for all stimulus conditions, but that the resolution for midsagittal plane locations

is much worse than for other planes. Moreover, we found a strong effect of head roll on the world-centered subjective auditory zenith, which provides the first evidence for an auditory A-effect.

METHODS

Listeners
Four male subjects (age: 20 to 22) participated in the experiments on a voluntary basis, including author BA. Subjects were free from vestibular or other neurological disorders, and had no hearing deficit.

Experimental setup
The listener sat in a completely dark, sound-attenuated room, in which black sound-absorbing foam effectively reduced echoes down to 500 Hz. A circular hoop with 58 speakers could rotate around the subject about a vertical axis with an angular resolution below one degree. Speakers were mounted with 5° spacing in elevation, but the 29 speakers on the frontal vs. back halves of the hoop were offset by 2.5°. Three orthogonal magnetic fields were generated by three pairs of squared coils along the edges of the room, which induced alternating voltages in a dual-search coil mounted on the subject's head to record 3D head orientation (Robinson, 1963). The coil signals verified whether the subject's head remained stable throughout the experiment. Apart from the coil signals, we recorded button presses on a button box. All signals were digitized at 1017.25 Hz/channel on Tucker Davis Technologies equipment (System 3).

Stimuli
Sounds were 150 ms of Gaussian White Noise (cut-off frequencies: 200 Hz HP and 20 kHz LP; e.g., Hofman and Van Opstal, 1998) with an intensity of 60 dBA (measured at the subject's head with a Brüel and Kjær microphone B&K 3134, and measuring amplifier B&K 2610). In contrast to tones, these noise bursts provided optimal localization cues to the auditory system. By varying the relative intensities of two nearby speakers on the hoop we implemented a spatial resolution down to 1.25° (Bremen et al., 2010).

Experimental Paradigms
Listeners were positioned with their head in the centre of the hoop. They responded in a two-alternative forced choice (2AFC) approach, by pressing either one of two buttons on the button box. When upright the listener responded to stimuli within four different stimulus planes presented in different blocks: frontal plane (FP), midsagittal plane (MSP), left-anterior/right-posterior plane (LARP) and right-anterior/left-posterior (RALP) plane (Fig. 5.2A). The subject had to indicate whether the sound was perceived to the left vs. right of the zenith in the FP, LARP and RALP planes, or at front vs. back in the MSP plane.

In a subsequent experimental session with the head in a static rolled position (either left-ear down or right-ear down by about 35°), stimuli were presented in the FP, and listeners indicated whether the sound was heard left vs. right of the head-centered (Z_H), or world-
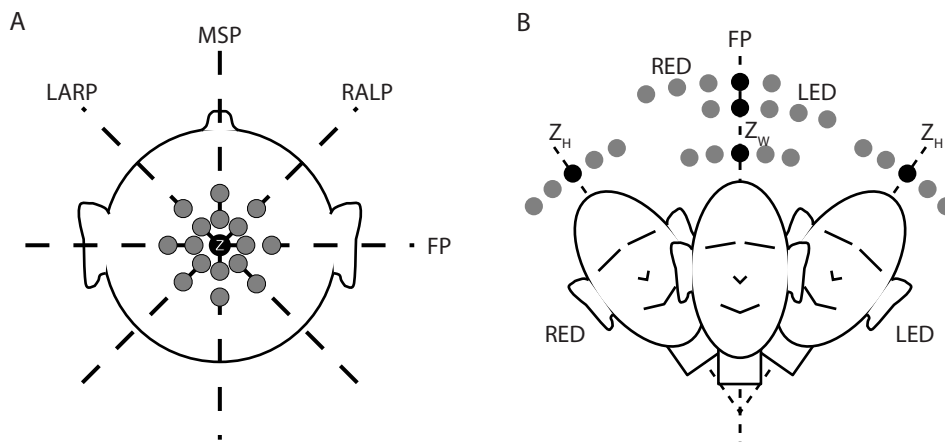
Figure 5.2   A) With the head upright sounds were presented in different planes around the auditory zenith (Z; top-view head). FP: frontal plane; MSP: midsagittal plane, LARP: left-anterior/right-posterior plane, RALP: right-anterior/left-posterior plane. B) Stimulus presentation in the FP with the head upright, or during a static active head roll of 35° RED, or LED. Subjects responded whether the sound (gray dots) was presented left or right from either the head-centered zenith (Z_H), or left or right from the world-centered zenith (Z_W). Note asymmetric stimulus arrays around Z_W for the RED/LED conditions.

centered (Z_W) zenith (Fig. 5.2B). Subjects responded open loop, as they never received any feedback about performance. That way we avoided potential effects of perceptual learning. If perceptual learning would have occurred in this fixed-order block design, response precision should improve over trials/blocks, which was not the case: MSP precision was always much worse than FP precision (see Results).

The subjects' answers were converted into psychometric curves (see Data Analysis). For a reliable fit, data should symmetrically cover the full perceptual range that includes the threshold (50% correct) and the upper (100% correct) and lower ends (0% correct). Therefore, to prevent oversampling (leading to unnecessarily long experiments), or measuring irrelevant regions of the psychometric curve, we used different physical speaker locations, resolutions and ranges for the different conditions, which were determined by pilot experiments.

In the FP, sounds were at [0 ±1.25 ±2.5 ±5 ±7.5]° (right positive) with respect to head-centered zenith. Because pilot experiments indicated a much poorer auditory spatial resolution in elevation around zenith, sounds were presented over a broader range in the MSP: [0 ±5 ±10 ±15 ±20 ±30 ±40]° (front positive). In the LARP/RALP planes we presented sounds at [0 ±2.5 ±5 ±7.5 ±12.5]° (anterior positive).

In static roll experiments the subject actively rolled the head by 35° (right ear down, RED), or -35° (left ear down, LED; Fig. 5.2B), which was about the maximal roll subjects could comfortably maintain. In the head-centered zenith task, sounds were presented between [-7.5, +7.5]° around the head-centered zenith (resolution as in upright FP). In the world-centered zenith task sounds were presented at [-40, -35, -30, -20, -15, -10, -5, +5, +10]° around the gravity zenith for LED, and at [-10, -5, +5, +10, +15, +20, +30, +35, +40]° re. zenith for RED. These physically asymmetric target sequences were chosen, as pilot experiments indicated that perceptually these target ranges were heard approximately symmetric around the perceived world-centered zenith. In this way, the listeners' responses covered the entire perceptual

range in an unbiased way, which was required for a reliable psychometric measurement. For all conditions, each sound location was presented 20 times, resulting in experimental blocks of about 8 minutes. The experiments with static head roll were divided in two blocks of 10 repetitions per sound location, to prevent discomfort for the listener.

Although the number of physical stimulus locations differed slightly for the different stimulus planes (13 for MSP, vs. 9 for FP), we think it's unlikely that response accuracy and precision were influenced by these differences, as all stimuli (20 repetitions each) were always presented in pseudorandom order, and subjects responded open loop, never receiving any feedback about performance.

Data Analysis
Off-line data analysis used custom-made routines in Matlab (Matlab 7.6, The Mathworks). Psychometric data were analyzed by calculating the proportion of 'right' (or 'front') responses for each stimulus location and fitting a cumulative normalized Gaussian through the data by using the method of maximum likelihood (Wichmann and Hill, 2001a). The psychometric curve, $\psi(x)$ (x is stimulus location), is thus given by:

$$\Psi(x) = \lambda + (1 - 2\lambda) \cdot erf(x; \mu, \sigma) \tag{5.1}$$

in which $erf(x;\mu,\sigma)$ is the error function (mean μ, standard deviation σ). The mean (threshold) represents the location of the subjective auditory zenith, which serves as a measure of accuracy. The standard deviation, which reflects the slope around threshold, measures response precision. The lapse parameter, λ, represents stimulus-independent errors that may be due to mistakes, a bias, or random guessing. It was constrained to maximally 10%.

RESULTS

The auditory zenith in upright listening
Figure 5.3 shows results for the four stimulus planes of listener KA sitting upright (Fig. 5.2A). The thresholds of the psychometric curves indicate an accurate percept of the auditory zenith in all four planes (mean close to zero: 0.08 ± 0.33°), but response precision was direction dependent. As standard deviations (precision) for the RALP/LARP and FP planes were highly similar (mean ± SD: 3.7 ± 1.3°), for the MSP it was clearly higher (11°).

Figure 5.4 presents accuracy and precision results of all listeners when estimating the head-centered auditory zenith for the different stimulus planes. All thresholds were within 5° (0.65 ± 0.57°; Fig. 5.4A) of the physical head/gravity zenith. The only exception concerned listener BA, whose responses to MSP stimuli were virtually random, leading to an unreliable psychometric fit. Excluding this one condition, the main trend is that upright listeners were quite accurate in defining the true auditory zenith (two-sided t-test between true and estimated zenith: P > 0.25 for all conditions).

Figure 5.4B shows a clear effect of stimulation plane on response precision (ANOVA with stimulation plane as factor: $F(3,11) = 14$, P = 0.0004; excluding BA_{MSP}). The precision
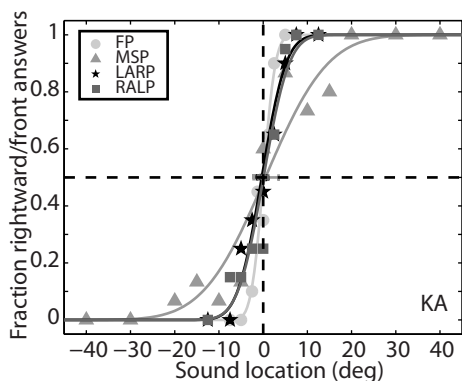
Figure 5.3   Responses to stimuli in the four planes with the head upright (subject KA): Psychometric curves for frontal plane (dots), midsagittal plane (triangles) and the LARP (stars) and RALP (squares) planes. Thresholds are determined by 50% rightward responses (horizontal/vertical dashed line), and measures response accuracy; the slope at threshold measures response precision (variance). In all four cases accuracy is high, as thresholds are close to 0°. MSP precision, however, is worse than for the other three planes.

measures for the FP, RALP and LARP planes were very similar, but the standard deviations for MSP stimuli were much higher (Bonferroni-corrected t-tests: P < 0.005).

Compensation for head roll

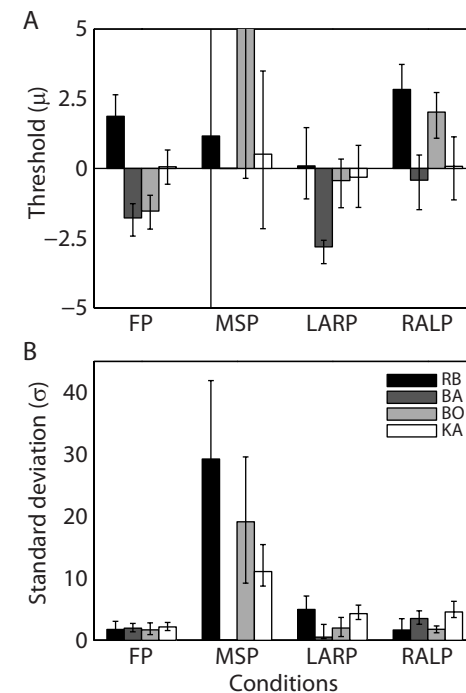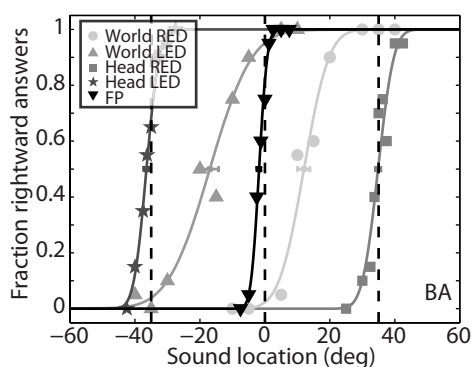Figure 5.5 compares the results of listener BA for the craniocentric zenith task for FP

Figure 5.4   A) Accuracy of the psychometric curves for all four subjects and stimulus planes with the head upright. All thresholds are within a few degrees (mean ± SD: 0.62 ± 0.57°) of the true auditory zenith, except for the MSP data of subject BA. All four subjects are quite accurate in determining craniocentric auditory zenith. Error bars denote 95% confidence intervals of fit. B) Precision data. For all subjects precision was high in FP and in the RALP/LARP planes, but much worse for MSP stimuli. Error bars denote 95% confidence intervals of fit.

stimuli when sitting upright (black triangles), with the head rolls of 35° RED (grey stars) and LED (grey squares). Note that the thresholds (small squares) in all three curves were close to the actual head axis (vertical dashed lines), indicating good accuracy for the three head

Figure 5.5   Psychometric curves during head roll of ±35° (subject BA). Stars and squares show the curves for the head-centered task. Vertical dashed lines: true head-centered zenith. Subject is accurate in localizing the head-centered zenith, as thresholds are close to the true locations (vertical dashed lines). Circles and gray triangles: world-centered zenith task for head rolls of ±35°. Thresholds shifted into the direction of head roll, and response variability increased when compared with head upright data for FP stimuli (black triangles).
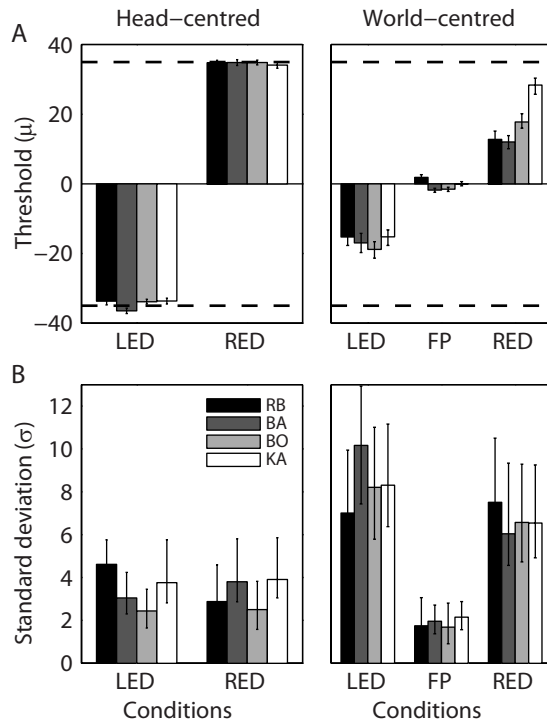
Figure 5.6 A) Response accuracy for all subjects during head roll for head-centered (left) and world-centered (right) zenith localization. Dashed lines: actual craniocentric zenith locations. All subjects were accurate in the head-centered task, whereas they made large systematic errors in the direction of head roll for the world-centered task (auditory A-effect). Error bars denote 95% confidence intervals of fit. B) During head roll, response precision was lower than for the upright orientation (FP) for either task. Error bars denote 95% confidence intervals of fit.

postures. The figure also shows the results of the world-centered zenith task for the head-roll conditions (LED: light-grey triangles, RED: light-grey dots). For an accurate world-zenith estimate, the curves should coincide with the central (FP) response curve around 0°. This is clearly not the case, as the two curves shifted in the direction of head roll (LED: -17°, RED: 12°). Note that also their standard deviations (LED: 10°, RED: 6.0°, FP: 1.9°) differ from the upright condition, indicating increased response variability.

Figure 5.6 presents the results for all subjects. The left-hand column shows thresholds (A) and standard deviations (B) of the psychometric curves for the head-centered zenith task under LED and RED conditions. The dashed lines correspond to the true head zenith. All subjects accurately estimated the craniocentric auditory zenith (two-sided t-test between true and estimated zenith: $P > 0.12$ for all conditions). The right-hand side shows the results of the world-centered task, with the upright FP data for comparison. The data indicate a substantial and consistent shift of the perceived auditory earth-vertical into the direction of head roll by about 10-15° (ANOVA with head roll as factor: $F_{(2,9)} = 56$, $P \ll 0.0001$).

The precision data of the head- (Fig. 5.6B, left) and world-centered (right) settings for the different head postures show an effect of head roll on response variability when compared to the upright FP estimates (ANOVA with head roll as factor: head-centered: $F_{(2,9)} = 6.4$, $P = 0.019$; world-centered: $F_{(2,9)} = 65$, $P \ll 0.0001$). Specifically, precision decreased for all listeners and for both tasks when they rolled their head (two-sided t-tests on precision differences between FP and head tilt: $P < 0.05$ for all conditions).

DISCUSSION

Effect of auditory cues

We tested accuracy and precision in determining the auditory zenith, either straight above the head, or along the direction of gravity. With the head upright we found (i) accurate localization of the zenith for all stimulus planes, but (ii) lower precision for sounds within the MSP, than for the other three planes (Fig. 5.4). Differences in accuracy and precision for FP vs. LARP/RALP were minor. These results therefore suggest that binaural difference cues dominated around head-centered auditory zenith, and only for the MSP configuration subjects exclusively relied on poorly defined spectral-shape cues.

Auditory Aubert effect

Accuracy of the craniocentric auditory zenith under the two head-roll orientations was similar as for head-upright (Figs 5.5 and 5.6A, left). However, precision of the head-centered estimates in roll was worse than for FP upright (Fig. 5.6B, left), which suggests an influence of head orientation on the precision of processing binaural difference cues.

When estimating the world-centered auditory zenith, however, subjects were inaccurate, with 10-15° errors in the direction of head roll (Fig. 5.6A, right). This finding resembles the visual Aubert effect (see Introduction), and may therefore be termed Auditory Aubert (AA)-effect. Compared to the visual A-effect, which starts for roll angles beyond about 60°, the AA-effect kicks in at a much smaller roll angle. The precise behavior of the effect will have to be assessed in future experiments; for this report we only determined the effect for a particular roll angle.

In addition, the variability of the world-centered responses was higher when compared to head-centered roll and head-upright data in the FP (Fig. 5.6B). It is not immediately obvious whether this increased variability is due to a (slight) deterioration of the binaural difference cues at more lateral azimuth angles, to an influence of head-roll, or to both. Spatial resolution of the auditory system is about one degree around zero azimuth, and declines with azimuth angle (Grantham, et al. 2003; Perrot and Saberi, 1990; Hofman and Van Opstal, 1998), with poorest performance near the interaural axis. Under roll conditions, stimuli were presented (in head-centered coordinates) around $[\alpha,\varepsilon] = [0,90]°$ (head-centered task) and $[\alpha,\varepsilon] = [\pm20,70]°$ (world-centered task). Therefore, an effect of cue resolution on response variability may have played only a minor role.

Other studies

Few studies investigated the influence of changes in head orientation on sound localization. Goossens and Van Opstal (1999) studied eye movements to pure tones with the head pitched, and found that responses were directed toward a location between a head-centered and world-centered reference frame, depending on tone frequency. Since eye movements toward broadband noise stimuli were accurate, the authors suggested that a static head-orientation signal interacts within the tonotopically-organized auditory system. Although the interaction might be due to a gravitational signal from the otoliths, Kopinska and Harris (2003) found that pointing errors toward dichotic auditory stimuli were mostly attributed to (yaw-induced)

head-on-neck signals. In a visual remembered-saccade task, Klier et al. (2005) showed that both efference copies of head movement (yaw rotation only) and gravitational signals (pitch and roll head orientations) contribute to spatial updating of saccades, and it is conceivable that this holds true for audition as well. Indeed, Goossens and Van Opstal (1999) and Vliegen et al. (2004) showed that intervening movements of the head in rapid eye-head gaze shifts are fully incorporated in sound-localization responses to broadband noises, suggesting the accurate on-line use of efferent feedback signals. This high accuracy contrasts with the errors observed in perceptual tasks employed in (off-line) lateralization experiments, or pointing tasks.

Others have also assessed the effect of changes in head orientation on sound lateralization. For example, passive whole-body rotational vestibular stimulation around the earth-vertical axis affects sound- lateralization (audiogyral illusion), in which the auditory median plane (where ITDs and ILDs are perceived as zero) shifts in the direction of rotation (Clark and Graybiel, 1949; Lewald and Karnath, 2001). Recently, Van Barneveld and Van Opstal (2010) argued that this effect is due to changes in mean eye position, caused by quick phases of vestibular nystagmus.

Stimulation of the otoliths by linear acceleration in a centrifuge (Graybiel and Niven, 1951; Dizio et al., 2001), or by passive whole-body roll (Lewald and Karnath, 2002) also affects sound lateralization: sounds at straight ahead shift a small amount towards the (perceived) upper ear (audiogravic illusion). In the head-centered zenith task we did not observe this effect (Fig. 5.6A, left). Possibly, the illusion disappears around the zenith, where the spectral cues are less reliable.

To our knowledge, the only study on the influence of static head roll on perceived world-centered auditory zenith was by Lechner-Steinleitner et al. (1981), who found no net effect of LED head roll after averaging their data from leftward and rightward sound presentations. However, they reported hysteresis: when sounds approached from the right, the perceived zenith shifted rightward, whereas a leftward shift was found for sounds on the left side. The origin of the hysteresis is not clear, but perhaps the repeated presentation of sounds on the same side may have drawn attention, or expectation, of sound locations toward that side. In the presence of such a biased nonlinearity, averaging data does not seem appropriate. A second difference with our study is the use of a low-frequency tone (323 Hz), instead of a well-localizable broadband noise burst. Such a tone only contains ITD information, as ILDs and spectral pinna cues are negligible. As a result, the ill-defined sound elevation could have caused the actual spatial percept of stimuli to move along a frontal straight-ahead path in azimuth. In any case, it seems unlikely that subjects perceived such stimuli around the world-centered zenith. We have attempted to use an unbiased approach: subjects were tested open loop, and never directly indicated the perceived zenith. They responded to broadband, well-localizable stimuli that were symmetrically arranged around the perceived task-related zenith. In addition, sounds were drawn at random, so that the likelihood of left vs. right was the same. Under these conditions we obtained a clear AA-effect on the percept of a world-centered auditory zenith.
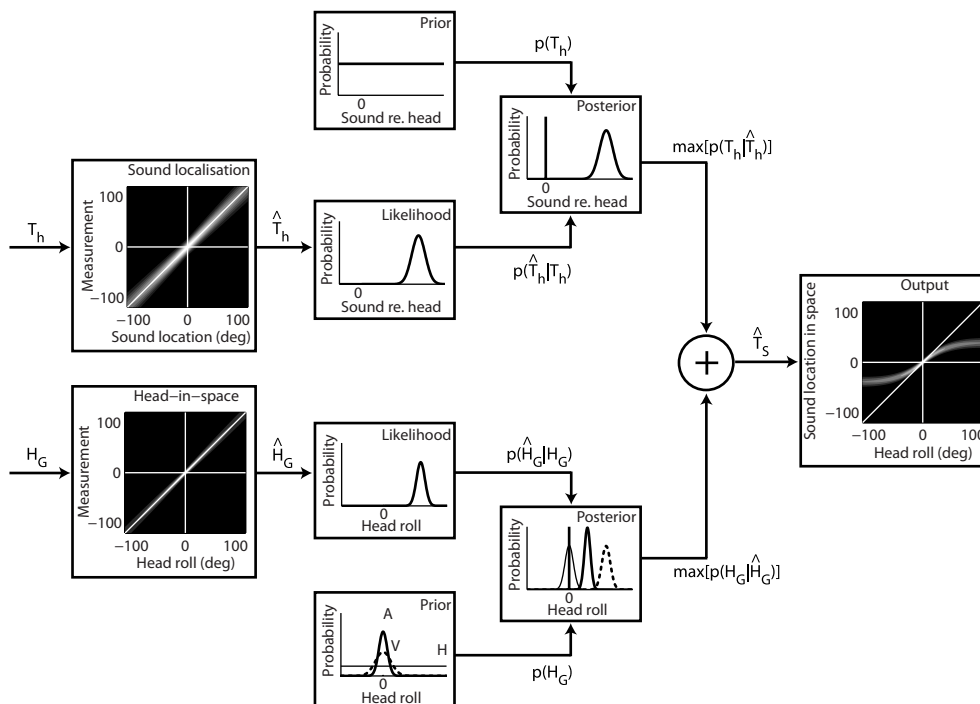
Figure 5.7   Model that explains the auditory A-effect. The head-re.-gravity estimation is based on the same Bayesian mechanism as discussed in De Vrijer et al. (2008): the actual head orientation re. gravity (H_G) induces an ambiguous otolith signal ($\hat{H}_G$ the same neural signal corresponds to many potential head orientations). This is represented by the likelihood function that is weighted against the prior expectation of possible head orientations, which peaks around upright (0°). The prior in the auditory task (A) is narrower than for visual stimuli (V), or for head-estimation (H, flat). The posterior distribution has smaller variance than the prior (thin black line) and likelihood (dashed line), but is biased toward the prior (Eqn 5.2). The auditory cues are noisy too, but the prior expectation of sounds is assumed uniform. As a result, the posterior estimate equals the likelihood. At the output, the sound location in space (T_s) estimate is biased toward the head-centered zenith.

Implications for models

The Bayesian model of De Vrijer et al. (2008) cannot readily explain our results. First, head-on-body roll in our experiments was only 35°, while the (visual) Aubert effect starts beyond 50-60°. Second, in the Bayesian model the retinal representation of the luminous line is close to perfect with little variability, so that the likelihood for visual stimuli resembles a delta peak at the actual retinal location. For audition, however, this is not the case: sound localization relies on the integration of different acoustic cues, each with varying reliabilities. It may be assumed that the acoustic likelihood function peaks around the true head-centered location, as sound localization is accurate, but with considerable direction-dependent variability. In a Bayesian model, this would invoke a prior about craniocentric sound locations to get optimal estimates with smaller variance. For example, the auditory system could assume that sounds typically originate from straight-ahead. The Bayesian estimate for a sound at the left would then shift towards the centre. Hence, in LED roll, a stimulus at the world-centered zenith (i.e. rightward with respect to the head) would be perceived left from the zenith. However, our results indicate an opposite effect (Fig. 5.5)!

The Bayesian model could account for our data under the assumption that the estimate of head orientation is biased, like in De Vrijer et al. (2008), in combination with an accurate representation of the sound's location (Fig. 5.7). Thus, sound locations have a uniform prior: they can originate anywhere with equal probability. To explain the earlier onset of the AA-effect, the prior for head orientation should have a narrower peak around upright for auditory than for visual stimuli, as the Bayesian posterior for head orientation is determined by:

$$\widehat{H}_{post} = \frac{\sigma_{prior}^2}{\sigma_{prior}^2 + \sigma_{otolith}^2} \cdot \widehat{H}_{otolith} + \frac{\sigma_{otolith}^2}{\sigma_{prior}^2 + \sigma_{otolith}^2} \cdot \widehat{H}_{prior} \qquad (5.2)$$

with σ_H the standard deviation of signal H, and $\hat{H}$ its mean. In case $\sigma_{prior} \ll \sigma_{otolith}$ Eqn 5.2 is dominated by the prior, resulting in a strong A-effect. In the head-centered task the head prior is supposed to be uniform, yielding an accurate estimate of head orientation. In other words, the influence of the prior would be task and modality dependent. The modality dependence underlies differences for auditory, visual, vestibular, and tactile stimuli, and could be determined by the reliability of the respective sensory inputs.

The results of response variability (Fig. 5.6B) may be qualitatively understood from the model too. The final stage adds two independent stochastic signals ($\widehat{T}_G = \widehat{T}_H + \widehat{H}_G$), and therefore the response variability increases as $\sigma_{H+A} = \sqrt{\sigma_A^2 + \sigma_H^2}$. In the upright task, the standard deviations of auditory and head-posture signals are minimal, and total response variability is expected to be smallest. In the tilted world-centered task the standard deviations of both signals increase, and therefore variability is highest for that task, with the tilted head-centered task yielding intermediate results.

ACKNOWLEDGEMENTS

Adapted from: Van Barneveld, D.C.P.B.M. and Van Opstal, A.J. (2010) Eye position determines audio-vestibular integration during whole-body rotation. Eur J Neurosci, 31, 920-930

6

Eye position determines audio-vestibular integration during whole-body rotation

Denise C.P.B.M. Van Barneveld
A. John Van Opstal

INTRODUCTION

Sound localization relies on the neural processing of acoustic cues, as binaural differences in timing (ITDs) and sound level (ILDs) specify horizontal sound positions, while direction-dependent pinna reflections determine vertical locations (Wightman and Kistler, 1989; Middlebrooks, 1992; Blauert, 1997). Free-field sound-localization studies indicate accurate behaviour, even in the absence of any feedback about performance (open-loop testing; Oldfield and Parker, 1984; Middlebrooks and Green, 1991; Hofman and Van Opstal, 1998; Vliegen et al., 2004).

To compensate intervening eye, head and body movements, head-centered acoustic inputs should be updated by proprioceptive body-posture signals, efference copies of motor commands, and vestibular signals. This multimodal integration appears accurate for auditory evoked gaze-orienting (Goossens and Van Opstal, 1999; Vliegen et al., 2004). Yet, small but systematic localization errors have been observed. For example, Goossens and Van Opstal (1999) noted that gaze-endpoints slightly overestimated eye position, causing small errors around auditory targets that opposed eye-in-head orientation. Recently, Razavi et al. (2007) reported that prolonged (up to 20 min) eccentric eye-fixation induced localization errors in the same direction as eye-in-head orientation.

In sound-lateralization studies subjects indicate whether sounds are heard either left or right from the head's midsagittal plane. Under normal headphone listening (dichotic hearing), with eyes and head stationary and straight-ahead, the so-called auditory median plane (AMP; Fig. 6.1) typically coincides with the midsagittal plane. However, when the eyes are held in an eccentric orientation, the AMP moves slightly in the same direction (Lewald and Ehrenstein, 1996).

Vestibular stimulation could also affect sound lateralization. Early free-field lateralization studies demonstrated a perceived shift of head-fixed sounds opposing the direction of passive whole-body rotation, a phenomenon known as the audiogyral illusion (AGI; Münsterberg and Pierce, 1894; Clark and Graybiel, 1949). As Figure 6.1 illustrates, the AMP would then shift in the same direction as perceived rotation.
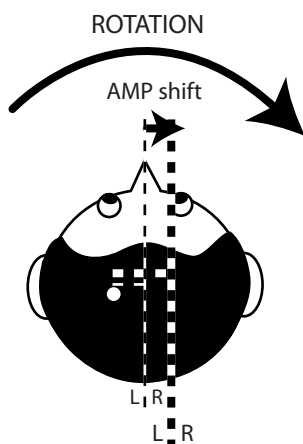

Figure 6.1   The audiogyral illusion (AGI). The vertical dashed line represents the auditory median plane of the head (AMP) under stationary hearing. Sounds presented on the AMP are perceived in the centre of the head. Note that acoustic parameters determine the AMP (it is defined as perceived ILD=0 and/or ITD=0), not a spatial reference (like, e.g. perceived straight-ahead). For example, a plugged ear would shift the AMP to the ipsilateral side, without affecting the perceived body or visual straight-ahead direction. If during vestibular stimulation the AMP shifts in the direction of rotation (thick versus dashed line), a head-fixed sound (black dot) would be heard displaced in the direction opposing rotation (thick leftward horizontal line). To prevent confusion, we describe effects of audio-vestibular integration in terms of (dichotic) AMP shifts (in dB ILD/µs ITD), rather than by corresponding opposite (free-field) sound-location shifts (in °).

To date, the source of this illusion is not well understood, though various hypotheses exist. Clark and Graybiel (1949) attributed the AGI to an erroneous sense of perceived rotation. Alternatively, it could arise from misperceived head-on-trunk orientation (kinaesthetic illusion; Lester and Morant, 1969; 1970; Lackner, 1974). Also, spatial attention may influence dichotic listening (Bohlander, 1984). Importantly, since in darkness quick phases of vestibular nystagmus shift mean eye-in-head position into the rotation direction (Chun and Robinson, 1978; Vidal et al., 1983; Carpenter, 1988), ocular nystagmus could potentially underlie the AGI (Arnoult, 1950; Thurlow and Kerr, 1970). In line with this, Quarck et al. (2009) noted that eye position affects perceived body-rotation.

When a fixation light suppresses vestibular nystagmus under dichotic listening, the reported AMP shift opposes perceived rotation, and thus would also oppose the AGI (Lewald and Karnath, 2001). However, even though a fixation light stabilises head-centered eye position, oculomotor control is far from inactive. Rather, ocular pursuit in the direction of rotation compensates for the vestibular slow phase (Barnes, 1993, for review), and this could induce an additional AMP shift that opposes vestibular rotation. Furthermore, the visual fixation point could affect perceived sound locations through either visual capture (ventriloquist illusion, Alais and Burr, 2004), or attention (Bohlander, 1984).

The present study attempts to identify the mechanism underlying the vestibular-induced shift in sound lateralization, and tests whether effects on the AMP are caused by changes in eye position. Subjects underwent sinusoidal rotation at different chair velocities while lateralising dichotic sounds, either in darkness, or with a fixation light. To investigate the influence of eye velocity on sound lateralization, stationary subjects also tracked moving visual stimuli in the same sound-lateralization task. Our results show that a shift in average eye position explains the AGI. We discuss potential neural mechanisms.

METHODS

Subjects

Eleven subjects (five females, six males; age 20 to 51) participated in this study. All subjects participated in the audio-vestibular experiments in darkness with a peak chair velocity of 107°/s (see below), while a subset of 9 subjects (AP, DB, EM, MV, JK, JO, RH, RHE and ST) also participated in the other experiments, including the smooth pursuit paradigms. We measured eye movements in four subjects (DB, MV, JK and JO) during a shortened version of the audio-vestibular experiments.

All subjects had normal hearing, except RHE who had slightly elevated thresholds in the low-frequency audiogram (< 2 kHz) of the right ear. This subject was nevertheless able to perform in these experiments, in which we employed broad-band noise bursts. Three subjects (including the authors) were familiar with the purpose of the experiments; all other subjects were kept naive. Prior to the first experiment, some practice trials were presented without vestibular stimulation to all subjects to allow them to get acquainted with the procedure and the different stimuli. All subjects had normal or corrected-to-normal vision except for JO, who is amblyopic in his right, recorded, eye.

Experiments were conducted after full understanding and written consent was obtained from the subject. The experimental procedures were approved by the Local Ethics Committee of the Radboud University Nijmegen and adhered to The Code of Ethics of the World Medical Association (Declaration of Helsinki), as printed in the British Medical Journal of July 18, 1964.

Apparatus and stimuli

Auditory stimuli

Auditory stimuli were digitized in Matlab (The Mathworks, Natick, MA). Signals consisted of a single 100 ms broadband Gaussian white noise burst (bandwidth 0.2-20 kHz), with 5 ms sine-squared onset and offset ramps. In order to provide the auditory localization cues with as much spatial information as possible, we applied co-varying interaural time and level differences to the broadband noise signal. The ILD ranged from -2 dB (unambiguously perceived left of the AMP) to +2 dB (always perceived right) in nine steps of 0.5 dB. Variations of ILD were symmetrical, i.e. if the ILD was +2 dB, the left ear was attenuated by 1 dB, whereas the right ear was amplified by 1 dB. For the ITDs we had to employ two different sets, due to differences in D/A-sampling rates of our setups. In the audio-vestibular sessions, sounds were played with a sample frequency of 50 kHz and the ITD ranged from -80 µs (left) to +80 µs (right), in nine steps of 20 µs. In the smooth pursuit sessions (measured in a different setup), the sample frequency was 44.1 kHz and the ITD ranged from -90 µs (left) to +90 µs (right), in steps of 22.5 µs.

Sounds were presented to the subject via headphones (Pioneer SE-205) at 53.3 dBA (calibrated with a Brüel and Kjær sound amplifier) in the ocular smooth pursuit experiments, and at 57.3 dBA in the vestibular experiments. Subjects consistently perceived the dichotic stimuli as intracranial sound images.

Vestibular stimuli

In the audio-vestibular experiments, the subject was seated in a computer-controlled vestibular chair (Vingerhoets et al., 2006). The trunk was tightly strapped with seat belts, while Velcro straps restrained the legs. The subject wore headphones and the head was stabilized in the natural upright position, looking straight ahead with a padded adjustable helmet. The present study employed sinusoidal yaw rotations of different amplitudes (90°, 115°, 140°) at a frequency of 0.125 Hz, which corresponded to three different peak chair velocities of 68, 87 and 107°/s, respectively.

Visual stimuli

Audio-vestibular experiments were conducted either in complete darkness, or with an optional fixation light (approximately 0.088 cd/m^2, measured at a distance of 1.1 m with Minolta LS-100 luminance meter) that was attached to the frame of the chair, such that it rotated along with the subject at a distance of 85 cm.

During the ocular smooth pursuit experiments, subjects sat in a darkened room (0.32 cd/m^2) with the head aligned to the centre of a computer screen, and fixated by a chin rest.

The visual target was a red dot (1.60 cd/m^2) that moved sinusoidally at a frequency of 0.24 Hz with peak amplitudes of 11.3° and 17.4°. These peak amplitudes were chosen to correspond approximately to the observed range of mean eye positions during the audio-vestibular experiments in darkness (see Results). The frequency was chosen to allow for comfortable eye tracking of the visual stimulus at peak-eye velocities of 16.9 and 26.0°/s, respectively.

Eye-movement measurements
In the oculomotor session, horizontal and vertical components of eye position were measured with the magnetic search-coil technique (Collewijn et al., 1975), using oscillating magnetic fields (30k and 40k Hz, respectively) generated by two sets of orthogonal coils (0.77 x 0.77 m) inside the vestibular stimulator. The horizontal and vertical eye-position signals were amplified, demodulated (PAR128A), and sampled at 500 Hz per channel before being stored on the computer's hard disk.

Response measures
Prior to the first experiment, all subjects were given a brief practice session without vestibular rotation to get acquainted with the psychophysical procedure. First, the outermost left and right auditory stimuli were presented alternately, after which all nine stimuli were presented in the left to right order. Subjects never received feedback about their performance.

To determine a subject's psychometric curve, we applied the method of constant stimuli. To that end, the nine sound stimuli were presented in pseudo-random order, whereby each stimulus was repeated 20 times. This procedure yielded a robust estimate of the psychometric curve. After the presentation of a sound, the subject judged its lateralization relative to the AMP (two-alternative forced choice, left/right) using a joystick that was operated with the right hand. The AMP was described to the subject as the plane bisecting the head in two halves, with the nose being on that plane. From the 180 individual answers the percentage rightward judgements of each stimulus (ITD/ILD combination) was computed off-line, resulting in a psychometric curve (% rightward as function of ILD/ITD). From this psychometric curve the AMP could be extracted by assessing the ILD/ITD value at which the subject responded 50% rightward (see Curve fitting).

Experimental paradigms
The experimental paradigms were designed to investigate the potential influence of the visual and oculomotor systems on the interaction between the vestibular and auditory systems.

Sinusoidal rotation with and without fixation light
An experimental session consisted of eight runs. The first and last runs, in which the subject was stationary, served as a consistency check of the subject's performance. Both runs consisted of 180 auditory stimuli (20 repetitions of nine stimuli, one psychometric curve). In the remaining six four-minute audio-vestibular runs, the subject was rotated sinusoidally about the Earth-vertical axis at 0.125 Hz with a peak velocity of either 68°/s, 87°/s or 107°/s (fixed within an experimental session). Each run consisted of 30 sine periods, during which four auditory stimuli were presented per period (Fig. 6.2). To avoid discontinuities in velocity and
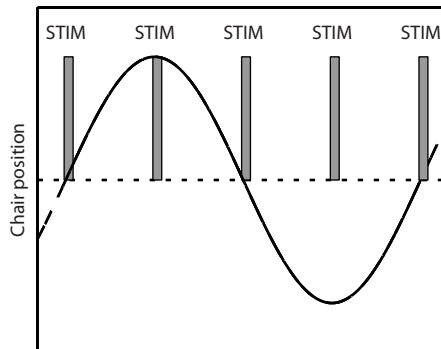
Figure 6.2 The vestibular chair rotated sinusoidally with a period of 8.0 seconds and at different amplitude displacements of 90, 115 or 140° (black line), such that the peak chair velocity was 68, 87 or 107°/s, respectively. Sound stimuli (marked by the gray bars) were presented both at left/right peak chair displacement (nrs 2 and 4) and at the zero crossings corresponding to the peak chair velocities (nrs 1, 3 and 5).

acceleration at motion onset, angular velocity increased linearly over the first two sinusoidal periods in which no auditory stimuli were presented (see Merfeld et al., 2005; Kaptein and Van Gisbergen, 2006).

Auditory stimuli were presented at peak chair amplitude, both left and right, and at peak chair velocity (i.e. at chair amplitude 0°), both in leftward and rightward movement directions (see Fig. 6.2) such that at each of these four chair positions, 20 repetitions of nine auditory stimuli were presented (four psychometric curves).

Smooth pursuit experiment
Subjects tracked a sinusoidally moving visual target without whole-body rotation, while dichotic stimuli were presented either at peak eye-position amplitude (11.3°, 17.4°), both left and right, or at peak eye velocity (26.0°/s), both in leftward and rightward direction. An experimental session consisted of four runs of 90 auditory stimuli, such that in total two psychometric curves were sampled.

Eye-movement measurements
In this experiment the subject wore an eye coil to measure the actual pattern of eye movements during vestibular stimulation. The session started with a calibration run in which 37 LEDs were presented (eccentricity re. straight ahead, $R = 0, 10, 20$ and $30°$, direction re. horizontal, $\Phi = 0$ to $360°$ in $30°$ steps), which the subject had to fixate. Subsequently the subject was sinusoidally rotated at 0.125 Hz for 30 cycles at different peak velocities in complete darkness (at 68, 87 and 107°/s), and with chair-fixed straight-ahead fixation light (only measured at 107°/s), while performing the same, although shortened, 2AFC task. Instructions were the same as in the vestibular experiments.

Data analyses and statistics

Curve fitting
Subjects made two-alternative forced choice lateralization judgments (left/right) on the 180 sound stimuli. The proportion of the subject's "rightward" judgements for each of the stimuli was determined as function of stimulus ILD/ITD for the different conditions. Data were subsequently modelled by a cumulative gaussian psychometric function, $F(x;\mu,\sigma)$ defined as

follows:

$$\Psi(x; \mu, \sigma, \gamma, \lambda) = \gamma + (1 - \gamma - \lambda) \cdot F(x; \mu, \sigma) \qquad (6.1)$$

with mean, μ, and standard deviation, σ, using the psignifit toolbox (ver. 2.5.6) for Matlab (http://bootstrap-software.org/psignifit/), which implements the maximum-likelihood method (Wichmann and Hill, 2001a;b). The stimulus-independent errors (so-called lapses) γ and λ were constrained to be symmetrical and were allowed to be maximally 10%. The auditory median plane (AMP) was defined as the 50% rightward threshold, thus corresponding to the mean of the cumulative gaussian. 95%-confidence intervals of the AMP were determined by the bootstrap method implemented by the psignifit toolbox based on 1000 simulations.

Data exclusion criteria

Pilot experiments (Fig. 6.3) showed that the control AMP could vary slightly, though not systematically, over days. Therefore as explained above, each vestibular experiment started and ended with a stationary run, to determine two stationary reference curves. Vestibular data were excluded for further analysis if the two stationary reference curves differed significantly (P > 0.05, 7/38 experiments). This was determined by the likelihood ratio test with four degrees of freedom, which tests the null hypothesis that two psychometric curves have the same underlying distribution.

In the smooth pursuit sessions no reference curves were measured. Accordingly, we did not apply the exclusion criteria to these experiments.

Eye movements

In the oculomotor audio-vestibular experiment, horizontal and vertical eye-coil signals were calibrated offline using two trained neural networks (for the horizontal and vertical channels) that had been obtained from fixation data in the eye-coil calibration run (for details, see Goossens and Van Opstal, 1997b). To determine the mean eye position during vestibular stimulation, the calibrated horizontal eye movement data were averaged over 30 chair cycles and fitted with a sine. Quick phases were not removed in this analysis. Since in this study the head is restrained with respect to the trunk, eye position in the head is the same as eye position relative to the body.

RESULTS

Effect of chair velocity in darkness on AMP

In Figure 6.4A we show two examples of typical psychometric curves that were obtained from the discrimination responses of subject RH at maximal chair velocity during leftward and rightward vestibular stimulation in darkness. At rightward rotation (107°/s) the psychometric curve, and hence the AMP, shifted to the right with respect to leftward rotation (-107°/s), a finding obtained in six of nine subjects (likelihood ratio test: P < 0.05). Consequently, perceived locations of auditory stimuli would shift in the opposite direction. For example, from the graphs in Figure 6.4A it can be deduced that the same stimulus at ILD = 0 dB (ITD
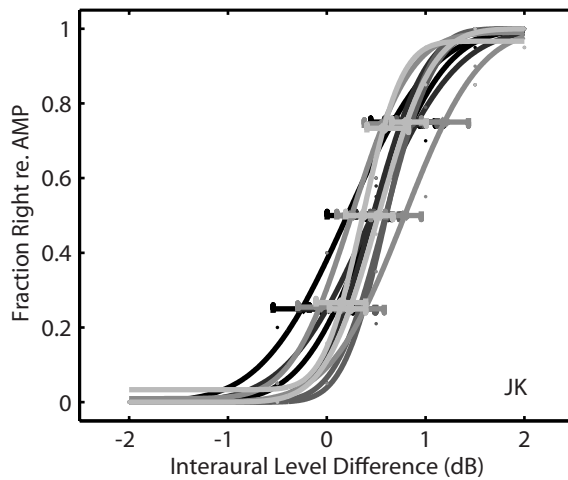
Figure 6.3   Psychometric curves of 10 repetitions of the stationary measurement of subject JK. Experiments were performed on 5 different days, each represented in a different shade of gray. The horizontal error bars represent the 95%-confidence intervals at 25%, 50% and 75% rightward judgements.

= 0 μs) was more likely to be perceived on the right side during leftward rotation (35%), than during rightward rotation (0%).

Figure 6.4B shows the AMPs during vestibular stimulation in the dark of all subjects, for a peak chair velocity of 107°/s. There was a significant difference in mean AMP between leftward and rightward peak velocity (one-sided t-test for matched pairs: $P = 3.7 \cdot 10^{-4}$). In other words, the mean AMP shifted significantly in the direction of rotation.

To determine whether the magnitude of the shift depended on vestibular input, subjects were rotated at different peak velocities (68, 87 or 107°/s). Subjects who did not reproduce the same static results before and after the dynamic experiment were not included in these analyses (number of subjects excluded: 68°/s: 1/9, 87°/s: 2/9, 107°/s: 2/11). The majority of subjects (68°/s: 4/8, 87°/s: 4/7 and 107°/s: 6/9) produced significantly different curves for leftward and rightward rotation (likelihood ratio test: $P < 0.05$), with a shift in the direction of rotation. An asymmetry (or bias) in the results may be noted, although at all three peak velocities, the mean AMP-shift during rightward peak chair velocity was significantly larger than during leftward velocity (see Fig. 6.4C, one-sided t-test for matched pairs: 68°/s: $P = 0.0064$, 87°/s: $P = 4.8 \cdot 10^{-5}$, 107°/s: $P = 3.7 \cdot 10^{-4}$). We also pooled the percentage "rightward" judgements of all subjects first and then fitted the pooled data with a cumulative gaussian to determine the mean AMP. This yielded the same results for all three velocities, i.e. a significant AMP shift in the direction of rotation (likelihood ratio test $P < 10^{-11}$, not shown).

The AMP shift increased slightly with chair velocity, which we quantified by linear regression on all AMPs of all subjects at all velocities. Figure 6.4D shows that despite the considerable variability the shift increased significantly with chair velocity (slope = 0.0024 ± 0.0007 dB/(°/s), r = 0.40, n = 72, $P = 5 \cdot 10^{-4}$). In summary, these results reflect a proper AGI.

Eye position during sinusoidal vestibular stimulation in darkness
During sinusoidal vestibular stimulation the average eye position is expected to shift in the direction of rotation at peak chair velocity, because the quick phases of vestibular nystagmus
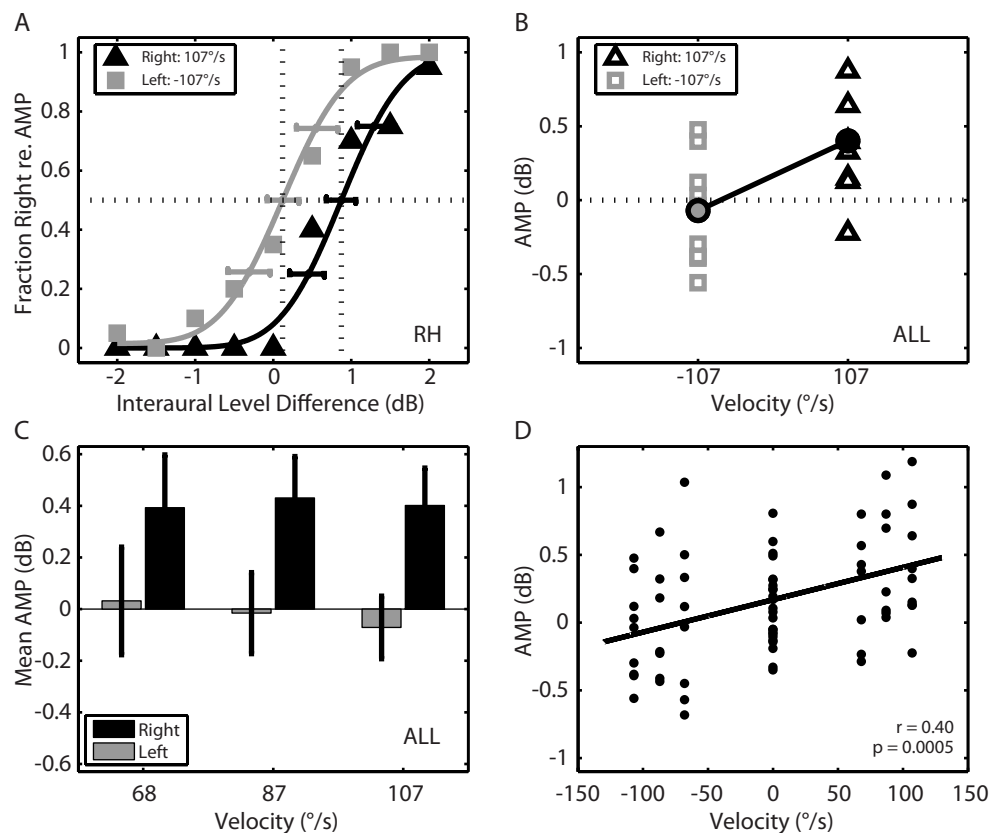
Figure 6.4 In darkness, the AMP shifts in the direction of whole-body rotation. A) Psychometric curve of subject RH. Gray squares indicate leftward rotation and black triangles indicate rightward rotation. The AMP is defined as the 50% rightward judgment threshold, marked by the dashed vertical lines. Error bars give the 95%-confidence intervals of 25%, 50% and 75% rightward judgements. B) All AMPs of all subjects (n = 9). Open symbols are the individual AMPs and filled circles are the means of all subjects. Note that an AMP of e.g. 0.5 dB corresponds to an ITD of 20 μs, due to co-varying ITD and ILD. C) Shift in AMP tends to increase with chair velocity. Gray bars indicate mean AMP shifts during leftward rotation; black bars indicate shifts for rightward rotation. Error bars give the standard error of the mean (SEM) (n = 8,7,9). D) Regression analysis on the individual AMPs (black circles) as a function of chair velocity. Slope: 0.0024 ± 0.0007, x-intersection: 0.17 ± 0.05. The correlation (r = 0.40) is indicated in the figure.

bring the eyes beyond the head-centered midline (Chun and Robinson, 1978; Vidal et al., 1983; Carpenter, 1988). To verify that this was also the case in our experiments, we measured the eye movements of four subjects in a separate session, and fitted the average eye-movement data (*e(t)*) with a sinusoid

$$e(t) = A \cdot sin(2\pi \cdot t/T + \phi) + B \tag{6.2}$$

with *A* the amplitude, *T* the period, *Φ* the phase and *B* the bias of the average eye-movement patterns. Quick phases were not removed from the recordings. The average results for the four subjects are given in Table 6.1. Note the slight increase of eye-movement amplitude, with chair velocity.

Table 6.1   Result of fitting a sinusoid through the average eye-movement data for the three different chair amplitudes in darkness. Results averaged over 4 subjects, given by mean ± standard deviation. Bias (*B*, Eqn 6.2) not included because of the large variation between subjects.

	Darkness		
Peak chair velocity	68°/s	87°/s	107°/s
A (°)	7.09 ± 3.12	7.68 ± 4.90	9.64 ± 4.95
T (s)	8.16 ± 0.45	8.21 ± 0.44	7.88 ± 0.17
Φ (°)	0.74 ± 6.49	-0.64 ± 12.24	-0.35 ± 2.39

Figure 6.5A shows mean eye position (averaged across 30 trials) together with chair velocity for subject DB. At peak leftward chair velocity (at time 2 s) the average eye position was -2.6°. The phase was -1°, i.e. mean eye position was virtually in phase with the chair's velocity. Also at the peak rightward chair velocity (at time 6 s), the average eye position reached a maximum of +10.5°, again in phase with chair velocity.

The sinusoidal movement of the eyes was generally not centered at the straight ahead direction (0°). This idiosyncratic bias could vary from day to day in a non-systematic way, but could not be recorded in all psychophysical sessions for practical reasons. Hence, we were not able to conclusively relate the eye-position asymmetry to the asymmetry observed in the AMP shifts for leftward vs. rightward rotation (Fig. 6.4C).

Effect of rotation with a fixation light on AMP

The shift of the AMP found in the experiments performed in darkness (Fig. 6.4), corresponds to the AGI. To investigate whether the AGI originates from a true audio-vestibular interaction or, alternatively, from an effect related to the subject's dynamic changes in eccentric eye position, we performed two additional experiments: a vestibular experiment without eye movements, and a smooth pursuit experiment without vestibular stimulation.

We first presented a fixation light during sinusoidal vestibular stimulation with a peak velocity of 107°/s, which enforced the eyes to their central, straight ahead position. Although subjects judged the task to be more difficult, they were well able to maintain their gaze centered during the entire run of the experiment (Fig. 6.5B). The mean amplitude of the eye-movement pattern was strongly reduced to about 0.3°.

Figure 6.6A shows typical psychometric curves measured during leftward and rightward peak chair velocity of subject EM in the presence of a fixation light. These curves did not differ significantly (likelihood ratio test: P = 0.37), a finding that was obtained for 5 out of 7 subjects. The remaining two subjects showed a small shift in, rather than against, the direction of rotation.

Figure 6.6B shows the mean AMPs of leftward and rightward rotations together with the SEM. We found no significant shift in AMPs between leftward and rightward rotation in the presence of a fixation light (two-sided t-test for matched pairs: P = 0.21). This finding contrasts with previous results, which showed a shift in the direction opposite to rotation (Lewald and Karnath, 2001).
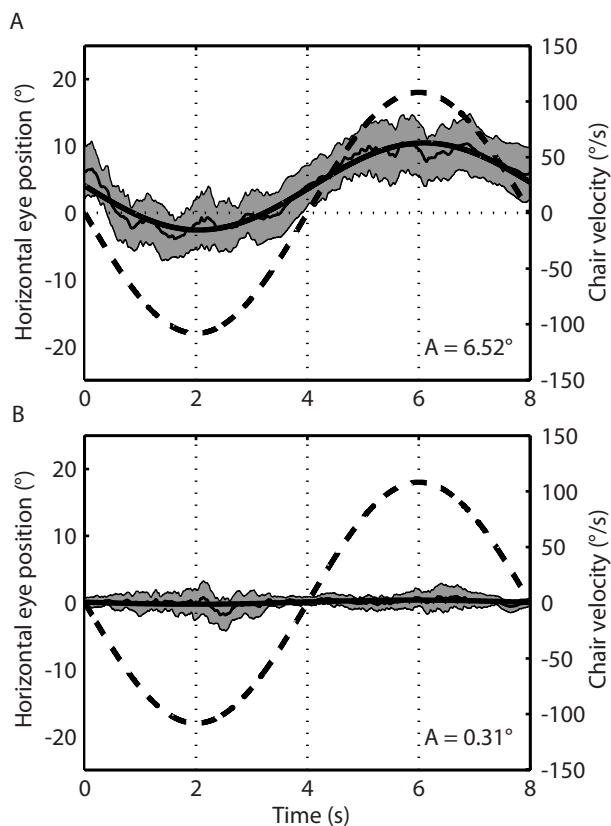
A

Figure 6.5 Mean eye position of subject DB during sinusoidal whole-body rotation in darkness (A), and while fixating a head-fixed fixation light (B), with peak chair velocity ±107°/s. A) Subject's mean gaze position was in the direction of rotation with an average amplitude of 6.52°. The gray area gives the standard deviation of the mean eye position (30 trials). The dashed line gives the corresponding chair velocity. B) On average, the subject was well able to maintain a centered gaze direction.

Sinusoidal smooth pursuit

The results described so far suggest that the vestibular-induced eye-movement patterns (Fig. 6.5A, Table 6.1) could underlie the AGI. In darkness the eyes are, on average, deviated in the direction of vestibular rotation. In the presence of a fixation light, however, a VOR cancellation signal (ocular pursuit) keeps the eyes at a fixed head-centered orientation.

Possibly, this putative cancellation signal shifts the AMP in a direction opposing the AGI, resulting in no net shift (Fig. 6.6). Alternatively, the AGI could result from the average eccentric eye-in-head orientation and thus have no vestibular origin. In that case, the absence of an AGI with a fixation light results from the straight-ahead fixation, rather than from the antagonist effects caused by two opposing eye velocity commands (slow phase of nystagmus vs. ocular pursuit).

To dissociate these two possibilities, we investigated how an ocular smooth-pursuit task influences the AMP. Stationary subjects tracked a sinusoidally moving visual target on a computer screen. Auditory stimuli were presented either when the visual target was on the outermost left and right position (i.e. at peak eye acceleration and amplitude) or when it crossed the centre of the screen (at peak eye velocity). These eye movements mimicked the average eye movement patterns seen during sinusoidal whole-body rotation in darkness (Fig. 6.5A).
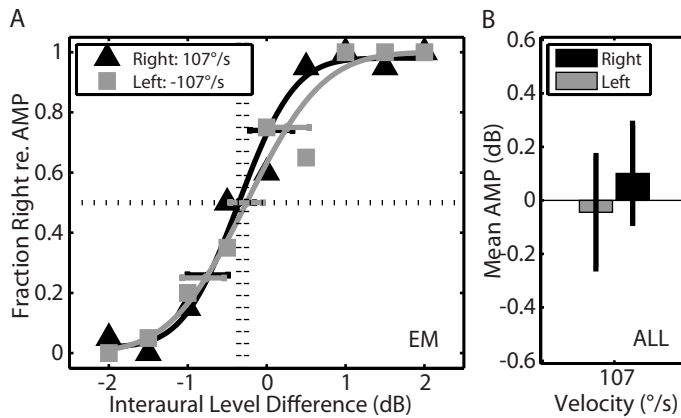
Figure 6.6 In the presence of a fixation light there is no difference in AMP between leftward and rightward rotation. A) Psychometric curve of subject EM. Same conventions as Fig. 6.4. B) Mean AMP during leftward rotation (gray bar) and during rightward rotation (black bar) together with SEM (n = 7).

Figure 6.7A exemplifies typical psychometric curves of subject MV for the left peak eye position (-17.4°) and right peak eye position (17.4°). At these two eye orientations, the eye velocity was 0°/s. The psychometric curves differed significantly, such that there was a clear shift in AMP in the direction of eye position (likelihood ratio test: $P = 6.4 \cdot 10^{-7}$). We tested two different sinusoidal movements, with peak eye position of ± 11.3° and ± 17.4°. In both conditions four out of nine subjects showed a significant shift in the direction of eye position (likelihood ratio test $P < 0.05$). One subject had a shift in the direction opposite to eye position, for the 17.4° case (likelihood ratio test: $P = 1.4 \cdot 10^{-6}$).

If the AMPs of all subjects are taken together, we see that for the peak eye amplitudes the AMP shifted significantly in the direction of eye position, (Fig. 6.7B, one-sided t-test for matched pairs: 11.3°: $P = 0.038$, 17.4°: $P = 0.037$).

The auditory targets were also presented when the visual target (and eyes) moved at peak velocity through the straight-ahead position, either to the left (at -26.0°/s) or to the right (at +26.0°/s). For eight out of nine subjects there was no significant difference between the psychometric curves of leftward vs. rightward eye velocities (likelihood ratio test: $P > 0.05$). As an example, Figure 6.8A presents the psychometric curves of subject MV. The AMPs of these two curves are not significantly different (likelihood ratio test: $P = 0.53$). Furthermore,
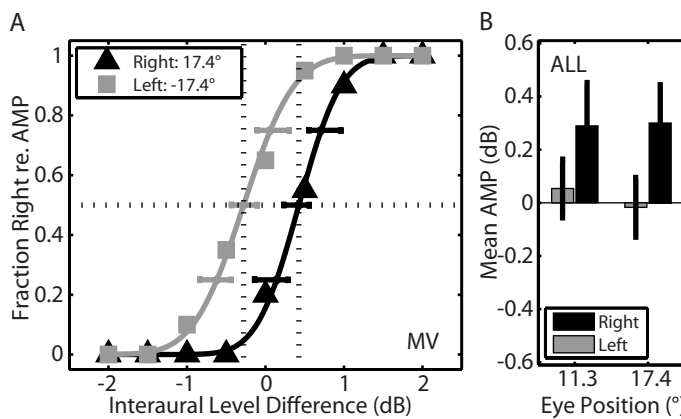

Figure 6.7 AMP at peak eye eccentricity shifts in the direction of eye position. A) Psychometric curves at left peak eye position (gray squares) and at right peak eye position (black triangles) of subject MV. B) Mean AMP (n = 9) at left (gray) and right (black) peak eye position as function of eye eccentricity, together with SEM.
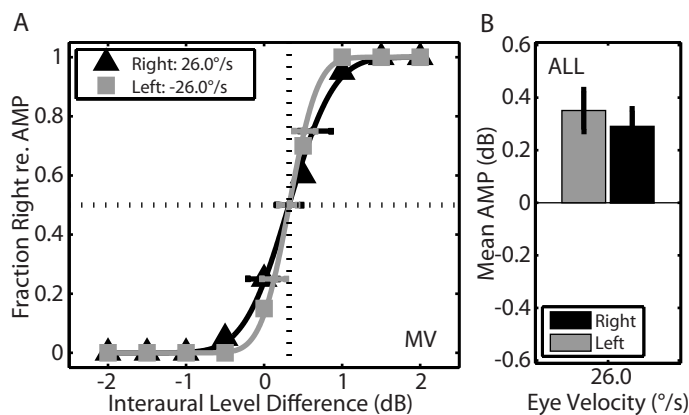
Figure 6.8   Eye velocity does not influence AMP. A) Psychometric functions at peak leftward eye velocity (gray squares) and peak rightward eye velocity (black triangles) of subject MV. B) Mean AMP (n = 9) at peak leftward (gray) and peak rightward (black) eye velocity together with the SEM.

the mean AMPs of the nine subjects for leftward vs. rightward eye velocities showed no significant difference (Fig. 6.8B, two-sided t-test for matched pairs: P = 0.44). Hence, these smooth pursuit experiments show that whereas eye position drives the AMP in the direction of eccentric fixation, eye velocity does not influence the AMP.

DISCUSSION

The present study set out to investigate to what extent vestibular stimulation influences sound lateralization, as quantified by the AMP. Sinusoidal rotation in darkness shifted the AMP in the direction of rotation. The magnitude of the shift increased slightly with chair velocity. In the presence of a fixation light, however, the AMP shift disappeared. Our smooth pursuit results showed that eye position, rather than eye velocity, influenced the AMP. Taken together, our data indicate that the AGI is due to an effect of eccentric eye position on sound lateralization, rather than to audio-vestibular interactions.

Comparison to earlier studies
The results obtained in darkness reflect a true AGI (Münsterberg and Pierce, 1894; Clark and Graybiel, 1949), whereas those obtained with a fixation light are not in line with an earlier report (Lewald and Karnath, 2001). In this latter study the AMP shifted opposite to the rotation direction. Several procedural differences could underlie the different results with the use of a fixation light. First, the vestibular stimulation profiles were different. Whereas Lewald and Karnath (2001) tested subjects with unidirectional stimulation at constant velocity, we rotated our subjects sinusoidally. This allowed a direct comparison of a subject's AMP for both leftward and rightward rotation within the same experimental session. Such a comparison turned out to be important, as subjects considered the psychophysical measurements a difficult task. We observed a considerable day-to-day variability within and between subjects, even for the stationary AMP measurements (Fig. 6.3), as well as an idiosyncratic and variable left-right bias (e.g. Fig. 6.4A). This renders it difficult to pool leftward vs. rightward results obtained from different sessions and subjects (Lewald and Karnath, 2001).

Second, Lewald and Karnath (2001) used pure tones (1 kHz) with only an ITD localization cue as sound stimuli, whereas the present study employed 100 ms broadband noise bursts with co-varying interaural time and level differences, to make the dichotic stimuli as informative as possible and to prevent potential frequency-dependent effects of eye and head orientation (Goossens and Van Opstal, 1999). These sound-stimulus differences, however, did not appear to influence the AGI in darkness, since pilot experiments with a pure 1 kHz tone and broadband noise stimuli yielded similar AMP shifts (not shown).

Others have shown an effect of eye position on sound lateralization too, although results seem inconsistent. Lewald and Ehrenstein (1996) reported an AMP shift in the direction of static eye position. The present study extends these results to dynamic eye-position changes. As illustrated in Figure 6.1, the free-field sound-localization percepts should then shift in a direction opposite to eye-in-head position. Indeed, Lewald and Getzmann (2006) reported such shifts for both horizontal and vertical static eye positions in a hand-pointing localization task. Although a natural orienting task towards sounds typically yields accurate localization responses, with no, or very small, average errors, the regression analysis of Goossens and Van Opstal (1999) reported a small, but systematic overestimation of horizontal eye-in-head orientation. As a result, gaze shifts slightly missed the sound location in a direction opposing eye position. Lewald (1998) had observed a similar shift.

In contrast to those studies, however, Razavi et al. (2007) demonstrated that prolonged eccentric fixation of the eyes (up to 20 min.) leads to a systematic mislocalization of free-field sounds in the same direction as eye position. Possibly, the effect of eye-in-head position reverses when the eyes are held eccentric sufficiently long. However, Lewald and Ehrenstein (1998a) obtained similar effects for much shorter fixation durations. In both studies subjects indicated the sound-source location with a laser pointer. As hypothesized by Lewald and Ehrenstein (1998a), this pointing method could influence localization responses, since eye position also influences visual localization, as in particular retinal eccentricity of visual stimuli is generally overestimated (Morgan, 1978; Bock, 1986). If this perceived visual shift exceeds the auditory shift, the net effect would be in the same direction as eye position.

An additional factor with visual pointing methods could be an influence of visual attention (e.g. Bohlander, 1984), which may, at least partly, underlie the seemingly conflicting results between studies.

Visual effects during VOR cancellation?

The presence of a head-fixed fixation light during vestibular stimulation might induce two visual-related spatial illusions that could interfere with the spatial representation of sound sources as well. The first is a visual-vestibular effect, and is known as the oculogyral illusion (OGI; Graybiel and Hupp, 1946). In this illusion a head-fixed visual target is seen shifted in the direction of whole-body rotation. If this visual reference seems to move, the AMP might do so accordingly, particularly when it is regarded relative to such a visual reference. The second effect could be due to audiovisual integration, when auditory and visual stimuli are presented simultaneously, but from different spatial locations. When the brain interprets this stimulus combination as a single audiovisual event, it is typically dominated by the visual percept (the ventriloquist effect; Alais and Burr, 2004). Both phenomena might influence vestibular sound

lateralization and localization results with a fixation light in the following way. If during rotation, the fixation light seems to shift in the direction of rotation (OGI), while at the same time audiovisual integration takes place, the subject's perceived sound lateralization might be attracted towards the perceived visual stimulus location in the direction of rotation. As a result, the AMP may shift in the direction opposite to rotation (Fig. 6.1). Since these visual effects may rely on the intensity of the visual stimulus, the "ventriloquist shift" might have fully cancelled the AGI in our experiments, whereas it might have overtaken the AGI in the experiments of Lewald and Karnath (2001).

Eye position or eye velocity?

Although the presence of a fixation light suppresses overt eye movements (Fig. 6.5B), it does not rule out the possibility that kinaesthetic factors, rather than audio-vestibular interactions, underlie the AGI. The nearly complete suppression of nystagmus is thought to be due to an internally generated VOR cancellation signal that is subtracted from the vestibular slow-phase eye-velocity signal. This cancellation signal might be an ocular pursuit signal, since clinical studies have shown that VOR suppression and smooth pursuit eye movements may arise from the same neural mechanisms. Firstly, the ability to suppress the VOR breaks down at similar frequencies as ocular pursuit. Secondly, patients with impaired VOR suppression also have degraded smooth pursuit (for review: Barnes, 1993).

Hence, rather than eliminating potential kinaesthetic factors, it might be argued that a fixation light introduces additional kinaesthetic factors. Since the VOR cancellation signal opposes the vestibular slow phase, its effect on the AMP could also oppose the vestibularly induced AMP shift. If the magnitudes of these two antagonistic effects are not identical, a net AMP shift remains, either in (vestibular effect larger) or opposite (pursuit effect larger) to the direction of vestibular rotation. Alternatively, if the AMP shift in darkness were not due to audio-vestibular causes, but secondary to an overall change in gaze direction, VOR cancellation would abolish the shift in AMP. In line with such a hypothesis there should be no shift of the AMP for pursuit eye velocity through the straight-ahead gaze direction either.

The smooth-pursuit experiments indicated that pursuit eye velocity indeed had no significant influence on the AMP (Fig. 6.8). Instead, an eccentric eye position of about 15° during pursuit consistently shifted the AMP in the direction of gaze (Fig. 6.7). The small, but asymmetric, effect of chair velocity on the magnitude of the AMP shift (Figs 6.4C,D) could be related to a similar increase in mean eye position with chair velocity (Table 6.1).

Taken together, we conclude that the dynamic AGI is due to an effect exerted by eccentric eye position on sound lateralization, rather than to a potential mismatch in audio-vestibular interactions. Our study shows that the effect also arises when eye position changes dynamically, regardless its cause (vestibular or pursuit).

Neural mechanisms

The immediate effect of eccentric eye position could be a shift in the direction of spatial orienting ('look where you go'), which would normally be associated with a voluntary head movement in the same direction. Indeed, eccentric fixation of the eyes is usually associated with the activation of neck muscles (Vidal et al., 1983). Eccentric head-on-body orientation has

been shown to influence sound localization (Lewald et al., 2000), as well as sound lateralization (Lewald and Ehrenstein, 1998b). Moreover, neck-muscle vibration in the absence of an actual head movement influences sound lateralization in the direction of perceived head orientation as well (Lewald et al., 1999). Thus, the observed shift in AMP during vestibular stimulation in darkness could eventually result from the integration of incomplete, or inaccurate, sensorimotor signals that under natural conditions would all jointly occur (Goossens and Van Opstal, 1997b; 1999; Vliegen et al., 2004). According to this view, the effect of eye position on AMP would be attributable to a secondary effect, i.e. the failure to accompany the eccentric eye fixation with either an appropriate head-movement command (in case of muscle vibration), or with an actual head movement (in case of passive rotation, and/or head fixation).

If the auditory system accounts for an upcoming head movement, the sound's location relative to the head would be expected to rotate in the opposite direction. Perhaps the sound-localization system predicts this upcoming shift of craniocentric sound location when the eyes change orientation. Such a prediction could be reminiscent to the mechanism of "predictive remapping" that has been reported by a number of seminal visuomotor studies in brain areas such as lateral parietal cortex (Duhamel et al., 1992), frontal eye fields (Umeno and Goldberg, 1997), and midbrain superior colliculus (Walker et al., 1995). However, when the head is not moving after prolonged fixation, this putative remapping response might fade and even reverse, as observed by Razavi et al. (2007), and could thus induce an 'after-effect' in the opposite direction of eye rotation.

Model of eye-position effect on sound localization and lateralization

To explain the effects observed in our experiments and those of others in the context of neural acoustic processing, we adopted the model of Zwiers et al. (2003). In this scheme, binaurally responsive neurons on both sides of the brainstem respond in a sigmoid fashion to ILDs (Fig. 6.9A). Each neuron has its own working range (set by its threshold) that spans a fraction of the azimuth domain. The total population of ILD neurons thus covers the entire azimuth space and azimuth localization results from the total summed population response (Fig. 6.9A, upper-right panel). This simple model accounts for the effect of visual compression on free-field sound localization by assuming that visual input modulates the weights of ILD neurons to the summation stage (Zwiers et al., 2003).

We added two features to this model: (i) we included an effect of eye position, and (ii) we considered sound lateralization as a perceptual process that compares the activities from left and right ILD populations (Fig. 6.9A, lower-right panel). The AMP is then determined by that acoustic input for which the left and right population activities are identical. In other words: if activity is higher for left-side cells, the stimulus is judged to be on the left. With this simple model, we simulated psychometric curves of 2AFC left/right judgements on binaural stimuli by taking the total activity of left and right cells as a measure for the probability of rightward judgements (black line Fig. 6.9B5).

The eye-position dependent shift in the AMP is then explained by assuming that a change in eye position changes the threshold of all ILD cells: it decreases (and hence, activity increases) when the eyes look leftward, whereas it increases for rightward eye positions. In this way, the total activity of the left and right cells is slightly modulated by eye position. Since
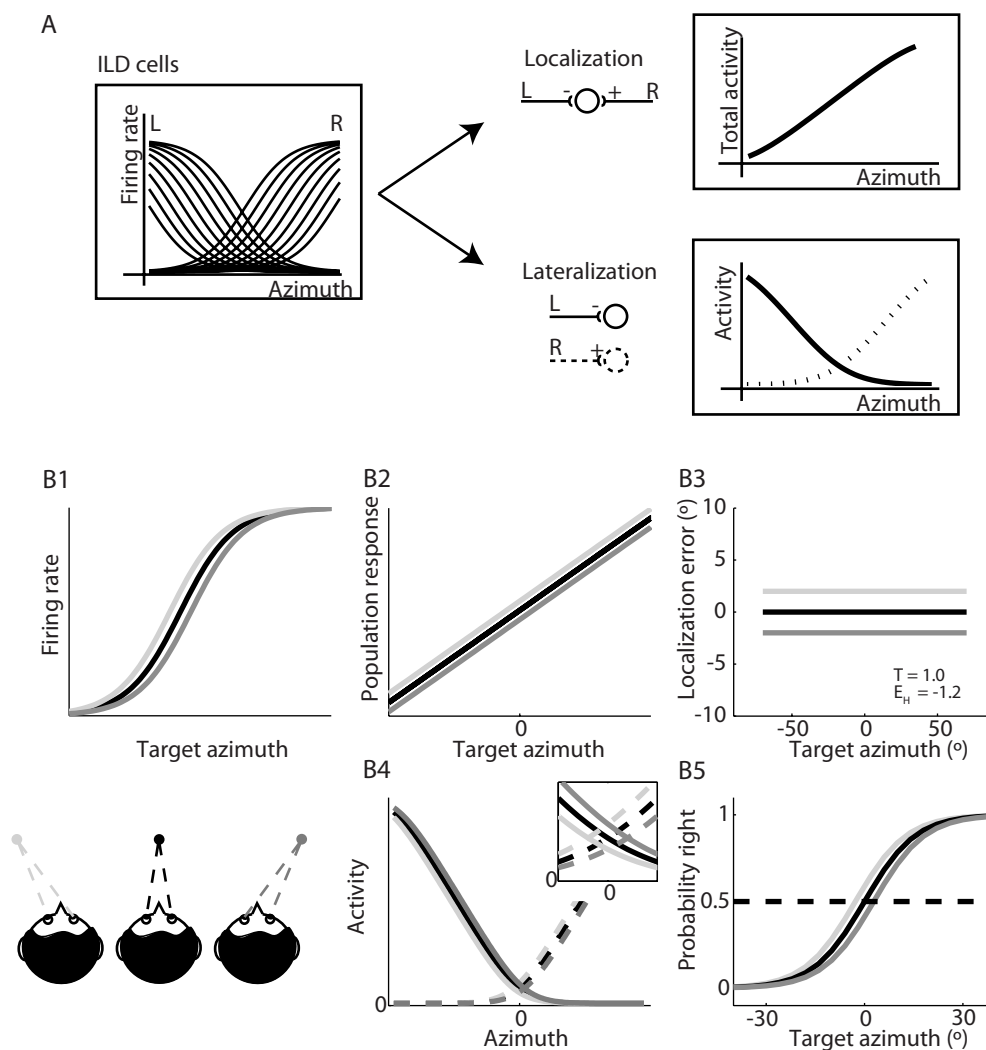
Figure 6.9   Model of ILD-cells encoding sound lateralization and localization. A) The model has 121 ILD units (60 left, 60 right and one centre), which respond in a sigmoid fashion to sound ILD in the horizontal plane. Azimuth localization is determined by the linear sum of the total population output (with left neurons having negative weights). Lateralization is based on comparing the left and the right populations. The AMP is determined as the ILD for which right and left side activities are equal. B) Simulation results. B1) The threshold of ILD cells shifts slightly in the direction of eye position. B2) The shift in thresholds modulates the population response, such that a target is shifted in the direction opposite to eye position. B3) Simulation result for a range of sound locations and eye positions. Multiple linear regression ($R = a \cdot T + b \cdot E_H + c$) shows that subjects incorporate target position correctly ($a = 1.0$), but overestimate eye-in-head position ($b = -1.2$; see Goossens and Van Opstal, 1999). B4) The activity of left and right cells is modulated with eye position. B5) The AMP is also affected by the eye-position-dependent threshold of ILD cells. Simulation shows that the AMP shifts in the direction of eye position.

the AMP is defined by the azimuth location for which the right and left population activities are equal, it will shift to the right when the eyes look rightward (Fig. 6.9B5).

For absolute localization, these threshold modulations result in a small bias in the opposite direction of eye position. For example, if the eyes look rightward, the population response for the same auditory stimulus is lower (corresponding to a leftward shift of the location) than when the eyes look straight ahead (Fig. 6.9B3). Similar effects of eye position within the auditory system have been reported for single-unit recordings in monkey Inferior Colliculus (Groh et al., 2001; Zwiers et al., 2004).

ACKNOWLEDGEMENTS

[1]Department of Biophysics, Donders Institute for Brain, Cognition and Behaviour, Radboud University Nijmegen, The Netherlands, [2]CNRS UMR 8194, Université Paris Descartes, Centre Universitaire des Saints-Pères, Paris, France, [3]ENT Department, Salpetriere Hospital, Paris, France

7

Sound lateralization is not affected in patients with acute unilateral vestibular neuronitis, nor during galvanic vestibular stimulation

Denise C.P.B.M. Van Barneveld[1]
Elodie Chioravano[2]
Catherine De Waele[2,3]
Pierre-Paul Vidal[2]
A. John Van Opstal[1]

INTRODUCTION

Horizontal sound localization relies on the neural evaluation of interaural time (ITD) and level differences (ILD) (Blauert, 1997). When navigating through space, intervening eye, head and body movements should also be incorporated to ensure a stable spatial percept. Behavioral experiments have shown that spatial updating is accurate for self-generated eye and head movements before and during stimulus presentation (Goossens and Van Opstal, 1999; Vliegen et al., 2004; Van Grootel and Van Opstal, 2010). During self-generated movements, spatial updating could rely on proprioceptive body-posture signals from neck muscles, on efference copies of planned eye and head movements and on vestibular signals that relate to head rotations and linear accelerations though space. In contrast, during passive whole-body rotation, the brain can rely only on vestibular information since proprioceptive and efference copy signals are absent. It has been shown that such stimulation in darkness induces the illusion that head-fixed sounds are heard at a displaced location in the direction opposing rotation (Münsterberg and Pierce, 1894), a phenomenon known as the audiogyral illusion (AGI).

The AGI can be quantified by assessing the subjective auditory median plane (AMP), which is the plane where interaural differences are perceived to be zero. Under dichotic hearing conditions with the eyes and head stationary and at straight ahead, the AMP of normal listeners typically coincides with the midsagittal plane of the head. During whole-body rotation, however, the AMP shifts in the direction of rotation, as sounds are perceived displaced in the opposite direction of rotation (Fig. 7.1; Clark and Graybiel, 1949; Van Barneveld and Van Opstal, 2010).

The origin of the AGI has been controversial for a long time, and several potential mechanisms have been proposed in the literature: Clark and Graybiel (1949) attributed the AGI to an erroneous sense of perceived rotation. Lester and Morant (1969; 1970) and Lackner (1974) attributed the AGI to a misperceived head-on-trunk orientation (kinaesthetic illusion). Bohlander (1984) suggested that spatial attention may influence dichotic listening and hence the location of the AMP. Arnold (1950), and Thurlow and Kerr (1970) proposed that vestibular ocular nystagmus could underlie the AGI. In line with this latter idea, Quarck et al. (2009) recently noted that a shift in eye position also affects the perceived body-rotation.

Recently, we attributed the AGI to an eccentric eye-position effect induced by the vestibulo-ocular reflex (VOR), rather than to a proper vestibular effect (Van Barneveld and Van Opstal, 2010). In darkness, the vestibular quick phases shift the mean eye position into the direction of head rotation (Chun and Robinson, 1978; Vidal et al., 1983; Carpenter, 1988). In addition, earlier studies had demonstrated that the AMP moves in the direction of static eccentric eye position without the use of vestibular stimulation (Lewald and Ehrenstein, 1996; Lewald and Getzmann, 2006; Lewald, 1998), and we recently showed that this effect also occurred for dynamic changes in eccentric eye position during smooth ocular pursuit in a visual tracking task (Van Barneveld and Van Opstal, 2010). Moreover, the shift in AMP disappeared during smooth pursuit when the eyes crossed straight ahead, and during whole-body rotation with a fixation light, which cancelled the VOR and kept the eyes centered in the head (Van Barneveld and Van Opstal, 2010). The AGI was also absent when ocular
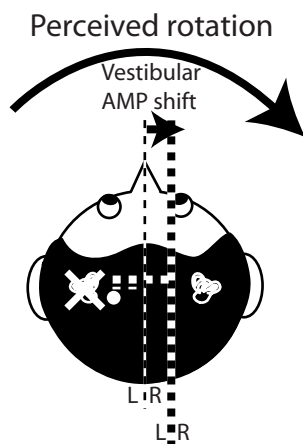
Perceived rotation

Figure 7.1   Rationale of the experiments. The thin vertical dashed line represents the auditory median plane of the head (AMP) under stationary hearing in healthy controls. Sounds presented on the AMP are perceived in the centre of the head. Note that acoustic parameters determine the AMP (it is defined as perceived ILD=0 and/or ITD=0), not a spatial reference (like, e.g. perceived straight-ahead). For example, a plugged ear would shift the AMP to the ipsilateral side, without affecting the perceived body or visual straight-ahead direction. If the AGI had a pure vestibular origin, AVN patients would show a shift in AMP in the direction of perceived rotation (thick dashed vertical line), thus away from the affected side (indicated by the white cross though the left vestibular organ). A head-fixed sound (white dot) would be heard displaced in the opposite direction, thus in the direction of the affected side (thick dashed leftward horizontal line). To prevent confusion, we describe effects of audio-vestibular integration in terms of (dichotic) AMP shifts (in dB ILD/µs ITD), rather than by corresponding opposite (free-field) sound-location shifts (in °).

nystagmus moved the eyes through the straight-ahead direction during vestibular stimulation in darkness (unpublished results), indicating that the presence or absence of a fixation light is not essential.

In the present study, we further tested the hypothesis that the AGI is not caused by a vestibular interaction with the auditory system in acute vestibular neuronitis patients (AVN, Fig. 7.1). Vestibular neuronitis is a syndrome characterized by the acute onset of vertigo with spontaneous nystagmus, postural imbalance and nausea without hearing deficits or neurological symptoms. It is thought to stem from an abrupt functional decrease in vestibular system function due to viral inflammation or ischemia. Patients suffering from AVN usually perceive a prominent head rotation away from the affected side that might be accompanied by a head tilt due to the asymmetric peripheral vestibular input.

Besides having postural imbalance, AVN patients have difficulties in spatial perception. They misjudge visual verticality and horizontality (Friedmann, 1970; Bohmer et al., 1995; 1996; Tabak et al., 1997; Min et al., 2007), like has been found in healthy subjects when tilted sideways. It is not known whether they also have problems with spatial hearing. Here we tested the sound lateralization abilities of AVN patients

In addition, we tested the AMP of healthy subjects by applying bilateral bipolar galvanic stimulation of the mastoids (GVS), either in total darkness, or while fixating straight ahead. GVS increases the firing rate of vestibular afferents at the cathode side and inhibits them at the anode (Fitzpatrick and Day, 2004). In doing so, it creates a sensation of tilt with a small yaw component both towards the cathode, which is accompanied by ocular nystagmus and torsion (Fitzpatrick and Day, 2004).

We conjectured that if the AGI results from an eye-position effect, it should be absent in AVN patients and during GVS stimulation, as long as the eyes are kept at straight ahead. A vestibular-induced AGI, in contrast, would shift the AMP contralateral to the affected side in patients and towards the stimulating cathode during GVS.

Our results show that ANV patients did not display a significant shift of the AMP when compared to healthy controls, when fixating at straight ahead. Also, while GVS did induce a clear vestibular sensation, as objectively measured by eye velocity in darkness, it did not

shift the AMP significantly, neither in darkness, nor when fixating at straight ahead. Taken together, these results support the hypothesis that the AGI is not due to an audio-vestibular interaction.

METHODS

Listeners

Experiments were conducted with nine patients (four females, five males, age: 49.0 ± 18.0 years) suffering from an acute (between two and up to 15 days post-lesion) complete unilateral vestibular loss (five at the left and four at the right side). They all met the clinical diagnostic criteria for vestibular neuritis, including sudden onset of prolonged vertigo more than one day with unidirectional spontaneous horizontal nystagmus, absence of other auditory or neurologic findings, reduced caloric responses (< 25%) and no previous history of neurologic diseases. Experiments were conducted in the Pitié-Salpêtrière hospital in Paris. The experimental procedures were approved by the Local Ethics Committee of the hospital, and adhered to The Code of Ethics of the World Medical Association (Declaration of Helsinki), as printed in the British Medical Journal of July 18, 1964.

As a control group we measured twenty age-matched healthy listeners (thirteen females, seven males, age: 40.4 ± 15.0 years). None of the controls had a history of motor disability, visual, auditory or vestibular disorder. Eight healthy listeners participated in the GVS experiments (two females, six males; age: 28.6 ± 3.5). All had normal hearing, and no history of motor disability, visual or vestibular malfunction. Experiments were conducted after we obtained full understanding and written consent from the subject. The experimental procedures were approved by the Local Ethics Committee of the Radboud University Nijmegen, and adhered to The Code of Ethics of the World Medical Association (Declaration of Helsinki), as printed in the British Medical Journal of July 18, 1964.

Experimental setup

Auditory stimuli

Auditory stimuli were digitally generated in Matlab (The Mathworks, Natick, MA, version R2008a). Signals consisted of a single 100 ms broadband Gaussian white noise burst (bandwidth 0.5-18 kHz, sample frequency 44.1 kHz), with 5 ms sine-squared onset and offset ramps. To provide the auditory localization cues with as much spatial information as possible, we provided the broadband noise burst with co-varying interaural time (ITD) and level differences (ILD). Variations of ILD were symmetrical, i.e. if the ILD was +8 dB, the left ear was attenuated by 4 dB, whereas the right ear was amplified by 4 dB. Listeners perceived the sounds inside the head, on the line connecting the two ears, either on the left or on the right of the centre of the head. A custom written program in Matlab on a computer (Mac iBook (galvanic study) or IMac (patient study)) presented the sounds via headphones (Sennheiser HD 457 (galvanic study) or HD 205 (patient study)). Subjects responded to the laterality of the sounds by giving a left or right button press.

Galvanic stimulation

Bilateral bipolar galvanic stimulation was delivered by a constant-current stimulator (Eldith, NeuroConn GmbH, Ilmenau, Germany) via two conductive rubber electrodes (5 x 7 cm²) inside saline-soaked sponges placed on the left (cathode) and right (anode) mastoids. Before the electrodes were placed, the skin was rigorously cleaned and lightly abraded to reduce impedance. The target skin impedance, as measured by the stimulator, was < 15 kΩ. To avoid abrupt sensations, the stimulation period (75 s at -2, 0 or 2 mA) was initiated by a fade-in period (10 s) and completed by a fade-out period (10 s). The auditory stimulation started immediately after the fade-in period. Note that a current of -2 mA implies that the cathode and anode are reversed.

Eye-movements measurements

During the galvanic experiments in darkness the listener sat comfortably in a chair with the head stabilized in an upright position with a padded adjustable helmet in the middle of a completely dark room (4.05 x 5.15 x 3.30 m³). We measured two-dimensional eye movements of the right eye with the double-magnetic induction technique (Bour et al., 1984; Bremen et al., 2007) using three orthogonal oscillating magnetic fields at 30, 48 and 60 kHz, respectively, generated by three pairs of orthogonal coils (0.77 x 0.77 m²) around the subject's head. The horizontal, vertical and frontal eye-position signals were amplified, demodulated by tuned lock-in amplifiers (Princeton Applied Research, NJ, USA, model PAR 128A), low-pass filtered (150 Hz, custom-built 4th order Bessel) and subsequently sampled at 500 Hz per channel (1401 Plus, using Spike 2 software, Cambridge Electronic Design, Cambridge, England) for storage on the computer's hard disk (Precision 360, Dell, Limerick, Ireland).

Experimental algorithm: accelerated stochastic approximation

A custom made program (Matlab) implemented an adaptive staircase method in which the step size is determined by accelerated stochastic approximation (Kesten, 1958). The idea behind the adaptive staircase method is to present a series of sounds with ascending and descending interaural differences in order to find the interaural differences at which the sound matches the AMP. Based upon the collected series of responses ('leftward' or rightward'), the presentation in the forthcoming run was adjusted in the requested direction. Thus, if the listener's response to the first stimulus was 'leftward' the next stimulus would be presented more to the right, and so on, until the response reversed from 'leftward' to 'rightward'. Such a response reversal started a staircase-type series of adjustments in opposite direction until the next reversal occurred. The step size was gradually decreased according to the accelerated stochastic approximation (Kesten, 1958), which incorporates the history of all answers of the listener. The ITD (in samples) of the next trial is determined by:

$$ILD_{n+1} = ITD_n - \frac{c}{n}(Z_n - \phi) \qquad n \leq 2 \qquad (7.1a)$$

$$ILD_{n+1} = ITD_n - \frac{c}{2 + m_{rev}}(Z_n - \phi) \qquad n > 2 \qquad (7.1b)$$

where m_{rev} is the number of reversals, c initial step size, φ is threshold probability (0.5), and Z_n the answer of the listener to the nth trial (left: $Z = 0$; right: $Z = 1$). Since the step

size in ITD is discrete (because of the discrete sampling of digital sound presentation at 44.1 kHz), we rounded the outcome of equations 7.1a and 7.1b. We used the accelerated stochastic approximation because it converges more rapidly than the traditional stochastic approximation (Robbins and Monro, 1951, for review see Treutwein, 1995).

The ILD was then determined by:

$$ILD = a \cdot ITD \qquad (7.2)$$

where a = 0.022 dB/μs, which resulted from a pragmatic data fit between ITD and ILD.

In a single run, two staircases were presented interleaved, the first started at one side and the second started at the other side of the head. The experiment always started with an extreme sound (8 dB/363 μs left or 7.5 dB/340 μs right) and with a large step size (4 dB/181 μs). Each staircase in the experiment ended either when the (unrounded) step size was reduced to 0.5 dB/22 μs (one digital sample) or after 25 sounds.

By using a staircase procedure, the AMP is determined by decreasing the interaural differences until the listener hears the sound in the middle. This implies that judging the laterality of the stimuli becomes more difficult further on in the experiment. To make the task easier, sounds with large interaural differences (randomly chosen between 6 dB/272 μs and 9.5 dB/430 μs left or right) were presented every fifth trial. These sounds were clearly perceived at either left or right.

Experimental procedure

Sound lateralization
The subject indicated the laterality of the sounds on a button box with a left and a right button, while fixating an LED (galvanic study) or a red dot on a gray computer screen (patients study) at straight ahead. The subject could take as much time as needed, but was instructed to answer rapidly. One and a half seconds after pressing the button, the next sound was presented. A typical run took about one minute, depending on the response time of the subject. In the patient study, listeners performed two runs while fixating at straight ahead.

During the galvanic experiments we ensured that the experiment was finished before the end of the galvanic stimulation. In the galvanic study, listeners performed 2 runs in darkness and 2 runs fixating straight ahead per galvanic current (-2 mA, 0 mA or 2 mA). The galvanic experiments in darkness started with a fixation light at straight ahead that was extinguished at the start of the galvanic stimulation. We measured horizontal and vertical eye position, during the course of the experiment.

Calibration of eye position (preceding galvanic experiments in darkness)
The galvanic experiments in darkness started with a calibration run, in which the subject fixated 37 LEDs that covered the oculomotor range (direction re. horizontal, $\Phi = 0°$ to 360° in 30° steps; eccentricity re. straight ahead, $R = 0, 13.2, 25$ and 35°). At fixation the subject pressed a joystick, which triggered 50 ms sampling of horizontal, vertical and frontal eye-position signals. These data were used for offline calibration of the eye-position signals.
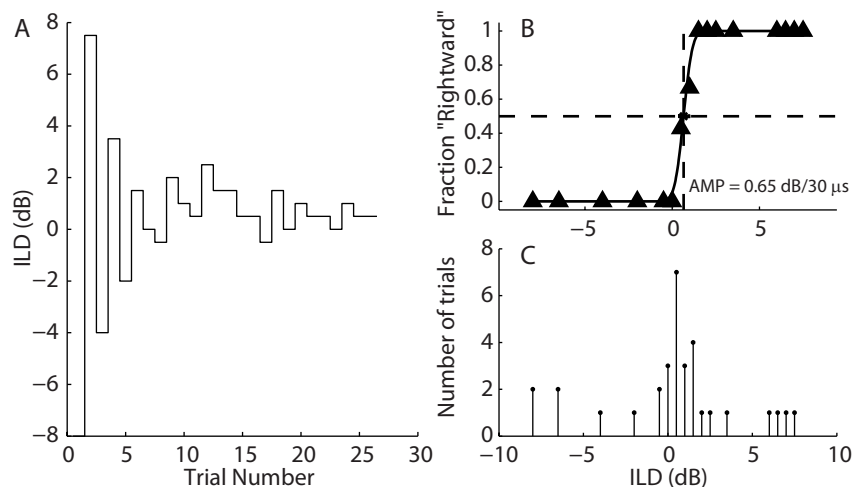
Figure 7.2   AMP measurements. A) Adaptive results for two interleaved staircases of acute right patient 4: one starting left (odd trial numbers) and one starting right (even trial numbers). At response "left" the next stimulus in that staircase was further right, and v.v.; the step size decreased gradually. B) Same data plus 'easy trials' (see Methods) converted into a psychometric curve (fraction "Rightward" judgements for each ILD/ITD combination). Data were modeled by a cumulative gaussian (solid line); the 50% threshold defines the AMP (dashed line). The steepness of the curve (i.e. the sensitivity of the listener to ILD/ITD) is quantified by the standard deviation (sigma). C) ILD histogram of data in B. Note that this example shows two staircases performed in one experimental block, while the majority of the listeners performed two blocks.

Data analysis

Determining the AMP

We reanalyzed the answers of the subjects by constructing psychometric curves of all trials of all blocks with the same conditions, including the "easy" trials with large ILD/ITD as illustrated in Figure 7.2. The proportion of the listener's 'rightward' judgements for each stimulus was determined as a function of stimulus ILD/ITD (Van Barneveld and Van Opstal, 2010). Data were subsequently modeled by a cumulative gaussian psychometric function, $F(x;\mu,\sigma)$ defined as follows:

$$\Psi(x; \mu, \sigma, \gamma, \lambda) = \gamma + (1 - \gamma - \lambda) \cdot F(x; \mu, \sigma) \tag{7.3}$$

with mean, μ, and standard deviation, σ, using the psignifit toolbox (ver. 2.5.6) for Matlab (http://bootstrap-software.org/psignifit/), which implements the maximum-likelihood method (Wichmann and Hill, 2001a,b). The stimulus-independent errors (so-called lapses) γ and λ were constrained to be symmetrical and were allowed to be maximally 10%. The AMP was defined as the 50% rightward threshold, thus corresponding to the mean of the cumulative gaussian. The 95% confidence intervals of the AMP were determined by the bootstrap method implemented by the psignifit toolbox based on 1000 simulations.

In the patient study, we normalized the AMPs of all patients and healthy controls by subtracting the mean AMP of the healthy controls. In the GSV experiments, we normalized the AMPs relative to the AMP during 0 mA current stimulation to test the influence of

stimulation current on AMP.

Eye-position and velocity

First, we calibrated the eye position signals. We determined the relation between raw eye-position signals and the corresponding LED positions by training two neural networks for the horizontal and vertical eye-position components, respectively (for details, see Goossens and Van Opstal, 1997b).

We determined the average horizontal and vertical eye position during the period of constant galvanic current of each block (two per stimulus current), yielding two eye-data points for each psychometric curve. To determine the average horizontal and vertical eye velocity we low-pass filtered the horizontal and vertical eye position signals at 80 Hz. We then differentiated the filtered signal to obtain eye-velocity signals, and removed the quick phases of ocular nystagmus by removing velocities exceeding 10°/s. We averaged the signals over the period of constant galvanic current.

Statistics

To test the influence of galvanic current on mean eye position and velocity we determined the optimal linear fit through the data (see Fig. 7.5). Parameters were found by minimizing the mean-squared error (Press et al., 1992). From the linear fit we also determined the coefficient of determination (r^2) between data and model prediction.

To test the significance of the effects we performed a one-way analysis of variance (ANOVA) with stimulation current as a factor (GVS) or with patient group as a factor (patient study).

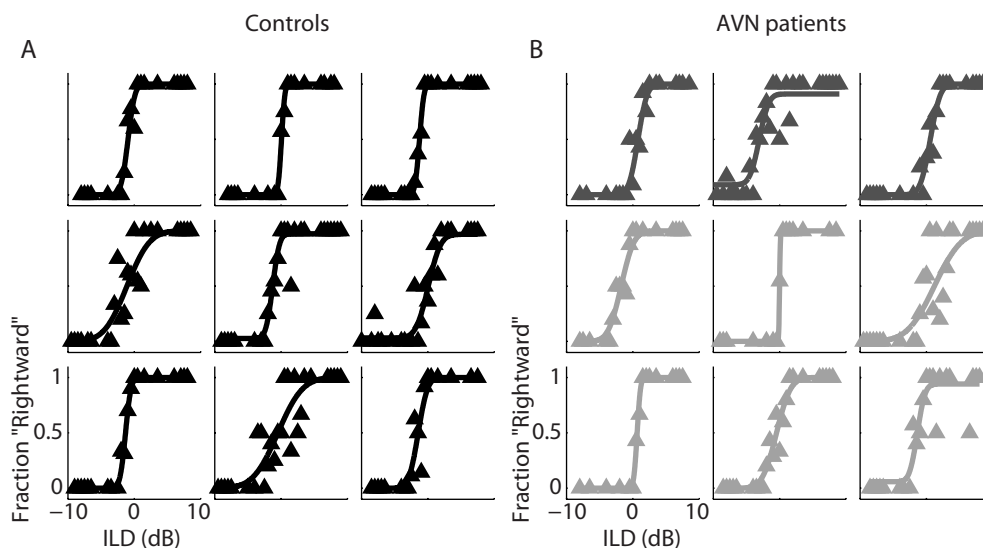Figure 7.3   Psychometric curves of 9 of healthy controls (A) and of AVN patients (B). The fraction "Rightward" answers is plotted against ILD. Left AVN patients are presented in dark gray and right AVN patients in light gray. Although most listeners produced well-defined psychometric relationships, some listeners generated more variable responses. The examples show that this occurred in both groups.

RESULTS

AVN patients

To test whether vestibular input would underlie the AGI, unilateral AVN patients and healthy controls lateralized sounds while they fixated at straight ahead. Figure 7.3 shows the psychometric curves of nine patients and nine healthy controls. Healthy controls as well as AVN patients were able to reliably perform the task: stimuli with large positive interaural differences (e.g. an ILD/ILD of 5 dB/127 μs)) were always judged rightward (fraction rightward equals 1) and large negative differences leftward (fraction rightward equals 0). Furthermore, the variability in the data was equal for healthy controls and AVN patients.

If vestibular input would underlie the AGI, the AMP of AVN patients would shift significantly contralateral to the affected side compared to healthy controls during fixation. If, on the other hand, the AGI indeed results from eccentric eye position during ocular nystagmus, there would be no difference between patients and healthy controls when listeners fixate straight ahead. In line with the latter hypothesis, the mean AMP of left and right AVN patients (second and third column Fig. 7.4A, respectively) did not differ significantly from healthy controls (first column Fig. 7.4A) (ANOVA: $F_{(2,26)} = 0.88$, $P = 0.43$).

Figure 7.4B demonstrates results on the steepness of the psychometric curve as indicated by the standard deviation of the fitted cumulative gaussian (sigma). There is no significant difference between healthy controls and AVN patients (ANOVA: $F_{(2,26)} = 0.18$, $P = 0.83$). This means that healthy controls and AVN patients had a comparable resolution of the interaural difference cues. Figure 7.4C summarizes the data in a two-dimensional scatter plot of AMP and sigma for the patients and healthy controls. Note that the distributions are highly similar.

Galvanic vestibular stimulation

To further test our hypothesis that the AGI has no vestibular origin, we applied GSV to healthy subjects. Galvanic stimulation of the mastoids produces a vestibular sensation, which can be appreciated from verbal reports of subjects, and from the average eye velocity data of all
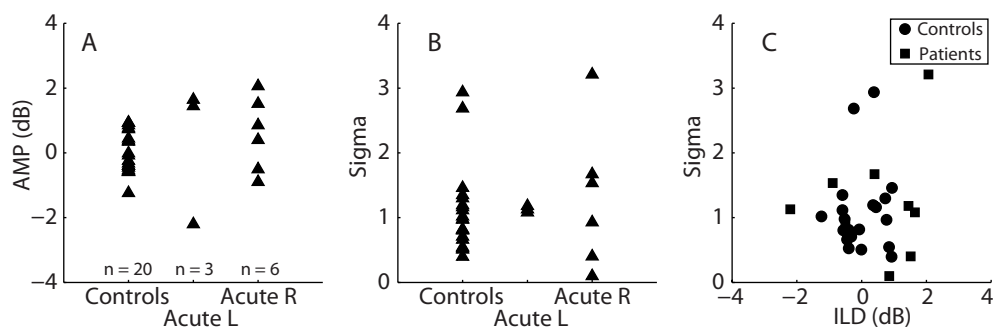

Figure 7.4   Patient AMPs. A) Individual AMPs of healthy controls and AVN patients (triangles) while fixating at straight ahead. B) The standard deviations (sigma) of the fitted cumulative gaussians of all listeners. C) A two-dimensional representation of AMP and sigma for the patients and healthy controls. The distributions are highly similar.
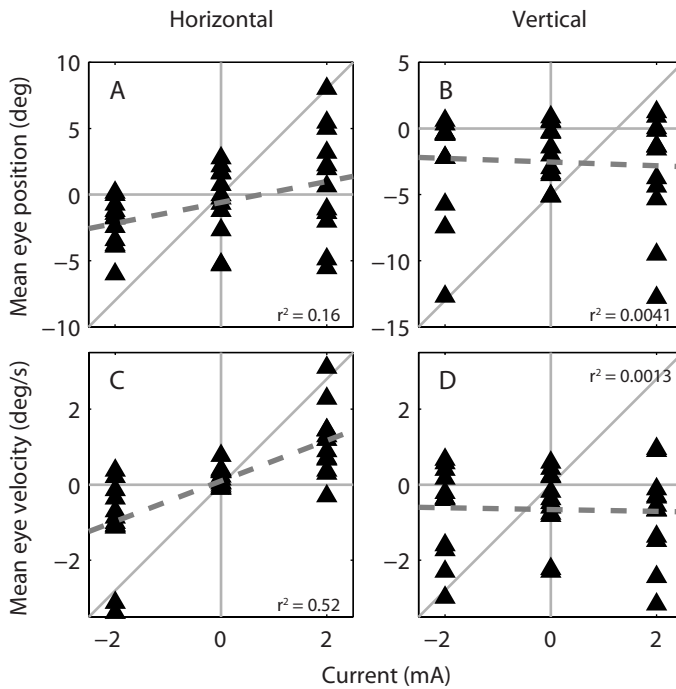
Figure 7.5 Eye data during galvanic vestibular stimulation in darkness. Average horizontal (A) and vertical (B) eye position and horizontal (C) and vertical (D) eye velocity as a function of stimulation current. Each open circle represents the average eye position/velocity during one block of galvanic vestibular stimulation of maximally 75 seconds. Coefficients of determination are given (r²).

single blocks (six per subject, two repetitions of three different currents) that are presented in Figure 7.5. The majority of subjects felt a sensation of tilt or rotation in the direction of the cathode. This corresponds to an average horizontal slow-phase eye velocity in the direction of the anode (Fig. 7.5C; ANOVA: $F_{(2,33)} = 18.5$, $P < 4.1 \cdot 10^{-6}$). GVS did not induce vertical eye movements (Fig. 7.5D; ANOVA: $F_{(2,33)} = 0.15$, $P = 0.86$). The induced horizontal eye movements did not co-occur with a large systematic deviation in average eye position from straight ahead, neither in the horizontal (Fig. 7.5A), nor in the vertical (Fig. 7.5B) direction (ANOVA: horizontal $F_{(2,33)} = 3.23$, $P = 0.05$); vertical $F_{(2,33)} = 0.4$, $P = 0.67$).

Figure 7.6 Individual normalized AMPs as a function of galvanic stimulation current during fixation (A) and in darkness (B).

We determined the AMP of subjects during galvanic vestibular stimulation by pooling all trials of two repetitions of one condition. Figures 7.6A and 7.6B show the normalized individual AMPs (see Methods) during fixation and in darkness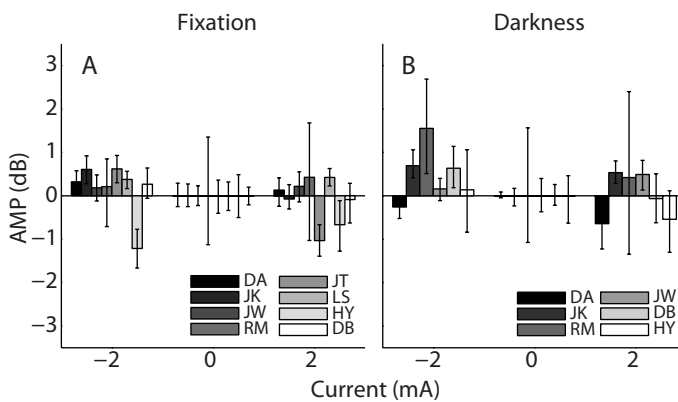, respectively. In both conditions there was no significant effect of galvanic stimulation on the AMP (ANOVA: fixation: $F(2,21) = 0.66$, $P = 0.53$, darkness: $F(2,15) = 1.97$, $P = 0.17$).

DISCUSSION

Summary
The present study set out to investigate the role of the vestibular system in the AGI. We conjectured that if the AGI is due to a pure audio-vestibular interaction, it is expected to be prominent in patients suffering from an acute vestibular loss, and during GVS, even when the eyes are kept at straight ahead. We showed that the AMP of patients with AVN was similar to that of healthy age-matched controls, both in accuracy and precision (Fig. 7.4). Furthermore, although GVS caused a clear vestibular sensation (Fig. 7.5C), it did not shift the AMP, neither in darkness, nor when actively fixating at straight ahead (Fig. 7.6). Taken together, these results strongly suggest that audio-vestibular interactions do not underlie the AGI.

Comparison to earlier studies
Previous research has suggested an effect of the vestibular system on sound lateralization for both whole-body rotation (Münsterberg and Pierce, 1894; Clark and Graybiel, 1949; Arnoult, 1950; Lester and Morant, 1969; 1970; Lewald and Karnath, 2001) and cold caloric stimulation (Lewald and Karnath, 2000), although the direction and the amount of the sound-source displacement differed profoundly between studies. Several causes might underlie these discrepancies. First, the spectral-temporal properties of the applied sounds differed among studies. Some studies used dichotic sounds (Lewald and Karnath, 2000; 2001), others free-field sounds (Münsterberg and Pierce, 1894; Clark and Graybiel, 1949; Arnoult, 1950; Lester and Morant, 1969; 1970). Also, some used narrow-band (Lewald and Karnath, 2000) or tone stimuli (Clark and Graybiel, 1949; Arnoult, 1950; Lester and Morant, 1969; 1970; Lewald and Karnath, 2001), which provided potentially conflicting ILD and ITD cues. We used broadband sounds with covarying ILDs and ITDs to make the dichotic stimuli as informative as possible, and to prevent potential frequency-dependent effects of eye and head orientation

Second, earlier studies have used different methods to stimulate the vestibular system. It is conceivable that caloric stimulation acts as an unnatural stimulation of vestibular afferents by only activating the vestibular organ at one side of the head. In contrast, both GVS and whole-body rotation provide stimulation of both sides, in a way that is more concordant with natural head rotations. Moreover, GVS and acute vestibular loss in patients might induce a head-tilt sensation (Fitzpatrick and Day, 2004), in addition to the clear sensation of rotation, which is evidenced by the eye movement recordings during GVS (Fig. 7.5), and by observations of the spontaneous nystagmus in AVN patients. Although head tilts might induce a perceptual shift of the AMP when assessed through dichotic sounds (Dizio et al. 2001; Lewald and Karnath, 2002), we recently showed that for free-field sounds, listeners accurately estimated the

head-centered zenith during relatively large (35°) head-on-body tilts. In such tilt conditions, the world-centered zenith, on the other hand, was mislocalized by more than 10 degrees (a phenomenon that was termed the Auditory Aubert effect; Van Barneveld et al., 2011b).

Importantly, although it might seem that the present results are in marked contrast with previous findings, they corresponded well with our previous results on audio-vestibular integration (Van Barneveld and Van Opstal, 2010), where we attributed the AMP shift during passive whole-body rotation to an eccentric eye position effect. The VOR shifts the average eye position in the direction of rotation. It has been shown that without vestibular stimulation both static (Lewald and Ehrenstein, 1996; Lewald and Getzmann, 2006; Lewald, 1998) and dynamic changes in eccentric eye position (Van Barneveld and Van Opstal, 2010) shift the AMP in the direction of eye position. Although GVS produced a clear horizontal vestibular nystagmus (Fig. 7.5C), the modest change in average eye position was not sufficient to produce a measurable shift in the AMP. The results in darkness and with the fixation light therefore yielded consistent results. These results also show that the absence of an AMP shift with a fixation light is not due to visual factors, like visual capture (ventriloquist effect), or an ocular pursuit signal that counteracts nystagmus.

Taken together, our results confirm the hypothesis that audio-vestibular interactions do not underlie the AGI.

ACKNOWLEDGEMENTS
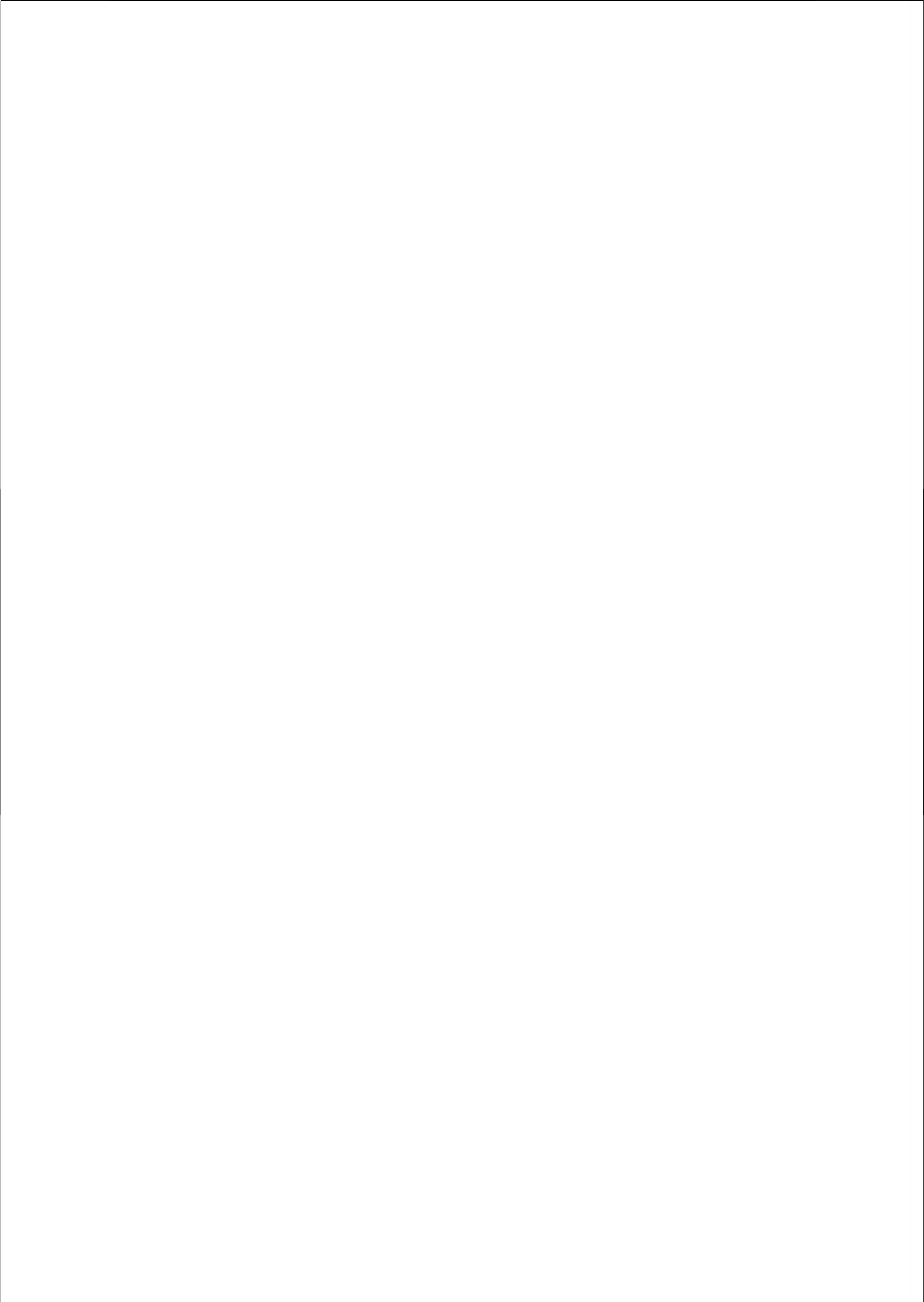
8

Summary

How the brain monitors the environment and our movements within it, so that we can successfully interact with, select, and orient to objects, has been a long-standing problem in systems neuroscience. Since different sensory systems contribute to this process, their information could be combined in a sophisticated manner to improve our perception of the world. This thesis describes a series of experiments designed to investigate different stages of multisensory integration: audio-vestibular integration (chapters 3, 5, 6 and 7), visual-vestibular integration (chapter 2) and audiovisual integration (chapter 4). In the next sections, I will provide a brief summary of the major results.

CHAPTER 2 – ABSENCE OF SPATIAL UPDATING WHEN THE VISUOMOTOR SYSTEM IS UNSURE ABOUT STIMULUS MOTION

Chapter 2 explored spatial updating of visual stimuli during passive whole-body rotation. For correct spatial updating the visuomotor system should decide whether a target is moving or stationary in space, or whether it moves relative to the eyes or head. But how does it do that? A visual flash during a rapid eye-head gaze shift produces a brief visual streak on the retina that could provide information about target motion, when appropriately combined with eye and head self-motion signals. Indeed, double-step experiments have demonstrated that the visuomotor system incorporates actively generated intervening gaze shifts in the final localization response. Also saccades to brief head-fixed flashes during passive whole-body rotation compensate for vestibular-induced ocular nystagmus. However, both the amount of retinal motion to invoke spatial updating, and the default strategy in the absence of detectable retinal motion remain unclear. To study these questions we determined the contribution of retinal motion and the vestibular canals to spatial updating of visual flashes during passive whole-body rotation. Head- and body-restrained humans made saccades toward very brief (0.5 and 4 ms) and long (100 ms) visual flashes during sinusoidal rotation around the vertical body axis in total darkness. Stimuli were either attached to the chair (head-fixed), or stationary in space, and were always well localizable. Surprisingly, spatial updating only occurred when retinal stimulus motion provided sufficient information: long-duration stimuli were always appropriately localized, thus adequately compensating for vestibular nystagmus and the passive head movement during the saccade reaction time. For the shortest stimuli, however, the target was kept in retinocentric coordinates, thus ignoring intervening nystagmus and passive head displacement, regardless whether the target was moving with the head, or not.

CHAPTER 3 – ABSENCE OF COMPENSATION FOR VESTIBULAR-EVOKED PASSIVE HEAD ROTATIONS IN HUMAN SOUND LOCALIZATION

Chapter 3 extends the results of chapter 2 into the auditory domain. A world-fixed sound presented to a moving head produces changing sound-localization cues, from which the audio-motor system could infer sound movement relative to the head. When appropriately combined with self-motion signals, sound localization remains spatially accurate. Indeed,

free-field orienting responses fully incorporate intervening eye-head movements of saccadic gaze shifts under open-loop conditions (i.e., in complete darkness, toward brief sounds). In chapter 3 we investigate the default strategy of the audio-motor system when localising sounds in the absence of efferent and proprioceptive head-movement signals. Head- and body-restrained listeners made saccadic eye movements in total darkness toward brief (3, 10, or 100 ms) broadband noise bursts, while being rotated sinusoidally (f = 1/9 Hz, V_{peak} = 112 °/s) around the vertical body axis. Since the loudspeakers were attached to the chair, the 100 ms sounds might be perceived as rotating along with the chair, and localized in a head-centered reference frame. We showed that during 3 and 10 ms stimuli, however, the amount of chair rotation remained well below the minimum audible movement angle. These brief sounds would therefore be perceived stationary in space and, like in open-loop gaze-orienting, expected to be localized in world-centered coordinates. Analysis of the saccades showed, however, that all stimuli were accurately localized on the basis of imposed acoustic cues, but remained in head-centered coordinates. These results suggest that in the absence of motor planning the audio-motor system keeps sounds in head-centered coordinates when unsure about sound motion relative to the head. To that end, it ignores vestibular canal signals of passive-induced head rotation, but incorporates intervening eye-displacements from vestibular nystagmus during the saccade-reaction time.

Taken together, the results of chapters 2 and 3 suggest that the default strategy of the auditory and visual systems under vestibular-only stimulation would be to keep targets in their initial reference frame (for audition this means: head-centered; for vision: eye-centered) until sufficient sensory evidence reveals stimulus motion relative to the head or eye, respectively. This default strategy may seem surprising, or even suboptimal, as in daily life it is highly unlikely that sounds move along with the head at exactly the same speed, or that visual stimuli are fixed on the retina.

CHAPTER 4 – REFERENCE FRAME OF THE VENTRILOQUIST EFFECT

Chapter 4 deals with audiovisual integration. Orienting responses to audiovisual events have shorter reaction times and better accuracy and precision when images and sounds in the environment are aligned in space and time. How the brain constructs an integrated audiovisual percept is a computational puzzle because the auditory and visual senses are represented in different reference frames: the retina encodes visual locations with respect to the eyes, whereas the sound-localization cues are referenced to the head. In the well-known ventriloquist effect, the auditory spatial percept of the ventriloquist's voice is attracted toward the synchronous visual image of the dummy, but does this audiovisual interaction occur at the initial stages or at a common stage? In chapter 4 we studied this question by independently varying initial eye and head orientations, and the amount of audiovisual spatial mismatch. Human subjects pointed head and/or gaze to auditory targets in elevation, and were instructed to ignore visual distracters. Results indicate that vision captures sounds in a common reference frame, rather than at a stage where audition and vision are still represented in their initial reference frames. Furthermore, our results suggest that humans accurately incorporate the different head and

eye orientations required for the appropriate sensorimotor coordinate transformations.

CHAPTER 5 – THE EFFECT OF HEAD ROLL ON PERCEIVED AUDITORY ZENITH

Whereas chapters 2 and 3 focus on the role of the vestibular canals in spatial updating, chapter 5 explores the effect of stimulating the vestibular otoliths on the perceived auditory zenith. Specifically, we studied the influence of static head roll on the perceived auditory zenith in head-centered and world-centered coordinates. Subjects sat either upright, or with their head left/right rolled sideways by about 35° relative to gravity, while judging whether a broadband sound was heard left or right from the head-centered or world-centered zenith. When upright, these reference frames coincide. Results showed that subjects judged the zenith accurately within different planes, although response variability increased for the midsagittal plane. With the head rolled, head-centered auditory zenith shifted by the same amount, and was located as accurately as for upright, indicating unaltered localization cues by head-on-body roll. Interestingly, when judging world-centered zenith subjects made large systematic errors (10-15°) in the direction of head roll, and response variability increased, which resembles the visual Aubert effect. These results demonstrated a significant influence of the vestibular-collic system on auditory spatial awareness, which sheds new light on the mechanisms underlying multisensory integration and spatial updating in sound-localization behaviour.

CHAPTER 6 – EYE POSITION DETERMINES AUDIO-VESTIBULAR INTEGRATION DURING WHOLE-BODY ROTATION

In chapters 4 and 5, we show that multisensory integration might cause systematic localization errors (the ventriloquist effect and the auditory Aubert effect, respectively). Chapter 6 investigates another type of error resulting from multisensory integration: the audiogyral illusion (AGI). When a sound is presented in the free field at a location that remains fixed to the head during whole-body rotation in darkness, it is heard displaced in the direction opposing the rotation (the AGI). Consequently, the subjective auditory median plane (AMP; the plane where the binaural difference cues for sound localization are perceived to be zero) shifts in the direction of body rotation. Recent experiments, however, have suggested opposite AMP results when using a fixation light that also moves with the head. Although in this condition the eyes remain stationary in the head, an ocular pursuit signal cancels the vestibulo-ocular reflex (VOR), which could induce an additional AMP shift. We tested whether the AMP is influenced by vestibular signals, eye position, or eye velocity. We rotated subjects sinusoidally at different velocities, either in darkness, or with a head-fixed fixation light, while they judged the laterality (left vs. right with respect to the midsagittal plane of the head) of broadband sounds presented over headphones. Subjects also performed the same task without vestibular stimulation while tracking a sinusoidally moving visual target, which mimicked the average eye-movement patterns of the vestibular experiments in darkness. Results showed that whole body rotation in darkness induces a shift of the AMP in the direction of body rotation. In

contrast, we obtained no significant AMP change when a fixation light was used. The pursuit experiments showed a shift of the AMP in the direction of eccentric eye position, but not at peak pursuit velocity. We therefore concluded that the vestibular-induced shift in average eye position underlies both the AGI and the AMP shift.

CHAPTER 7 - SOUND LATERALIZATION IS NOT AFFECTED IN PATIENTS WITH ACUTE UNILATERAL VESTIBULAR NEURONITIS, NOR DURING GALVANIC VESTIBULAR STIMULATION

In chapter 6, we attributed the AGI to an eccentric eye-position effect due to vestibular nystagmus, rather than to a proper vestibular effect, as the AGI disappeared during vestibulo-ocular reflex cancellation with a fixation light. Moreover, our smooth pursuit experiments indicated that eccentric eye position and not the peak pursuit eye-velocity through straight-ahead shifted the AMP. In chapter 7, we further examined this hypothesis in acute vestibular neuronitis (AVN) patients, who perceive head rotation away from the affected side accompanied by ocular nystagmus. Stationary listeners lateralized sounds while fixating at straight ahead. We found, like in normal controls, that the AGI in AVN patients was absent when they fixated straight ahead to counteract nystagmus. In addition, we tested the AMP of healthy subjects with bilateral bipolar galvanic vestibular stimulation (GVS) of the mastoids either in total darkness of while fixating straight ahead. GVS did not induce a shift of the AMP in either condition. These results provide further support for the hypothesis that the AGI is not caused by a proper vestibular interaction with binaural auditory processing.
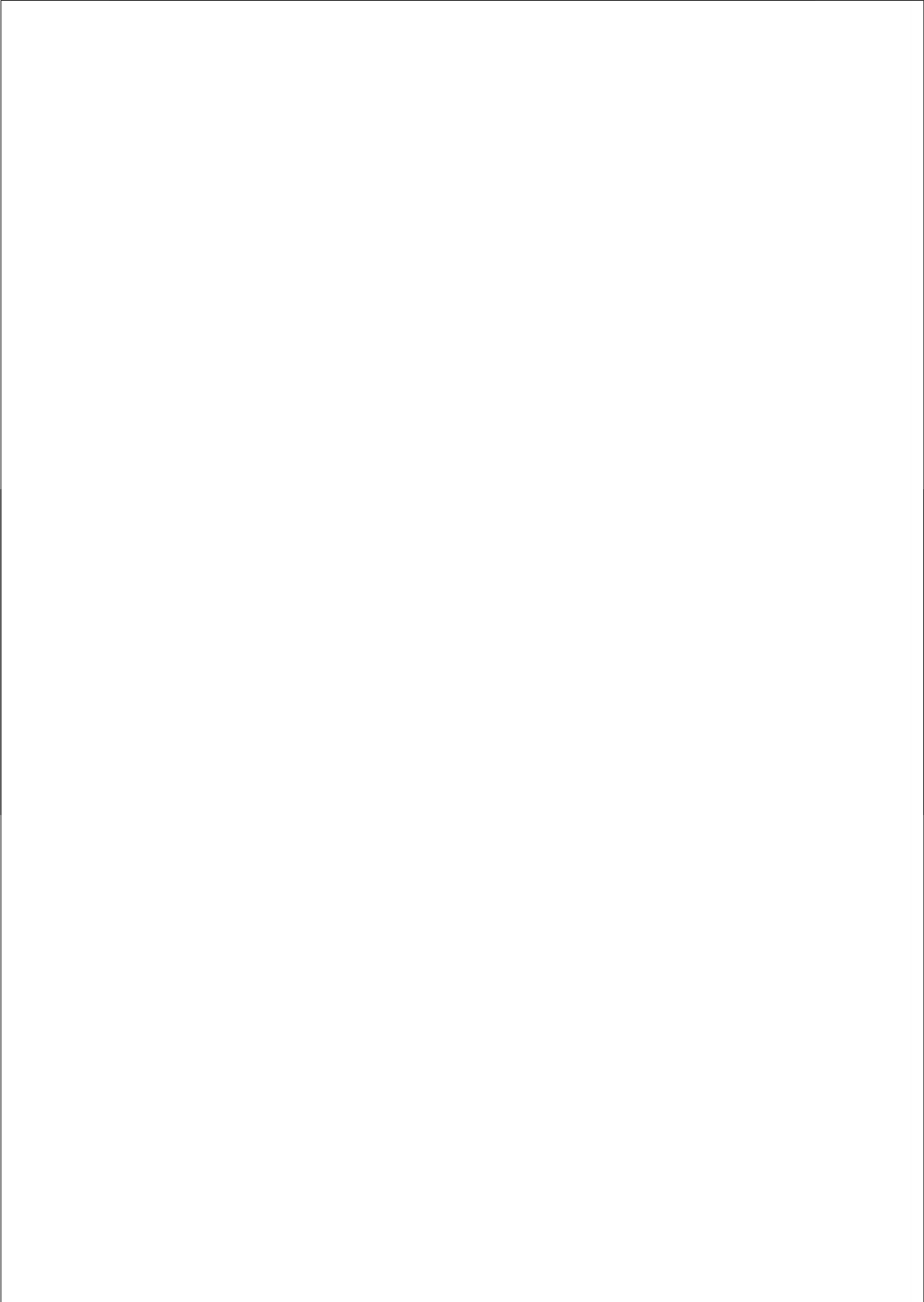
9

De integratie van interne en externe
signalen voor ruimtelijke localisatie

Nederlandse samenvatting

Als je over straat loopt en je hoort iemand je naam roepen, dan kijk je om naar wie je riep. Dit lijkt een gemakkelijke handeling die we automatisch uitvoeren, maar is dit wel zo eenvoudig voor ons brein als het lijkt? Ons brein krijgt signalen binnen van verschillende zintuigen en moet complexe berekeningen maken om zulk doelgericht gedrag te kunnen vertonen. Een bijkomend probleem is dat elk zintuig informatie binnenkrijgt in een bepaald referentiekader. Visuele informatie valt op het netvlies en wordt gecodeerd ten opzichte van de kijkrichting, geluiden komen binnen via de oren die aan het hoofd vastzitten en worden dus gecodeerd in hoofdcentrische coördinaten. Deze informatie moet getransfomeerd worden naar ruimtelijke coördinaten, zodat er een coherent beeld van de omgeving ontstaat. Vaak houdt dit in dat informatie uit verschillende zintuigen (sensoren) gecombineerd moet worden, een proces dat we multisensorische integratie noemen. Daarnaast moeten onze hersenen rekening houden met alle bewegingen die we maken, zodat we correct waarnemen dat wij door een voornamelijk stilstaande wereld heen bewegen. Dit proces heet spatial updating.

Hieronder geeft ik een korte introductie van de relevante onderwerpen die bij multisensorische integratie en spatial updating een rol spelen en van de problemen die de hersenen tegenkomen als informatie van meerdere zintuigen moet worden gecombineerd. Ook volgt er een gedetailleerde samenvatting van het onderzoek dat beschreven staat in hoofdstuk 2 t/m 7.

HET VISUEEL SYSTEEM

Om veilig door de wereld heen te bewegen, is het belangrijk om obstakels te vermijden. Het visueel systeem is het belangrijkste zintuig dat we gebruiken om de locatie van deze obstakels te bepalen. Visuele informatie komt onze hersenen binnen via de ogen. De lens projecteert objecten topografisch op de twee retina's (netvliezen), zodat aangrenzende punten op de retina aangrenzende punten in de buitenwereld coderen. Deze retinotope organisatie blijft behouden tot aan de visuele cortex (Sereno et al., 1995). Zoals hieronder zal blijken, is alleen retinale informatie over de obstakels niet genoeg voor correcte ruimtelijke lokalisatie in het dagelijks leven. Het systeem moet namelijk ook rekeninghouden met de positie van de ogen in de oogkas en van het hoofd op de romp en in de ruimte bij het berekenen van de absolute posities van objecten in de wereld.

Ondanks dat we een groot visueel veld hebben, is maar een klein gedeelte (de gele vlek of fovea) van de retina gespecialiseerd in gedetailleerd en scherp zien. De gele vlek bevindt zich in het centrum van de retina en bestaat uit een dichte hoeveelheid kleurgevoelige kegeltjes. Het perifere netvlies heeft een lage receptordichtheid (staafjes) en is minder gespecialiseerd in scherp en kleuren zien, maar heeft wel een hoge sensitiviteit in het donker en voor beweging. Als gevolg hiervan moeten we de fovea naar perifere objecten richten, wanneer we deze in detail willen bekijken. Hiervoor hebben primaten (en andere dieren met een fovea, zoals de kat) de mogelijkheid gekregen snelle oogbewegingen, saccades, te kunnen maken die de kijklijn naar een nieuw punt kunnen verschuiven.

De snelle oogbewegingen zorgen echter voor een serieus probleem voor het visueel systeem dat opgelost moet worden: elke oogbeweging laat de visuele wereld over het netvlies

bewegen en zorgt ervoor dat een object op een andere plaats op de retina valt. Daarom moet het visuele systeem zijn interne representatie van de wereld bijstellen na iedere oogbeweging ('spatial updating') om correct waar te nemen dat de ogen door een stilstaande wereld bewegen en niet dat de wereld rond de waarnemer beweegt. Hieronder zal ik spatial updating en de bijbehorende coördinatentransformaties in meer detail bespreken.

GELUIDSLOKALISATIE

Ondanks dat onze ogen belangrijke zintuigen zijn voor het lokaliseren van objecten in de wereld om ons heen, moet de rol van het gehoor niet worden onderschat; we kunnen geluiden van achteren, ver buiten ons gezichtsveld horen en hun locaties nauwkeurig bepalen in totale duisternis. De eerste stadia van het auditieve systeem zijn, in tegenstelling tot het visueel systeem, niet in een spatieel

Figure 9.1   Schematische representatie van het oor en binnenoor.

formaat georganiseerd. Ze zijn tonotopisch georganiseerd: elk punt op het basilaire membraan reageert op een toon van een bepaalde frequentie, ongeacht de locatie van deze geluiden. Het slakkenhuis rafelt het geluid dus uiteen in afzonderlijke tonen en heeft niet direct informatie over de locatie. Daarom moet het auditieve systeem positie-informatie van geluiden op een andere manier achterhalen dan het visuele systeem. Het berekent de positie van een geluidsbron dankzij de interactie van de geluidgolven met de oren, het hoofd en de torso.

Geluidslokalisatie in azimut

Geluidslokalisatie in het horizontale vlak (azimut) wordt gebaseerd op verschillen in aankomsttijd en luidheid tussen de twee oren (interaurale tijd en luidheidsverschillen; Blauert, 1997). Geluidsgolven bereiken eerst het oor het dichtst bij de geluidsbron en later het andere
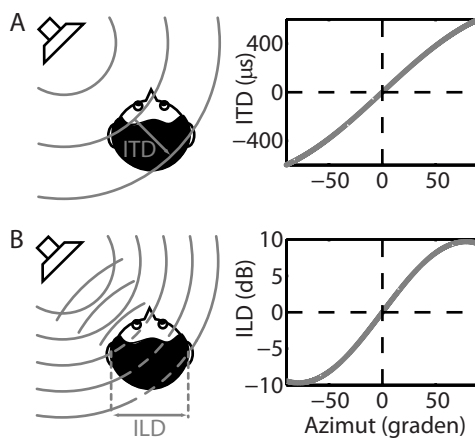
Figure 9.2   Geluidslokalisatie in azimut: interaural tijd- (ITD) en luidheidsverschillen (ILD). A) De relatie tussen azimut (α) en ITD wordt benaderd voor een bolvormig hoofd met *ITD=r/c (α+sinα)*, waarbij r de straal van het hoofd (ongeveer 8 cm) is en c de geluidssnelheid 343 m/s. B) De ILD relatie voor breedbandige geluiden wordt beschreven door *ILD=9.7·sin(0.02·α)* (Van Wanrooij and Van Opstal, 2004).
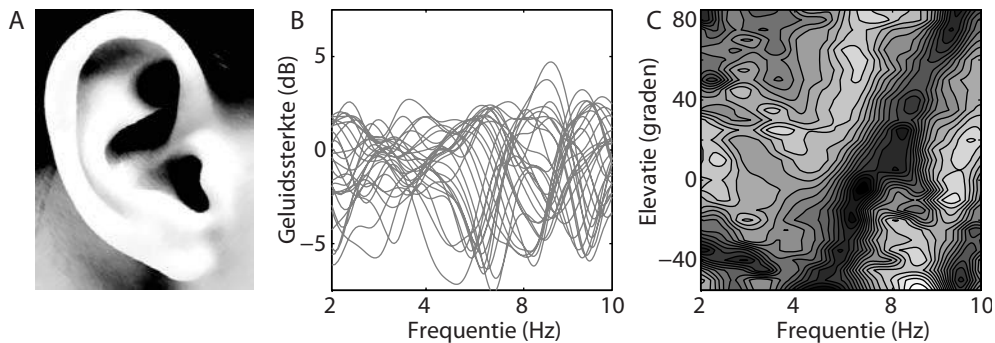
Figure 9.3 Richtinsafhankelijke filtering door de oorschelp (A), hoofd en schouders. B) Metingen van de geluidssterkte ter hoogte van het trommelvlies als functie van frequentie voor geluiden van verschillende elevatie. C) Hoogteplot van dezelfde metingen waarbij de grijswaarde de geluidssterkte weergeeft (zwart: laag, wit: hoog). Er is een duidelijk richtsings- en frequentieafhankelijk dal te zien.

oor, waardoor er een interauraal tijdsverschil ontstaat (Fig. 9.2A; Engels: interaural time difference: ITD). ITDs variëren systematisch met de horizontale locatie van het geluid. Het auditief systeem kan echter alleen vertrouwen op tijdsverschillen voor tonen met een lage frequentie (beneden ongeveer 1500-2000 Hz). Bij hogere frequenties is het tijdsverschil niet langer een unieke code. Echter, voor deze frequenties wordt het hoofd een significant obstakel voor de geluidsgolven. Dit zorgt voor een hoofdschaduw: de intensiteit van het geluid in het oor dichtst bij de bron is hoger dan in het andere oor. Oftewel er treden interaurale luidsheidsverschillen op (Fig. 9.2B; Engels: interaural level difference: ILD).

Geluidslokalisatie in elevatie

De binaurale verschillen variëren systematisch met azimut, maar niet met de verticale locatie van de bron (elevatie), omdat de oren meestal op dezelfde hoogte zitten. Ook gespiegelde voor-achter locaties hebben dezelfde ILD en ITD. Nauwkeuriger uitgedrukt, er is een hele kegel met locaties met identieke ITD en ILD: de verwarringskegel (of: cone of confusion in het Engels). Om lokalisatie in het verticale vlak mogelijk te maken, interpreteert het brein de complexe spectrale vervorming van het geluid door de oorschelp, hoofd en schouders. Het geluid wordt gereflecteerd door de plooien van de oorschelp en hoofd en schouders waardoor sommige tonen harder doorkomen, en andere juist zwakker, zodat ter hoogte van het trommelvlies een patroon van versterkingen en verzwakkingen ontstaat dat op een gecompliceerde manier afhangt van de richting waaruit het geluid komt (Fig. 9.3; Wightman en Kistler, 1989; Middlebrooks, 1992). Door de geluidssterkte in verschillende frequentiebanden met elkaar te vergelijken kan het brein de verticale positie van het geluid bepalen (Hofman en Van Opstal, 2002).

HET EVENWICHTSSYSTEEM

In het dagelijks leven bewegen we continu en om een stabiel beeld van de wereld om ons heen te krijgen, moet het brein deze bewegingen bijhouden. Hiervoor kan het verschillende signalen gebruiken. Omdat we meestal zelf onze bewegingen plannen, heeft het brein de beschikking
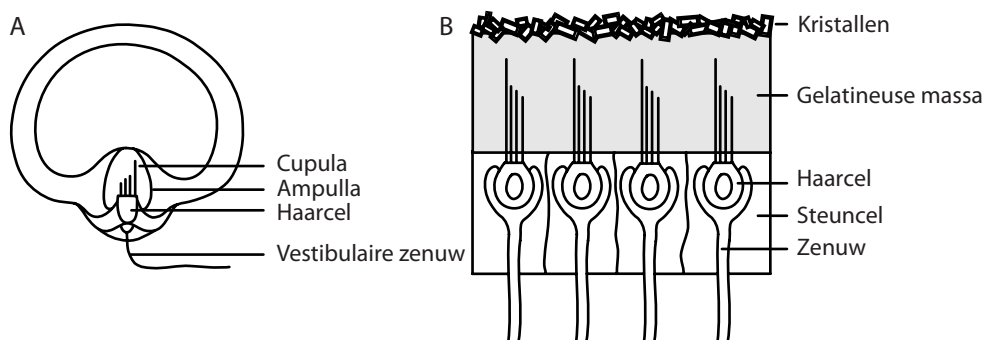
Figure 9.4   Schematische representatie van de anatomie van (A) halfcirkelvormige kanalen en (B) otolieten.

over efferente kopieën van signalen die naar de spieren gaan om deze aan te sturen (Crapse and Sommer, 2008). Verder detecteren spierspoeltjes de bewegingen van het hoofd op het bovenlichaam en die van het bovenlichaam op de heupen etc. (proprioceptie; Armstrong et al., 2008). Daarnaast worden onze hoofdbewegingen door de ruimte gedetecteerd door het evenwichtsorgaan. Het evenwichtssysteem vertaalt continu de hoofdbewegingen en hoofdoriëntatie ten opzichte van de zwaartekracht in neuronale signalen die naar de hersenstam worden gezonden (Angelaki en Cullen, 2008). Al deze verschillende interoceptieve signalen kunnen gecombineerd worden om onze lichaamsoriëntatie in de ruimte en veranderingen hierin te detecteren.

In dit proefschrift heb ik me beperkt tot de rol van het evenwichtssysteem in ruimtelijke lokalisatie. Het evenwichtsorgaan bevindt zich in het binnenoor aan beide zijden van het hoofd (Fig. 9.4). Het bestaat uit drie halfcirkelvormige kanalen die hoofddraaiing detecteren en twee otolieten, de uriculus en saccules, die hoofdversnelling (en dus ook de richting van de zwaartekracht) detecteren.

MULTISENSORISCHE INTEGRATIE

Doorgaans krijgen meerdere sensoren informatie over de wereld om ons heen en de orientatië van ons eigen lichaam binnen. Het integreren van deze signalen, een proces dat multisensorische integratie wordt genoemd, kan nuttig zijn om een aantal redenen. Allereerst kan de ene sensor informatie aanvullen die andere zintuigen missen. We kunnen bijvoorbeeld audiovisuele doelen die zich achter ons bevinden niet zien, maar we kunnen deze wel horen. Daarnaast kan het combineren van informatie uit meerdere sensoren mogelijk ambigue informatie die een enkele sensor levert, oplossen. Aan de hand van efferente kopieën van oogbewegingssignalen bijvoorbeeld, kan het brein bepalen of visuele beweging op de retina het gevolg is van een bewegend object ten opzichte van een stilstaand oog of van een stilstaand object ten opzichte van een bewegend oog. Verder kan het combineren van signalen leiden tot preciezere lokalisatieresponsies en verkorte saccadische reactietijden zoals bekend is van audiovisuele integratie (Frens et al., 1995; Colonius en Arndt, 2001; Corneil et al., 2002).

REFERENTIEKADERTRANSFORMATIES

Een probleem bij multisensorische integratie is dat sensoren en spieren informatie in verschillende referentiekaders coderen. Zoals ik hierboven al aangaf, wordt auditieve informatie gecodeerd ten opzichte van het hoofd oftewel in hoofdcentrische coördinaten, terwijl visuele informatie in retinotope of oogcentrische coördinaten binnenkomt. Om doelgericht oogbewegingen naar geluiden of beelden te maken, moet de sensorische signalen getransformeerd worden naar oogcentrische bewegingscommando's die naar de spieren gestuurd worden. Bij het transformeren van geluiden moet er ook rekening worden gehouden met oog-in-hoofd stand, terwijl dit voor visuele informatie niet nodig is.

SPATIAL UPDATING

Normaalgesproken staan we meestal niet stil als we doelgerichte oog- en hoofdbewegingen plannen. De initiële oogcentrische doellocaties zijn onbruikbaar zodra de ogen in een andere richting kijken. Bovendien moet er ook rekening gehouden worden met lichaamsbewegingen waardoor het hoofd in de ruimte wordt verplaatst. Bijvoorbeeld een kopje op tafel dat zich 45 graden rechts van me bevindt, verschuift naar 45 graden links van me wanneer ik me 90 graden naar rechts draai. Als er bij de planning van een oogbeweging wordt uitgegaan van de initiële doellocatie heeft dit dus significante lokalisatiefouten tot gevolg. Het systeem zou kunnen wachten op visuele terugkoppeling (feedback) voor het bepalen van de nieuwe locatie van het object, maar dit zou te veel tijd kosten. Om vertragingen te voorkomen moet het brein de nieuwe locatie berekenen: een proces dat spatial updating heet.

Spatial updating kan worden beschouwd als een referentiekadertransformatie. Voor een reactie naar een visueel doel dat vast staat in de wereld, moeten de initiële retinotope coördinaten getransformeerd worden naar in bewegingscommando's voor de oogspieren, waarbij er rekening moet worden gehouden met oog- een hoofdverplaatsingen die plaatsvinden in de reactietijd. Om te reageren naar een doel dat met het hoofd meebeweegt, daarentegen, hoeft er niet gecompenseerd te worden voor de hoofdverplaatsing, maar wel voor oogverplaatsing.

In **hoofdstuk 2** bestudeerden we spatial updating van visuele stimuli tijdens passieve lichaamsrotatie. Voor correcte spatial updating moet het visuomotor systeem bepalen of een doel beweegt of stilstaat in de ruimte, of dat het beweegt ten opzichte van de ogen of het hoofd. Maar hoe doet het dat? Een geflitst doel tijdens een snelle oog-hoofdbeweging zorgt voor een korte visuele streep op het netvlies, die informatie zou kunnen bieden over de doelbeweging mits deze op de juiste manier wordt gecombineerd met oog- en hoofdbewegingssignalen. Dubbelstapexperimenten, waarbij ogen en hoofd actief bewogen worden tussen doelpresentatie en respons, hebben dan ook laten zien dat het visuomotor systeem bij de lokalisatieresponsies rekening houdt met deze actief gegenereerde oog-hoofdverplaatsingen. Ook saccades naar korte hoofd-vaste flitsen die werden aangeboden tijdens passieve lichaamsrotatie corrigeerden voor de vestibulaire nystagmus, oogbewegingen geïnduceerd tijdens hoofdrotatie. Het is echter niet bekend hoeveel visuele beweging op het netvlies er nodig is voor spatial updating en wat

de standaard strategie van het systeem is als er onvoldoende visuele beweging op het netvlies valt. Om deze vragen te bestuderen, hebben we de bijdrage van de beweging op het netvlies en van de vestibulaire kanalen aan spatial updating van geflitste doelen bepaald tijdens passieve rotatie van het gehele lichaam. Proefpersonen werden met het hoofd en lichaam vastgezet in een vestibulaire stoel en maakten saccades naar hele korte (0.5 en 4 ms) en langere (100 ms) flitsen tijdens passieve sinusvormige rotatie rond de vertikale lichaamsas in totale duisternis. Het LED-bord waarmee de flitsen werden aangeboden, zat vast aan de stoel (hoofd-vast), of stond in de ruimte (wereld-vast). De flitsen waren altijd goed zichtbaar en lokaliseerbaar. Verrassend genoeg vond er alleen spatial updating plaats als de beweging op het netvlies voldoende informatie bood over stimulusbeweging: de lange stimuli werden altijd op de juiste wijze gelokaliseerd. Dus bij stoelvaste stimuli werden oogverplaatsing en hoofdverplaatsing tijdens de reactietijd gecompenseerd en bij hoofdvaste stimuli alleen de oogverplaatsing. De kortste stimuli, echter, werden gelokaliseerd in oogcentrische coördinaten: het visuomotor systeem negeerde zowel oog- als hoofdverplaatsingen, ongeacht of het doel met het hoofd meebewoog of niet.

Hoofdstuk 3 breidt de resultaten van hoofdstuk 2 uit naar het auditieve domein. Een wereld-vast geluid dat gepresenteerd wordt aan een bewegend hoofd veroorzaakt veranderende geluidslokalisatiecues, waardoor het audiomotor systeem kan afleiden of het geluid bewoog ten opzichte van het hoofd. Als deze op de juiste manier worden gecombineerd met zelfbewegingssignalen, blijft geluidslokalisatie spatiëel accuraat. Inderdaad, bij het maken van lokalisatieresponsies naar vrije-veldgeluiden houdt het brein rekening met oog- en hoofdverplaatsingen die tussen stimuluspresentatie en respons plaatsvinden in "open-loop" condities (zonder feedback in totale duisternis). In hoofdstuk 3 onderzochten we de standaard strategie van het audiomotor systeem bij geluidslokalisatie in de afwezigheid van efferente en proprioceptieve hoofdbewegingssignalen. Proefpersonen werden met het hoofd en lichaam vastgezet in een vestibulaire stoel en maakten saccades naar korte (3, 10 en 100 ms) breedbandige geluiden in totale duisternis, terwijl ze sinusvormig rond de vertikale lichaamsas gedraaid werden. Omdat de luidsprekers aan de stoel bevestigd waren, verwachtten we dat de 100 ms geluiden correct werden waargenomen als meedraaiend en dus werden gelokaliseerd in een hoofdcentrisch referentiekader. We lieten zien dat de stoelverplaatsing gedurende 3 en 10 ms veel kleiner was dan de minimaal hoorbare bewegingshoek. Deze stimuli zouden daardoor kunnen worden beschouwd als stilstaand in de wereld. Wij zouden daarom verwachten, zoals bij open-loop lokalisatie, dat deze gelokaliseerd worden in wereldcentrische coördinaten. De analyse van de saccades laat echter zien dat alle stimuli goed gelokaliseerd werden op basis van de acoustische eigenschappen, maar dat de responsies in hoofdcentrische coördinaten bleven. Deze resultaten suggereren dat in de afwezigheid van motorplanning het audiomotor systeem geluiden in hoofdcentrische coödinaten houdt als het onzeker is over de beweging van het geluid ten opzichte van het geluid. Daartoe negeert het de signalen uit de vestibulaire kanalen over passieve hoofdverplaatsing, maar houdt het wel rekening met oogverplaatsingen als gevolg van vestibulaire nystagmus tijdens de reactietijd.

De resultaten van hoofdstuk 2 en 3 suggereren dat het auditieve en visuele systeem standaard doelen in hun initiële referentiekader houden, totdat er voldoende sensorische infomatie is om te bepalen of doelen bewegen ten opzichte van hoofd of oog, respectievelijk.

Voor het gehoor is dit initiële referentiekader hoofdcentrisch en voor visuele doelen oogcentrisch. Deze standaard strategie lijkt erg verrassend, of zelf suboptimaal, omdat het in het dagelijks leven erg onwaarschijnlijk is dat geluiden met dezelfde snelheid met het hoofd meebewegen, of dat visuele stimuli vast zitten op het netvlies.

MULTISENSORISCHE INTEGRATIE KAN TOT FOUTEN LEIDEN

Ondanks dat multisensorische integratie gunstig kan zijn in meerdere opzichten, kan het ook tot fouten leiden. In dit proefschrift heb ik drie typen van zulke fouten onderzocht: het buiksprekerseffect (hoofdstuk 4), het auditieve Aubert-effect (hoofdstuk 5) en de audiogyrale illusie (hoofdstuk 6 en 7).

Het buiksprekerseffect
Van oudsher wordt gedacht dat visuele informatie in ruimtelijke perceptie superieur en dominant is over de andere sensorische systemen (Welch en Warren, 1980). Een bekend voorbeeld is het buiksprekerseffect, waarbij de buikspreker de mond van de pop laat bewegen terwijl hij praat (Fig. 9.5). Daardoor lijkt het of het geluid van de pop afkomstig is, terwijl we toch echt wel weten dat de buikspreker praat en niet de pop. Hoewel multisensorische integratie hier fout lijkt te gaan, kan het verklaard worden door statistisch optimale integratie van multimodale stimuli (Alais en Burr, 2004; Körding et al., 2007). Volgens deze theorie worden het auditieve en visuele percept gewogen met elkaar gemiddeld waarbij het gewicht afhangt van de betrouwbaarheid van het signaal: hoe betrouwbaarder het signaal, hoe meer gewicht het krijgt. Hierdoor treden er weliswaar lokalisatiefouten op, maar is de onzekerheid van het audiovisuele percept kleiner dan die van de unimodale percepten. Audiovisuele experimenten lieten dit fenomeen duidelijk zien bij responsies naar audiovisuele doelen: deze waren preciezer dan responsies naar unimodale stimuli (Van Wanrooij et al., 2009; 2010).

Het lijkt nogal vanzelfsprekend dat alleen signalen die vanuit dezelfde gebeurtenis en locatie geïntegreerd mogen worden. Experimenten hebben inderdaad laten zien dat hoe groter de dispariteit (afstand in de ruimte) tussen geluid en beeld, hoe minder invloed het beeld heeft op geluid (Bertelson en Radeau, 1981; Frens et al., 1995; Van Wanrooij et al., 2009). Om te weten of signalen van dezelfde gebeurtenis afkomstig zijn, moet het brein de unimodale locaties van beeld en geluid bepalen, beslissen of de auditieve en visuele signalen van dezelfde bron afkomstig zijn (Körding et al., 2007; Van Wanrooij et al., 2010), de

Figure 9.5   Buikspreker met pop

signalen integreren volgens de beslissing (Alais en Burr, 2004) en een reactie voorbereiden en uitvoeren naar het doel (Corneil et al., 2002). Maar omdat auditieve informatie het brein binnenkomt in een hoofdcentrisch referentiekader en visuele informatie wordt gecodeerd in oogcentrische coördinaten, moeten deze signalen worden getransformeerd naar een gemeenschappelijk referentiekader voordat het brein kan bepalen of deze signalen vanuit dezelfde plaats in de ruimte afkwamen.

Dit is geen triviale hypothese, omdat neurofysiologische data suggereert dat neuronen in hersengebieden die betrokken zijn bij multimodaal lokalisatiegedrag auditieve en visuele receptieve velden (locaties in de ruimte waar presentatie van een stimulus leidt tot een respons in de cellen) hebben die niet in een gemeenschappelijk referentiekader gecodeerd worden (Jay en Sparks, 1984; Mullette-Gillman et al., 2005; Schlack et al., 2005). Bovendien suggereert gedragsdata een ruimtelijk-incorrecte integratie bij perceptuele beslissingen bij audiovisuele fusiegebieden (Hartnagel et al., 2007) en voor de recalibratie van geluiden bij het buikspreker-naeffect (Kopčo et al., 2009).

In **hoofdstuk 4** onderzochten we of het buiksprekerseffect inderdaad in een gemeenschappelijk referentiekader plaatsvindt. Proefpersonen maakte snelle oog-hoofdbewegingen naar audiovisuele doelen. Ze werden daarbij geïnstrueerd het geluid te lokaliseren en de visuele flits te negeren. Daarbij varieerden we initiële oog- en hoofdoriëntaties en de grootte van de audiovisuele dispariteit. De resultaten lieten zien dat audiovisuele integratie inderdaad plaatsvindt in een gemeenschappelijk referentiekader. Verder suggereren de resultaten dat mensen corrigeren voor de verschillende oog- en hoofdstanden wat nodig is voor de juiste coördinatentransformaties.

Het auditieve Aubert-effect

Normaal gesproken is de richting en sterkte van de zwaartekracht constant. Daarom zouden we kunnen aannemen dat het weten van de richting van de zwaartekracht voldoende zou zijn om lichaamskanteling ten opzichte van de aarde te kunnen schatten en om te kunnen schatten wanneer een object verticaal in de wereld staat. Paradoxaal genoeg kunnen gekantelde proefpersonen wel nauwkeurig aangeven hoeveel ze zijn gekanteld (stippellijn Fig. 9.6; Mittelstaedt, 1983; Mast and Jarchow, 1996; Van Beuzekom et al., 2001), maar zijn zij niet in staat een lijn verticaal in de wereld te zetten (dikke lijn Fig. 9.6). Hun fouten hangen systematisch af van kantelhoek (Aubert, 1861; Mittelstaedt, 1983; Kaptein and Van Gisbergen, 2004) of van hoofd-op-lichaam oriëntatie (Van Beuzekom et al., 2001). Rechtop maken mensen verwaarloosbare fouten. Bij kleine kantelhoeken overcompenseren proefpersonen hun kantelhoek, terwijl ze ondercompenseren bij grote kantelhoeken. Wanneer een proefpersoon bijvoorbeeld op zijn rechter zij ligt (90 graden naar rechs gekanteld), lijkt een lijn die in werkelijkheid verticaal in de wereld staat wel 30 graden naar links gekanteld. Ook dit fenomeen kan verklaard worden door statistisch optimale integratie van signalen, waarbij er wordt aangenomen dat het hoofd meestal rechtop in de wereld staat (De Vrijer et al., 2008).

In **hoofdstuk 5** hebben we deze visuele resultaten uitgebreid naar het auditieve domein. We onderzochten de rol van de otolieten en proprioceptie van de nekspieren bij het bepalen van de auditieve zenit (het punt recht boven het hoofd) als analoog aan de visuele verticaal. Proefpersonen zaten ofwel rechtop, ofwel met hun hoofd naar links of rechts gekanteld tot
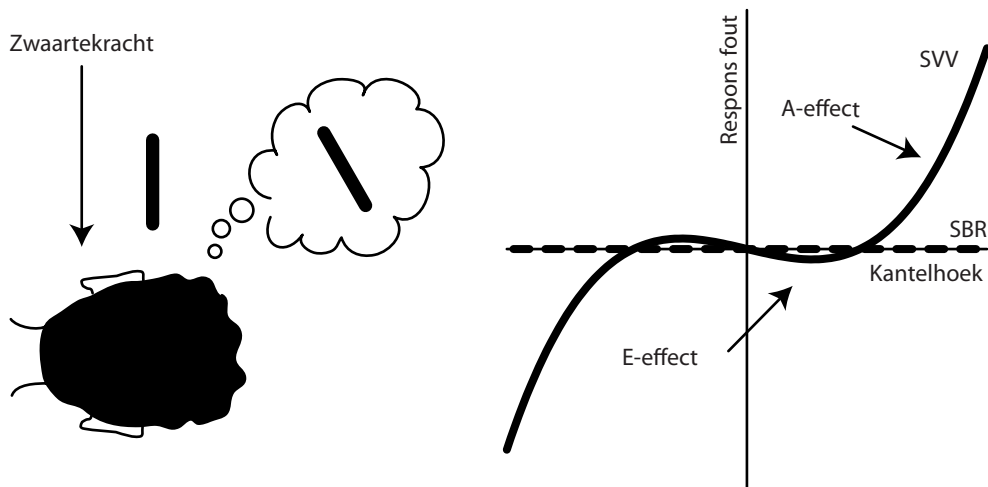
Figure 9.6   Aubert-effect. Een lijn die in werkelijkheid evenwijdig aan de zwaartekracht staat, lijkt 30° gekanteld voor een persoon die 90° gekanteld is. Proefpersonen maken grote fouten als ze een lijn evenwijdig aan de verticaal moeten zetten wanneer ze gekanteld zijn. tilt (roll). De subjectieve visuele verticaal (SVV; dikke doorgetokken lijn) laat overcompensatie zien (E-effect) bij kleine kantelhoeken en ondercompensatie bij grote kantelhoeken (A-effect). Schatting van lichaamschatting (Eng: subjective body roll, SBR; gestippelde horizontale lijn), daarentegen, gaat wel foutloos.

ongeveer 35°, terwijl ze van breedbandige geluiden aangaven of deze links of rechts van de hoofdcentrische of wereldcentrische zenit hoorden. Als proefpersonen rechtop zitten overlappen deze referentiekaders. De resultaten laten zien dat proefpersonen de locatie van de auditieve zenit nauwkeurig kunnen inschatten, maar dat de responsvariabiliteit toeneemt voor het midsagittale vlak. Tijdens hoofdkanteling verschoof de hoofdcentrische zenit met een gelijke hoeveelheid en bleef dus recht boven het hoofd. Ook werd de hoofdcentrische zenit even nauwkeurig gelokaliseerd als rechtop, wat erop duidt dat de gevoeligheid van geluidslokalisatiecues niet verandert tijdens hoofdkanteling. Interessant genoeg maakten proefpersonen grote systematische fouten (10-15°) in de richting van hoofdkanteling wanneer ze de wereldcentrische zenit moesten aangeven. Ook nam de responsvariailiteit toe, wat lijkt op het visuele Aubert-effect. Deze resultaten laten een significante invloed van het vestibulaire-collische systeem op het auditieve ruimtelijk oriëntatie zien, en geven nieuwe inzichten in de mechanismen die ten grondslag liggen aan multisensorische integratie en spatial updating bij geluidslokalisatie.

De audiogyrale illusie
Actieve hoofdbewegingen voor en tijdens saccades naar korte breedbandige geluiden hebben geen invloed op de nauwkeurigheid van het lokalisatiegedrag (Goossens en Van Opstal, 1999; Vliegen et al., 2004). Passieve lichaamsrotatie in totale duisternis introduceert echter systematische fouten waarbij hoofdvaste geluiden lijken te verschuiven in de richting tegenovergesteld aan de rotatie. Dit fenomeen wordt de audiogyrale illusie genoemd (AGI; Münsterberg en Pierce, 1894; Clark en Graybiel, 1949). Door deze verschuiving van het geluid verschuift het auditieve middenvlak (AMP, het vlak waar de binaurale verschillen als nul worden waargenomen) in de tegengestelde richting, dus in de richting van rotatie. Daarom
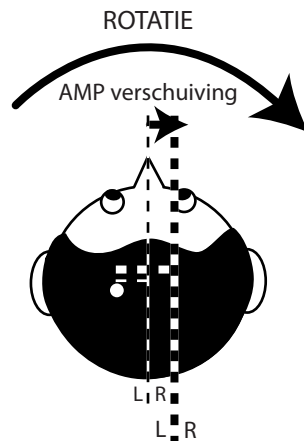
ROTATIE

AMP verschuiving

L R
L R

Figure 9.7   De audiogyrale illusie. Geluiden die aangeboden worden in het AMP worden waargenomen in het midden van het hoofd. Voor normaalhorende en stilstaande proefpersonen komt dit overeen met geluiden waarbij ILD = 0 dB en ITD = 0 µs (dunne verticale stippellijn). Als de AMP tijdens lichaamsrotatie in totale duisternis in de richting van rotatie verschuift (dikke verticale stippellijn), verschuift een hoofd-vast geluid (witte stip) in tegenovergestelde richting, wat hier wordt weergegeven door de langere dikke horizontale stippellijn.

moeten geluiden in de richting van rotatie gepresenteerd worden om in het midden van het hoofd te worden waargenomen. Recente experimenten suggereren een tegenovergestelde verschuiving van het AMP als proefpersonen fixeerden op een fixatielampje recht vooruit werd gebruikt dat met het hoofdmee bewoog (Lewald and Karnath, 2001).

Er zijn verschillende hypotheses voorgesteld om het onderliggende mechanisme van de AGI te verklaren. Eerst dacht men dat het kwam doordat mensen de lichaamsrotatie niet goed waarnemen (Clark en Graybiel, 1949). Ook zou het kunnen liggen aan een verkeerd percept van hoofd-op-lichaam oriëntatie (Lester en Morant, 1969; 1970; Lackner, 1974). Daarnaast kan ruimtelijke aandacht geluidslokalisatie beïnvloeden (Bohlander, 1984). Verder staan de ogen tijdens hoofdrotatie in totale duisternis niet stil in het hoofd door de vestibulo-oculaire reflex. De ogen draaien tijdens rotatie namelijk in tegengestelde richting om het beeld stil op het netvlies te houden en schieten af en toe snel in de richting van rotatie, omdat de ogen niet 360° kunnen draaien. Deze snelle oogbewegingen zorgen ervoor dat de gemiddelde oogstand in de richting van hoofdrotatie is (Chun en Robinson, 1978; Vidal et al., 1983; Carpenter, 1988). Zowel dit oogbewegingspatroon (Arnoult, 1950; Thurlow en Kerr, 1970) als eccentrische oogpositie (Lewald en Ehrenstein, 1996) kunnen een effect hebben op geluidslokalisatie alsmede op de perceptie van lichaamsoriëntatie (Quarck et al., 2009).

In hoofdstuk 6 en 7 van dit proefschrift hebben we de hypothese getest dat de verschuiving in gemiddelde oogpositie ten grondslag ligt aan de AGI. In **hoofdstuk 6** hebben we getest of het AMP wordt beïnvloed door vestibulaire signalen, oogpositiesignalen of oogsnelheidssignalen. Proefpersonen werden op verschillende snelheden sinusvormig geroteerd, ofwel in totale duisternis ofwel met een hoofdvast fixatielampje, terwijl ze van breedbandige geluiden aangaven of deze zich links of rechts van het auditieve middenvlak bevonden. Deze geluiden werden via een hoofdtelefoon gepresenteerd. Proefpersonen voerden deze taak ook uit zonder vestibulaire stimulatie, terwijl ze een visueel target volgden dat volgens een sinusvormig patroonbewoog. Dit patroon bootste het gemiddelde oogbewegingspatroon tijdens vestibulaire stimulatie in het donker na. De resultaten laten zien dat lichaamsrotatie in het donker een verschuiving van het AMP in de richting van de rotatie teweeg brengt. In tegensteling tot eerdere experimenten vonden we geen significante verschuiving van het

AMP wanneer er een fixatielampje gebruikt werd. De volgbewegingsexperimenten lieten een verschuiving van het AMP zien in de richting van eccentrische oogpositie, maar niet van de maximale oogsnelheid. Daarom concludeerden we dat de verschuiving in gemiddelde oogpositie die geïnduceerd werd door vestibulaire stimulatie ten grondslag ligt aan de AGI en de verschuiving van het AMP.

In **hoofdstuk 7** hebben we deze hypothese verder onderzocht in patiënten met acuut-optredende neuritis vestibularis, waarschijnlijk een ontsteking van het evenwichtsorgaan of evenwichtszenuw aan een zijde van het hoofd. Deze patiënten ervaren een hoofddraaiing weg van de aangedane zijde die samengaat met oculaire nystagmus (onwillekeurige bewegingen van de ogen) in het donker. Stilstaande patiënten gaven van geluiden aan of deze zich links of rechts van het auditieve middenvlak bevonden terwijl zij recht vooruit fixeerden. De resultaten lieten zien dat de AGI, net als in gezonde proefpersonen, afwezig was in patiënten. Daarnaast hebben we de AMP van gezonde proefpersonen getest tijdens bipolaire bilaterale galvanische stimulatie (GVS) van de het evenwichtsorgaan in totale duisternis of tijdens fixatie recht vooruit. GVS leidde in beide condities niet tot een verschuiving van de AMP. Deze resultaten ondersteunen de hypothese dat de AGI niet wordt veroorzaakt door een echte vestibulaire interactie met binaurale auditieve verwerking.

10

References

Agterberg, M.J., Snik, A.F., Hol, M.K., van Esch, T.E., Cremers, C.W., Van Wanrooij, M.M. and Van Opstal, A.J. (2011) Improved horizontal directional hearing in bone conduction device users with acquired unilateral conductive hearing loss. J Assoc Res Otolaryngol, 12, 1-11.

Arnoult, M.D. (1950) Post-rotatory localization of sound. Am J Psychol, 63, 229-236.

Aubert, H. (1861) Eine scheinbare bedeutende Drehung von Objecten bei Neigung des Kopfes nach Rechts oder Links. Virchows Archiv, 20, 381-393.

Alais, D. and Burr, D. (2004) The ventriloquist effect results from near-optimal bimodal integration. Curr Biol, 14, 257-262.

Angelaki, D.E. and Cullen, K.E. (2008) Vestibular system: The many facets of a multimodal sense. Annu Rev Neurosci, 31, 125-150.

Armstrong, B., McNair, P. and Taylor, D. (2008) Head and neck position sense. Sports Med, 38, 101-117.

Arnoult, M.D. (1950) Post-rotatory localization of sound. Am J Psychol, 63, 229-236.

Aubert, H. (1861) Eine Scheinbare Bedeutende Drehung von Objecten bei Neigung des Kopfes nach Rechts oder Links. Virchows Archiv 20, 381-393.

Baker, J.T., Harper, T.M. and Snyder, L.H. (2003) Spatial memory following shifts of gaze. I. Saccades to memorized world-fixed and gaze-fixed targets. J Neurophysiol 89, 2564-2576.

Barnes, G.R. (1993) Visual-vestibular interaction in the control of head and eye-movement - the role of visual feedback and predictive mechanisms. Prog Neurobiol, 41, 435-472.

Battaglia, P.W., Jacobs, R.A. and Aslin, R.N. (2003) Bayesian integration of visual and auditory signals for spatial localization. J Opt Soc Am A, 20, 1391-1397.

Becker, W. (1989) Metrics. In Wurtz, R., Goldberg, M. (eds) The neurobiology of saccadic eye movements. Elsevier, Amsterdam, pp. 13-66.

Becker, W., Jurgens, R. (1979) An analysis of the saccadic system by means of double step stimuli. Vision Res 19, 967-983.

Bertelson, P., Pavani, F., Ladavas, E., Vroomen, J. and de Gelder, B. (2000) Ventriloquism in patients with unilateral visual neglect. Neuropsychologia, 38, 1634-1642.

Bertelson, P. and Radeau, M. (1981) Cross-modal bias and perceptual fusion with auditory-visual spatial discordance. Percept Psychophys, 29, 578-584.

Bertini, C., Leo, F., Avenanti, A. and Ladavas, E. (2010) Independent mechanisms for ventriloquism and multisensory integration as revealed by theta-burst stimulation. Eur J Neurosci, 31, 1791-1799.

Biguer, B., Donaldson, I.M., Hein, A. and Jeannerod, M. (1988) Neck muscle vibration modifies the representation of visual motion and direction in man. Brain 111, 1405-1424.

Bizley, J.K. and King, A.J. (2008) Visual-auditory spatial processing in auditory cortical neurons. Brain Res, 1242, 24-36.

Bizley, J.K., Nodal, F.R., Bajo, V.M., Nelken, I. and King, A.J. (2007) Physiological and anatomical evidence for multisensory interactions in auditory cortex. Cereb Cortex, 17, 2172-2189.

Blauert, J. (1997) Spatial hearing: the psychophysics of human sound localization. MIT Press, Cambridge, Mass.

Blohm, G., Missal, M. and Lefevre, P. (2003) Interaction between smooth anticipation and saccades during ocular orientation in darkness. J Neurophysiol 89, 1423-1433.

Blohm, G., Missal, M. and Lefevre, P. (2005) Processing of retinal and extraretinal signals for memory-guided saccades during smooth pursuit. J Neurophysiol 93, 1510-1522.

Blouin, J., Gauthier, G.M. and Vercher ,J.L. (1995a) Failure to update the egocentric representation of the visual space through labyrinthine signal. Brain Cogn 29, 1-22.

Blouin, J., Gauthier, G.M. and Vercher, J.L. (1997) Visual object localization through vestibular and neck inputs. 2: Updating off-mid-sagittal-plane target positions. J Vestib Res 7, 137-143.

Blouin, J., Gauthier G.M., van Donkelaar, P. and Vercher, J.L. (1995b) Encoding the position of a flashed visual target after passive body rotations. Neuroreport 6, 1165-1168.

Blouin, J., Labrousse L., Simoneau M., Vercher J.L and Gauthier, G.M. (1998) Updating visual space during passive and voluntary head-in-space movements. Exp Brain Res 122, 93-100.

Bock, O. (1986) Contribution of retinal versus extraretinal signals towards visual localization in goal-directed movements. Exp Brain Res, 64, 476-482.

Bohlander, R.W. (1984) Eye position and visual attention influence perceived auditory direction. Percept. Mot. Skills, 59, 483-510.

Bohmer, A., Mast, F. and Jarchow, T. (1996) Can a unilateral loss of otolithic function be clinically detected by assessment of the subjective visual vertical? Brain research bulletin, 40, 423-427; discussion 427-429.

Bohmer, A. and Rickenmann, J. (1995) The subjective visual vertical as a clinical parameter of vestibular function in peripheral vestibular diseases. J Vestib Res, 5, 35-45.

Bonath, B., Noesselt, T., Martinez, A., Mishra, J., Schwiecker, K., Heinze, H.J. and Hillyard, S.A. (2007) Neural basis of the ventriloquist illusion. Curr Biol, 17, 1697-1703.

Bour, L.J., van Gisbergen, J.A., Bruijns, J. and Ottes, F.P. (1984) The double magnetic induction method for measuring eye movement--results in monkey and man. IEEE Trans Biomed Eng 31, 419-427.

Bremen, P., Van Wanrooij, M.M. and Van Opstal, A.J. (2010) Pinna cues determine orienting response modes to synchronous sounds in elevation. J Neurosci 30, 194-204.

Bremen, P., Van der Willigen, R.F. and Van Opstal, A.J. (2007) Using double-magnetic induction to measure head-unrestrained gaze shifts: I. Theory and validation. J Neurosci Methods 160, 75-84.

Carpenter, R.H.S. (1988) Movements of the eyes. Pion Ltd.

Chandler, D.W. and Grantham, D.W. (1992) Minimum audible movement angle in the horizontal plane as a function of stimulus frequency and bandwidth, source azimuth, and velocity. J Acoust Soc Am, 91, 1624-1636.

Chun, K.S. and Robinson, D.A. (1978) A model of quick phase generation in the vestibuloocular reflex. Biol Cybern, 28, 209-221.

Clark, B. and Graybiel, A. (1949) The effect of angural acceleration on sound localization: The audiogyral illusion. J Psychol, 28, 235-244.

Cohen, Y.E. and Andersen, R.A. (2000) Reaches to sounds encoded in an eye-centered reference frame. Neuron, 27, 647-652.

Collewijn, H., van der Mark, F. and Jansen, T.C. (1975) Precise recording of human eye movements. Vision Res, 15, 447-450.

Collewijn, H., Erkelens, C.J. and Steinman, R.M. (1988) Binocular co-ordination of human vertical saccadic eye movements. J Physiol, 404, 183-197.

Colonius, H. and Arndt, P. (2001) A two-stage model for visual-auditory interaction in saccadic latencies. Percept Psychophys, 63, 126-147.

Colonius, H. and Diederich, A. (2004) Why aren't all deep superior colliculus neurons multisensory? A Bayes' ratio analysis. Cognit Affect Behav Neurosci, 4, 344-353.

Colonius, H. and Diederich, A. (2011) Computing an optimal time window of audiovisual integration in focused attention tasks: illustrated by studies on effect of age and prior

knowledge. Exp Brain Res, 212, 327-337.

Corneil, B.D. and Andersen, R.A. (2004) Dorsal neck muscle vibration induces upward shifts in the endpoints of memory-guided saccades in monkeys. J Neurophysiol 92, 553-566.

Corneil, B.D., Van Wanrooij, M., Munoz, D.P. and Van Opstal, A.J. (2002) Auditory-visual interactions subserving goal-directed saccades in a complex scene. J Neurophysiol, 88, 438-454.

Crapse, T.B. and Sommer, M.A. (2008) Corollary discharge across the animal kingdom. Nature Rev Neurosci 9, 587-600.

Crawford, J.D., Henriques, D.Y. and Medendorp, W.P. (2011) Three-dimensional transformations for goal-directed action. Annu Rev Neurosci, 34, 309-331.

Dayan, P. and Abbott L.F. (2001) Theoretical neuroscience: Computational and mathematical modeling of neural systems. The MIT Press.

Daye, P.M., Blohm, G. and Lefevre, P. (2010) Saccadic compensation for smooth eye and head movements during head-unrestrained two-dimensional tracking. J Neurophysiol 103, 543-556.

De Vrijer, M., Medendorp, W.P. and Van Gisbergen, J.A.M. (2008) Shared computational mechanism for tilt compensation accounts for biased verticality percepts in motion and pattern vision. J Neurophysiol 99, 915-930.

De Vrijer, M., Medendorp, W.P. and Van Gisbergen, J.A.M. (2009) Accuracy-precision trade-off in visual orientation constancy. J Vision, 9, 1-15.

DiZio, P., Held, R., Lackner, J.R., Shinn-Cunningham, B. and Durlach N. (2001) Gravitoinertial force magnitude and direction influence head-centric auditory localization. J Neurophysiol 85, 2455-2460.

Duhamel, J.R., Colby, C.L. and Goldberg, M.E. (1992) The updating of the representation of visual space in parietal cortex by intended eye movements. Science, 255, 90-92.

Duysens, J., Orban, G.A., Cremieux, J. and Maes, H. (1985) Visual cortical correlates of visible persistence. Vision Res 25, 171-178.

Falchier, A., Clavagnier, S., Barone, P. and Kennedy, H. (2002) Anatomical evidence of multimodal integration in primate striate cortex. J Neurosci, 22, 5749-5759.

Festinger, L. and Holtzman J.D. (1978) Retinal image smear as a source of information about magnitude of eye movement. J Exp Psychol Hum Percept Perform 4, 573-585.

Fitzpatrick, R.C. and Day, B.L. (2004) Probing the human vestibular system with galvanic stimulation. J Appl Physiol, 96, 2301-2316.

Foxe, J.J. and Schroeder, C.E. (2005) The case for feedforward multisensory convergence during early cortical processing. Neuroreport, 16, 419-423.

Frassinetti, F., Bolognini, N. and Ladavas, E. (2002) Enhancement of visual perception by crossmodal visuo-auditory interaction. Exp Brain Res, 147, 332-343.

Frens, M.A. and Opstal, A.J. (1994) Transfer of short-term adaptation in human saccadic eye movements. Exp Brain Res, 100, 293-306.

Frens M.A., Van Opstal A.J. (1995) A quantitative study of auditory-evoked saccadic eye movements in two dimensions. Exp Brain Res 107, 103-117.

Frens, M.A., Van Opstal, A.J. and Van der Willigen, R.F. (1995) Spatial and temporal factors determine auditory-visual interactions in human saccadic eye movements. Percept Psychophys, 57, 802-816.

Friedmann, G. (1970) The judgement of the visual vertical and horizontal with peripheral and central vestibular lesions. Brain, 93, 313-328.

Fu, K.M., Shah, A.S., O'Connell, M.N., McGinnis, T., Eckholdt, H., Lakatos, P., Smiley, J. and Schroeder, C.E. (2004) Timing and laminar profile of eye-position effects on auditory

responses in primate auditory cortex. J Neurophysiol, 92, 3522-3531.

Ghazanfar, A.A. and Schroeder, C.E. (2006) Is neocortex essentially multisensory? Trends Cogn Sci, 10, 278-285.

Goldberg, M.E. and Bruce, C.J. (1990) Primate frontal eye fields. III. Maintenance of a spatially accurate saccade signal. J Neurophysiol, 64, 489-508.

Goossens, H.H.L.M and Van Opstal, A.J. (1997a) Local feedback signals are not distorted by prior eye movements: Evidence from visually evoked double saccades. J Neurophysiol 78, 533-538.

Goossens, H.H.L.M. and Van Opstal AJ (1997b) Human eye-head coordination in two dimensions under different sensorimotor conditions. Exp Brain Res 114, 542-560.

Goossens, H.H.L.M. and Van Opstal, A.J. (1999) Influence of head position on the spatial representation of acoustic targets. J Neurophysiol, 81, 2720-2736.

Grantham, D.W., Hornsby, B.W.Y. and Erpenbeck, E.A. (2003) Auditory spatial resolution in horizontal, vertical, and diagonal planes. J Acoust Soc Am 114, 1009-1022.

Graybiel, A. and Hupp, D. (1946) The oculogyral illusion: a form of apparent motion which may be observed following stimulation of the semicircular canals. Aerospace Med, 3, 1-12.

Graybiel, A. and Niven, J.I. (1951) The effect of a change in direction of resultant force on sound localization: the audiogravic illusion. J Exp Psychol 42, 227-230.

Groh, J.M., Trause, A.S., Underhill, A.M., Clark, K.R. and Inati, S. (2001) Eye position influences auditory responses in primate inferior colliculus. Neuron, 29, 509-518.

Gu, Y., Angelaki, D.E. and Deangelis, G.C. (2008) Neural correlates of multisensory cue integration in macaque MSTd. Nat Neurosci, 11, 1201-1210.

Hairston, W.D., Wallace, M.T., Vaughan, J.W., Stein, B.E., Norris, J.L. and Schirillo, J.A. (2003) Visual localization ability influences cross-modal bias. J Cogn Neurosci, 15, 20-29.

Hallett, P.E. and Lightstone, A.D. (1976) Saccadic eye movements towards stimuli triggered by prior saccades. Vision Res 16, 99-106.

Harrington, L.K. and Peck, C.K. (1998) Spatial disparity affects visual-auditory interactions in human sensorimotor processing. Exp Brain Res, 122, 247-252.

Harris, C.M. (1995) Does saccadic undershoot minimize saccadic flight-time? A Monte-Carlo study. Vision Res, 35, 691-701.

Hartline, P.H., Vimal, R.L., King, A.J., Kurylo, D.D. and Northmore, D.P. (1995) Effects of eye position on auditory localization and neural representation of space in superior colliculus of cats. Exp Brain Res, 104, 402-408.

Hartnagel, D., Bichot, A. and Roumes, C. (2007) Eye position affects audio-visual fusion in darkness. Perception, 36, 1487-1496.

Held, R. (1955) Shifts in binaural localization after prolonged exposures to atypical combinations of stimuli. Am J Psych, 68, 526-548.

Herter, T.M. and Guitton, D. (1998) Human head-free gaze saccades to targets flashed before gaze-pursuit are spatially accurate. J Neurophysiol 80, 2785-2789.

Hillis, J.M., Ernst, M.O., Banks, M.S. and Landy, M.S. (2002) Combining sensory information: mandatory fusion within, but not between, senses. Science (New York, N.Y, 298, 1627-1630.

Hofman, P.M. and Van Opstal, A.J. (1998) Spectro-temporal factors in two-dimensional human sound localization. J Acoust Soc Am, 103, 2634-2648.

Hofman, P.M. and Van Opstal, A.J. (2002) Bayesian reconstruction of sound localization cues from responses to random spectra. Biol Cybern, 86, 305-316.

Howard, I.P. and Templeton, W.B. (1966) Human spatial orientation. Wiley, New York.

Hughes, H.C., Nelson, M.D. and Aronchick, D.M. (1998) Spatial characteristics of visual-

auditory summation in human saccades. Vision Res, 38, 3955-3963.

Hughes, H.C., Reuter-Lorenz, P.A., Nozawa, G. and Fendrich, R. (1994) Visual-auditory interactions in sensorimotor processing: saccades versus manual responses. J Exp Psychol Hum Percept Perform, 20, 131-153.

Israel I., Ventre-Dominey J., Denise P. (1999) Vestibular information contributes to update retinotopic maps. Neuroreport 10, 3479-3483.

Jack, C.E. and Thurlow, W.R. (1973) Effects of degree of visual association and angle of displacement on the "ventriloquism" effect. Percept Mot Skills, 37, 967-979.

Jay, M.F. and Sparks, D.L. (1984) Auditory receptive fields in primate superior colliculus shift with changes in eye position. Nature, 309, 345-347.

Jay, M.F. and Sparks, D.L. (1987a) Sensorimotor integration in the primate superior colliculus. I. Motor convergence. J Neurophysiol, 57, 22-34.

Jay, M.F. and Sparks, D.L. (1987b) Sensorimotor integration in the primate superior colliculus. II. Coordinates of auditory signals. J Neurophysiol, 57, 35-55.

Jurgens, R., Becker, W. and Kornhuber, H.H. (1981) Natural and drug-induced variations of velocity and duration of human saccadic eye movements: evidence for a control of the neural pulse generator by local feedback. Biol Cybern, 39, 87-96.

Kaptein, R.G. and Van Gisbergen, J.A.M. (2004) Interpretation of a discontinuity in the sense of verticality at large body tilt. J Neurophysiol 91, 2205-2214.

Kaptein R.G. and Van Gisbergen, J.A.M. (2005) Nature of the transition between two modes of external space perception in tilted subjects. J Neurophysiol 93, 3356-3369.

Kaptein, R.G. and Van Gisbergen, J.A.M. (2006) Canal and otolith contributions to visual orientation constancy during sinusoidal roll rotation. J Neurophysiol, 95, 1936-1948.

Kayser, C. and Logothetis, N.K. (2007) Do early sensory cortices integrate cross-modal information? Brain Struct Funct, 212, 121-132.

Kayser, C., Petkov, C.I., Augath, M. and Logothetis, N.K. (2007) Functional imaging reveals visual modulation of specific fields in auditory cortex. J Neurosci, 27, 1824-1835.

Koelewijn, T., Bronkhorst, A. and Theeuwes, J. (2010) Attention and the multiple stages of multisensory integration: A review of audiovisual studies. Acta Psychol (Amst), 134, 372-384.

Kesten, H. (1958) Accelerated stochastic approximation. Ann Math Stat, 29, 41-59.

Klier, E.M., Angelaki, D.E. and Hess, B.J.M. (2005) Roles of gravitational cues and efference copy signals in the rotational updating of memory saccades. J Neurophysiol 94, 468-478.

Klier, E.M., Hess, B.J. and Angelaki, D.E. (2006) Differences in the accuracy of human visuospatial memory after yaw and roll rotations. J Neurophysiol 95, 2692-2697.

Knudsen, E.I. and Konishi M. (1979) Mechanisms of sound localization in the barn owl (tyto-alba). J Comp Physiol 133, 13-21.

Knudsen, E.I., Blasdel, G.G. and Konishi, M. (1979) Sound Localization by the Barn Owl (Tyto-Alba) Measured with the Search Coil Technique. J Comp Physiol, 133, 1-11.

Kopčo, N., Lin, I.F., Shinn-Cunningham, B.G. and Groh, J.M. (2009) Reference frame of the ventriloquism aftereffect. J Neurosci, 29, 13809-13814.

Kopinska, A. and Harris, L.R. (2003) Spatial representation in body coordinates: Evidence from errors in remembering positions of visual and auditory targets after active eye, head, and. body movements. Can J Exp Psychol 57, 23-37

Königs, K., Knoll, J. and Bremmer, F. (2007) Localization of auditory targets during optokinetic nystagmus. Perception, 36, 1507-1512.

Körding, K.P., Beierholm, U., Ma, W.J., Quartz, S., Tenenbaum, J.B. and Shams, L. (2007)

Causal inference in multisensory perception. PloS one, 2, 943.

Lackner, J.R. (1974) The role of posture in sound localization. Q J Exp Psychol, 26, 235-251.

Lechner-Steinleitner, S., Schone, H. and Steinleitner, A. (1981) The auditory subjective vertical as a function of body tilt. Acta Otolaryngol 92, 71-74.

Lemij, H.G. and Collewijn, H. (1989) Differences in accuracy of human saccades between stationary and jumping targets. Vision research, 29, 1737-1748.

Leo, F., Bolognini, N., Passamonti, C., Stein, B.E. and Ladavas, E. (2008) Cross-modal localization in hemianopia: new insights on multisensory integration. Brain, 131, 855-865.

Lester, G. and Morant, R.B. (1969) The role of the felt position of the head in the audiogyral illusion. Acta Psychol, 31, 375-384.

Lester, G. and Morant, R.B. (1970) Apparent sound displacement during vestibular stimulation. Am J Psychol, 83, 554-566.

Lewald, J. (1997) Eye-position effects in directional hearing. Behav Brain Res, 87, 35-48.

Lewald, J. (1998) The effect of gaze eccentricity on perceived sound direction and its relation to visual localization. Hear Res, 115, 206-216.

Lewald, J. (2002) Rapid adaptation to auditory-visual spatial disparity. Learn Mem, 9, 268-278.

Lewald, J., Dorrscheidt, G.J. and Ehrenstein, W.H. (2000) Sound localization with eccentric head position. Behav Brain Res, 108, 105-125.

Lewald, J. and Ehrenstein, W.H. (1996) The effect of eye position on auditory lateralization. Exp Brain Res, 108, 473-485.

Lewald, J. and Ehrenstein, W.H. (1998a) Auditory-visual spatial integration: A new psychophysical approach using laser pointing to acoustic targets. J Acoust Soc Am, 104, 1586-1597.

Lewald, J. and Ehrenstein, W.H. (1998b) Influence of head-to-trunk position on sound lateralization. Experimental Brain Research, 121, 230-238.

Lewald, J. and Getzmann, S. (2006) Horizontal and vertical effects of eye-position on sound localization. Hear Res, 213, 99-106.

Lewald, J. and Guski, R. (2003) Cross-modal perceptual integration of spatially and temporally disparate auditory and visual stimuli. Brain Res, 16, 468-478.

Lewald, J. and Karnath, H.O. (2000) Vestibular influence on human auditory space perception. J Neurophysiol, 84, 1107-1111.

Lewald, J. and Karnath, H.O. (2001) Sound lateralization during passive whole-body rotation. Eur J Neurosci, 13, 2268-2272.

Lewald J, Karnath HO (2002) The effect of whole-body tilt on sound lateralization. Eur J Neurosci 16, 761-766.

Lewald, J., Karnath, H.O. and Ehrenstein, W.H. (1999) Neck-proprioceptive influence on auditory lateralization. Exp Brain Res, 125, 389-396.

Li, N., Wei, M. and Angelaki, D.E. (2005) Primate memory saccade amplitude after intervened motion depends on target distance. J Neurophysiol 94, 722-733.

Linden, J.F., Grunewald, A. and Andersen, R.A. (1999) Responses to auditory stimuli in macaque lateral intraparietal area. II. Behavioral modulation. J Neurophysiol, 82, 343-358.

Maier, J.X. and Groh, J.M. (2010) Comparison of gain-like properties of eye position signals in inferior colliculus versus auditory cortex of primates. Front Integr Neurosci, 4.

Martuzzi, R., Murray, M.M., Michel, C.M., Thiran, J.P., Maeder, P.P., Clarke, S. and Meuli, R.A. (2007) Multisensory interactions within human primary cortices revealed by BOLD dynamics. Cereb Cortex, 17, 1672-1679.

Mast, F. and Jarchow, T. (1996) Perceived body position and the visual horizontal. Brain Res Bull 40, 393-397.

Mays, L.E. and Sparks D.L. (1980) Saccades are spatially, not retinocentrically, coded. Science 208, 1163-1165.

McKenzie, A. and Lisberger S.G. (1986) Properties of signals that determine the amplitude and direction of saccadic eye-movements in monkeys. J Neurophysiol 56, 196-207.

McGuire, L.M. and Sabes, P.N. (2011) Heterogeneous representations in the superior parietal lobule are common across reaches to visual and proprioceptive targets. J Neurosci, 31, 6661-6673.

Meienbrock, A., Naumer, M.J., Doehrmann, O., Singer, W. and Muckli, L. (2007) Retinotopic effects during spatial audio-visual integration. Neuropsychologia, 45, 531-539.

Meredith, M.A. and Stein, B.E. (1983) Interactions among converging sensory inputs in the superior colliculus. Science 221:389-391.

Meredith, M.A. and Stein, B.E. (1986a) Spatial factors determine the activity of multisensory neurons in cat superior colliculus. Brain Res 365:350-354.

Meredith, M.A. and Stein, B.E. (1986b) Visual, auditory, and somatosensory convergence on cells in superior colliculus results in multisensory integration. J Neurophysiol 56:640-662.

Merfeld, D.M., Park, S., Gianna-Poulin, C., Black, F.O. and Wood, S. (2005) Vestibular perception and action employ qualitatively different mechanisms. I. Frequency response of VOR and perceptual responses during translation and tilt. J Neurophysiol, 94, 186-198.

Middlebrooks, J.C. (1992) Narrow-band sound localization related to external ear acoustics. J Acoust Soc Am 92, 2607-2624.

Middlebrooks, J.C. and Green, D.M. (1991) Sound localization by human listeners. Annu Rev Psychol 42, 135-159.

Mills, A.W. (1958) On the Minimum Audible Angle. J Acoust Soc Am, 30, 237-246.

Min, K.K., Ha, J.S., Kim, M.J., Cho, C.H., Cha, H.E. and Lee, J.H. (2007) Clinical use of subjective visual horizontal and vertical in patients of unilateral vestibular neuritis. Otol Neurotol, 28, 520-525.

Mittelstaedt, H. (1983) A new solution to the problem of the subjective vertical. Naturwissenschaften 70, 272-281.

Molholm, S., Ritter, W., Murray, M.M., Javitt, D.C., Schroeder, C.E. and Foxe, J.J. (2002) Multisensory auditory-visual interactions during early sensory processing in humans: a high-density electrical mapping study. Brain Res, 14, 115-128.

Morgan, C.L. (1978) Constancy of egocentric visual direction. Percept Psychophys, 23, 61-68.

Morrell, F. (1972) Visual system's view of acoustic space. Nature, 238, 44-46.

Müller, G.E. (1916) Über das Aubertsche Phänomen. Zeitschrift für Sinnesphysiologie 49, 109-246.

Mullette-Gillman, O.A., Cohen, Y.E. and Groh, J.M. (2005) Eye-centered, head-centered, and complex coding of visual and auditory targets in the intraparietal sulcus. J Neurophysiol, 94, 2331-2352.

Mullette-Gillman, O.A., Cohen, Y.E. and Groh, J.M. (2009) Motor-related signals in the intraparietal cortex encode locations in a hybrid, rather than eye-centered reference frame. Cereb Cortex, 19, 1761-1775.

Münsterberg, C.H. and Pierce, A.H. (1894) The localization of sound. Psychol rev, 1, 461-476.

Niemeier, M., Crawford, J.D. and Tweed, D.B. (2003) Optimal transsaccadic integration

explains distorted spatial perception. Nature, 422, 76-80.

Nodal, F.R., Bajo, V.M., Parsons, C.H., Schnupp, J.W. and King, A.J. (2008) Sound localization behavior in ferrets: comparison of acoustic orientation and approach-to-target responses. Neuroscience, 154, 397-408.

Oldfield, S.R. and Parker, S.P.A. (1984) Acuity of Sound Localization - a Topography of Auditory Space .1. Normal Hearing Conditions. Perception, 13, 581-600.

Passamonti, C., Bertini, C. and Ladavas, E. (2009) Audio-visual stimulation improves oculomotor patterns in patients with hemianopia. Neuropsychologia, 47, 546-555.

Perrott, D.R., Ambarsoom, H. and Tucker, J. (1987) Changes in head position as a measure of auditory localization performance: auditory psychomotor coordination under monaural and binaural listening conditions. J Acoust Soc Am, 82, 1637-1645.

Perrott, D.R. and Saberi, K. (1990) Minimum audible angle thresholds for sources varying in both elevation and azimuth. J Acoust Soc Am 87, 1728-1731.

Phan, M.L., Schendel, K.L., Recanzone, G.H. and Robertson, L.C. (2000) Auditory and visual spatial localization deficits following bilateral parietal lobe lesions in a patient with Balint's syndrome. J Cogn Neurosc, 12, 583-600.

Poppel, E. (1973) Comment on "visual system's view of acoustic space". Nature, 243, 231.

Populin, L.C. and Yin, T.C. (1998) Behavioral studies of sound localization in the cat. J Neurosci, 18, 2147-2160.

Press, W.H., Flannery, B.P., Teukolsky, S.A. and Vettering, W.T. (1992) Numerical recipes in C: the art of scientific computing. Cambridge University Press, Cambridge, MA.

Quarck, G., Lhuisset, L., Etard, O. and Denise, P. (2009) Eye eccentricity modifies the perception of whole-body rotation. Exp Brain Res, 196, 295-301.

Radeau, M. and Bertelson, P. (1977) Adaptation to auditory-visual discordance and ventriloquism in semirealistic situations. Percept Psychophys, 22, 137-146.

Radeau, M. and Bertelson, P. (1978) Cognitive factors and adaptation to auditory-visual discordance. Percept Psychophys, 23, 341-343.

Razavi, B., O'Neill, W.E. and Paige, G.D. (2007) Auditory spatial perception dynamically realigns with changing eye position. J Neurosci, 27, 10249-10258.

Recanzone, G.H. (1998) Rapidly induced auditory plasticity: the ventriloquism aftereffect. Proc Natl Acad Sci U S A, 95, 869-875.

Robbins, H. and Monro, S. (1951) A Stochastic Approximation Method. Ann Math Stat, 22, 400-407.

Robinson, D.A. (1963) A method of measuring eye movement using a scleral search coil in a magnetic field. IEEE T Bio-med Eng BME-10, 137-145.

Robinson, D.A. (1975) Oculomotor control signals. In Iennerstrand, G., Bach-y-Rita, P. (eds) Basic Mechanisms of Ocular Motility and Their Clinical Implications. Pergamon Press, Oxford, pp. 337-374.

Robinson, D.A. (1989) Integrating with neurons. Annu Rev Neurosci, 12, 33-45.

Rockland, K.S. and Ojima, H. (2003) Multisensory convergence in calcarine visual areas in macaque monkey. Int J Psychophysiol, 50, 19-26.

Rosenhall, U. (1972) Vestibular macular mapping in man. Ann Otol Rhinol Laryngol, 81, 339-351.

Romei, V., Murray, M.M., Merabet, L.B. and Thut, G. (2007) Occipital transcranial magnetic stimulation has opposing effects on visual and auditory stimulus detection: implications for multisensory interactions. J Neurosci, 27, 11465-11472.

Russo, G.S. and Bruce, C.J. (1994) Frontal eye field activity preceding aurally guided saccades. J Neurophysiol, 71, 1250-1253.

Saberi, K. and Perrott, D.R. (1990) Minimum audible movement angles as a function of sound

source trajectory. J Acoust Soc Am, 88, 2639-2644.

Schlack, A., Sterbing-D'Angelo, S.J., Hartung, K., Hoffmann, K.P. and Bremmer, F. (2005) Multisensory space representations in the macaque ventral intraparietal area. J Neurosci, 25, 4616-4625.

Schlag, J., Schlagrey, M. and Dassonville, P. (1990) Saccades can be aimed at the spatial location of targets flashed during pursuit. J Neurophysiol 64:575-581.

Schröder, M.R. (1970) Synthesis of low-peak-factor signals and binary sequences with low autocorrelation. IEEE Trans Inf Theory 16, 85-89.

Schröder, C.E. and Foxe, J. (2005) Multisensory contributions to low-level, 'unisensory' processing. Curr Opin Neurobiol, 15, 454-458.

Sereno, M.I., Dale, A.M., Reppas, J.B., Kwong, K.K., Belliveau, J.W., Brady, T.J., Rosen, B.R. and Tootell, R.B. (1995) Borders of multiple visual areas in humans revealed by functional magnetic resonance imaging. Science, 268, 889-893.

Slutsky, D.A. and Recanzone, G.H. (2001) Temporal and spatial dependency of the ventriloquism effect. Neuroreport, 12, 7-10.

Sommer, M.A. and Wurtz, R.H. (2002) A pathway in primate brain for internal monitoring of movements. Science 296, 1480-1482.

Sparks, D.L. and Mays, L.E. (1983) Spatial localization of saccade targets. I. Compensation for stimulation-induced perturbations in eye position. J Neurophysiol 49, 45-63.

Sparks, D.L., Mays, L.E. and Porter, J.D. (1987) Eye-movements induced by pontine stimulation: Interaction with visually triggered saccades. J Neurophysiol 58, 300-318.

Stein, B.E. and Meredith, M.A. (1993) The merging of the senses. The MIT press, Cambrigde, MA.

Stein, B.E. and Stanford, T.R. (2008) Multisensory integration: current issues from the perspective of the single neuron. Nat Rev Neurosci, 9, 255-266.

Stekelenburg, J.J., Vroomen, J. and de Gelder, B. (2004) Illusory sound shifts induced by the ventriloquist illusion evoke the mismatch negativity. Neurosci Lett, 357, 163-166.

Stricanne, B., Andersen, R.A. and Mazzoni, P. (1996) Eye-centered, head-centered, and intermediate coding of remembered sound locations in area LIP. J Neurophysiol, 76, 2071-2076.

Tabak, S., Collewijn, H. and Boumans, L.J. (1997) Deviation of the subjective vertical in long-standing unilateral vestibular loss. Acta Otolaryngol, 117, 1-6.

Treutwein, B. (1995) Adaptive psychophysical procedures. Vision Res, 35, 2503-2522.

Thurlow, W.R. and Jack, C.E. (1973) Certain determinants of the "ventriloquism effect". Perceptual and motor skills, 36, 1171-1184.

Thurlow, W.R. and Kerr, T.P. (1970) Effect of a moving visual environment on localization of sound. Am J Psychol, 83, 112-118.

Umeno, M.M. and Goldberg, M.E. (1997) Spatial processing in the monkey frontal eye field. I. Predictive visual responses. J Neurophysiol, 78, 1373-1383.

Van Barneveld, D.C.P.B.M., Kiemeneij, A.C.M. and Van Opstal, A.J. (2011a) Absence of spatial updating when the visuomotor system is unsure about stimulus motion. J Neurosci, 31, 10558-10568.

Van Barneveld, D.C.P.B.M., Van Grootel, T.J., Alberts, B. and Van Opstal, A.J. (2011b) The effect of head roll on perceived auditory zenith. Exp Brain Res, 213, 235-243.

Van Barneveld, D.C.P.B.M. and Van Opstal, A.J. (2010) Eye position determines audio-vestibular integration during whole-body rotation. Eur J Neurosci, 31, 920-930.

Van Beuzekom, A.D., Medendorp, W.P. and Van Gisbergen, J.A.M. (2001) The subjective vertical and the sense of self orientation during active body tilt. Vision Res 41, 3229-3242.

Van Beuzekom, A.D. and Van Gisbergen, J.A.M. (2002) Interaction between visual and vestibular signals for the control of rapid eye movements. J Neurophysiol 88, 306-322.

Van Grootel, T.J. (2010) On the role of eye and head position in spatial localization behaviour: PhD Thesis. Donders Institute for Brain, Cognition and Behaviour. Donders Series, nr. 47. Radboud University Nijmegen, The Netherlands.

Van Grootel, T.J. and Van Opstal, A.J. (2009) Human sound-localization behaviour after multiple changes in eye position. Eur J Neurosci, 29, 2233-2246.

Van Grootel, T.J. and Van Opstal, A.J. (2010) Human sound localization accounts for ocular drift. J Neurophysiol, 103, 1927-1936.

Van Grootel, T.J., Van Wanrooij, M.M. and Van Opstal, A.J. (in press) Influence of static eye and head position on tone-evoked gaze shifts. J Neurosci

Van Wanrooij, M.M., Bell, A.H., Munoz, D.P. and Van Opstal, A.J. (2009) The effect of spatial-temporal audiovisual disparities on saccades in a complex scene. Exp Brain Res, 198, 425-437.

Van Wanrooij, M.M., Bremen, P. and Van Opstal, A.J. (2010) Acquired prior knowledge modulates audiovisual integration. Eur J Neurosci, 31, 1763-1771.

Van Wanrooij, M.M. and Van Opstal, A.J. (2004) Contribution of head shadow and pinna cues to chronic monaural sound localization. J Neurosci, 24, 4163-4171.

Vidal, P.P., Roucoux, A., Berthoz, A. and Crommelinck, M. (1983) Eye position-related activity in deep neck muscles of the alert cat. Adv Oto-Rhino-Laryng, 30, 27-29.

Vingerhoets, R.A.A., Medendorp, W.P. and Van Gisbergen, J.A.M. (2006) Time course and magnitude of illusory translation perception during off-vertical axis rotation. J Neurophysiol, 95, 1571-1587.

Vliegen, J., Van Grootel, T.J. and Van Opstal, A.J. (2004) Dynamic sound localization during rapid eye-head gaze shifts. J Neurosci, 24, 9291-9302.

Vliegen, J., Van Grootel, T.J. and Van Opstal, A.J. (2005) Gaze orienting in dynamic visual double steps. J Neurophysiol 94, 4300-4313.

Wallace, M.T., Roberson, G.E., Hairston, W.D., Stein, B.E., Vaughan, J.W. and Schirillo, J.A. (2004) Unifying multisensory signals across time and space. Exp Brain Res, 158, 252-258.

Walker, M.F., Fitzgibbon, E.J. and Goldberg, M.E. (1995) Neurons in the monkey superior colliculus predict the visual result of impending saccadic eye movements. J Neurophysiol, 73, 1988-2003.

Wei, M., Li, N., Newlands, S.D., Dickman, J.D. and Angelaki, D.E. (2006) Deficits and recovery in visuospatial memory during head motion after bilateral labyrinthine lesion. J Neurophysiol 96, 1676-1682.

Welch, R.B. and Warren, D.H. (1980) Immediate perceptual response to intersensory discrepancy. Psychological bulletin, 88, 638-667.

Werner-Reiss, U., Kelly, K.A., Trause, A.S., Underhill, A.M. and Groh, J.M. (2003) Eye position affects activity in primary auditory cortex of primates. Curr Biol, 13, 554-562.

Weyand, T.G. and Malpeli, J.G. (1993) Responses of neurons in primary visual cortex are modulated by eye position. J Neurophysiol, 69, 2258-2260.

Wichmann, F.A. and Hill, N.J. (2001a) The psychometric function: I. Fitting, sampling, and goodness of fit. Percept Psychophys, 63, 1293-1313.

Wichmann, F.A. and Hill, N.J. (2001b) The psychometric function: II. Bootstrap-based confidence intervals and sampling. Percept Psychophys, 63, 1314-1329.

Wightman, F.L. and Kistler, D.J. (1989) Headphone simulation of free-field listening. I: Stimulus synthesis. J Acoust Soc Am, 85, 858-867.

Woods, T.M. and Recanzone, G.H. (2004) Visually induced plasticity of auditory spatial perception in macaques. Curr Biol, 14, 1559-1564.

Wozny, D.R. and Shams, L. (2011) Recalibration of auditory space following milliseconds of cross-modal discrepancy. J Neurosci, 31, 4607-4612.

Yao, L. and Peck, C.K. (1997) Saccadic eye movements to visual and auditory targets. Exp Brain Res, 115, 25-34.

Yin, T. (2002) Neural mechanisms of encoding binaural localization cues in the auditory brainstem. In Oertel, D., Fay, R., Popper, A. (eds) Integrative functions in the mammalian auditory pathway. Springer, Heidelberg, pp. 99-159.

Young, E. and Davis, K. (2002) Circuitry and function of the dorsal cochlear nucleus. In Oertel, D., Fay, R., Popper, A. (eds) Integrative functions in the mammalian auditory pathway. Springer, Heidelberg, pp. 160-206.

Young, L.R. (1984) Perception of the body in space: mechanisms. In Geiger, S.R. (ed) Handbook of physiology, section 1. Bethesda: American Physiological Society, pp. 1023-1066.

Zwiers, M.P., Van Opstal, A.J. and Paige, G.D. (2003) Plasticity in human sound localization induced by compressed spatial vision. Nat Neurosci, 6, 175-181.

Zwiers, M.P., Versnel, H. and Van Opstal, A.J. (2004) Involvement of monkey inferior colliculus in spatial hearing. J Neurosci, 24, 4145-4156.
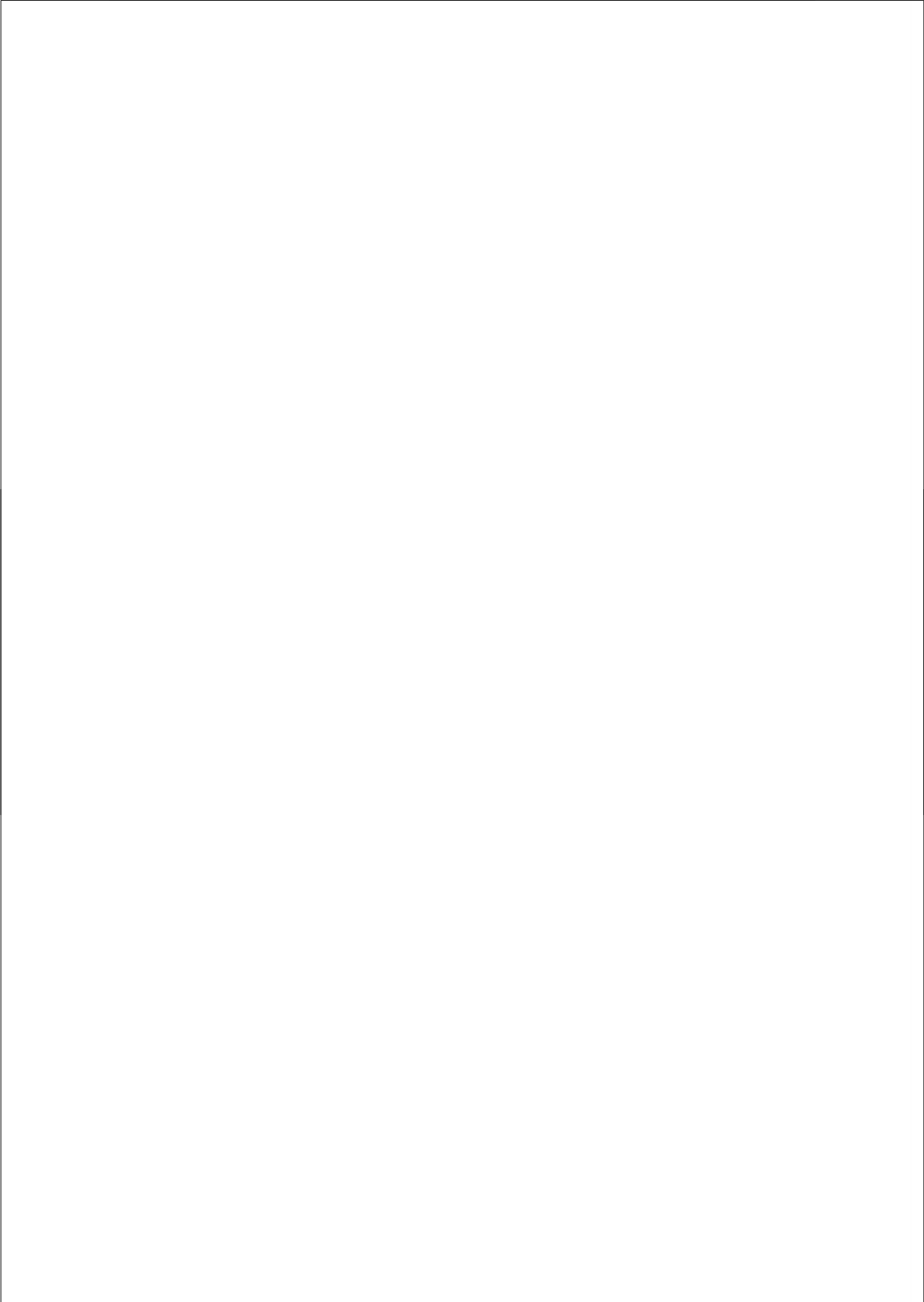
11

Epilogue

DANKWOORD

Het werk voor mijn promotie heb ik uiteraard niet alleen gedaan. Dit proefschrift was nooit tot stand kunnen komen zonder hulp van een heleboel mensen. Hier wil ik van de gelegenheid gebruik maken deze mensen te bedanken.

Allereerst wil ik mijn promotor John van Opstal bedanken. John, het was een genoegen om met de mooiste kermisattractie van Nijmegen, de vestibulaire stoel, te mogen werken. Ik wil je bedanken voor je enthousiasme. Een werkoverleg met jou zorgde altijd voor nieuwe energie en positieve gedachten. En ondanks je overvolle agenda de afgelopen maanden door je werkzaamheden als afdelingshoofd, wist je toch altijd tijd vrij te maken om met mijn onderzoek bezig te zijn en mijn teksten te beoordelen.

Als tweede wil ik mijn copromotor Marc van Wanrooij bedanken. Marc, je bent een goede John nr 2! Je bent een echte wetenschapper met een sterke mening. Het zou zonde zijn als je je wetenschappelijke carrière niet voortzet! Ondanks dat ik het tijdens onze samenwerking van het laatste jaar van mijn promotie vaak niet met je eens was wist je me toch iedere keer te overtuigen dat we meer saccades moesten meten of de analyses toch anders moesten aanpakken. Hoe vaak heb ik je niet horen zeggen: 'nee het moet helemaal anders!', of: 'ik weet nog niet of dit de uiteindelijke figuren gaan worden'. Uiteindelijk heeft dit geleid tot een mooi manuscript en zullen we zien wat de reviewers ervan vinden!

De data in dit proefschirft zijn deels verzameld door stagestudenten: Janneke, Eline, Stijn, Floor, Bart, Anne en Romy. Jullie hebben me veel werk uit handen genomen! Dit heeft geresulteerd in een aantal mooie publicaties. Bedankt!

Daarnaast wil ik alle collega's bedanken voor de leuke tijd die ik op de afdeling gehad heb. In het bijzonder wil ik David, Julian, Maaike, Joke, Josien, Tom, Jurrian, Douwe, Sep, Joyce, Rens, Kees, Rembrandt, Thom, Wim, John, Judith, Marieke, Cerien en alle studenten bedanken voor de gezellige koffiepauzes en lunches in de kantine, de colloquiumkamer of lekker in het zonnetje op het grasveld. Ook heb ik veel hulp gekregen van de auditieve groep Marc, Rob, Peter, Tom, Yoolla en Martijn. Tom, leuk dat onze samenwerking heeft geresulteerd in een mooie publicatie over het auditieve Aubert-effect.

Ook mijn kamergenootjes Maaike, Julian, Douwe, en natuurlijk Elvis, verdienen een plaatsje in het dankwoord. Het was erg gezellig om met jullie een kamer te delen! Het is een wonder dat we nog aan werken zijn toegekomen! Julian, veel succes met het laatste jaartje van je promotie en zorg goed voor Elvis. Julian en Maaike, ik vind het super leuk dat jullie mijn paranimfen willen zijn.

Verder wil ik de heren technici bedanken. Jullie stonden altijd voor me klaar! Hans om de coils te repareren als er weer eens een proefpersoon in de stoel zat en de coil stuk ging. Dick als de boog kuren had. Günter voor al mijn computerproblemen. Stijn voor allerhande stoelklusjes en de jaarlijkse controle, zodat de stoel altijd veilig kon draaien. Ger voor het omzetten van stoelsoftware naar Matlab. En Perry als opvolger van Hans.

Catherine de Waele and Pierre-Paul Vidal, I would like to thank you for giving me the opportunity to visit Paris for a month to measure vestibular loss patients and for introducing galvanic vestibular stimulation to me. It was a valuable experience. I also would like to thank Elodie Chiarovano for providing more patient data after I left Paris. This cooperation resulted

in chapter 7 of this thesis.

Het leven is meer dan alleen promotieonderzoek. Gelukkig kon ik rekenen op veel gezelligheid en afleiding van vrienden. In het bijzonder wil ik Marlou en Eveline bedanken voor vele telefoontjes, de gezellige avondjes samen eten of stappen, de heerlijke weekendjes, vakanties en Lowlands-uitjes! Jammer dat Vincent en ik de laatste twee jaar niet meekonden, volgend jaar gaan we gewoon weer mee (als we kaartjes weten te bemachtigen)!

Ook wil ik mijn familie bedanken voor alle steun en vertrouwen. Papa, mama, jullie zijn de beste ouders die een kind zich kan wensen. Jullie staan altijd voor me klaar en tonen jullie interesse met vele telefoontjes en bezoekjes. Kevin, je hebt zelf ook wel al ervaren dat onderzoek doen erg leuk, maar ook best zwaar kan zijn! Ik wens jou veel succes met je onderzoek. Opa en oma, ik wil jullie bedanken voor de steun en interesse in mijn carrière. En natuurlijk voor alle ijsjes die jullie me gegeven hebben. Opa, ook al wist je dat dit toch gewoon een baan was, je toonde altijd je betrokkenheid door te vragen hoe het op school was. Ik vind het heel fijn dat ik je mijn manuscript heb kunnen laten zien.

Tot slot: lieve Vincent, ik ben heel blij met jou! Je luistert altijd naar me en bent een grote steun. Het is ook erg leuk dat we samen over ons onderzoek kunnen praten. Ik wens jou veel succes met de laatste loodjes van jou proefschrift. Het is bijna klaar! Ik ben trots op je.

PUBLICATIONS

Van Barneveld, D.C.P.B.M. and Van Wanrooij M.M. The reference frame of the ventriloquist effect. Submitted to J Neurosci, 2011

Van Barneveld, D.C.P.B.M., Binkhorst F. and Van Opstal, A.J. (2011) Absence of compensation for vestibular-evoked passive head rotations in human sound localization. Eur J Neurosci, 34, 1149-1160

Van Barneveld, D.C.P.B.M., Van Grootel, T.J., Alberts, B. and Van Opstal, A.J. (2011) The effect of head roll on perceived auditory zenith. Exp Brain Res, 21, 235-243

Van Barneveld, D.C.P.B.M., Kiemeneij, A.C.M. and Van Opstal, A.J. (2011) Absence of spatial updating when the visuomotor system is unsure about stimulus motion. J Neurosci, 31, 10558-10568

Van Barneveld, D.C.P.B.M. and Van Opstal, A.J. (2010) Eye position determines audio-vestibular integration during whole-body rotation. Eur J Neurosci, 31, 920-930

ABSTRACTS AND POSTERS

Van Barneveld D.C.P.B.M., Van Wanrooij M.M. and Van Opstal A.J. (2011) The reference frame of the ventriloquist effect TU/e Dag van de Perceptie 2011

Van Opstal A.J. and **Van Barneveld D.C.P.B.M.** (2011) Audio-vestibular interactions in human orienting, Vergadering Werkgemeenschap Auditief Systeem

Van Barneveld D.C.P.B.M., Kiemeneij A.C.M. and Van Opstal (2010) Free-field sound localization during passive whole-body rotation Association for Research in Otolaryngology Midwinter Meeting 2010, 174

Kiemeneij A.C.M., **Van Barneveld D.C.P.B.M.** and Van Opstal A.J. (2010) Saccades to brief visual flashes presented during passive vestibular whole-body rotation FENS abstract, vol. 5, 084.8

Van Barneveld D.C.P.B.M., Binkhorst F. and Van Opstal A.J. (2010) Failure to compensate for vestibularly-evoked passive head rotations in human sound localization FENS abstract, vol. 5, 083.11

Van Barneveld D.C.P.B.M. and Van Opstal A.J. (2008) Influence of eye position on audio-vestibular interaction during whole-body rotation Neuroscience Meeting Planner. Washington, DC: Society for Neuroscience 367.11

Van Barneveld D.C.P.B.M., Meijerink, E. and Van Opstal A.J. (2008) Influence of eye position on audio-vestibular interactions during whole-body rotation TNO Soesterberg Dag van de Perceptie 2008

CURRICULUM VITAE

Denise van Barneveld werd op 1 juli 1983 geboren in Geleen. Hier ging zij naar basisschool De Driesprong en vervolgens naar de Albert Schweitzer Scholengemeenschap (later gefuseerd tot het Graaf Huijn College), waar ze in 2001 cum laude haar VWO diploma behaalde. Hierna verhuisde zij naar Nijmegen om daar de opleiding Natuurwetenschappen te volgen aan de Radboud Universiteit. Als snel werd duidelijk dat haar hart lag bij de biofysica, met name de werking van de hersenen. Een logisch vervolg op de bachelor Natuurwetenschappen was dan ook de research master Cognitive Neuroscience, waaraan zij in 2004 begon. Tegelijkertijd heeft zij de master Natuurwetenschappen afgerond. Na het beëindigen van deze twee opleidingen, is zij in 2007 als promovenda aan de slag gegaan bij de afdeling Biofysica aan de Radboud Universiteit, onder begeleiding van Prof. Dr. A. John van Opstal. Deze afdeling is in 2008 opgegaan in het Donders Institute for Brain, Cognition and Behaviour. De resultaten van het onderzoek dat zij daar gedaan heeft, staan beschreven in dit proefschrift. Sinds 1 november 2011 werkt zij aan het Leids Universitair Medisch Centrum, waar ze bij de afdeling KNO onderzoek doet naar de verbetering van spraakverstaaan in een ruizige omgeving van patiënten met een cochleair implantaat.

DONDERS GRADUATE SCHOOL FOR COGNITIVE NEUROSCIENCE SERIES

1. van Aalderen-Smeets, S.I. (2007). Neural dynamics of visual selection. Maastricht University, Maastricht, the Netherlands.
2. Schoffelen, J.M. (2007). Neuronal communication through coherence in the human motor system. Radboud University Nijmegen, Nijmegen, the Netherlands.
3. de Lange, F.P. (2008). Neural mechanisms of motor imagery. Radboud University Nijmegen, Nijmegen, the Netherlands.
4. Grol, M.J. (2008). Parieto-frontal circuitry in visuomotor control. University Utrecht, Utrecht, the Netherlands.
5. Bauer, M. (2008). Functional roles of rhythmic neuronal activity in the human visual and somatosensory system. Radboud University Nijmegen, Nijmegen, the Netherlands.
6. Mazaheri, A. (2008). The Influence of Ongoing Oscillatory Brain Activity on Evoked Responses and Behaviour. Radboud University Nijmegen, Nijmegen, the Netherlands.
7. Hooijmans, C.R. (2008). Impact of nutritional lipids and vascular factors in Alzheimer's Disease. Radboud University Nijmegen, Nijmegen, the Netherlands.
8. Gaszner, B. (2008). Plastic responses to stress by the rodent urocortinergic Edinger-Westphal nucleus. Radboud University Nijmegen, Nijmegen, the Netherlands.
9. Willems, R.M. (2009). Neural reflections of meaning in gesture, language and action. Radboud University Nijmegen, Nijmegen, the Netherlands.
10. Van Pelt, S. (2009). Dynamic neural representations of human visuomotor space. Radboud University Nijmegen, Nijmegen, the Netherlands.
11. Lommertzen, J. (2009). Visuomotor coupling at different levels of complexity. Radboud University Nijmegen, Nijmegen, the Netherlands.
12. Poljac, E. (2009). Dynamics of cognitive control in task switching: Looking beyond the switch cost. Radboud University Nijmegen, Nijmegen, the Netherlands.
13. Poser, B.A. (2009) Techniques for BOLD and blood volume weighted fMRI. Radboud University Nijmegen, Nijmegen, the Netherlands.
14. Baggio, G. (2009). Semantics and the electrophysiology of meaning. Tense, aspect, event structure. Radboud University Nijmegen, Nijmegen, the Netherlands.
15. van Wingen, G.A. (2009). Biological determinants of amygdala functioning. Radboud University Nijmegen Medical Centre, Nijmegen, the Netherlands.
16. Bakker, M. (2009). Supraspinal control of walking: lessons from motor imagery. Radboud University Nijmegen Medical Centre, Nijmegen, the Netherlands.
17. Aarts, E. (2009). Resisting temptation: the role of the anterior cingulate cortex in adjusting cognitive control. Radboud University Nijmegen, Nijmegen, the Netherlands.
18. Prinz, S. (2009). Waterbath stunning of chickens – Effects of electrical parameters on the electroencephalogram and physical reflexes of broilers. Radboud University Nijmegen, Nijmegen, the Netherlands.
19. Knippenberg, J.M.J. (2009). The N150 of the Auditory Evoked Potential from the rat amygdala: In search for its functional significance. Radboud University Nijmegen, Nijmegen, the Netherlands.

20. Dumont, G.J.H. (2009). Cognitive and physiological effects of 3,4-methylenedioxymethamphetamine (MDMA or 'ecstasy') in combination with alcohol or cannabis in humans Radboud University Nijmegen, Nijmegen, the Netherlands.

21. Pijnacker, J. (2010). Defeasible inference in autism: a behavioral and electrophysiogical approach. Radboud Universiteit Nijmegen, the Netherlands.

22. de Vrijer, M. (2010). Multisensory integration in spatial orientation. Radboud University Nijmegen, Nijmegen, the Netherlands.

23. Vergeer, M. (2010). Perceptual visibility and appearance: Effects of color and form. Radboud University Nijmegen, Nijmegen, the Netherlands.

24. Levy, J. (2010). In Cerebro Unveiling Unconscious Mechanisms during Reading. Radboud University Nijmegen, Nijmegen, the Netherlands.

25. Treder, M. S. (2010). Symmetry in (inter)action. Radboud University Nijmegen, Nijmegen, the Netherlands.

26. Horlings C.G.C. (2010). A Weak balance; balance and falls in patients with neuromuscular disorders. Radboud University Nijmegen, Nijmegen, the Netherlands

27. Snaphaan, L.J.A.E. (2010). Epidemiology of post-stroke behavioural consequences. Radboud University Nijmegen Medical Centre, Nijmegen, the Netherlands.

28. Dado – Van Beek, H.E.A. (2010). The regulation of cerebral perfusion in patients with Alzheimer's disease. Radboud University Nijmegen Medical Centre, Nijmegen, the Netherlands.

29. Derks, N.M. (2010). The role of the non-preganglionic Edinger-Westphal nucleus in sex-dependent stress adaptation in rodents. Radboud University Nijmegen, Nijmegen, the Netherlands.

30. Wyczesany, M. (2010). Covariation of mood and brain activity. Integration of subjective self-report data with quantitative EEG measures. Radboud University Nijmegen, Nijmegen, the Netherlands.

31. Beurze S.M. (2010). Cortical mechanisms for reach planning. Radboud University Nijmegen, Nijmegen, the Netherlands.

32. van Dijk, J.P. (2010). On the Number of Motor Units. Radboud University Nijmegen, the Netherlands .

33. Lapatki, B.G. (2010). The Facial Musculature – Characterization at a Motor Unit Level. Radboud University Nijmegen, Nijmegen, the Netherlands.

34. Kok, P. (2010). Word Order and Verb Inflection in Agrammatic Sentence Production. Radboud University Nijmegen, Nijmegen, the Netherlands.

35. van Elk, M. (2010). Action semantics: Functional and neural dynamics. Radboud University Nijmegen, Nijmegen, the Netherlands.

36. Majdandzic, J. (2010). Cerebral mechanisms of processing action goals in self and others. Radboud University Nijmegen, Nijmegen, the Netherlands.

37. Snijders, T.M. (2010). More than words – neural and genetic dynamics of syntactic unification. Radboud University Nijmegen, Nijmegen, the Netherlands.

38. Grootens, K.P. (2010). Cognitive dysfunction and effects of antipsychotics in schizophrenia and borderline personality disorder. Radboud University Nijmegen Medical Centre, Nijmegen, the Netherlands.

39. Nieuwenhuis, I.L.C. (2010). Memory consolidation: A process of integration – Converging evidence from MEG, fMRI and behavior. Radboud University Nijmegen Medical Centre, Nijmegen, the Netherlands.

40. Menenti, L.M.E. (2010). The right language: differential hemispheric contributions to language production and comprehension in context. Radboud University Nijmegen, Nijmegen, the Netherlands.

41. van Dijk, H.P. (2010). The state of the brain, how alpha oscillations shape behaviour and event related responses. Radboud University Nijmegen, Nijmegen, the Netherlands.

42. Meulenbroek, O.V. (2010). Neural correlates of episodic memory in healthy aging and Alzheimer's disease. Radboud University Nijmegen, Nijmegen, the Netherlands.

43. Oude Nijhuis, L.B. (2010). Modulation of human balance reactions. Radboud University Nijmegen, Nijmegen, the Netherlands.

44. Qin, S. (2010) Adaptive memory: imaging medial temporal and prefrontal memory systems. Radboud University Nijmegen, the Netherlands.

45. Timmer, N.M. (2011). The interaction of heparan sulfate proteoglycans with the amyloid β protein. Radboud University Nijmegen, Nijmegen, the Netherlands.

46. Crajé, C. (2011). (A)typical motor planning and motor imagery. Radboud University Nijmegen, Nijmegen, the Netherlands.

47. van Grootel, T.J. (2011). On the role of eye and head position in spatial localisation behaviour. Radboud University Nijmegen, Nijmegen, the Netherlands.

48. Lamers, M.J.M. (2011). Levels of selective attention in action planning. Radboud University Nijmegen, Nijmegen, the Netherlands.

49. Van der Werf, J. (2011). Cortical oscillatory activity in human visuomotor integration. Radboud University Nijmegen, Nijmegen, the Netherlands.

50. Scheeringa, R. (2011). On the relation between oscillatory EEG activity and the BOLD signal. Radboud University Nijmegen, Nijmegen, the Netherlands.

51. Bögels, S. (2011). The role of prosody in language comprehension: when prosodic breaks and pitch accents come into play. Radboud University Nijmegen, Nijmegen, the Netherlands.

52. Ossewaarde, L. (2011). The mood cycle: hormonal influences on the female brain. Radboud University Nijmegen, Nijmegen, the Netherlands.

53. Kuribara, M. (2011). Environment-induced activation and growth of pituitary melanotrope cells of Xenopus laevis. Radboud University Nijmegen, Nijmegen, the Netherlands.

54. Helmich, R.C.G. (2011). Cerebral reorganization in Parkinson's disease. Radboud University Nijmegen, Nijmegen, the Netherlands.

55. Boelen, D. (2011). Order out of chaos? Assessment and treatment of executive disorders in brain-injured patients. Radboud University Nijmegen, Nijmegen, the Netherlands.

56. Koopmans, P.J. (2011). fMRI of cortical layers. Radboud University Nijmegen, Nijmegen, the Netherlands.

57. van der Linden, M.H. (2011). Experience-based cortical plasticity in object category representation. Radboud University Nijmegen, Nijmegen, the Netherlands.

58. Kleine, B.U. (2010). Motor unit discharges - Physiological and diagnostic studies in ALS. Radboud University Nijmegen Medical Centre, Nijmegen, the Netherlands.

59. Paulus, M. (2011). Development of action perception: Neurocognitive mechanisms underlying children's processing of others' actions. Radboud University Nijmegen, Nijmegen, the Netherlands.

60. Tieleman, A.A. (2011). Myotonic dystrophy type 2. A newly diagnosed disease in the Netherlands. Radboud University Nijmegen Medical Centre, Nijmegen, the Netherlands.

61. van Leeuwen, T.M. (2011). 'How one can see what is not there': Neural mechanisms of grapheme-colour synaesthesia. Radboud University Nijmegen, Nijmegen, the Netherlands.

62. van Tilborg, I.A.D.A. (2011). Procedural learning in cognitively impaired patients and its application in clinical practice. Radboud University Nijmegen, Nijmegen, the Netherlands.

63. Bruinsma, I.B. (2011). Amyloidogenic proteins in Alzheimer's disease and Parkinson's disease: interaction with chaperones and inflammation. Radboud University Nijmegen, Nijmegen, the Netherlands.

64. Voermans, N. (2011) Neuromuscular features of Ehlers-Danlos syndrome and Marfan syndrome; expanding the phenotype of inherited connective tissue disorders and investigating the role of the extracellular matrix in muscle. Radboud University Nijmegen Medical Centre, Nijmegen, the Netherlands.

65. Reelick, M. (2011) One step at a time. Disentangling the complexity of preventing falls in frail older persons. Radboud University Nijmegen Medical Centre, Nijmegen, the Netherlands.

66. Buur, P.F. (2011). Imaging in motion. Applications of multi-echo fMRI. Radboud University Nijmegen, Nijmegen, the Netherlands.

67. Schaefer, R.S. (2011). Measuring the mind's ear: EEG of music imagery. Radboud University Nijmegen, Nijmegen, the Netherlands.

68. Xu, L. (2011). The non-preganglionic Edinger-Westphal nucleus: an integration center for energy balance and stress adaptation. Radboud University Nijmegen, Nijmegen, the Netherlands.

69. Schellekens, A.F.A. (2011). Gene-environment interaction and intermediate phenotypes in alcohol dependence. Radboud University Nijmegen, Nijmegen, The Netherlands.

70. van Marle, H.J.F. (2011). The amygdala on alert: A neuroimaging investigation into amygdala function during acute stress and its aftermath. Radboud University Nijmegen, Nijmegen, the Netherlands.

71. De Laat, K.F. Motor performance in individuals with cerebral small vessel disease: an MRI study. Radboud University Nijmegen Medical Centre, Nijmegen, the Netherlands.

72. Mädebach, A. (2011). Lexical access in speaking: Studies on lexical selection and cascading activation. Radboud University Nijmegen, Nijmegen, the Netherlands.

73. Poelmans, G.J.V. (2011). Genes and protein networks for neurodevelopmental disorders. Radboud University Nijmegen, Nijmegen, the Netherlands.

74. Van Norden, A.G.W. (2011). Cognitive function in elderly individuals with cerebral small vessel disease. An MRI study. Radboud University Nijmegen Medical Centre, Nijmegen, the Netherlands

75. Jansen, E.J.R. (2011). New insights into V-ATPase functioning: the role of its accessory subunit Ac45 and a novel brain-specific Ac45 paralog. Radboud University Nijmegen, Nijmegen, the Netherlands.

76. Haaxma, C.A. (2011). New perspectives on preclinical and early stage Parkinson's disease. Radboud University Nijmegen Medical Centre, Nijmegen, the Netherlands.

77. Haegens, S. (2012). On the functional role of oscillatory neuronal activity in the somatosensory system. Radboud University Nijmegen, Nijmegen, the Netherlands

78. Van Barneveld, D.C.P.B.M. (2012). Integration of exteroceptive and interoceptive cues in spatial localization. Radboud University Nijmegen, Nijmegen, the Netherlands.